Characterization of the ubiquitin ligase E6AP by small molecules

Dissertation

zur Erlangung des akademischen Grades eines

Doktors der Naturwissenschaften (Dr.rer.nat.)

vorgelegt von

Fabian Offensperger

an der

Mathematisch-Naturwissenschaftliche Sektion

Fachbereich Biologie

Tag der mündlichen Prüfung: 26.06.2020

1. Referent: Prof. Dr. Martin Scheffner

2. Referent: Prof. Dr. Florian Stengel

3. Referent: Prof. Dr. Andreas Marx

Table of contents

Abstract

Alteration of the activity of a single enzyme can have major impacts on proper human development and health. The ubiquitin ligase E6AP is a prime example for this notion due to its causal association with three distinct pathologies: (I) Reduced activity of E6AP because of deletion of or point mutation in *UBE3A,* the gene encoding E6AP, results in the neuro-developmental disorder Angelman syndrome. (II) Hyperactivation of E6AP, due to *UBE3A* copy number variation, is associated with the Dup15q syndrome, an autism spectrum disorder. (III) Complex formation with high-risk human papillomavirus (HPV) E6 oncoproteins induces activation as well as alteration of the substrate spectrum of E6AP. Hence, the tumor suppressor p53 is efficiently targeted for ubiquitination and degradation, ultimately contributing to the formation of cervical carcinoma and other types of cancer. In principle, a therapy for all three disorders is feasible by readjusting their molecular cause, namely the altered enzymatic activity of E6AP. To do so, among other approaches, small molecules which correct the respective dysfunction can be envisioned. However, presumably due to the lack of robust high-throughput methods to identify ubiquitin ligase modulators, small molecules acting on E6AP have not been reported so far, despite their sincere need.

For this purpose, a novel fluorescence polarization-based method to monitor ubiquitination reactions was developed in the present study. It was then applied to screen a library containing around 50,000 diverse and drug-like chemicals to identify inhibitors of the E6-E6AP complex as well as activators of E6AP. In the screen for E6-E6AP inhibitors 351 hits were obtained. However, secondary assays revealed that they were either false-positive hits or acted unspecifically on earlier steps of the ubiquitination cascade. In contrast, the screen for E6AP activators yielded 53 hits of which several could be confirmed as specific activators of E6AP. Furthermore, Tamoxifen was found in this study as potent and specific activator of E6AP. Additionally, some of the small molecule activators rescue at least partially the activity of catalytically impaired Angelman syndrome-derived point mutants of E6AP. Finally, quantitative chemical crosslinking coupled to mass spectrometry (known as qXL-MS) was used to explore conformational rearrangements induced by HPV-16 E6 or small molecule activators. The obtained data indicate that binding of both HPV-16 E6 and the small molecule activators affect the structural dynamics of E6AP and the Angelman syndrome-derived mutants in such a way that upon binding the N and C termini come into closer proximity. These findings underpin our model that E6AP is typically present in a low-activity conformation, that can however be transferred into a high-activity conformation.

Generally speaking, the newly developed FP-based ubiquitination assay offers a broadly applicable tool to identify modulators of ubiquitin-associated enzymes and to characterize mutants thereof. Moreover, the identified small molecule activators represent a first step towards an Angelman

syndrome therapy by stimulation and reactivation of the enzymatic activity of E6AP and certain catalytically impaired E6AP mutants, respectively.

Zusammenfassung

Eine Veränderung der Aktivität eines einzelnen Enzyms kann einen entscheidenden Einfluss auf die normale Entwicklung und Gesundheit eines Menschen haben. Hierfür ist die Ubiquitinligase E6AP ein Musterbeispiel, da sie mit drei verschiedenen Krankheitsbildern ursächlich verknüpft ist: (I) Eine verminderte Aktivität von E6AP bedingt durch Deletion oder Punktmutation im *UBE3A* Gen, welches E6AP kodiert, führt zu der neurologischen Entwicklungsstörung Angelman-Syndrom. (II) Eine Hyperaktivierung von E6AP verursacht durch eine Amplifikation des *UBE3A* Gens ist mit dem Dup15q-Syndrom, einer Autismus-Spektrum-Störung, assoziiert. (III) Eine Komplexbildung mit E6 Onkoproteinen von ''Hochrisikotypen'' humaner Papillomaviren (HPV) induziert sowohl eine Aktivierung als auch eine Veränderung des Substratspektrums von E6AP. Infolgedessen wird der Tumorsuppressor p53 effizient polyubiquitiniert und abgebaut, was schlussendlich zur Entstehung von Gebärmutterhalskarzinomen und weiteren Krebsarten wesentlich beiträgt. Im Prinzip ist eine Behandlung aller dieser drei Krankheitsbilder denkbar, indem deren molekulare Ursache, nämlich die Deregulierung der enzymatischen Aktivität E6APs, korrigiert wird. Hierfür sind neben anderen Herangehensweisen kleine Moleküle, die der jeweiligen Fehlfunktion entgegenwirken, durchaus vorstellbar. Ein Mangel an robusten Hochdurchsatzmethoden zur Identifikation von kleinen Molekülen, welche die Aktivität von Ubiquitinligasen modulieren können, hat jedoch dazu geführt, dass, trotz des dringenden Bedarfs, bisher noch keine kleinen Moleküle, welche spezifisch auf E6AP wirken, berichtet wurden.

Zu diesem Zweck wurde in der vorliegenden Studie eine neuartige, auf Fluoreszenzpolarisation basierende Methode entwickelt, um Ubiquitinierungsreaktionen zeitlich aufgelöst verfolgen zu können. Diese wurde anschließend angewandt, um eine Bibliothek von circa 50.000 verschiedenen wirkstoffartigen kleinen Molekülen sowohl auf eine Inhibierung des E6-E6AP Komplexes als auch auf eine Aktivierung von E6AP zu testen. Dabei wurden insgesamt 351 chemische Verbindungen identifiziert, welche den E6-E6AP Komplex inhibieren. Folgeexperimente zeigten jedoch, dass deren Wirkung entweder nicht reproduzierbar war oder auf unspezifischer Inhibierung früherer Schritte der Ubiquitinierungskaskade beruhte. Im Screen für E6AP Aktivatoren wurden hingegen 53 kleine Moleküle identifiziert, von denen mehrere als E6AP-spezifisch bestätigt wurden. Außerdem wurde in dieser Studie Tamoxifen als spezifischer Aktivator von E6AP gefunden. Des Weiteren konnten einige der Aktivatoren die Aktivität katalytisch stark beeinträchtigter, Angelman-Syndrom verursachender E6AP-Mutanten, zumindest teilweise wiederherstellen. Schließlich wurde ''quantitatives chemisches Crosslinking verknüpft mit Massenspektrometrie'' (auch bekannt als qXL-MS) eingesetzt, um Konformationsänderungen von E6AP, die potenziell durch Bindung von HPV-16 E6 oder den Aktivatoren induziert werden, zu erforschen. Die erhaltenen Daten deuten darauf hin, dass die

strukturelle Dynamik von E6AP und der Angelman-Syndrom Mutanten tatsächlich beeinflusst wird, insofern dass der N- und der C-Terminus durch Bindung von HPV-16 E6 oder der Aktivatoren in räumliche Nähe gelangen. Diese Forschungsergebnisse untermauern unser Modell, dass E6AP allein meist in einem Zustand geringer Aktivität vorliegt, jedoch durch Interaktionspartner in eine hochaktive Konformation überführt werden kann.

Zusammengefasst bietet der neu entwickelte Ubiquitinierungsassay ein allgemein anwendbares Werkzeug, um Modulatoren von Enzymen des Ubiquitinierungssystems und deren Mutanten zu identifizieren und zu charakterisieren. Darüber hinaus stellen die identifizierten Moleküle einen ersten Schritt in Richtung einer Therapie für das Angelman-Syndrom dar, da sie sowohl E6AP stimulieren als auch bestimmte katalytisch beeinträchtigte Angelman-Syndrom Mutanten reaktivieren können.

1 Introduction

The central topic of this work is E6AP, an exceptionally health-relevant and mechanistically fascinating enzyme. E6AP acts as a ubiquitin ligase and is thus part of the ubiquitin-proteasome system. In the following sections of this dissertation, first, the ubiquitin-proteasome system and the role of E6AP in it will be introduced. Then, the current knowledge about structure and mechanism of action, as well as known substrates and interaction partners of E6AP will be summarized. Afterwards, disorders caused by malfunction of E6AP, namely cervical cancer, Angelman syndrome (AS) and Dup15q syndrome will be described, and the mechanism how E6AP is involved as well as potential approaches for therapeutic intervention will be outlined. Finally, an overview over existing methods to identify small molecule modulators of ubiquitin ligases and over already identified modulators targeting other ubiquitin ligases will be given. Additionally, fluorescence polarization, the method applied in the present study to identify small molecule modulators of E6AP, will be discussed.

1.1 The ubiquitin-proteasome system

In 2004, Aaron Ciechanover, Avram Hershko and Irwin Rose received the Nobel Prize in chemistry 'for the discovery of the ubiquitin-mediated protein degradation'. Ubiquitin is a small protein that is attached via an isopeptide bond between its C-terminal carboxyl group and the ε-amino group of a lysine residue or the N-terminal amino group of a substrate protein. This post-translational modification is called ubiquitination or ubiquitylation and is mediated by an enzymatic process that will be described in more detail below (chapter 1.1.2). Ubiquitination influences a myriad of cellular processes including cell cycle regulation, DNA repair, cell growth, apoptosis, immune function, vesicular trafficking pathways including autophagy, regulation of histone modification, viral budding and many more (Hershko et al., 2000, Nath & Shadan, 2009, Komander & Rape, 2012, Varshavsky, 2012, Swatek & Komander, 2016, Dikic, 2017, Kwon & Ciechanover, 2017, Zheng & Shabek, 2017).
Ubiquitin itself contains seven lysine residues with a primary amine group and another amino group at its N-terminal methionine, all of which can be used for ubiquitination, so that not only a single ubiquitin residue (mono-ubiquitination) but also ubiquitin chains (poly-ubiquitination) can be attached to a substrate. Ubiquitination results in different fates of the modified substrate depending on the number and linkage type of attached ubiquitin residues (Swatek & Komander, 2016). For example, a well accepted doctrine is that ubiquitination with K11- or K48-linked chains leads to degradation of the labeled protein by the proteasome (Kerscher et al., 2006). The proteasome is a huge protein complex of approximately 1700 kDa which cleaves proteins into short peptides and in a simplistic view consists of several proteases and regulatory proteins. For detailed information about the structure, mechanism and function of the proteasome see (Voges et al., 1999, Dikic, 2017, Bard et al., 2018).

1.1.1 Structure and function of ubiquitin

Ubiquitin is a small (8.5 kDa) protein found in all eukaryotes. It consists of 76 highly conserved amino acids and has a globular structure with a flexible, six amino acids long C-terminal tail. Its canonical fold is a 5-stranded β-sheet, a short 3_{10}-helix and a 3.5-turn α-helix (Vijay-Kumar et al., 1987). The surface of ubiquitin is further characterized by a canonical hydrophobic patch mainly formed by I44, L8 and V70. This hydrophobic patch plays a crucial role in interactions of ubiquitin with proteins bearing ubiquitin binding domains that are for example involved in the recognition of differently linked ubiquitin chains at the proteasome (Dikic et al., 2009). Hydrophobic patch mutants are well studied and show for instance defects in the activation by E1 and recognition by E6AP and the 26 S proteasome (Beal et al., 1996, Sloper-Mould et al., 2001, Mortensen et al., 2015, Singh et al., 2017).

1.1.2 The ubiquitination cascade

For attachment to substrate proteins, ubiquitin is activated and transferred via a three-step enzymatic cascade comprising E1 ubiquitin-activating enzymes, E2 ubiquitin-conjugating enzymes and E3 ubiquitin ligases (figure 1 and (Oh et al., 2018)). The first step of the ubiquitination cascade is the activation of ubiquitin by E1 enzymes under ATP consumption. The carboxyl group of ubiquitin's C-terminal glycine is activated by formation of a high-energy bond to adenosine monophosphate. Subsequently, the catalytically active cysteine of E1 attacks this bond resulting in an E1-ubiquitin thioester conjugate. In the next step, ubiquitin is transthiolated from E1 to the catalytic cysteine on an E2 enzyme forming another thioester. Finally, it is transferred from E2 to the substrate through E3 ubiquitin ligases by forming a stable isopeptide bond. Two E1, approximately 40 E2s and over 600 potential E3 enzymes are encoded in the human genome (Li et al., 2008, Stewart et al., 2016). These ascending numbers of the components of the ubiquitination cascade indicate that E3 ubiquitin ligases are responsible for substrate specificity and that a huge number of substrates can be specifically targeted for ubiquitination illustrating the enormous impact of ubiquitination on cellular life. The ubiquitination cascade is counteracted by deubiquitinating enzymes (DUBs), which remove ubiquitin from substrates or cleave ubiquitin chains.

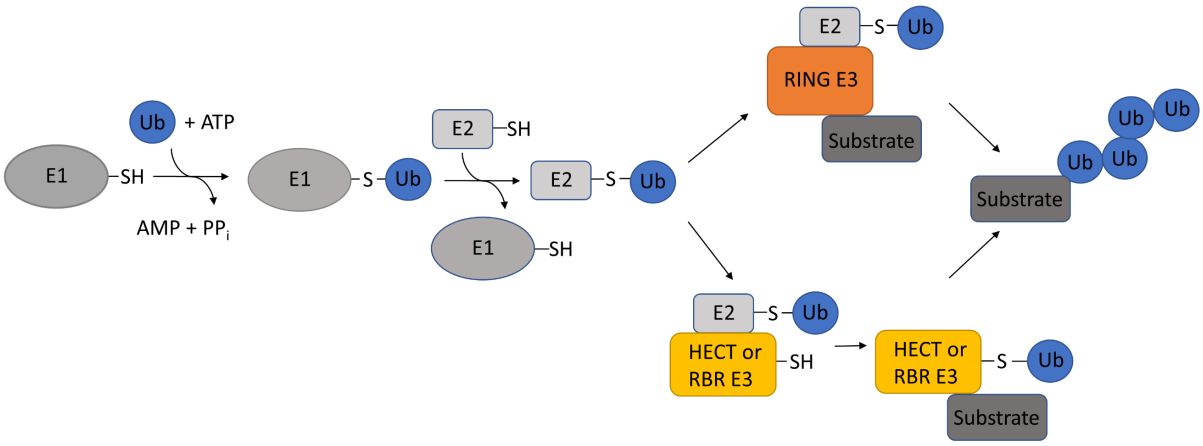

Figure 1: Schematic overview over the ubiquitination cascade
In the ubiquitination cascade, an E1 ubiquitin activating enzyme forms a 'high energy' thioester with the C-terminal carboxyl group of ubiquitin under ATP consumption. Next, ubiquitin is passed to the catalytic cysteine of an E2 ubiquitin conjugating enzyme in a transthiolation reaction. The last step is the transfer of ubiquitin to the substrate facilitated by an E3 ubiquitin ligase. Three different families of E3 ubiquitin ligases exist. RING E3 ligases act as scaffolds and activators of the direct transfer of ubiquitin from E2~Ub thioester to the substrate, whereas HECT and RBR E3 ligases form a further thioester with ubiquitin before it is transferred to the substrate, thereby being directly involved in the catalysis.

1.1.3 E3 ubiquitin ligases

E3 ubiquitin ligases are, by reason of shared structural elements and distinct transfer mechanisms, subdivided into three subgroups, namely RING (with over 600 members in humans), HECT (28 human members), and RBR E3 ligases (14 human members). RING (Really Interesting New Gene) ligases contain a so-called RING domain that coordinates a pair of zinc ions which are involved in E2 binding. RING ligases themselves are not directly catalytically implicated in the transfer of ubiquitin from E2 to the substrate, but rather act as scaffolds to bring ubiquitin-charged E2s and their substrates into proximity. In addition, they activate E2 enzymes allosterically to facilitate an efficient reaction (Deshaies & Joazeiro, 2009, Metzger et al., 2014). In contrast, HECT (Homologous to E6AP C Terminus) ubiquitin ligases contain a cysteine residue as catalytic center that forms a thioester intermediate with ubiquitin, so that HECT ligases are directly catalytically involved in ubiquitination (reviewed in (Rotin & Kumar, 2009, Lorenz, 2018, Sluimer & Distel, 2018, Weber et al., 2019)). In addition, RBR (RING-between-RING) E3 ligases appeared as a third subgroup as hybrids between RING and HECT E3 ligases harboring two RING domains, one of which contains a catalytically active cysteine (Eisenhaber et al., 2007, Wenzel et al., 2011, Riley et al., 2013, Dove & Klevit, 2017, Reiter & Klevit, 2018).

Besides E6AP, three different E3 ligases (HDM2, RLIM, HUWE1) with pathological relevance have been investigated in this study and will thus be shortly introduced in this section. HDM2 (the human orthologue of MDM2) is a RING E3 ligase that ubiquitinates the tumor suppressor p53 leading to its

degradation. This makes HDM2 an important target in cancer research (Haupt et al., 1997, Honda et al., 1997, Kubbutat et al., 1997, Urso et al., 2016). RLIM is a RING-H2 zinc finger protein that acts as negative co-regulator of LIM homeodomain transcription factors, which are involved in specification of cell lineages and regulation of differentiation during development. Altered RLIM expression has also been associated with cancer (Ostendorff et al., 2000, Ostendorff et al., 2002). In addition, pathogenic variants of RLIM lead to a syndromic X-linked intellectual disability and behavioral disorder (Frints et al., 2019). HUWE1 (also known as HECTH9, ARF-BP1, URE-B1, LASU1 or Mule) is a HECT E3 ligase which among other targets ubiquitinates the transcription factor Myc with mixed K6-, K48-, and K63-linked poly-ubiquitin chains (Adhikary et al., 2005). Subsequently, transactivation of multiple target genes is induced, the coactivator p300 is recruited, and cell proliferation is turned on. HUWE1 is overexpressed in multiple human tumors and is essential for proliferation of a subset of tumor cells, underlining its key role in cancer (Adhikary et al., 2005, Kao et al., 2018).

1.2 The HECT ligase E6AP

The main focus of this study is on the ubiquitin ligase E6AP (E6-associated protein), which was the first known member of the HECT ubiquitin ligase family, to that 27 other human members with a conserved C-terminal so-called HECT domain were affiliated (Huibregtse et al., 1995). E6AP is known to attach mainly K48-linked ubiquitin chains to substrates resulting in their proteasomal degradation (Wang & Pickart, 2005, Kim & Huibregtse, 2009). As already mentioned, malfunction of E6AP is associated with three distinct disorders: cervical cancer, Angelman syndrome and Dup15q syndrome (Matentzoglu & Scheffner, 2008, Scheffner & Kumar, 2014, Khatri & Man, 2019). Understanding the mechanisms that regulate its activity is therefore fundamentally important to develop strategies to interfere with E6AP malfunction in the mentioned human disorders. For this reason, all available structural information of E6AP will be summarized.

1.2.1 Structure of E6AP (in comparison to other HECT E3s)

Originally the E6AP cDNA was described to be 2700 bp long encoding about 850 amino acids (Huibregtse et al., 1993a). Later, E6AP was found to be expressed from the *UBE3A* gene on the long arm of chromosome 15 in the 15q11.2-q13.3 region and that three different isoforms are produced by alternative splicing (Yamamoto et al., 1997). The three isoforms differ in their extreme N termini with isoform one being the shortest form with a length of 852 amino acids. Isoform two and three own an N-terminal extension of 23 or 20 amino acids, respectively (figure 2). Although similar ubiquitination activity was confirmed, it remains elusive whether substrate specificity is altered due to the extensions (Yamamoto et al., 1997). Recent studies revealed that the different isoforms of E6AP are localized in

different subcellular compartments (Avagliano Trezza et al., 2019). Another recent study identified a non-coding function of an alternative *UBE3A* transcript, lacking the catalytic domain region of E6AP, in dendritic protein synthesis (Valluy et al., 2015). Potential different localization and roles of the different isoforms need to be kept in mind as in the present study isoform one was investigated only.

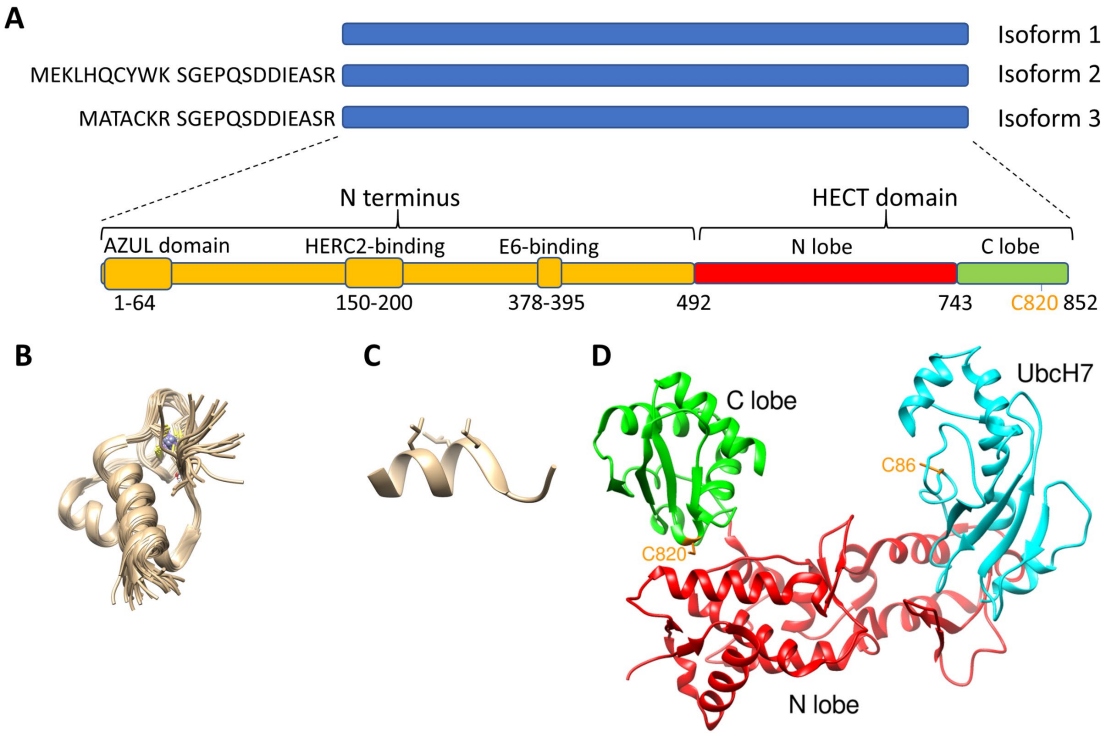

Figure 2: Structural knowledge of E6AP
*(A) The three isoforms of E6AP according to (Yamamoto et al., 1997). Isoform 1 is the shortest expressed version of E6AP with 852 amino acid residues and the catalytic center at position 820. All positions in this dissertation refer to isoform 1. Isoform 2 and 3 have a 23 or 20, respectively, amino acids long N-terminal extension. The scheme below shows known domains and binding sites within E6AP. (B) Ensemble of NMR structures of the AZUL domain of E6AP with the coordinated zinc ion colored in blue (pdb entry 2KR1) (Lemak et al., 2011). (C) E6-binding α-helix of E6AP containing residues 383-394 (ELT**L**QE**LL**GEER) with leucine residues from the LXXLL motif shown (pdb entry 4GIZ) (Zanier et al., 2013). (D) Crystal structure of the HECT domain of E6AP with the cognate E2 enzyme UbcH7 bound (pdb entry 1C4Z) (Huang et al., 1999). The structures shown were modified with UCSF chimera software (Pettersen et al., 2004).*

Soon after its discovery, regions of E6AP responsible for E6 and p53 binding and regions responsible for ubiquitin ligase activity were determined (Huibregtse et al., 1993b). Shortly afterwards, a family of proteins that are structurally and functionally related to E6AP was discovered, which all share a C-terminal, ~350 amino acids long domain with a highly conserved catalytically active cysteine (Huibregtse et al., 1995). 20 years ago, the structure of the HECT domain of E6AP with a bound cognate E2 enzyme could be solved by X-ray crystallography (Huang et al., 1999). To note, for the full-length protein or the whole N-terminal part of E6AP no structures could be obtained yet. The HECT domain forms an L-shape with two lobes, the N lobe and the C lobe. The C lobe harbors the catalytically active

cysteine and the N lobe contains the E2 binding site. Two aspects are interesting in this crystal structure: first, the catalytic cysteines of the E2 and E6AP are 41 Å apart so that no direct transfer of ubiquitin from the catalytic cysteine of the E2 to the catalytic cysteine of E6AP can take place without major structural rearrangements. The second interesting new finding was that the HECT domain forms a trimer that was, however, concluded to represent an artifact due to high crystal packaging forces. Later, also structures of the HECT domains of WWP1 (Verdecia et al., 2003), Smurf1 (Ogunjimi et al., 2005) and NEDD4L (Kamadurai et al., 2009) were solved. The structures of the two lobes are for each HECT domain highly similar, but the orientation of the two lobes differs by a rotation around a hinge region between the two of them. This possibility to swivel around an axis between the two lobes indicates large structural rearrangements during catalysis. Indeed, the two lobes of the HECT domains seem to be able to swivel in an angle of about 100° allowing to accept ubiquitin from the E2 enzyme and to pass it to the substrate. Mutational analysis of this hinge region proved that rotation is essential for catalysis (Verdecia et al., 2003). Additionally, modelling and molecular dynamic simulations of the interaction between the HECT domain of the E3 ubiquitin ligase Itch and the E2 enzyme UbcH7 showed two different hinge regions in the HECT domain, the known one between the N and C lobe and another between two subdomains of the N lobe (Raimondo et al., 2008). Additionally, the structure of the HECT domain of NEDD4 was solved on its own and in complex with ubiquitin showing a new binding mode that involves two surfaces on ubiquitin and both subdomains of the N lobe (Maspero et al., 2011). However, this regulatory interaction seems to be only valid for NEDD4-type HECT ligases, as the key interacting cysteine is not present in other HECT ligase family members (Maspero et al., 2011). Furthermore, the structure of a ubiquitin loaded HECT domain of NEDD4 revealed the molecular basis for catalytic priming by providing insight into interactions between the C lobe of the HECT domain and ubiquitin. It could be revealed that ubiquitin is locked in an extended conformation resulting in the formation of specific K63-linked ubiquitin chains (Maspero et al., 2013), while the determinants for K48-linked chains formed by E6AP are not known yet. Another study determined experimentally the complete ^{1}H, ^{13}C, and ^{15}N backbone and side chain resonance assignments for the C lobe of the HECT domain of ITCH (residues 784–903) using heteronuclear, multidimensional NMR spectroscopy. The resonance assignments can be used in future NMR-based studies to examine dynamics and conformational flexibility in ubiquitination by HECT ligases. Moreover, the structural and biochemical basis for ubiquitin chain synthesis and specificity can thus be investigated (Beasley et al., 2019). Taken together, structures of HECT domains shed some light on the molecular mechanism of ubiquitin ligation to substrates, however questions remain, for example, how different chain specificities are maintained.

Besides the HECT domain, the structure of two other parts of E6AP (AZUL domain and E6-interacting α-helix) have been solved yet so that 50% of the structure of E6AP is known at this time. The structure

of the AZUL (Amino-terminal Zn-finger of Ube3a Ligase) domain was solved by solution NMR of a truncated construct spanning residues 1-64 according to isoform 1 of E6AP (Lemak et al., 2011). The AZUL domain adopts a helix-loop-helix architecture with an atypical, C4 type zinc finger with the Zn^{2+} ion coordinated by four cysteine residues arranged in a C-X_4-C-X_4-C-X_{28}-C motif (with X representing any other amino acid). Interestingly, a mutation of C21, one of the Zn^{2+} ion coordinating residues, was found in an AS patient (Cooper et al., 2004), and was further characterized in the present work.

The other structural feature of E6AP of which the three-dimensional structure is known is the E6-binding motif containing α-helix. It spans residues 372-383 with the core LXXLL motif. The E6-binding motif forms an α-helix which was solved first by NMR (Be et al., 2001). Mutational analysis in the same study proved that all three leucine residues form a hydrophobic patch that is essential for E6 binding and substitution of any of the amino acids in the α-helix disrupted the interaction. Later, the structure of the E6-binding motif was also solved by X-ray crystallography, first in complex with full-length HPV-16 E6 (Zanier et al., 2013) and then also in a ternary complex with full-length HPV-16 E6 and the core domain of p53 (Martinez-Zapien et al., 2016).

The 28 human HECT E3 ligases have been grouped based on shared structural domains into the NEDD4-like family with nine members, the HERC-like family with six members and 'others', which do not share any structural feature in the N terminus with other HECT ligases like it is the case for E6AP. For a detailed description and classification of the HECT ligases see (Scheffner & Kumar, 2014, Lorenz, 2018, Sluimer & Distel, 2018). To recapitulate the most essential information it can be said that size as well as structural motifs are divergent and regulatory mechanisms like asymmetric auto-inhibiting dimerization of HUWE1 (Sander et al., 2017), auto-inhibitory interaction of N-terminal domains with the HECT domain of NEDD4 subfamily as shown for SMURF1 (Wan et al., 2011), SMURF2 (Wiesner et al., 2007), ITCH (Gallagher et al., 2006, Riling et al., 2015, Zhu et al., 2017), NEDD4 (Mari et al., 2014, Chen et al., 2017), NEDD4L (Escobedo et al., 2014) or the ubiquitin-binding domain controlled oligomerization resulting in inhibition of Rsp5 (the yeast ortholog of NEDD4) (Attali et al., 2017) are only valid for the particular ligase and cannot be transferred to other members of the HECT family. Additionally, HECT ligases form distinct ubiquitin chains regardless of the paired E2 enzyme from which ubiquitin is received (Weber et al., 2019).

1.2.2 Cellular interaction partners of E6AP

E6AP was found to be expressed in all cell types and tissues (Su et al., 2004). Moreover, E6AP is localized in the nucleus since it harbors a nuclear localization signal sequence but it is also localized in the cytoplasm (Hatakeyama et al., 1997, Avagliano Trezza et al., 2019). This spatial presence suggests that E6AP interacts with diverse cellular proteins.

1.2.2.1 Non-substrate interaction partners of E6AP

The protein-protein interaction database BioGRID (version 3.5.177 (Oughtred et al., 2019)) recognizes 318 potential protein interaction partners of E6AP found in 133 publications. Only a limited number of these interactions has been validated as E6AP substrates while some of the interaction partners have been shown not to be substrates, but to have other functions. Other functions are for example regulation of E6AP activity or to act as adaptors, which modify the substrate spectrum of E6AP.

Obviously, E2 enzymes need to bind to E6AP for ubiquitin transfer from themselves to E6AP. The sequence properties of E2 enzymes needed for E6AP binding were investigated, shedding some light on the question of E2-E3 specificity (Eletr & Kuhlman, 2007). UbcH5, UbcH7 and UbcH8 were identified as cognate E2 enzymes for E6AP.

Besides E2 enzymes, the E6 protein of high-risk human papilloma viruses (see chapter 1.2.4.1.2) is well known to serve as adaptor between E6AP and p53. While ubiquitination of E6 proteins by E6AP *in cellula* might happen to some extent (Li et al., 2019), HPV-16 E6 is in *in vitro* ubiquitination assays not ubiquitinated (Ebner, 2019). Another example for an adaptor function is the interaction of the AZUL domain of E6AP with PSMD4 which mediates binding of E6AP to the proteasome (Kühnle et al., 2018) and for which the structure was solved recently (Buel et al., 2020). The AZUL domain is a zinc coordinating domain and zinc fingers are known to interact with DNA, however E6AP-DNA interaction was not reported yet.

Furthermore, two proteins that act as allosteric activators of E6AP have been characterized so far, namely HERC2 and HPV-16 E6. The giant HECT ligase HERC2 was identified to bind to the N-terminal part of E6AP (encompassing amino acid residues 150 to 200 according to isoform 1) and thereby to stimulate E6AP's catalytic activity (Kühnle et al., 2011). In an early study, HPV-16 E6 was shown to induce self-ubiquitination of E6AP (Kao et al., 2000). In a later study, HPV-16 E6 could be confirmed as allosteric activator of E6AP in auto- as well as substrate ubiquitination assays (Mortensen et al., 2015). Moreover, binding of HPV-16 E6 enables the rescue of the catalytically impaired Angelman syndrome (AS) mutant E6AP Y533A (Ronchi et al., 2014).

Besides the mentioned interaction partners that act either as scaffolds or allosteric activators, several other unrelated interaction partners were identified. A couple of studies suggest interaction of E6AP with estrogen and progesterone receptors as well as a possible co-transactivation activity of E6AP and ERα independent of the ubiquitin ligase activity of E6AP (Nawaz et al., 1999, Dhananjayan et al., 2006, El Hokayem et al., 2018, Obeid et al., 2018). E6AP contains three LXXLL motifs, which are in general important for receptor interaction (Heery et al., 1997). However, further evidence is needed to support the regulation of nuclear hormone receptors by E6AP and whether this interaction plays a role in the neurological disorders AS or Dup15q syndrome. Furthermore, the synapse regulating protein Arc was suggested as a substrate of E6AP (Greer et al., 2010); however no ubiquitination *in vitro* was

recognizable and a transcriptional regulation of the Arc gene by E6AP was suggested (Kühnle et al., 2013). Moreover, further potential interaction partners of E6AP were found by mass spectrometry, where E6AP was shown to be in complex with the proteasome or in a high-molecular weight complex of approximately 2 MDa with HERC2, NEURL4 and MAPK6 (Martinez-Noel et al., 2012). Network analysis of E6AP associated proteins (including MCM6, SUGT1, EIF3C, and ASPP2) identified in affinity purification coupled to mass spectrometry (AP-MS) and yeast two- or three-hybrid assays, revealed that E6AP-associated proteins are involved in several fundamental cellular processes including translation, DNA replication, intracellular trafficking, and centrosome regulation (Martinez-Noel et al., 2018). For most interaction partners, it is not finally clarified whether they are substrates of E6AP or act as adaptors or regulators of E6AP activity.

1.2.2.2 Substrates of E6AP

The main mode of action of E3 ligases is the specific recognition and modification of target proteins with ubiquitin, why it is of fundamental importance to know the targets of an E3 ligase to understand its physiological functions. In the past, a most studies searched for substrates of E6AP in presence of HPV E6 proteins (Vande Pol & Klingelhutz, 2013). In the meantime, an increasing number of studies also aimed at identifying substrates of E6AP alone. A summary of identified substrates will be given in the following section.

Firstly, E6AP has been identified to serve as its own substrate, in a process called auto-ubiquitination, as it holds true for most E3 ligases (Nuber et al., 1998). Next, HHR23A, one of the human homologues of the yeast DNA repair protein Rad23, was identified in a yeast two-hybrid screen with E6AP as bait, and could be confirmed as substrate of E6AP in absence of HPV E6 proteins (Kumar et al., 1999). In addition, the PRC1-like complex member Ring1B is a well-established substrate (Zaaroor-Regev et al., 2010)). Ring1B is itself an E3 ligase, monoubiquitinates histone H2A and can thereby substantially impact global gene expression. To selectively inactivate its E3 function thereby facilitating the characterization of E6AP-mediated ubiquitination in *in vitro* and *in cellula* experiments, Ring1B is rendered catalytically inactive by mutation of isoleucine 53 to serine (Ben-Saadon et al., 2006). Furthermore, the proteasomal shuttling factor RPN10 (also known as PSMD4 or S5A) and other regulators of the proteasome were identified as direct targets for DUBE3A (the *Drosophila* analogue of E6AP) in a neuronal cell culture system (Lee et al., 2014), and several subunits of the proteasome were shown to be ubiquitinated *in situ* by E6AP (Jacobson et al., 2014). However, this stands in contrast to a study reporting that PSMD4 is only an interaction partner of E6AP and is not ubiquitinated by it (Kühnle et al., 2018).

Further reported potential substrates of E6AP are BLK (Oda et al., 1999), MCM7 (Kuhne & Banks, 1998), UBQLN1/2 (Kleijnen et al., 2000, Kleijnen et al., 2003), the Estrogen Receptor α (Li et al., 2006),

hepatitis C virus core protein (Shirakura et al., 2007, Shoji et al., 2007), TSC2 (Zheng et al., 2008), ANNEXIN A1 (Shimoji et al., 2009), α-Synuclein (Mulherkar et al., 2009), the tumor suppressor PML (Louria-Hayon et al., 2009), Peroxiredoxin (Nasu et al., 2010), Ephexin5 (Margolis et al., 2010), the core clock component ARNTL/BMAL1 (Gossan et al., 2014), the potassium channel SK2 (Sun et al., 2015, Sun et al., 2019), MNT (Kapoor et al., 2016), clusterin (Gulati et al., 2018), p18/LAMTOR1 (Sun et al., 2018), XIAP (Khatri et al., 2018), PTPA (Wang et al., 2019) and ENO1 (Mishra et al., 2019). Furthermore, a recent proteomics study used an orthogonal ubiquitin transfer approach to identify 130 substrates from which MAPK1, CDK1, CDK4, PRMT5, β-catenin and UbxD8 were reported to be directly ubiquitinated by E6AP *in vitro* and *in cellula* (Wang et al., 2017b) with β-catenin being supported as E6AP substrate by an independent study (Kuslansky et al., 2016). However, many other of the mentioned identified substrates have not been confirmed nor have been followed up as physiological substrates of E6AP yet. In any case, to be able to make final conclusions about the function of an E3 ligase and to understand its enzymatic mechanism, it is necessary to know the full range of substrates. Therefore, the mentioned potential E6AP substrates should be evaluated carefully in future studies. However, it should be kept in mind that ubiquitination of a given substrate may only be relevant for certain tissues or during certain phases of differentiation or development (Scheffner & Kumar, 2014). Tissue specific substartes in neurons are of special interest due to the connection of E6AP to neurodevelopmental disorders (Khatri & Man, 2019).

1.2.3 Mechanism of function and activity regulation of E6AP

Most of the recent scientific reviews covering HECT ubiquitin ligases presume that E6AP is active as a trimer. The origin of this hypothesis lies in the crystal structure of the HECT domain of E6AP forming a trimer, that was, however, originally ascribed to an artifact due to crystal packaging forces (Huang et al., 1999). In contrast to that explanation, a later study claimed that the actual active form of E6AP is indeed a trimer as indicated by the size of recombinantly expressed E6AP determined by static light scattering measurements and size-exclusion chromatography (Ronchi et al., 2014). In the same study, mutational analysis of Phe727, that is absolutely conserved in HECT ligases and interacts with a hydrophobic pocket in the adjacent subunit in the crystal structure, showed that mutation to aspartic acid led to a dramatic decrease of auto-ubiquitination activity. It was furthermore reported that *N*-acetyl-phenylalanyl-amide reversibly antagonized trimer formation and inhibited catalytic activity with a K_i of 12 mM supporting the trimer model. On the contrary, the authors of another study overexpressed HA-tagged E6AP in mammalian cells and investigated the lysate by size-exclusion chromatography. They found E6AP either present in huge complexes with the proteasome or with HERC2, NEURL4 and MAPK6 or, and actually the majority, E6AP was found in lower molecular-mass complexes ranging from 100 to 200 kDa, indicating a monomeric state of E6AP (Martinez-Noel et al.,

2012). Besides, as already described above (chapter 1.2.2.2), biochemical experiments revealed that E6AP for its own mainly performs auto-ubiquitination in a *trans* mechanism (ubiquitination of one E6AP molecule by another E6AP molecule) (Nuber et al., 1998), whereas addition of HPV-16 E6 shifted E6AP auto-ubiquitination mainly to a *cis* mechanism (meaning transfer of ubiquitin from the catalytic cysteine residue to a lysine residue on the very same E6AP molecule) (Kao et al., 2000). These findings also indicated transient interactions between E6AP molecules which could be reduced in presence of HPV-16 E6.

Apart from oligomerization, post-translational modification is believed to regulate activity of E6AP. E6AP performs efficient auto-ubiquitination. Additionally, it was reported that E6AP is ubiquitinated by the HECT ligase UBR5 (Tomaic et al., 2011) and possibly also by other E3 ligases, as ubiquitination of other ubiquitin ligases is a common feature of several E3 ligases (de Bie & Ciechanover, 2011). To date, auto-ubiquitination of E6AP has only been regarded as negative feedback loop to counteract hyperactivity of E6AP by its degradation through the proteasome. Mono-ubiquitination may, however, also influence the catalytic activity of E6AP as mono-ubiquitination has been shown to activate NEDD4-like HECT ligases (Chen et al., 2017).

Besides ubiquitination, phosphorylation plays a potential role in E6AP regulation as E6AP was found in different proteomic studies to be ubiquitinated and phosphorylated (PhosphoSitePlus v.6.5.8 (Hornbeck et al., 2015)). For example, tyrosine at position 636 was proposed to be phosphorylated by c-Abl kinase (Chan et al., 2013). This modification was considered to disrupt putative trimer formation of the HECT domain and consequently act inhibitory on ligase activity. Another known phosphorylation site of E6AP is T485. This mutation was identified as an autism-linked mutation (Yi et al., 2015). This study showed that E6AP T485A is hyperactive and that this mutation leads to increased synapse formation *in vivo*. In contrast, a phospho-mimetic mutation of position 485 to glutamate decreased ligase activity. Thus, it was concluded that phosphorylation of T485 inhibits ligase activity of E6AP (Yi et al., 2015). Additionally, serine at position 195 was identified to be phosphorylated in proteomic studies, however no functional consequence has been associated to this modification site yet (Matsuoka et al., 2007, Mayya et al., 2009).

Besides understanding the regulation of E6AP by interaction partners or post-translational modification, knowledge about the mechanism by which E6AP modifies substrates with K48-linked ubiquitin chains is helpful to be able to manipulate it. To do so, Krist et al. developed a novel acid-cleavable photo-crosslinker to identify catalytic important residues of E6AP (Krist & Statsyuk, 2015). Except of the catalytic cysteine C820, two residues (K799 and K847) reacted with the photo-crosslinker which was loaded on the catalytic cysteine of a cognate E2 enzyme. K847 is required for the formation of K48-linked poly-ubiquitin chains, while a K799A mutant was hyperactive in producing K48-linked ubiquitin chains. However, a major drawback of this study is that, like in many other studies, only the

HECT domain but not full-length E6AP was utilized. Full-length E6AP forms linkage-specific K48 chains in auto- as well as substrate ubiquitination, whereas the HECT domain only creates mono- and to a smaller amount di- and tri-ubiquitinated species in auto-ubiquitination assays and does not ubiquitinate substrates. Mass spectrometric analysis revealed that also free dimers are formed by E6AP HECT, which, however, do not show any specificity in linkage type (Kobayashi et al., 2018).

Another study probed the interactions of the HECT domain of E6AP with ubiquitin by NMR and mutational analysis. Ries and colleagues identified distinct surface regions which are important for the initial step of catalysis, the trans-thiolation reaction, as well as other regions that are important for the subsequent step, the isopeptide bond formation between two ubiquitin molecules (Ries et al., 2019).

In addition, it was suggested that the HECT domain of E6AP harbors two distinct E2 binding sites (Ronchi et al., 2013, Ronchi et al., 2017), providing a possible mechanism by which ubiquitin chain elongation may occur, but further studies are needed to substantiate the proposed model. In general, despite intense efforts over the last two decades, the molecular details underlying the synthesis of ubiquitin chains is still not completely understood. Two alternative, but not mutually exclusive models exist. In one, one ubiquitin moiety is transferred at a time to a growing substrate-linked chain (sequential addition model); in the other, a pre-assembled ubiquitin chain is transferred to a substrate (*en bloc* model) (Deol et al., 2019).

Taken together, a number of studies investigated potential physiological functions of E6AP and how its activity is regulated. However, despite this increasing knowledge, many questions remain to be solved including how chain specificity is achieved, how the N terminal half of E6AP is structured, how E6AP changes its conformation in the catalytic cycle to attach K48-linked ubiquitin chains to substrates, where on E6AP different substrates bind, and if common binding sites exist for different substrates.

1.2.4 Role of E6AP in human health and disease

1.2.4.1 E6AP and cervical cancer

1.2.4.1.1 Human papillomaviruses (HPVs)

Human papillomaviruses (HPVs) are small DNA viruses leading to hyperproliferative lesions of the skin and mucosal epithelia (Doorbar et al., 2015). HPVs infecting mucosal epithelia can be subdivided into low-risk types such as type 6 or 11, which induce benign lesions like warts, and high-risk types such as type 16, 18, 31, 33, 45 which can cause the formation of epithelial cancers (Giuliano et al., 2008, Klingelhutz & Roman, 2012). HPV-16 and -18 are the most abundant high-risk types found in at least 70% of cervical cancers. Infection with high-risk HPVs has been associated with virtually all cases (99.7%) of cervical cancer (zurHausen, 1996). Moreover, high-risk HPV infection is also the source of additional cancers in the anogenital tract and the head and neck region, with about 5% of total human

cancers being attributable to HPV infection (de Martel et al., 2017). High-risk HPVs thus represent a global clinical problem (Bosch et al., 2013).

The key viral factors promoting cancer development are the early proteins E6 and E7 which are constitutively expressed in HPV-positive cancer cells and appear to associate with a plethora of host cellular proteins. When expression of either E6 or E7 is extinguished, the cellular senescence program is rapidly executed (Goodwin et al., 2000). This indicates that HPV infected cells are oncogene-addicted so that they need continuous E6 and E7 expression for their proliferation and neoplastic progression, presenting a great potential for molecular treatment options off HPV-related pre(neo)plastic lesions (Manzo-Merino et al., 2013, Hoppe-Seyler et al., 2018).

The E7 protein targets several cellular pathways, with the most prominent target being the tumor suppressor pRB (retinoblastoma protein) leading to dissociation of the E2F1 transcription factor which in turn induces transition from G1 to S phase, ultimately leading to cell cycle progression and replication of the viral genome (Mittal & Banks, 2017). The role of the E6 protein will be explained in more detail in the following chapter.

1.2.4.1.2 Deregulation of E6AP by viral E6 proteins

The interrelation of E6, E6AP and p53 and the following consequences for HPV-infected cells are reviewed in (Scheffner & Whitaker, 2003, Beaudenon & Huibregtse, 2008, Lehoux et al., 2009, Hoppe-Seyler et al., 2018). Briefly, HPV E6 proteins were originally found to stimulate the degradation of p53 (Scheffner et al., 1990). Next, it was shown that a cellular protein mediates association of p53 with the E6 oncoprotein of HPV types 16 or 18 (Huibregtse et al., 1991). Shortly afterwards, it could be shown that E6-associated protein (that is how E6AP received its name) leads in complex with HPV E6 to proteasomal degradation of the tumor suppressor p53 (Huibregtse et al., 1993a, Scheffner et al., 1993). This concerted degradation of p53 and other proteins by the E6-E6AP complex is crucial to by-pass host-cell defenses and to prevent apoptosis, thus presenting a major mechanism of carcinogenesis of infected cells (Howie et al., 2009). The E6-E6AP complex is known to ubiquitinate p53 at several sites by a stepwise mechanism (Masuda et al., 2019).

Several studies showed that stabilization of p53 (or an increase in p53 levels) can be achieved by depletion of the E6 oncoprotein. For instance, it has been shown that inhibition of E6 and E7 expression by expressing the HPV E2 protein via a recombinant virus (Goodwin & DiMaio, 2000) or by transfection (Wells et al., 2000) leads to apoptosis. This means that the malignant phenotype of HPV-positive cancer cells is critically dependent on the expression of the E6 and E7 oncogenes, but is in principle reversible by interfering with their activities (Zanier et al., 2014). In this regard, HPV-positive cells fulfill the criteria for oncogene addiction (Weinstein & Joe, 2008), providing a promising therapeutic approach by the functional inhibition of E6 and/or E7 and, furthermore, the conceptual advantage of no or

reduced side effects on uninfected cells. Especially E6 has emerged as target by different approaches like antisense RNA (BeerRomero et al., 1997), peptide aptamers (Butz et al., 2000), siRNA (Butz et al., 2003, Yamato et al., 2006), or intracellular antibodies (Griffin et al., 2006, Lagrange et al., 2007). Later on, it could be confirmed in a mouse model that E6 requires E6AP to cause cervical cancer (Shai et al., 2010) and that E6 and E7 act synergistically to cause head and neck cancer in mice (Jabbar et al., 2010). All studies emphasize that targeting E6 restores p53 levels and induces consequently cell cycle arrest and/ or apoptosis of HPV-positive cells.

The crystal structure of HPV-16 E6 in complex with the E6-binding α-helix of E6AP revealed a pocket that presents a possible target site for E6 specific inhibitors (Zanier et al., 2013). In a follow-up study including the core domain of p53 in addition to the E6AP α-helix and E6, it was shown that binding of E6AP renders the conformation of E6 competent for interaction with p53 by structuring a p53-binding cleft on E6 (Martinez-Zapien et al., 2016). The structure of the complex should aid in finding small molecules that interfere with E6-p53 complex formation, possibly by rational design of small molecules fitting into the E6AP binding site of E6. All solved structures and functions of E6 and E7 proteins are reviewed in (Suarez & Trave, 2018).

1.2.4.1.3 Small molecule inhibitors of the E6-E6AP complex

The available vaccines (Cervarix® or Gardasil 9®) protect against infection with the most common high-risk HPV types, but they are ineligible to prevent the progression of or to eliminate cervical cancer (Schiffman et al., 2016). Despite several studies which aimed to identify peptides or small molecules that prevent the complex formation of HPV-16 E6 with E6AP and thereby the targeted degradation of p53, no therapeutic treatments are currently available for already infected individuals.

An early approach to inhibit formation of the E6-E6AP complex was the design of α-helical peptides containing the LQELLGE motif critical for binding to E6 with the goal to utilize them in a dominant-negative manner in HPV infected cells(Liu et al., 2004). Two peptides, containing different extensions for stabilization, were created and shown to be stable and correctly folded in aqueous solutions. These peptides showed inhibition of binding of *in vitro* translated S^{35}-labeled HPV-16 E6 to a GST fusion protein of E6AP in pulldown experiments (Liu et al., 2004). A follow-up study used the structure of the α-helical LXXLL motif as pharmacophore for an *in silico* screen, however, identified hits had no or only a low potency in *in vitro* competitive binding assays (Baleja et al., 2006). A new high-throughput binding assay was developed in the same group resulting in the identification of Luteolin, a yellow flavonoid, found in different plants and suggested already for a long time as natural medicine for various cancers and other diseases. In that study, Luteolin and several other flavonoids displayed a high degree of specificity to inhibit proliferation of HPV-positive cells (Cherry et al., 2013). In a follow-up study, the authors derivatized the flavonoid scaffold to several differently 2,6-disubstituted benzopyranones,

which were probed by induced fit modelling to the E6 binding groove of E6AP. The results were also compared to *in vitro* binding assays and cell proliferation experiments. This led to the identification of a group of flexible arginine residues from E6 forming a rim-cap over the helix binding groove that offers a compensatory role in binding and plays a key role in recognition of the small molecule probes (Rietz et al., 2016).

Other studies focused on peptides unrelated to the LXXLL motif containing E6 binding peptide, since the LXXLL containing peptide did not show anti-proliferative effects in HPV-positive cells. Therefore, a yeast two-hybrid screen was performed and different linear peptides that bound E6 were identified (Dymalla et al., 2009). The peptides were further optimized with respect to solubility and shown to occupy the binding pocket of E6 in NMR studies (Zanier et al., 2014). Optimized versions of these peptides inhibited proliferation specifically in HPV-positive cells and were intracellularly shown to bind E6 and to reshape it such that E6 interacts with p53 (Stutz et al., 2015). Giving the proof-of-principle that the E6 binding pocket can be occupied by peptides with sequences other than the LXXLL α-helix and that this blockage leads to p53 accumulation, provides evidence that the E6 binding pocket is druggable. However, peptides are difficult to deliver inside human tissues, so that the identified peptides can be regarded rather as blueprints to identify small molecules with similar properties.

Several studies aimed to identify small molecules acting on E6. A large high-throughput screen (HTS) with over 88,000 compounds yielded 30 validated hits that disrupted binding of an MBP-fusion construct of the LXXLL α-helix to a GST fusion protein of HPV-16 E6 (Malecka et al., 2014). Several hits were validated by p53 stabilization *in vitro* (30 compounds) and in HPV-positive cells compared to HPV-negative cells (7 compounds). One hit was a flavonoid (gossypetin) so that another flavonoid (baicalein) that was not identified in the screen but has a structural similarity to gossypetin even blocked p53 degradation and inhibited proliferation in cells stably transfected with HPV-16 E6 (Malecka et al., 2014). In addition, another study underlines the effect of flavonol and imidazole derivatives to block E6 activities and reactivate pro-apoptotic pathways in HPV-positive cells by screening a 2,000 small molecule containing library and characterizing the two best hits (spinacine and myricetin) by *in vitro* binding and showing that the compounds can sensitize HPV-positive cells to chemotherapeutics (Yuan et al., 2016). Also, a Bristol-Myers Squibb's group performed a phenotypic high-throughput cell culture screen that identified a series of quinoxaline compounds that inhibited proliferation of HPV-transformed cell lines approximately 10-fold stronger than HPV-negative cell lines. Unexpectedly, however, the compounds did not act via the E6 or E7 proteins, but induced apoptosis via the extrinsic, death receptor-mediated pathway (Sheaffer et al., 2016).

Another approach is based on the structural information of the crystal structure of E6 with the bound E6AP α-helical peptide as pharmacophore and to screen *in silico* for small molecules fitting in the binding pocket. A recent, small bioinformatic study did so and modeled binding of a few marine

substances (Dhamodharan et al., 2018). Furthermore, another study developed an *in silico* pipeline to identify small molecule inhibitors of the E6-E6AP complex that was applied to screen a large library. The top three hits were compared with Luteolin in molecular dynamics simulations (Ricci-Lopez et al., 2019).

An alternative approach is to target the E6-p53 interaction interface. One study used the crystal structure of the ternary complex for an *in silico* screen and identified a compound that could restore p53 intracellular levels and transcriptional activity, thus reducing viability and proliferation of HPV-positive cancer cells (Celegato et al., 2019). The compound could even block formation of 3D cervospheres of HPV-positive cells. Mechanistic studies revealed that the anti-tumor activity of this compound mainly relies on induction of cell cycle arrest and senescence (Celegato et al., 2019). A quantitative LumiFluo assay to test inhibitory compounds blocking p53 degradation by HPV E6 in living cells was developed and published by the same group previously (Messa et al., 2018).

Moreover, single compounds were tested, for example a copper anthracenyl-terpyridine complex that induced E6 aggregation thereby stabilizing p53 in HPV-positive cells (Kumar et al., 2018). In line with this, zinc-ejecting compounds have been proposed and successfully tested to destabilize the E6 protein and to lead to apoptosis in HPV-positive cells (Beerheide et al., 1999, Foster & Phelps, 1999). Another study investigated the effect of iron chelating substances with the example of the topical antifungal agent ciclopirox that strongly repressed HPV E6/E7 oncogene expression both at the transcript and protein level (Braun et al., 2019). Moreover, a strong repression of cellular proliferation in both 2D and 3D cell culture and induction of cellular senescence could be achieved (Braun et al., 2019). To note, cells inside cervical tumors seem to fall in dormancy, so that patients need probably to undergo multiple treatments with a drug (Hoppe-Seyler et al., 2017).

Notwithstanding the distinct correlation between induction of apoptosis by targeting E6 in HPV-positive cells and the mentioned substantial efforts to identify and evaluate new compounds, still no drug for HPV-induced cancers was launched on the market, making it indispensable to continue the quest for new lead molecules.

1.2.4.2 E6AP and Angelman syndrome

Angelman syndrome (AS) is a rare neuro-developmental disorder, first described in 1965 by the pediatrician Harry Angelman as 'happy puppet syndrome'. The name originated from the distinctive phenotype and behavior of three affected children which conveyed the association of puppets to him (Angelman, 1965). AS was later named after Angelman and became known as debilitating developmental disorder with virtual absence of speech and jerky movements as the most prominent symptoms (Williams et al., 1995, Williams et al., 2006). AS is clinically further characterized by severe mental retardation, movement and balance anomalies, ataxia, epileptic seizures, sleep disturbances

and abnormal behaviors like excessive laughter and an overall happy demeanor, tongue protrusions and hyperactivity (Bird, 2014, Bindels-de Heus et al., 2019, Khatri & Man, 2019). The incidence of AS is estimated to be between 1 in 10,000 (Petersen et al., 1995), 12,000 (Steffenburg et al., 1996), 15,000 (Clayton-Smith, 1993), 20,000 (Clayton-Smith & Pembrey, 1992, Buckley et al., 1998) or 24,000 (Mertz et al., 2013). As the special needs of AS individuals are so demanding that they are unable to live independently and as the AS symptoms have such a devastating impact on the quality of life of AS-affected individuals and their caregivers, the development of still missing therapeutic approaches is highly desired.

1.2.4.2.1 Role of E6AP in Angelman syndrome

E6AP was originally ascertained to play a key role in AS development through the identification of several heterozygous mutations in the maternal allele of the *UBE3A* gene in different AS individuals (Kishino et al., 1997, Matsuura et al., 1997). Thus, several other genes could be ruled out which were previously also considered as candidate genes since they were as well as the *UBE3A* gene affected by large chromosomal deletion. In addition to single point mutations in the *UBE3A* gene, mutations found in AS patients can either be deletion (Magenis et al., 1987, Pembrey et al., 1989), uniparental disomy (Wagstaff et al., 1992) or imprinting mutations (Reis et al., 1993, Saitoh et al., 1997) of chromosomal region 15q11.2-q13.3. Subsequently, *UBE3A* was identified to be genomically imprinted specifically in the brain, so that only the maternal allele is expressed (Rougeulle et al., 1997, Vu & Hoffman, 1997), while both alleles are expressed in other tissues (Nakao et al., 1994). These findings explained the deleterious effects of the heterozygous gene defects present on the maternal allele, which had already been evident for some time, since improper expression of the maternal allele results in absence of functional E6AP in neurons. To note, the 15q11.2-13.3 region is also associated with the Prader-Willi syndrome, a disorder with certain symptoms related to AS, with affected people showing absence of expression of several genes due to paternal deletion, maternal uniparental disomy or in rare cases due to imprinting defects; E6AP, however, does not play a central role in this disorder (Driscoll et al., 2017). According to distinct gene defects underlying the loss of E6AP function, AS individuals can be subdivided into five classes (Lossie et al., 2001, Clayton-Smith & Laan, 2003) (the following percentages of affected individuals are adopted from (Daily et al., 2012)). In class I, large deletions are found in the 15q11.2-13.3 chromosomal region of the maternal allele. Class I is by far the largest subgroup associated with approximately 70% of the investigated cases. In class II (2 to 3%), paternal uniparental disomy of chromosome 15 results in loss of *UBE3A* expression in neurons, and class III (7 to 9%) is characterized through imprinting defects due to abnormal methylation of certain regions of chromosome 15, also resulting in loss of maternal *UBE3A* expression. Class IV (12-15%) patients have point mutations in the maternal allele of *UBE3A* (Fang et al., 1999, Sadikovic et al., 2014). For most of

the mutations found in AS, a strong correlation with loss of E6AP ubiquitination activity has been discovered (Cooper et al., 2004). A further study showed that the AS phenotype results from a defect in the ubiquitin ligase activity of E6AP and not from a proposed coactivation role of the nuclear hormone receptor superfamily (Nawaz et al., 1999). Missense mutations are distributed all over the *UBE3A* gene (Sadikovic et al., 2014) with clusters located in exon 9 which contains the HECT domain and several other mutations being located in the hinge region between the two lobes of the HECT domain (Cooper et al., 2004, Yi et al., 2015). Finally, patients with no genetic abnormalities identified on chromosome 15 but with Angelman syndrome-like phenotypes are grouped in class V that is increasingly called Angelman-like syndrome. Class V contains either individuals with another syndrome with similar symptoms like AS, mostly caused by microdeletions or microduplications of other chromosomal segments or genes (Tan et al., 2014, Luk, 2016), or cases with genetic defects leading to indirect targeting of E6AP, for example by mutations in the *HERC2* gene, a known interactor and modulator of the catalytic activity of E6AP (Kühnle et al., 2011, Puffenberger et al., 2012, Harlalka et al., 2013, Cubillos-Rojas et al., 2016).

In order to develop a therapy for AS, it is important to gain a comprehensive understanding of the temporal and spatial silencing of *UBE3A* in the brain. Silencing of *UBE3A* is mediated by an extremely long non-coding RNA (named UBE3A-ATS) that is only paternally expressed and overlaps the paternal *UBE3A* gene (Rougeulle et al., 1998). The UBE3A-ATS has a size of ~460 kb and is under the coordinated control of an imprinting center (IC) at the 5' end of the SNURF-SNRPN gene (Runte et al., 2001). Murine Ube3a-ATS is an atypical RNA polymerase II transcript that represses expression of *Ube3a* from the paternal chromosome (Meng et al., 2012), probably due to collision of the two polymerases transcribing *UBE3A* and *UBE3A-ATS*, respectively (Meng et al., 2013).

Early studies found that genomic imprinting of *UBE3A* is restricted to cerebellar Purkinje cells, hippocampal neurons and mitral cells of the olfactory bulb (Lalande & Calciano, 2007) or as described in another study to the hippocampus, hypothalamus, olfactory bulb, cerebral cortex, striatum, thalamus, midbrain, and cerebellum (Gustin et al., 2010) while both alleles are active in glial cells and peripheral tissues (Yamasaki et al., 2003). In contrast, more recent studies showed imprinting also in neural tissues of the spinal cord and sciatic nerve but confirmed no imprinting in oligodendrocytes and astrocytes (Grier et al., 2015).

Similar imprinting in *UBE3A* also exists in rats and mice (Albrecht et al., 1997) also mediated by a paternal Ube3a-ATS that is restricted to the brain (Chamberlain & Brannan, 2001). Several different AS mouse models exist with all of them exhibiting similar symptoms as human AS individuals (Mabb et al., 2011). Two Angelman mouse models, harboring a null mutation in exon 2 (Jiang et al., 1998), or a deletion comprising a part of exon 15 and complete exon 16 of *Ube3a* (coding for the HECT domain of E6AP) (Miura et al., 2002) are the most prevalently used. Much of the state-of-the-art knowledge about

the molecular and biochemical changes in the central nervous system associated with AS has been obtained through these murine models. Additional sophisticated test batteries to evaluate drugs or other approaches to rescue the AS phenotype in mouse models have been established (Sonzogni et al., 2018).

Despite the imprinting defects, it needs to be kept in mind that paternal expression of the *UBE3A* gene is, however, not totally silenced as indicated by E6AP protein detected by western-blot analysis of mice with a knock-out of the maternal *Ube3a* allele (*Ube3a*$^{m-/p+}$) and *post mortem* samples from AS patients (Daily et al., 2012). Moreover, relaxed imprinting of *Ube3a* in neurons of the postnatal developing cortex could be observed, however not in structures with already more complete neurogenesis and migration where more stringent imprinting was observed (Grier et al., 2015). This finding supports the notion that at least certain stages of neuronal development occur also in AS patients under biallelic expression of the *UBE3A* gene, maintaining a relative preservation of *Ube3a* expression during this crucial stage of early development and resulting in a complete development of the brain before birth (Grier et al., 2015). A further study identified persistent expression of E6AP from both alleles in neurons of the suprachiasmatic nucleus, the master circadian pacemaker, highlighting the complexity of *Ube3a* imprinting in the brain (Jones et al., 2016). That the time point during development seems to play a critical role for *UBE3A* imprinting was shown in different *Ube3a*$^{m-/p+}$ mouse model studies revealing that E6AP is expressed during the first one (Judson et al., 2014), two (Sato & Stryker, 2010) or four weeks after birth (Stanurova et al., 2016) from the paternal allele but afterwards its expression is strongly reduced. In line with these results, induced pluripotent stem cells (iPSCs) isolated from human patients displayed late on-set of paternal *UBE3A* silencing (Stanurova et al., 2016). In contrast, a single study demonstrated that genomic imprinting does not reduce the dosage of E6AP in neurons (Hillman et al., 2017). This result argues against a dosage-regulating mechanism that has been widely used to explain why certain genes are imprinted; however no alternative explanation for why the paternal *UBE3A* allele is imprinted was provided in this study.

Besides the mechanism of imprinting, intracellular localization of E6AP protein is also of interest. Investigation of a transgenic mouse model expressing maternally a Ube3a-YFP fusion protein showed that E6AP is *in vivo* intracellularly located in the nucleus as well as in dendrites and that it is in cultured hippocampal neurons located in the nucleus as well as pre- and postsynaptic compartments (Dindot et al., 2008). High-resolution light and electron microscopic immunocytochemistry of E6AP has shown a broad neuronal distribution including both axon terminals and euchromatin-rich nuclear domains (Burette et al., 2017, Burette et al., 2018). Taken all mentioned studies together, E6AP seems to be expressed biallelically for a short period of time in all tissues but afterwards the paternal allele is silenced in all neurons of the CNS but not in peripheral tissues. The efficiency of the silencing is not

quantified in any of the studies, but roughly estimated 5 - 10% of wild-type E6AP may still be present in AS conditions.

1.2.4.2.2 Approaches for AS therapy

To date most treatments focus on alleviating symptoms of AS. Examples are pharmaceuticals to control mood and sleep disorders, which have been partially effective (Clayton-Smith & Laan, 2003), or Levodopa (L-Dopa), which is commonly used to treat Parkinsonian symptoms, proved partially effective in treating late onset movement disorders in a subset of AS patients (Harbord, 2001). However, no drug exists targeting the actual source of AS, the reduced E6AP levels in neurons; however, several studies probed various approaches to interfere with the molecular mechanisms resulting in AS.

The genetic variety underlying AS makes it more demanding to tackle, however for most cases the paternal *UBE3A* allele is still intact so that several recent approaches aim to unsilence the dormant paternal allele (Mabb et al., 2011). Unsilencing was achieved in one approach by indenoisoquinoline-derived topoisomerase inhibitors with topotecan, the most potent compound, showing upregulation of E6AP protein in neurons of AS mice (Huang et al., 2012, Lee et al., 2018). Another strategy was induction of global methylation by dietary supplements (i.e. betaine or folic acid), however, with no significant effects visible in clinical studies (Bacino et al., 2001, Peters et al., 2010, Han et al., 2019). Alternatively, unsilencing was achieved by expression of a truncated UBE3A-ATS that proved to ameliorate behavioral deficits in AS mice (Meng et al., 2013, Meng et al., 2015).

Restoring E6AP expression in general proved to be beneficial as it was shown to suppress epileptic seizures in GABAergic neurons (Gu et al., 2019). In addition, two studies using Cre-dependent temporally controlled induction of the maternal *Ube3a* allele in mice showed that during early development a rescue of the behavioral phenotype was possible and that in adults electrophysiological deficits in layer 5 pyramidal neurons could be extenuated (Silva-Santos et al., 2015, Rotaru et al., 2018). The same group deleted E6AP at three different time points during brain development. They found that only early embryonic deletion and not deletion after 3 or 12 weeks after birth recapitulates all behavioral deficits of AS mice (Sonzogni et al., 2019). The authors concluded that E6AP critically impacts early brain development but plays a more limited role in adulthood. These results suggest that even transient *UBE3A* reinstatement during a critical window of early development is likely to prevent most adverse Angelman syndrome phenotypes (Sonzogni et al., 2019). This means that treatment during the prenatal period could greatly reduce the severity of symptoms or even prevent AS from developing (Zylka, 2019). Besides, inducible pluripotent stem cells (iPSCs) derived from AS patients have allowed researchers to investigate AS in a more human relevant context (Chamberlain et al., 2010). De novo targeting of CGI methylation was used in such iPSCs resulting in normal UBE3A

expression (Takahashi et al., 2017). Moreover, new and highly sensitive non-invasive prenatal tests that take advantage of single-cell genome sequencing technologies are expected to enter the clinic in the coming years. These technologies are sensitive enough to sequence fetal-derived DNA that is circulating in the mother's blood (Zylka, 2019).

Taken together, all mentioned studies underline that restoration of E6AP expression or activity is a feasible approach for AS therapy. However, the presented approaches are not readily applicable as cure for AS due to specificity or delivery issues. Nevertheless, chances exist that low levels of remaining paternally expressed E6AP can be used to restore the physiological duties of E6AP.

1.2.4.3 E6AP and Dup15q syndrome

1.2.4.3.1 Dup15q syndrome - an autism spectrum disorder

Autism spectrum disorders (ASDs) are characterized by decreased communication, impaired social interest, and increased repetitive behavior (Levy et al., 2009). These three core clinical symptoms are often accompanied by developmental comorbidities, like cognitive and intellectual disability, language deficits, attention problems, hyperactivity, and motor delays; furthermore, psychiatric and -related behavioral comorbidities including anxiety, depression, obsessive-compulsive disorder, defiant and aggressive behavior, and self-injurious behavior; moreover other common comorbid features like seizures and epilepsy, gastrointestinal difficulties, and sleep disruption go along with ASDs (Khatri & Man, 2019). Environmental factors such as prenatal exposure to air pollution and short inter-pregnancy intervals have been well-studied to contribute to ASD etiology aside from genetic factors (Lyall et al., 2017). Nowadays, the median worldwide prevalence of autism is 0.62 – 0.70%, although higher estimates of 1 to 2% have been made in the latest large-scale surveys (Lai et al., 2014, Baxter et al., 2015, Lyall et al., 2017). To note, it becomes more and more accepted that high rates of comorbidity across ASD, schizophrenia, intellectual disability and other brain-based disorders exist, and recent studies using chromosomal microarray analysis and whole exome sequencing detected many of the same pathogenic copy number and sequence level variants across cohorts with these different clinical classifications (Finucane et al., 2016). Consequently, the more general term of 'developmental brain dysfunction' has been proposed to encompass disorders arising from impaired neuro-development that can manifest clinically in diverse ways (Mitchell, 2015). For this reason, it must be kept in mind that prevalence numbers of affected people need to be taken with caution, also since ASDs are solely diagnosed based on behavioral criteria. However, also genetic evidence exists for ASD like small genomic DNA copy number variants that are found in 10 to 20% of cases (Morrow et al., 2008, Glessner et al., 2009, Pinto et al., 2010). Among those, maternally inherited duplications and triplications of the 15q11.2-13.3 chromosomal region are the most common and penetrant genomic CNVs observed in

individuals with ASD identified in 1 to 3% of the entirety of affected persons (Glessner et al., 2009, Hogart et al., 2010).

1.2.4.3.2 Role of E6AP in Dup15q syndrome

As the *UBE3A* gene is located on the 15q11.2-13.3 chromosomal region it has become a candidate gene for a subset of ASD cases (Glessner et al., 2009). In the CNVs of the 15q11.2-13.3 chromosomal region is in some cases one additional copy of the maternal allele present through interstitial insertion. This situation is known as dup15q (Browne et al., 1997, Mao et al., 2000, Thomas et al., 2003). In other cases, two additional copies from an extranumerary isodicentric chromosome 15 are present (referred to as idic15). In cases with two maternal gene copies only mild symptoms are present, whereas in cases with three maternal gene copies much more severe phenotypes are observed (Borgatti et al., 2001, Hogart et al., 2010). However, both cases are classified as Dup15q syndrome. Although about 40 genes are located in the affected chromosomal region, overexpression of *UBE3A* gene is thought to be the predominant molecular cause of the phenotypes observed in Dup15q syndrome (Finucane et al., 2016). This has become obvious as one study narrowed down the possible candidate genes to *UBE3A*, since a patient harbored a duplication encompassing only the *UBE3A* gene (Noor et al., 2015). Besides that, another study showed a clear-cut correlation between increase of *UBE3A* and autism traits by introducing two extra copies of *Ube3a* in mice (Smith et al., 2011). These mice showed autism-related behavioral deficits including impaired sociability, diminished conspecific ultrasonic vocalizations and heightened repetitive self-grooming. Moreover, consistent with neuronal imprinting of the *UBE3A* gene known from AS, only maternal but not paternal CNVs have been associated with ASD (Cook et al., 1997). Taken together, genetic analysis associated E6AP with certain subtypes of ASD that are known as Dup15q syndrome.

In addition, another hint that Dup15q syndrome is linked with E6AP is the circumstance that a high percentage of individuals with Angelman syndrome show phenotypes (i.e. impaired communication, absence of speech, attentional deficits, hyperactivity, feeding and sleeping problems, and delay of motor development) with some similarity to symptoms of individuals with Dup15q syndrome (Samaco et al., 2005, Williams et al., 2006, Bonati et al., 2007). The actual mechanism how loss of both function and gain of function result in the same symptoms is, however, not fully elucidated yet. Having said this, a role of several potential E6AP substrates in regulation of synaptic plasticity and function has been suggested, critically depending on the presence of a small window of defined E6AP concentration to maintain physiological function and prevent impaired neuro-development (Vatsa & Jana, 2018).

As mentioned above in this chapter, Smith and coworkers demonstrated that *Ube3a*2x mice (displaying a ~3-fold increase in total E6AP protein) display deficits in glutamate synaptic transmission and consequently autism traits (Smith et al., 2011). A follow-up study identified 190 up- and 408 down-

regulated genes in an affymetrix microarray analysis of total RNA from entire cortices of adult *Ube3a*2x and wild type littermate mice. Pursuing characterization showed that *Cbln1* (the glutamatergic synapse organizer cerebellin-1), one of the genes downregulated by E6AP, is a key node in the expanding protein interaction network of autism genes and is needed for sociability in mice (Krishnan et al., 2017). It must be taken into consideration, however, that Kühnle et al. found that addition of a C-terminal FLAG-tag, which was the case for the utilized mouse model, renders E6AP catalytically inactive, suggesting rather an E6AP dominant-negative effect instead of an overexpression mode of action or effects that are independent of the ubiquitin ligase function of E6AP (Kühnle et al., 2013). Besides, another transgenic mouse model has been created, overexpressing *Ube3a* isoform 2 in excitatory forebrain neurons (Copping et al., 2017). These mice exhibited increased anxiety-like behaviors, learning impairments, and reduced seizure thresholds. However, these mice displayed undisturbed social approach and interactions and no repetitive motor stereotypies, indicating limitations of this model organism (Copping et al., 2017). Iossifov and colleagues identified in a whole exome sequencing study that aimed to identify the contribution of *de novo* coding mutations to autism spectrum disorder an E6AP T485A mutation in a proband (Iossifov et al., 2014). This mutation resulted in hyperactivity of E6AP ubiquitin ligase activity as mentioned above (chapter 1.2.3) (Yi et al., 2015). The authors of this study showed that phosphorylation of threonine 485 by PKA reduced ubiquitin ligase activity. Moreover, activation of PKA by chronic treatment with forskolin or rolipram increased E6AP levels in neurons presumably by reducing its auto-ubiquitination activity. This opens the possibility to interfere with up-stream pathways to regulate the activity of E6AP to finally restore normal enzymatic activity.
As described in this chapter and reviewed in (Lopez et al., 2019), cellular pathways affected by E6AP and the genome-wide impact of alterations in *UBE3A* expression levels are currently investigated to gain deeper insights into how E6AP affects the developing brain and how gain of E6AP function leads to Dup15q syndrome. However, no therapy for Dup15q is available yet, so that small molecule inhibitors of E6AP may open a first avenue for therapeutic intervention.

1.2.4.4 Further pathological conditions associated with E6AP

Apart from the three disorders already discussed, E6AP has been suggested to be associated with additional diseases. For example, E6AP was proposed to drive cancer progression in B-cell lymphoma by degrading PML (promyelocytic leukemia protein) allowing tumor cells to by-pass PML-induced senescence (Wolyniec et al., 2012). Furthermore, a few publications claim a possible tumor-suppressive function of E6AP in breast and prostate cancer and non-small cell lung cancer (Srinivasan & Nawaz, 2011, Levav-Cohen et al., 2012, Ramamoorthy et al., 2012, Birch et al., 2014, Gamell et al., 2017, Gamell et al., 2019). However, one study supporting this connection (Mansour et al., 2016) was retracted recently (Mansour et al., 2019). Nonetheless, E6AP may, in addition to its well-established

role in cervical cancer, AS, and Dup15q syndrome, also be associated with several other viral-induced (like hepatitis C and encephalomyocarditis virus) and non-viral cancers as reviewed in (Bandilovska et al., 2019). Even HIV infection was associated with E6AP in a recent publication (Pyeon et al., 2019). The role of E6AP in the proposed diseases, however, needs to be investigated in more detail. This will possibly expand our knowledge of the physiological role of E6AP in proteostasis in general and potentially represents further applications for small molecule modulators of E6AP.

1.3 Small molecule modulation of ubiquitin ligase activity

The ubiquitin system plays a key role in proteostasis and its malfunction has hence been tightly linked to various diseases like neurodegenerative diseases including Alzheimer's disease, Huntington's disease and amyotrophic lateral sclerosis as well as neuronal disorders like ataxia (Hegde & Upadhya, 2011, George et al., 2018) and numerous types of cancers (Hoeller et al., 2006, Wang et al., 2017a, Ong & Torres, 2019). To develop therapies for diseases associated with the ubiquitin system, E3 ubiquitin ligases are the most selective components and should be preferred as targets over E1 or E2 enzymes or the proteasome in order to reduce side-effects (Landre et al., 2014, Zhang & Sidhu, 2014). Despite the multitude of connections between E3 ubiquitin ligases and health and disease, to date, not many small molecule modulators of E3 ubiquitin ligases have been identified. Moreover, the ubiquitination system is ill-reputed as being undruggable (Huang & Dixit, 2016). Nonetheless, E6AP is a key player in cervical cancer, AS and Dup15q syndrome. Hence, it is of fundamental interest to identify approaches to interfere with malfunction of E6AP. One often applied strategy to alter an enzyme's activity are small molecules. The following chapters will summarize strategies to identify such small molecules acting on E3 ligases developed by others. Also, examples of identified small molecule modulators will be given. Finally, fluorescence polarization, the method applied to develop a novel ubiquitination assay in the present study, will be introduced.

1.3.1 HTS methods to identify small molecule modulators of E3 ligases

A major bottleneck for the identification of compounds acting on E3 ligases is the lack of simple and robust assays to determine the effect of small molecules on the ubiquitin ligase activity of the E3 ligase of interest. One reason for this is the complexity of the ubiquitination cascade consisting of three consecutive steps performed by three different classes of enzymes (see chapter 1.1.2). Furthermore, the speed of the ubiquitination reaction makes it difficult to be recorded (Pierce et al., 2009, Melvin et al., 2013). In addition, the outcome of ubiquitination reactions is difficult to monitor. In former days, laborious and in an HTS format error-prone SDS-PAGE analyses or detection of ubiquitin chains by special reagents coupled to antibodies were commonly utilized, making real-time monitoring and high-

throughput screenings rather unfeasible. More recently, several assays with different underlying detection methods were developed to identify small molecules modulating the activity of distinct E3 ligases (Landre et al., 2014).

One feature of the ubiquitination reaction is that ubiquitin is covalently attached to the substrate for which ubiquitin and the substrate have to come into close proximity. Two different methods to determine proximity have been applied for the ubiquitination reaction, namely FRET and AlphaScreen technology. FRET assays were already developed 20 years ago. As a proof of principle, a rather complex assay design was conceptualized: europium-labeled anti-GST antibody bound to GST-tagged RSC (serving as substrate) that was modified under ubiquitination conditions with biotinylated ubiquitin; upon ubiquitination, APC-strepavidin was bound to the biotinylated ubiquitin. Bringing europium and APC in proximity resulted in FRET enabling real-time monitoring of the ubiquitination reaction (Boisclair et al., 2000). A similar HTS FRET assay was developed for p53 ubiquitination (Murray et al., 2007). An advance was the development of a ubiquitin chain assembly assay by labeling ubiquitin with a FRET donor and another ubiquitin with a corresponding FRET acceptor, so that ubiquitin chain formation could be monitored (Hong et al., 2003, Gururaja et al., 2005). This assay design has the advantage that it can be used for all different types of E3 ligases and deubiquitinating enzymes. More recently, a commercial company (SouthBayBio) started selling kits for time resolved FRET with ubiquitin FRET donors and ubiquitin FRET acceptors. Furthermore, AlphaScreen technology was used to identify inhibitors of E6-E6AP (Sehr et al., 2007) and of E6AP only (Street et al., 2012) resulting in multiple hits. However, both screens were not followed up nor yielded an established inhibitor so far. An alternative assay principle was used to identify inhibitors of HUWE1 (Peter et al., 2014). The biotinylated HECT domain of HUWE1 was captured on streptavidin-coated plates and incubated under ubiquitination conditions with MYC-tagged ubiquitin. After washing, europium-labeled anti-MYC antibodies were added to detect MYC-tagged ubiquitin used for auto-ubiquitination and being thus still present in the wells after washing (Peter et al., 2014). This method has, besides the rather complex ELISA-like capturing method with the need for tagging ubiquitin as well as the target protein and the expensive antibody conjugates, the drawback of error-prone washing steps. Another study used glutathione-coated paramagnetic beads to capture GST-tagged HDM2 with which *in vitro* ubiquitination assays were performed (Davydov et al., 2004). Afterwards, an ORIGEN-tagged antibody against ubiquitin was added and electro-chemiluminescence signals were measured. This assay was used in an HTS to identify inhibitors of HDM2 auto-ubiquitination (Yang et al., 2005). The identified inhibitors were later further developed and shown to bind to the RING domain of HDM2 and thus prevented p53 ubiquitination (Roxburgh et al., 2012).

With advancing technologies new methods surfaced, as seen for a fluorescent confocal on-bead microscopy assay (Koszela et al., 2018) or a MALDI-TOF *in cellula* ubiquitination assay (De Cesare et al.,

2018), which were however not applied to screen for small molecules so far. Additionally, an assay was developed with ubiquitin traps to capture ubiquitinated species from cell lysates that were then quantified by AlphaLISA or DELFIA (Mata-Cantero et al., 2015). Another cell-based HTS assay based on a ubiquitin-reference technique was utilized to test a 5,000 compounds library for SMURF1 inhibitors (Tian et al., 2019). Most of the described assays were revealed to be prone to identify false-positives due to effects on the level of the E1 and E2 enzymes, so that Krist et al. developed a by-passing system with chemically activated ubiquitin that can be directly used by the tested HECT ubiquitin ligase thereby bypassing the enzymatic cascade (Krist et al., 2016). This method can also be applied to screen for small molecule inhibitors of RBR ubiquitin ligases as shown for PARKIN (Park et al., 2017). However, interference of the assay by reaction of the chemically modified ubiquitin with reactive compounds and altered modes of interaction of the modified ubiquitin with the E3 ligases due to the modification or the absence of cognate E2 enzymes are possible limitations of the method.

Although the outlined methods to monitor ubiquitination in a high-throughput format are available, none of them has been established in the scientific research community (*i.e.* they have not been used by other laboratories), so that there is still a major demand for novel, robust, and broadly transferable HTS assays.

1.3.2 Reported small molecule modulators of E3 ligases

Ubiquitin ligases, and especially HECT ligases, share certain features, so that information about small molecules, their identification and characterization process can possibly be transferred to E6AP.

Considerable progress in identification of small molecule inhibitors of RING ubiquitin ligases has been made. Examples are Siah1/2 inhibitors which proved to have activity in melanoma and prostate cancer cells (Feng et al., 2019), inhibitors for HDM2/HDMX (Herman et al., 2011), and inhibitors for RNF5 that could rescue expression levels of F508del-CFTR in cystic fibrosis airway epithelia (Sondo et al., 2018). Additionally, several inhibitors were identified for SCF RING ubiquitin ligase complexes and VHL, the substrate recognition component of a ubiquitin ligase complex, as well as inhibitors specific HDM2-mediated ubiquitination of p53 (e.g. nutlins). These compounds are summarized in (Nalepa et al., 2006, Buckley & Crews, 2014, Bielskiene et al., 2015). In addition, gliotoxin was identified in an HTS that reduced signal-induced NF-κB activation by selectively inhibiting LUBAC-mediated linear ubiquitin chain formation (Sakamoto et al., 2015).

In contrast to RING ubiquitin ligases, only few inhibitors of HECT ubiquitin ligases have been reported (Chen et al., 2018). Mund and coworkers were the first to describe HECT ligase inhibitors (Mund et al., 2014). They isolated bicyclic peptides that targeted the E2 binding sites on the HECT domains of SMURF2, NEDD4, HUWE1, and WWP1 by phage display, and thus act as specific inhibitors of the E2-E3 interaction. Next, they screened for displacement of one of these peptides from the SMURF2 HECT

domain by small molecules and thereby identified a compound called Heclin that inhibited several HECT ligases in tissue culture cells. *In vitro* experiments showed that heclin, however, does not block E2 binding but causes a conformational change that results in oxidation of the active site cysteine. Although the mechanism of action is inconclusive, this demonstrated that HECT domains are potentially druggable (Mund et al., 2014). Moreover, indole-3-cabinol (I3C) was found to interact with NEDD4 and to inhibit NEDD4-mediated PTEN degradation (Aronchik et al., 2014). To overcome disadvantages of I3C such as low affinity and chemical instability, derivatives were generated and tested with 1-benzyl-I3C being the most potent one, with inhibition of NEDD4 auto-ubiquitination and inhibition of melanoma cell proliferation in the low micromolar range(Quirit et al., 2017). Hence, I3C derivatives have been proposed as novel set of anti-cancer compounds for treatment of human melanomas and other cancers. Furthermore, a small molecule was identified that could switch NEDD4-mediated ubiquitination from a processive to a distributive enzymatic mechanism (Kathman et al., 2015). Two small molecule inhibitors for HUWE1 were identified that showed great potency and selectivity in *in vitro* assays but were not suited for *in vivo* applications due to unfavorable pharmacokinetic properties (Peter et al., 2014). Other studies identified inhibitors of the HECT ligase SMURF1 (Cao et al., 2014, Zhang et al., 2017), and 1,4-Naphthoquinones were identified as inhibitors of the HECT ligase ITCH (Liu et al., 2017b). Moreover, clomipramine was identified in another HTS study to inhibit ITCH and several other HECT ligases including E6AP in *in vitro* assays (Rossi et al., 2014). Furthermore, natural product-like macrocyclic N-methyl-peptide inhibitors against E6AP were uncovered from a ribosome-expressed *de novo* library (Yamagishi et al., 2011). However, the effect of E6AP inhibitors is quite modest or not specific. More than anything, no small molecule activators of E3 ubiquitin ligases have been identified, despite the fact that in particular HECT and RBR ubiquitin ligases can be activated as they are present in an auto-inhibited state that can be released in different ways.

1.3.3 Fluorescence polarization as readout for ubiquitination

Fluorescence polarization (FP) is an in-solution, biophysical method that can be used to monitor changes of the molecular weight of an investigated molecule (Lakowicz, 2006). FP can detect covalent as well as non-covalent binding or respective release of the investigated molecule to other molecules. FP has been widely used in HTS to identify small molecules interfering with binding or the enzymatic function of the investigated protein (Lea & Simeonov, 2011, Du, 2015, Hall et al., 2016, Kim et al., 2017, Rinken et al., 2018). To be able to measure FP a fluorophore needs to be attached to the investigated molecule. This fluorophore is excited with linearly polarized light. After a specific time (called fluorescence lifetime of the fluorophore) light is emitted again with an altered wavelength. The orientation of the fluorophore may have changed substantially in that time if attached to a small molecule but remained mostly unchanged if bound to a large molecule or complex of several

molecules. As readout, the emitted light is measured with two detectors, one with a polarization filter with the same orientation as the excitation filter (F_I) and the other with a perpendicular orientated filter ($F_\perp$). FP can be calculated from these values according to equation $FP = (F_I - F_\perp)/(F_I + F_\perp)$. Consequently, low values indicate attachment of the fluorophore to smaller molecules while high FP values indicate conjugation to larger molecules.

In the ubiquitin field, FP was mainly used so far to investigate non-covalent interactions of fluorophore-labeled ubiquitin with different ubiquitin-interacting proteins (Maspero et al., 2011). An example for such an application are competition assays to monitor interaction of ubiquitin binders to different ubiquitin chains (Clerici et al., 2014, Du & Strieter, 2018). Another application of FP in the ubiquitin field is C-terminally fluorophore-tagged ubiquitin to determine the activity of deubiquitinating enzymes (DUBs). DUBs cleave off the fluorophore resulting in a strong decrease of FP values (Tirat et al., 2005, Geurink et al., 2012). Another application is a ubiquitin variant to which a fluorophore is C-terminally attached via a thiol-reactive bond. This reactive probe can be utilized to measure HECT or RBR ligase activity in an assay in the absence of E1 or E2 enzymes (Krist et al., 2016, Park et al., 2017). Finally, fluorophore-labeled ubiquitin was used to monitor formation of free ubiquitin chains (von Delbruck et al., 2016) or substrate ubiquitination (Mot et al., 2018). However, FP of fluorophore-labeled ubiquitin was so far not used to study enzymatic activities of E3 enzymes in a high-throughput manner and it was not used to identify small molecule modulators of such enzymes. Consequently, the development of an HTS assay that takes advantage of the large differences in FP values between free ubiquitin and products of ubiquitination reactions as readout would be an advance for ubiquitin research.

2 Aims of the study

Nowadays, vaccines can protect against infection with the most common types of human papillomaviruses and can thus prevent formation of cervical and other HPV-related cancers. However, harsh and unspecific procedures like surgery, chemotherapy or radiotherapy are still the only treatment option for infected individuals that already developed tumors. The reason for this is that, despite considerable research efforts, no drug against cervical and other HPV-related cancer has been released yet. Complex formation of the viral E6 protein with the human ubiquitin ligase E6AP plays a key role in HPV-induced cancer formation. This complex formation leads to the activation of E6AP as well as to an altered substrate spectrum of E6AP, resulting ultimately in p53 degradation, a main mechanism of HPV-induced carcinogenesis. Several studies confirmed that disruption of the E6-E6AP complex is sufficient to induce apoptosis of infected cells. Inhibition of the E6-E6AP complex represents thus a promising approach for therapeutic intervention. Therefore, this work aimed to identify small molecules that inhibit the E3 activity of the E6-E6AP complex and thus could serve as lead structures for the development of therapeutics for HPV-related cancers.

Since activation of E6AP by HPV-16 E6 is one of the consequences of E6-E6AP complex formation, ubiquitin ligase activity can be used as read-out for complex formation and in turn also for inhibition of the complex by small molecules. However, robust and easy to use *in vitro* methods to monitor ubiquitination reactions in a high-throughput format are lacking. Therefore, to identify inhibitors of the E6-E6AP complex, a method had first to be developed that can be applied in the setting of a high-throughput screen.

In addition, loss of function of E6AP underlies the rare neuro-developmental disorder Angelman syndrome. As E6AP can be activated by HERC2 or HPV-16 E6, it should be possible to activate E6AP by small molecules. In fact, compounds with stimulating effects on the catalytic activity of E6AP may represent a novel approach to treat individuals with Angelman syndrome, for which no therapy is available yet. Therefore, another aim of this study was to apply the newly developed ubiquitination assay in a second high-throughput screen to identify small molecule activators of E6AP. Such compounds may eventually serve as lead structures for the development of drugs for the Angelman syndrome. Moreover, investigation of their mode of action on E6AP should help to gain a deeper understanding how E6AP functions mechanistically and how its activity is regulated.

3 Material and Methods

3.1 Material

Chemical	Manufacturer
4'OH-Tamoxifen (Cat#H6278)	Sigma-Aldrich
4,4,5,5-deuterated lysine	Cambridge Isotope Laboratories
^{13}C6/^{15}N4-labeled arginine	Cambridge Isotope Laboratories
Acetic acid	Sigma-Aldrich
Acriflavin (Cat#A8126)	Sigma-Aldrich
Acrylamide/Bisacrylamide solution 37.5%	Serva Electrophoresis
Alloxazine (Cat#A28651)	Sigma-Aldrich
Ampicillin	Carl Roth
Aprotinin (Cat#A162)	Carl Roth
ATP (sodium salt)	Sigma-Aldrich
Chloramphenicol	Carl Roth
Chloroacetamide	Sigma-Aldrich
Coomassie brilliant blue R250	Carl Roth
DMSO (gaschromatography grade)	Merck
DpnI (Cat#R0176)	NEB
DSS-H12/D12 (Disuccinimidyl suberate) (Cat#001S)	Creative Molecules
DTT (Dithiothreitol)	Carl Roth
E/Z view anti-HA agarose beads (Cat#E6779)	Sigma-Aldrich
Endoxifen (Cat#E8284)	Sigma-Aldrich
Gentamycin (10,000 U/ml)	Carl Roth
Glutathione, reduced	Sigma-Aldrich
Glutathione Sepharose 4 Fast Flow	GE Healthcare
Glycerol	Carl Roth
Heclin	Sigma-Aldrich
Imidazole	Carl Roth
IPTG (Isopropyl-thio-β-D-galacto-pyranoside)	Carl Roth
Kanamycin	Carl Roth
LB (Luria Broth)	Carl Roth

Leupeptin (Cat#CN33)	Sigma-Aldrich
Lipofectamine 2000	ThermoFisher
Luteolin (Cat#ALX-385-007)	Enzo Life-Sciences
Methanol	Sigma-Aldrich
$MgCl_2$ (Magnesiumchloride)	Carl Roth
MTT	Sigma-Aldrich
NaCl (Sodiumchloride)	Carl Roth
NaOAc	Carl Roth
NH_4OAc (Ammoniumacetate)	Sigma-Aldrich
Nickel-NTA beads	QIAGEN
OF100 - OF124	see appendix table I
OF201 - OF238	see appendix table II
PBS (Phosphate buffered saline)	Life Technologies
Pefabloc (Cat#154)	Carl Roth
Pen/Strep (10,000 U/mL Penicillin, 10,000 µg/mL Streptomycin)	Gibco
PFU Turbo polymerase (Cat#600250)	Agilent
Q-Sepharose beads	GE Healthcare
Raloxifen	Sigma-Aldrich
S^{35}-methionine	PerkinElmer
SDS (Sodiumdodecylsulfate)	Carl Roth
Tamoxifen (Cat#5648)	Sigma-Aldrich
TAMRA-NHS (SE, 5-and-6-isomer) (Cat#C1171)	Life Technologies
TEMED (N,N,N',N'-Tetramethylethylendiamine)	Carl Roth
Triton X-100	Carl Roth
Trizma®Base	Sigma-Aldrich
Trypsin (Cat#V511C)	Promega
Tryptone	Carl Roth
Tyrphostin 47 (Cat# BML-EI188-0005)	Enzo Life Sciences
Ubiquitin from bovine erythrocytes (Cat#U6352)	Sigma-Aldrich
HCCA (α-Cyano-4-hydroxycinnamic acid)	Sigma-Aldrich
β-Mercaptoethanol	Merck
Crystal violet	Serva

Compound library	**Manufacturer**
Maybridge HitFinder™ Collection	Thermo Fisher Scientific, Waltham, MA, USA
Screen-Well® ICCB known Bioactives Library	Enzo Life Sciences, Lörrach, Germany
AnalytiCon Discovery	AnalytiCon Discovery GmbH, Potsdam, Germany
NATx semi-synthetic screening compounds	AnalytiCon Discovery GmbH, Potsdam, Germany
ChemDiv	ChemDiv, San Diego, CA, USA
ChemBioNet 1-4	ChemBioNet, Germany
In-house synthetic compound library (MDB library)	Screening facility, University of Konstanz

Kit	**Manufacturer**
Bac-to-Bac®	Invitrogen
PureYield Plasmid Midiprep	Promega
Pierce BCA Protein Assay	Life technologies
High-molecular weight calibration for SEC	GE Healthcare
T7-coupled TNT *in vitro* translation system	Promega

Buffers and solutions	**Composition or supplier**
$T_{25}N_{50}$	25 mM Tris-HCl pH 7.5, 50 mM NaCl
2x Laemmli SDS-PAGE sample buffer	125 mM Tris-HCl (pH 6.8), 200 mM DTT, 4% SDS, 0.001% Bromphenol blue
5x Laemmli SDS-PAGE sample buffer	312.5 mM Tris-HCl (pH 6.8), 500 mM DTT, 10% SDS, 0.001% Bromphenol blue
Colloidal Coomassie staining solution	Carl Roth
Coomassie staining solution	2 g/L Coomassie brilliant blue solved in 50% MilliQ, 40% methanol, 10% acetic acid
Destain solution	50% MilliQ, 40% methanol, 10% acetic acid
Laemmli SDS-PAGE running buffer	25 mM Tris-HCl (pH 8.4), 200 mM glycine, 0.1% (w/v) SDS
Lightning Autoradiography Enhancer	PerkinElmer
ONPG	4 mg/mL in 100 mM Na_2HPO_4 (pH 7.0)
Puffer Z	100 mM Na_2HPO_4/NaH_2PO_4 (pH 7.0), 10 mM KCl, 1 mM $MgSO_4$, 50 mM β−Mercaptoethanol
Roti-Block solution	Carl Roth
SDS-PAGE separating gel buffer	1.5 M Tris-HCl pH 8.8, 0.4% SDS

SDS-PAGE stacking gel buffer	0.5 M Tris-HCl pH 6.8, 0.4% SDS, 0.0001% Bromophenol blue
TNE-T	50 mM Tris-HCl (pH 7.6), 50 mM NaCl, 2.5 mM EDTA, 0.1% (v/v) Tween 20
TNN buffer	100 mM Tris-HCl pH 8, 100 mM NaCl, 1% NP40, 1 µg/mL A/L, 100 µM Pefabloc, 1 mM DTT
WB detection reagent	ThermoScientific
WB transfer buffer	12.5 mM Tris-HCl (pH 8.3), 100 mM glycine

Protein and DNA marker	**Supplier**
Unstained Protein Ladder (Cat#26614)	Thermo Scientific
Prestained Protein Ladder (Cat#26616)	Thermo Scientific
1 kb Plus DNA Ladder (Cat#SM1331)	Thermo Scientific

Antibody	**Species**	**Dilution**	**Supplier**
HA.11 (Clone 16B12)	mouse	1:2500	BioLegend Covance
E6AP	rabbit	1:500	AG Scheffner
HRP-coupled α-mouse	goat	1:30,000	Dianova
HRP-coupled α-rabbit	goat	1:30,000	Dianova

Media	**Supplier**
SOC (20 g/l tryptone, 5 g/l yeast extract, 0.5 g/l NaCl, 20 mM glucose)	Carl Roth
LB (10 g/l NaCl, 5 g/l yeast extract, 10 g/l tryptone (pH 7.5))	Carl Roth
DMEM (4.5 g/L D-Glucose, L-Glutamine, pyruvate free)	Gibco
OptiMEM	Gibco
FCS	Biochrome AG

Bacterial cells	**Strain**
E. coli BL21 (DE3)	F-*ompT gal lon hsdS*$_B$ (rB- mB-) λ(DE3 [lacI lacUV5-T7 gene 1 ind1 sam7 nin5])

E. coli BL21 (DE3) Rosetta 2	F^- *ompT hsdS*$_B$ (r_B^- m_B^-) *gal dcm* (DE3) pLysSRARE (Cam^R)
E. coli BL21 (DE3) ril	F^-*ompT hsdS*$_B$ (r_B^- m_B^-) *dcm*$^+$ Tetrgal λ(DE3) endA *Hte* [argU ileY leuWCam^r]
E. coli BL21 (DE3) pLysS	F–, *omp*T, *hsd*S$_B$ (r_B–, m_B–), *dcm*, *gal*, λ(DE3), pLysS, Cm^r
E. coli DH5 α	F- endA1 glnV44 thi-1 recA1 relA1 gyrA96 deoR nupG purB20 ϕ80dlacZΔM15 Δ(lacZYA-argF) U169, hsdR17(rK- mK+), λ–
E. coli XL-10 gold	Tet^{r}delta- (*mcrA)183 delta- (mcrCB-hsdSMR-mrr)173 endA1 supE44 thi-1 recA1 gyrA96 relA1 lac* Hte [F′ *proAB lacI*^{q}*ZDM15* Tn*10* (Tet^r) Amy Cam^r]

Eukaryotic cells	**Description**
High Five (BTI-Tn-5B1-4)	Insect cell line isolated from *Trichoplusia ni*
HeLa	Human cervical cancer cell line
H1299	Human non-small cell lung carcinoma cell line
H1299 K3	Single clonal E6AP knockdown (siRNA mediated) cell line derived from H1299 cells created in AG Scheffner (Kuballa et al., 2007)
H1299 E6AP 1C3	CRISPR-Cas mediated E6AP knockout cell line (clone 1C3) derived from H1299 cells created in AG Scheffner (Schroff, 2017)

Equipment	**Manufacturer**
384 well plate, PS, non-binding, black, flat bottom	Greiner BIO-ONE
96 well plates transparent, flat bottom	Sarstedt
Cell culture dishes	Sarstedt
ÄKTA UPC-900 series	Amersham Biosciences
Dialysis membrane (MWCO 12,000 to 14,000 Da)	Carl Roth
FLA-5000 gel scanner	Fujifilm

Freedom Evo (HTS workstation)	Tecan
Gravity-flow column (10 mL)	Bio-Rad
Heraeus B6 Microbial incubator	Thermo Scientific
HisTrap™ FF crude 5 mL	GE Healthcare
HiTrap™ Q HP 1 mL	GE Healthcare
HiTrap™ SP HP 1 mL	GE Healthcare
VICTOR multilabel plate reader	PerkinElmer
Infinite F500 plate reader	Tecan
LAS-3000 imaging system	Fujifilm
BAS MS-2040 imaging plate	Fujifilm
MicroFlex MALDI-TOF instrument	Bruker
Sorvall RC6 Plus	Thermo Scientific
VaCo2-II (Lyophilizer)	Zirbus technology
0.22 µm syringe filter, CME membrane, sterile	Carl Roth
Amicon (ultra centrifugal units)	Merck-Millipore
Amersham Hybond PVDF membrane 0.22 µm	GE Healthcare
COUNTess automated cell counter	Thermo Fisher
VIAFLO electronic pipettes	Integra

Software	**Company**
AIDA image analysis software	Elysia-Raytest
Prism 6	GraphPad
KNIME 4.1.0	KNIME AG (Berthold et al., 2008)
Clone Manager 9	Sci-Ed software
UCSF Chimera 1.14	UCSF (Pettersen et al., 2004)

3.2 Methods

3.2.1 Cell culture

3.2.1.1 Bacterial cell culture

Bacterial cells were incubated at 37°C and 180 rpm shaking in liquid Luria broth (LB) medium containing appropriate antibiotics in the following concentrations: Ampicillin (50 mg/L), Kanamycin (12.5 mg/L), Chloramphenicol (34 mg/L).

3.2.1.2 Insect cell culture

High Five insect cells (BTI-TN-5B1-4) were grown in 10 cm cell culture dishes at 26 to 28°C. Cells were split in a 1 to 5 ratio every 2 to 3 days in serum free insect medium (TC-100 insect medium supplemented with 10% FCS and 50 mg/L Gentamycin). For E1 and E6AP expression cells were transfected with recombinant baculovirus generated previously with the Bac-to-Bac® kit (Life technologies).

3.2.1.3 Mammalian cell culture

Mammalian cells were cultivated in 10 cm cell culture dishes at 37°C, 95% humidity and 5% CO_2 in 4.5 g/L D-Glucose, L-Glutamine, pyruvate free DMEM (Dulbecco's Modified Eagle Medium) supplemented with 10% FCS and 1:100 Pen/Strep solution.

For longtime storage mammalian cells were washed with PBS, trypsinated with 2 mL Trypsin-EDTA (0.05%) and washed again with 10 mL cell culture media. Cells were resuspended in 2 mL sterile FCS supplemented with 10% DMSO and cells were slowly frozen in an isopropanol bath at - 80°C before they were transferred into a liquid nitrogen tank. To cultivate them again, cells were thawed at room temperature, washed with cell culture media and resuspended in 10 mL cell culture media.

3.2.2 Recombinant gene expression

3.2.2.1 Site-directed mutagenesis

To introduce point-mutations into a gene PCR based Quik-change site-directed mutagenesis was carried out with overlapping primers harboring the desired nucleotide mutation and PFU Turbo polymerase. Subsequent DpnI digest of template DNA was performed according to the manufacturer's instructions (NEB) prior to transformation in super-competent *E. coli* XL-10 gold cells.

3.2.2.2 Transformation of chemically competent E. coli cells

An aliquot of 100 µL of chemically competent *E. coli* cells were thawed on ice, mixed with 10 ng plasmid DNA and incubated for 30 min on ice. For transformation a 90 seconds heat-shock at 42°C and 2 min incubation on ice followed. Bacteria transformed with plasmids with Kanamycin selection marker were resuspended in 500 µL SOC medium and incubated for 1 h at 37°C prior to transfer to agar plates containing LB plus appropriate antibiotics.

3.2.2.3 Preparation of plasmid DNA and sequencing procedure

Plasmid DNA was purified using the PureYield Plasmid Midiprep kit (Promega) according to the manufacturer's instructions. Purified DNA was sequenced by GATC (Konstanz) with an ABI 3730XL DNA analyzer. For sample preparation 5 µL plasmid DNA (100 ng/µL) were mixed with 5 µL of the respective primer (5 µM).

3.2.3 Gene expression and protein purification

3.2.3.1 Production of UbLIA

UbLIA was expressed in *E. coli* BL21 (DE3) cells. After induction with 500 µM IPTG at OD_{600} of about 0.6 cells were cultured at 37°C for 5 h. Pellets from 1 L bacterial culture were resuspended in 20 mL $T_{25}N_{50}$ containing 1 µg/mL Aprotinin, 1 µg/mL Leupeptin and 100 µM Pefabloc. The solution was sonicated and centrifuged for 15 min at 4°C and 30,000 x g. The supernatant was heated up to 70°C for 20 min and afterwards centrifuged with 30,000 x g. The supernatant was additionally purified via ion-exchange chromatography using a 1 mL HiTrap SP HP column and size exclusion chromatography using a HiLoad 26/60 Superdex75 prep grade column with an ÄKTA FPLC system.

3.2.3.2 Production of E1 enzyme

For E1 (UBA1) expression, confluent High Five insect cells were resuspended and plated to 60% confluency. After 90 min, media was exchanged and 200 µL E1 baculovirus stock solution was added to each plate. After 44 h incubation at 27°C, cells were harvested and washed with PBS. Next, they were resuspended in TNN cell lysis buffer and incubated on ice for 90 min. 1 mL Q-Sepharose beads for each 10 plates was loaded on a gravity-flow column and equilibrated with 20 mL $T_{25}N_{125}$ (pH 7.4). The protein solution was cleared by centrifugation (20 min, 4°C, 30,000 x g) and the supernatant was loaded on the beads. Next, the beads were washed with 25 mL $T_{25}N_{125}$ and E1 was eluted in 1 mL fractions with elution buffer ($T_{25}N_{300}$, 1 µg/mL Aprotinin and Leupeptin, 100 µM Pefabloc, 1 mM DTT, pH 7.4). Fractions containing E1 were pooled and diluted with $T_{25}N_{25}$ containing 1 mM DTT (pH 7.4), and protein was stored in aliquots at - 80°C.

3.2.3.3 Production of E2 enzymes

C-terminal His-tagged UbcH5b and UbcH7 was expressed in *E. coli* BL21 (DE3) cells. After induction with 500 µM IPTG at OD_{600} of about 0.6 cells were cultured at 37°C for 5 h. Pellets from 500 mL bacterial culture were resuspended in 10 mL lysis buffer (PBS, 1% Triton X-100, 10 mM imidazole, 1 mM DTT, 1 µg/mL Aprotinin and Leupeptin, 100 µM Pefabloc). After 10 min incubation on ice, cells were sonicated and centrifuged (15 min, 30,000 x g, 4°C). The supernatant was incubated with 1 mL, with lysis buffer pre-equilibrated, Ni-NTA beads. After 1 h to overnight incubation at 4°C, beads were spun down, washed first with 15 mL wash buffer 1 (PBS, 0.1% Triton X-100) and then with 20 mL wash buffer 2 (PBS, 0.1% Triton X-100, 1 mM DTT, 50 mM imidazole). Afterwards, beads were resuspended in 10 mL wash buffer 3 ($T_{25}N_{300}$, 0.1% Triton X-100, 1 mM DTT, 50 mM imidazole, pH 7.5) and loaded onto a gravity-flow column. Beads were washed with 10 mL wash buffer 3 and eluted six times with 1 mL elution buffer ($T_{25}N_{300}$, 1 mM DTT, 250 mM imidazole, 1 µg/mL Aprotinin and Leupeptin, 100 µM Pefabloc, pH 7.5). United fractions containing E2 enzyme were dialyzed against 2 L of dialysis buffer ($T_{25}N_{300}$, 0.2 mM DTT, 5% glycerol, pH 7.5). The dialyzed protein solution was diluted with storage buffer ($T_{25}N_{100}$, 5% glycerol, 1 mM DTT, 1 µg/mL Aprotinin and Leupeptin, 100 µM Pefabloc, pH 7.5) to 100 ng/µL and stored in aliquots at - 80°C.

3.2.3.4 Production of E6AP

N-terminal His-tagged E6AP as well as point or truncation mutants thereof were expressed in *E. coli* Rosetta2 (DE3) cells. After induction with 500 µM IPTG at OD_{600} of about 0.6 cells were cultured at 20°C overnight. Pellets from 1 L bacterial culture were resuspended in 50 mL lysis buffer ($T_{25}N_{50}$, 0.1% Triton-X-100, 1 mM DTT, 1 µg/mL Aprotinin and Leupeptin, 100 µM Pefabloc, pH 7.5), sonicated and centrifuged (30,000 x g, 4°C, 15 min). The supernatant was first purified via Nickel-NTA chromatography (5 mL HisTrap FF crude column) with 8 CV 4% buffer B followed by a gradient to 100% buffer B in 20 CV with buffer A ($T_{25}N_{50}$, 1 mM DTT, pH 7.5) and buffer B ($T_{25}N_{50}$, 1 mM DTT, 500 mM imidazole, pH 7.5). Fractions containing E6AP were united and subjected to a second purification step via anion-exchange chromatography (1 mL HiTrap Q HP column), with a gradient from 0 to 50% buffer B in 20 CV with buffer A ($T_{25}N_{50}$, 1 mM DTT, pH 7.5) and buffer B ($T_{25}N_{1000}$, 1 mM DTT, pH 7.5). Elution fractions containing E6AP were united and subjected to buffer exchange ($T_{25}N_{50}$, 1 mM DTT, pH 7.5) with 4 mL Amicon Ultra Centrifugal Units with a cut-off of 30 kDa. Concentration was adjusted to 100 ng/µL in storage buffer ($T_{25}N_{50}$, 10% glycerol, 1 mM DTT, 1 µg/mL Aprotinin and Leupeptin, 100 µM Pefabloc, pH 7.5) and protein was stored in aliquots at - 80°C.

3.2.3.5 Production of heavy (stable isotope labeled) E6AP

For SILAC experiments heavy (stable isotope labeled) E6AP was generated. An *E. coli* strain auxotrophic for arginine and lysine (Matic et al., 2011) was used to incorporate 4,4,5,5-deuterated lysine (K +4.025108 Da) and $^{13}C6/^{15}N4$-labeled arginine (R +10.00826 Da). Expression was performed overnight at 20 °C in M9 minimal media (7.52 g/L Na_2HPO_4, 3 g/L KH_2PO_4, 0.5 g/L NaCl, 0.5 g/L NH_4Cl) containing 0.4 % glucose, 1 mM $MgSO_4$, 0.3 mM $CaCl_2$, 1 µg/L biotin, 1 µg/L thiamine, 134 µM EDTA, 31 µM $FeCl_3$, 6.2 µM $ZnCl_2$, 0.76 µM $CuCl_2$, 0.42 µM $CoCl_2$, 1.62 µM H_3BO_3, and 81 nM $MnCl_2$. Purification of isotope-labeled E6AP was performed as described above (chapter 3.2.3.4) for His-E6AP.

3.2.3.6 Production of E6AP_HECT

N-terminal His-tagged HECT domain of E6AP (E6AP_HECT) was expressed in *E. coli* Rosetta2 (DE3) cells. After induction with 500 µM IPTG at OD_{600} of about 0.6 cells were cultured at 20°C overnight. Pellets from 1 L bacterial culture were resuspended in 50 mL lysis buffer ($T_{25}N_{50}$, 0.1% Triton X-100, 1 mM DTT, 1 µg/mL Aprotinin and Leupeptin, 100 µM Pefabloc, pH 7.5), sonicated and centrifuged (30,000 x g, 4°C, 15 min). The supernatant was first purified via Nickel-NTA chromatography (5 mL HisTrap FF crude column) with 8 CV 4% buffer B followed by a gradient to 100% buffer B in 20 CV with buffer A ($T_{25}N_{50}$, 1 mM DTT, pH 7.5) and buffer B ($T_{25}N_{50}$, 1 mM DTT, 500 mM imidazole, pH 7.5). Fractions containing E6AP_HECT were pooled and dialyzed against 2 L dialysis buffer ($T_{25}N_{50}$, 0.2 mM DTT, pH 7.5). The dialyzed protein solution was adjusted to 100 ng/µL, and 1 µg/mL Aprotinin and Leupeptin, 100 µM Pefabloc and 1 mM DTT final concentration was added. The purified protein was stored in aliquots at - 80°C.

3.2.3.7 Production of GST fusion proteins of HPV E6 proteins, HDM2_RING, RLIM_RING, and HUWE1_trunc

GST fusion proteins of HPV-11 E6, HPV-16 E6, HPV-16 E6_L50E, HPV-18 E6, HDM2_RING, RLIM_RING and HUWE1_trunc were expressed in *E. coli* BL21 (DE3) pLysS cells. After induction with 500 µM IPTG at OD_{600} of about 0.6 cells were cultured at 20°C overnight. Pellets from 1 L bacterial culture were resuspended in 50 mL lysis buffer (PBS, 1% Triton X-100, 1 mM DTT, 1 µg/mL Aprotinin and Leupeptin, 100 µM Pefabloc), sonicated and centrifuged with 30,000 x g at 4°C for 15 min. The supernatant was added to 150 µL, with lysis buffer pre-equilibrated, Glutathione Sepharose 4B beads. After incubation at 4°C for 90 min in a tube roller incubator, beads were spun down afterwards, washed 3 times with 1 mL washing buffer (PBS, 0.1% Triton X-100, 1 mM DTT) and protein of interest was eluted six times with 500 µL elution buffer (25 mM Tris-HCl, 10 mM glutathione, 1 mM DTT, pH 8.0).

3.2.3.8 Production of HDM2

HDM2 was expressed and purified as described previously (Tang, 2017). In brief, after a heat-shock for increased chaperone presence and induction using low concentrations of IPTG, proteins were produced over 48 h in TB media. Since the proteins contain an N-terminal GST-SUMO tag, it was cleaved off by ULP1 protease to obtain pure and active protein.

3.2.3.9 Ubiquitin-TAMRA coupling and purification of Ub-T

In order to attach the fluorescent dye 5(6)-carboxytetramethylrhodamine (TAMRA) to ubiquitin, ubiquitin from bovine erythrocytes was solved in 50 mM NaOAc (pH 7.2) and incubated for at least 30 min on ice. TAMRA-NHS was freshly dissolved in DMSO and added in a molar ratio of 1:3 and mixed well. The final reaction concentrations were 3 mg/mL ubiquitin, 0.55 mg/mL TAMRA-NHS and 10% DMSO (v/v). After overnight incubation at 4°C, the reaction was quenched with 50 mM Tris-HCl pH 8.0 for 30 min at 30°C. The reaction mixture was added to 30 mL of 25 mM NaOAc (pH 4.0), the pH was adjusted to 4.0 and the solution was filtrated with a 0.22 µm syringe filter.

Ub-T (TAMRA-labeled ubiquitin) was next purified with an ÄKTA FPLC system using a 1 mL HiTrap SP HP column with a gradient to 100% buffer B in 20 CV with buffer A (25 mM NaOAc, pH 4.0) and buffer B (25 mM NaOAc, 1 M NaCl, pH 4.0). 4 mL Amicon Ultra filter devices with 3 kDa cut-off were used for buffer exchange to 25 mM Tris-HCl, 50 mM NaCl, 1 mM DTT, pH 7.5 and to concentrate the sample to 2 µg/µL. Purified protein was stored at - 80°C.

3.2.4 Fluorescence polarization measurements with Ub-T

3.2.4.1 Reader settings for FP measurements

A Tecan Infinite F500 micro plate reader was employed to determine FP of Ub-T. Measurements were carried out in 384 well plates (flat bottom, black, non-binding) in 80 µL volume. Ub-T was excited at 550 nm with linear polarized light and excited light passed through polarization filters (either parallel or peripendicular orientated to the excitation filter) with 580 nm before detection. The G-factor of the instrument was determined to be 0.90657 by using 10 nM free TAMRA solution and a theoretical FP value of 22 mP (millipolarization units) therefore. The Z-position (distance between detector and plate) was adjusted to 22 mm and the gain of the photomultiplier tube was set to 70 using 23 nM Ub-T solution as reference for all measurements.

3.2.4.2 FP-based ubiquitination assays

In vitro ubiquitination assays with Ub-T were monitored with FP measurements. Reactions were started by adding 20 µL of premix 2 (containing E1, E2, Ub and Ub-T) to 60 µL of premix 1 (containing

ATP and E6AP and may additionally contain HPV-16 E6 or compounds). Final amounts (and concentrations) of components were the following: 25 ng E1 (3 nM), 20 ng E2 (27 nM), various amounts of E6AP or other E3 ligases as indicated, 160 ng Ub (234 nM), 16 ng Ub-T (23 nM) in 25 mM Tris-HCl, 50 mM NaCl, 0.01% Triton X-100, 0.5 mM ATP, 2 mM $MgCl_2$, 1 mM DTT, pH 7.5. All reactions contained the same concentration of DMSO. Plates were incubated at 30°C inside the reader during reaction and FP was measured every 10 min for 2 h. Data was evaluated with GraphPad Prism 6 software. Error bars indicate standard deviations of three technical replicates.

3.2.4.3 High-throughput screening of small molecule libraries

The FP *in vitro* ubiquitination assay as described above (chapter 3.2.4.2) was used for high-throughput screening (HTS) of small molecule libraries. For automation, assays were carried out by a Tecan EVO Freedom HTS workstation. A screen for inhibitors of E6-E6AP and another for activators of E6AP were performed.

Premix 1 and 2 were stored in open vessels cooled to 4°C during one run with 10 to 20 plates. The room was constantly kept at 22°C using air conditioning. Plates were started every 27 min (inhibitor screen) or 28.5 min (activator screen), respectively. The last column of each plate was filled manually with reaction buffer as blank prior to screening runs. For HTS, first, 60 µL premix 1 containing 100 ng (12 nM) E6AP and 50 ng (15 nM) GST tagged HPV-16 E6 as well as 0.5 mM ATP in the inhibitor screen or 100 ng E6AP only in the activator screen as well as 0.5 mM ATP were transferred in all sample and negative control wells. Next, 60 µL of the positive control (containing no HPV-16 E6 in the inhibitor screen or containing additionally 100 ng HPV-16 E6 in the activator screen) were transferred into the respective wells. Next, compounds were transferred with a compound transfer tool from 10 mM stock solutions in DMSO in the library plates to the assay plate so that final assay concentrations of 50 µM were obtained. Plates were incubated at 30°C and 500 rpm shaking for 20 min in incubation towers with heating floors. Then, reactions were started by addition of 20 µL of premix 2 (containing E1, UbcH7, Ub and Ub-T) by a Tecan Multidrop device. FP was measured after 0 min and 35 min (inhibitor screen) or after 0, 45 and 55 min (activator screen) with short plate shaking in advance of each measurement. In total, 50,961 (E6-E6AP inhibitor screen) or 48,077 (activator screen) small molecules from commercially available libraries (Maybridge HitKit9000, ChemBioNet 1-3, ChemDiv, Analyticon Discovery I (1,000 natural compounds), Analyticon Discovery II (5,000 semi-natural compounds) and Biomol ICCB (480 FDA approved drugs with known targets)) were screened with 50 µM and 675 small molecules from an in-house library (MDB) were screened with 12.5 µM. Screening data were evaluated using KNIME (Konstanz Information Miner) software (Berthold et al., 2008) with following node packages: *KNIME Core, KNIME Database* and *KNIME HCS Tools* (provided by Max Planck Institute of Molecular Cell Biology and Genetics, Dresden, Germany).

3.2.5 Methods for protein characterization

3.2.5.1 SDS-PAGE

To separate proteins according to their size, sodium dodecyl sulfate polyacrylamide gel electrophoresis (SDS-PAGE) was applied. Gels were cast in Bio-Rad gel frames according to table 1. Acrylamide concentrations of the resolving gel varied depending on the size of the investigated proteins between 8 and 15%. The stacking gel contained 5% acrylamide. Samples were mixed with the respective volume of 2x or 5x SDS-PAGE sample buffer and boiled for 5 min prior to loading. 6 µL pre- or unstained protein marker was used. 18 x 8 cm pocket gels were run for 45 min with 70 mA in Lämmli running buffer.

Table 1: Composition of SDS-PA gel ingredients. Indicated volumes suffice for 18 x 8 x 0.1 cm gels.

	resolving gel (8%)	resolving gel (10%)	resolving gel (12%)	resolving gel (15%)	stacking gel (5%)
MilliQ	14.5 mL	12.5 mL	10.5 mL	7.5 mL	8.75 mL
Separating gel buffer	7.5 mL	7.5 mL	7.5 mL	7.5 mL	-
Stacking gel buffer	-	-	-	-	3.75 mL
30% Acrylamide	8 mL	10 mL	12 mL	15 mL	2.5 mL
10% APS	300 µL	300 µL	300 µL	300 µL	150 µL
TEMED	30 µL	30 µL	30 µL	30 µL	15 µL

3.2.5.2 Fluorescence scan of SDS-PA gels

Gels were incubated in MilliQ on an orbital shaker until bromophenol blue from the running front diffused out of the gel. Then, gels were scanned with a FLA-5000 (Fujifilm) using 532 nm laser excitation and 575 nm (LPG) emission filter with 800 V detection mode.

3.2.5.3 Coomassie blue staining of SDS-PA gels

Gels were stained with Coomassie stain solution for 1 h. Afterwards gels were incubated in destain solution until the background was colorless. Then, gels were stored in MilliQ and pictures were taken with a LAS-3000 imager. For detection of low protein amounts Colloidal Coomassie solution (Carl Roth) was used according to the manufacturer's instructions for overnight staining of SDS-PA gels. Gels were destained with 40% methanol in MilliQ and stored afterwards in MilliQ for complete destain.

3.2.5.4 Western blot analysis

For western blot analysis gels were blotted onto a 0.22 µm Amersham Hybond PVDF membrane. 1x Roti-Block solution was used for blocking for 1 h at room temperature or overnight at 4°C. After 3 times 5 min washing with TNE-T, the membrane was incubated with primary antibody for 1 h at room temperature or overnight at 4°C. After 3 times 5 min washing with TNE-T, the membrane was incubated with HRP-coupled corresponding secondary antibody for 1 h at room temperature. After washing 3 times 5 min with TNE-T, enhanced chemiluminescence solution was used for detection with LAS-3000 imager.

3.2.5.5 Fluorography of SDS-PA gels with radio-labeled proteins

S^{35} radio-labeled proteins were separated by electrophoresis with 12% SDS-PA gels, fixed for 15 min in destain solution and incubated afterwards for 15 min in Lightning Autoradiography Enhancer solution. Subsequently, gels were dried at 80°C and vacuum, subjected to a BAS MS-2040 imaging plate for 4 to 12 h. Signals were read out with a FLA-5000 scanner.

3.2.5.6 BCA assay for protein concentration determination

In order to determine total protein concentration of a sample, the Pierce BCA Protein Assay kit was applied according to the manufacturer's instruction.

3.2.5.7 In vitro thermal shift assays

In order to determine stabilizing or destabilizing effects on proteins due to binding of a compound *in vitro* thermal shift assays were performed similar as described previously (Molina et al., 2013). In brief, proteins of interest were pre-incubated with compounds for 10 min on ice. Then a 2 min step at indicated temperatures in a PCR cycler was followed by 15 min centrifugation at 16,000 x g. The supernatant was transferred into a fresh reaction tube and analyzed by SDS-PAGE and Coomassie staining.

3.2.5.8 Size-exclusion chromatography

Size exclusion chromatography was performed to determine oligomerization behavior of E6AP. 100 µg E6AP were loaded on a Superdex75 10I300 column (GE Healthcare) and $T_{25}N_{150}$ with 1 mM DTT was used for gelfiltration. Proteins of the high-molecular weight calibration kit from GE Healthcare were used as standards for molecular weight determination.

3.2.5.9 HPLC analysis of Ub-T

Samples were analyzed by UHPLC (Ultra High-Performance Liquid Chromatography) on a Dionex UltiMate3000 (Thermo Fisher Scientific) using an analytical Aeris WIDEPORE XB-C8 column (150 mm x 2.1 mm) with 3.6 µm silica as a stationary phase (Phenomenex). Prior to purification, all samples were acidified with 0.1% TFA. Gradient elution (2 min at 0% B; in 38 min to 70% B; then in 7 min to 100% B and finally for 5 min at 100% B) with eluent A (0.04% TFA in water) and eluent B (0.04% TFA in acetonitrile/water (80:20, v/v)) was performed at a flow rate of 250 µl/min. The signals were monitored by UV absorbance at 220 nm.

3.2.5.10 Mass spectrometric analysis

3.2.5.10.1 MALDI-TOF-MS of Ub-T

Reaction product of TAMRA to ubiquitin coupling was investigated by MALDI-TOF mass spectrometry with a MicroFlex MALDI-TOF instrument from Bruker. 1 µL α-cyano-4-hydroxycinnamic acid (HCCA) was spotted as matrix on the sample target chip. 2 µg sample in 2 µL aqueous solution was mixed with the matrix and measured after drying. The instrument was calibrated before with commercially available protein standards from Bruker.

3.2.5.10.2 ESI-MS of Ub-T

Intact proteins from UHPLC peak fractions of Ub-T were analyzed by direct infusion on an amaZon speed ETD mass spectrometer (Bruker Daltonics) with a flow rate of 4 µl/min. The mass spectrometric data were acquired for about 6 min and the final mass spectrum was averaged over the whole acquisition time. Mass spectrometric data were evaluated and deconvoluted using the Compass Data Analysis Version 4.4 (Bruker Daltonics) software.

3.2.5.10.3 LC-MS/MS analysis of tryptic digested proteins

In order to identify modification sites of ubiquitin with TAMRA and E6AP with ubiquitin LC-MS/MS measurements were performed. Ub-T and E6AP autoubiquitinated with Ub-T were separated using SDS-PAGE. Bands of interest were cut out, stored in 50 mM NH_4HCO_3, destained with acetonitrile/NH_4HCO_3 (1:1, v/v) solution and dried in acetonitrile. Samples containing E6AP were reduced with 10 mM DTT for 1 h at 56°C and alkylated with chloroacetamide for 1 h at room temperature. After washing twice for 5 min with acetonitrile/NH_4HCO_3 (1:1, v/v) solution, samples were stored in 1 mM DTT at 4°C. Later, gel pieces were dried with acetonitrile and covered with 10 µg/mL trypsin solution in 50 mM NH_4HCO_3 for 1 h at 4°C. After removing the supernatant proteins were in-gel digested at 30°C overnight. On the next day, peptides were eluted with 0.1% formic acid

during 1 h incubation at 4°C. Peptides were desalted and concentrated using C18-ZipTip (Millipore) according to the manufacturer's instructions.

All digested samples were analyzed by reversed phase liquid chromatography nanospray tandem mass spectrometry (LC-MS/MS) using an LTQ-Orbitrap mass spectrometer (Thermo Fisher) and an Easy-nLC 1,000 (Thermo Fisher). The dimensions of the reversed-phase LC column were 3 µm, 100 Å pore size C18 resin in a 75 µm i.d. × 15 cm long piece of fused silica capillary (Acclaim PepMap100, Thermo Scientific). After sample injection, the column was washed for 5 min with 94% mobile phase A (0.1% formic acid) and 6% mobile phase B (0.1% formic acid in acetonitrile), and peptides were eluted using a linear gradient of 6% mobile phase B to 36% mobile phase B in 45 min, then to 100% B in an additional 5 min, at 300 nL/min. The LTQ-Orbitrap mass spectrometer was operated in a data dependent mode in which each full MS scan (30,000 resolving power) was followed by five MS/MS scans where the five most abundant molecular ions were dynamically selected and fragmented by collision-induced dissociation (CID) using a normalized collision energy of 35% in the LTQ ion trap. Dynamic exclusion was allowed. Tandem mass spectra were searched against a StandardProt database using Proteome Discoverer 1.4 (Thermo Scientific) and an in-house Mascot Server 2.5 (Matrix Science) with "Trypsin/P" enzyme cleavage, static cysteine alkylation by chloroacetamide and variable methionine oxidation as well as variable TAMRA modification at lysine residues.

3.2.6 *In vitro* enzyme assays

3.2.6.1 E1 activity assays

The influence of E6-E6AP inhibitors on E1 activity was determined by monitoring ATP cleavage as described previously (Hacker et al., 2013). To do so, 10 µM Probe IV (Cy3-Cy5-dilabeled ATP analogue), 500 nM E1, 60 µM ubiquitin, 1 mM DTT, and the respective concentration of compounds (pre-solved in DMSO) in 30 µL of $T_{25}N_{50}$ pH 7.5 reaction buffer. Measurements were started with addition of 10 mM $MgCl_2$. Reactions were incubated at 37°C and monitored with a Tecan Infinite F500 reader with 525 nm excitation filter and 590 nm emission filter with a gain of 35.

At a later time, an improved version of the ATP sensor cleavage assay was developed (Hammler et al., 2020). This assay was applied for the E6AP activators. 5 µM DH582 (ATP sensor), 250 nM E1, 23 µM ubiquitin, 1 mM DTT, and the respective concentration of compounds (pre-solved in DMSO) in 30 µL reaction buffer ($T_{25}N_{50}$ pH 7.5). Measurements were started with addition of 10 mM $MgCl_2$. Reactions were incubated at 30°C and monitored in a Tecan Infinite F500 reader with 360 nm excitation filter, 465 nm emission filter and a gain of 75.

3.2.6.2 Conventional *in vitro* auto-ubiquitination assays

Conventional in vitro auto-ubiquitination assays were performed in 30 µL volume essentially as described previously (Nuber et al., 1998). The assay mixture with 150 ng E1 (50 nM), 75 ng E2 (166 nM), 750 ng E6AP (250 nM), 2 µg ubiquitin (7.78 µM) in reaction buffer (25 mM Tris-HCl, 50 mM NaCl, 2 mM ATP, 2 mM $MgCl_2$, 2 mM DTT, pH 7.5) was incubated for 90 min or indicated time at 30 °C or the indicated temperature. Reactions were stopped by addition of 7.5 µL 5x Laemmli buffer and boiling for 5 min. Proteins were separated by electrophoresis in a 12% SDS-PA gel and detected by Coomassie blue staining.

3.2.6.3 *In vitro* substrate ubiquitination assays

To investigate substrate ubiquitination HA-tagged Ring1B_I53S was *in vitro* translated with S^{35}-methionine using the T7-coupled TNT *in vitro* reticulocyte lysate translation system according to the manufacturer's instructions. HA-Ring1B_I53S was purified with E/Z view anti-HA agarose beads. For purification, beads were washed two times with 500 µL $T_{25}N_{50}$ pH 7.5. 1 µL bead slurry and 1 µL *in vitro* translated proteins were used for each ubiquitination assay sample. After 1 h incubation with 1,000 rpm shaking at 4°C, beads were washed 3 times with 500 µL $T_{25}N_{50}$ pH 7.5. Next, *in vitro* auto-ubiquitination assays were performed in 30 µL volumes. The assay mixture with 150 ng E1 (50 nM), 75 ng E2 (166 nM), 400 ng E6AP (100 nM), 10 µg Ub (39 µM) and 1 µL *in vitro* translated on beads immobilized HA-Ring1B_I53S in reaction buffer (25 mM Tris-HCl, 50 mM NaCl, 2 mM ATP, 2 mM $MgCl_2$, 2 mM DTT, pH 7.5) was incubated for 90 min or indicated time points at 30°C. Reactions were stopped by addition of 7.5 µL 5x Laemmli buffer and boiling for 5 min. Proteins were separated by electrophoresis with a 12% SDS-PA gel that was subsequently subjected to fluorography analysis.

3.2.7 Mammalian cell culture experiments

3.2.7.1 Transient transfection of mammalian cells

Mammalian cells were transfected by using Lipofectamine 2000 according to the manufacturer's instruction. 2 µL Lipofectamine 2000 were used for each 1 ng plasmid DNA to be transfected. To adjust transfection efficiencies 300 ng beta-galactosidase vector were co-transfected.

3.2.7.2 Harvest of mammalian cells

To harvest mammalian cells, they were cooled on ice, media was removed, and cells were washed with 2 mL ice-cold PBS. Then, 1 mL ice-cold PBS was added, and cells were detached with a cell scraper. Cells were centrifuged (4°C, 1,000 x g, 30 min), the supernatant was removed, and pellets were stored at - 80°C or processed directly.

3.2.7.3 Lysis of mammalian cells

For lysis, pellets were resuspended in 90 µL TNN lysis buffer, the suspension was vortexed and incubated 30 min on ice before it was cleared by centrifugation (30 min, 16 400 x g, 4°C). The supernatant was transferred into fresh Eppendorf tubes and β-Gal assays were performed.

3.2.7.4 Beta-Galactosidase assays (β-Gal assays)

To determine and adjust transfection efficiencies β-galactosidase (β-Gal) assays were performed. β-Gal assays were done in duplicates in 96 well plates (transparent, flat bottom). 5 µL lysate were mixed with a mixture of 5 µL ONPG and 120 µL buffer Z. A blank control with TNN lysis buffer only was run to distract background signal. After 5 min incubation at 37°C absorbance at 405 nm was measured with a VICTOR multilabel plate reader.

3.2.7.5 *In cellula* Ring1B degradation assays

Mammalian cells were seeded in 6 well tissue culture plates. At 80 to 90% confluency, cells were transiently transfected with the indicated amounts of vectors as described above (chapter 3.2.7.1). After 5 h media was exchanged with fresh media containing compounds. The same volume DMSO was added to each well. After 16 h cells were harvested and lysed. Loading amounts were adjusted according to results of the β-Gal assays. SDS-PAGE and WB analysis with anti-HA antibody was executed and band intensities were determined with AIDA image analysis software.

3.2.7.6 Colony formation cytotoxicity assays

H1299 or HeLa cells were resuspended in cell culture media and counted with a COUNTess automated cell counter. 50,000 cells were seeded in 500 µL media in 24 well tissue culture plates. After 20 h media was exchanged with media containing compound in the indicated concentrations. After 24 h or 48 h treatment cells were twice carefully washed with ice-cold PBS. 500 µL crystal violet/formaldehyde solution were added. After 20 min incubation on a rocking incubator, cells were washed carefully with tap water, dried at room temperature, and pictures were taken with LAS-3000 imager.

4 Results

Ubiquitination is an abundant post-translational modification that regulates properties and/or localization and thus cellular functions of a myriad of proteins. Consequently, it has an impact on virtually all cellular processes (Kwon & Ciechanover, 2017, Oh et al., 2018), and malfunction of ubiquitination has been associated with diverse pathologies including developmental disorders, neuro-degenerative diseases, cancers or diseases caused by bacteria or viruses which hijack the ubiquitination system (Nath & Shadan, 2009, Wang et al., 2017a). In most cases, no therapy has been developed acting directly on the molecular defect of the respective component of the ubiquitin-proteasome system. A main reason for this is that no practicable and robust method to monitor ubiquitination in a high-throughput format has been available so far. Therefore, a novel method to monitor ubiquitination that is based on fluorescence polarization (abbreviated as FP) of fluorophore-labeled ubiquitin was developed in the present study.

4.1 Development of FP-based ubiquitination assays

To date, ubiquitination reactions of E3 ligases are routinely investigated in *in vitro* assays with recombinant enzymes. Sodium dodecyl sulfate-polyacrylamide gel electrophoresis (SDS-PAGE) for separation of the reaction products followed for instance by Coomassie blue staining or Western blot analysis is performed as readout (figure 3 A). Such procedures are laborious and error-prone when performed in a high-throughput manner. Additionally, the reaction is difficult to follow in real-time in a quantitative manner. In order to monitor E6AP-mediated ubiquitination in real-time and in a high-throughput manner, a first version of an assay to monitor ubiquitination using fluorescence polarization (FP) as readout was initially set up during my master thesis (Offensperger, 2015). In this study, this approach was significantly improved and expanded to the analysis of additional ubiquitin ligases.

The basic idea of the FP-based ubiquitination assay is that free ubiquitin is small compared to the ubiquitination reaction product. In fact, due to the small size of ubiquitin, typical reaction products are approximately 5- to 20-fold larger than free ubiquitin, allowing for clear separation of these two species according to their size difference. FP is a commonly applied method to investigate the size of a molecule that is labeled by a fluorophore (Hall et al., 2016). Hence, ubiquitin was labeled with the fluorescent dye TAMRA to monitor its increase in size upon attachment to other proteins. In general, to measure FP a fluorophore is excited with linearly polarized light. After a certain time, the so-called fluorescence lifetime, light is emitted by the fluorophore. Small molecules tumble fast as the velocity of rotation of a molecule is dependent on its molecular mass due to Brownian motion. Consequently, the orientation of smaller molecules changes significantly during the fluorescence lifetime, leading in

average to depolarization of the originally polarized light and consequently low fluorescence polarization values. In contrast, larger molecules tumble slowly, maintaining a more similar orientation after the fluorescence lifetime so that the light emitted is still mainly polarized, resulting in high fluorescence polarization values (figure 3 B).

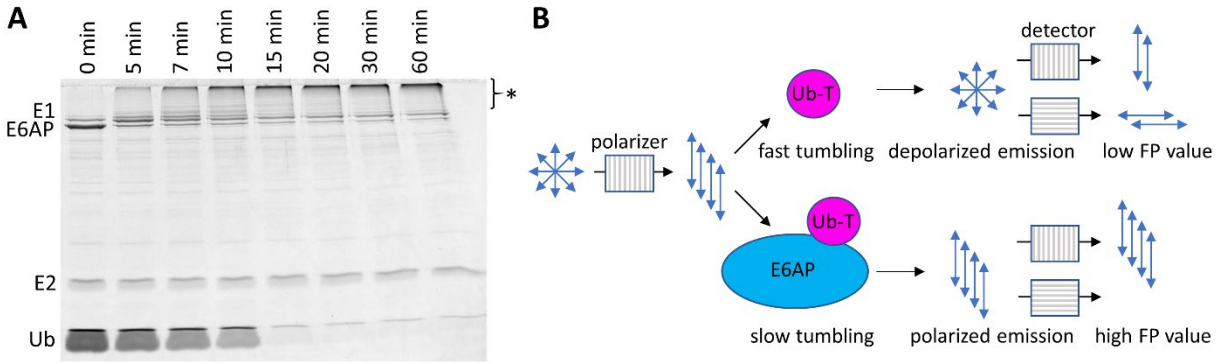

Figure 3: Principles of conventional in vitro ubiquitination assays and the envisioned fluorescence polarization (FP)-based ubiquitination assay

(A) Coomassie stained SDS-PA gel of in vitro E6AP auto-ubiquitination assays (in this study referred to as conventional in vitro ubiquitination assays) stopped at indicated times. Proteins are labeled and ubiquitinated forms of E6AP are marked by an asterisk. (B) Scheme of the principle of FP as basis for the envisioned FP-based ubiquitination assay.

4.1.1 Generation of TAMRA-labeled ubiquitin (Ub-T)

To be able to measure FP, ubiquitin was labeled with the fluorescent dye TAMRA (5-/6-Carboxytetramethylrhodamine) via N-hydroxysuccinimide (NHS) coupling with NHS-activated TAMRA. Reactions were carried out basically as described for the modification of ubiquitin with NHS-activated biotin (Shang et al., 2005). MALDI-TOF-MS analysis of purified reaction products showed that mainly a single TAMRA molecule was attached to ubiquitin, as the molecular mass shifts from 8565 Da, which corresponds to the mass of unmodified ubiquitin, to 8981 Da corresponding to the mass of one TAMRA molecule linked via an isopeptide bond to a primary amine of ubiquitin (figure 4 A). HPLC analysis confirmed that mainly mono-modified ubiquitin (peak 2, 55% according to integration of areas under the peak) and only smaller amounts of multiple-modified ubiquitin species (peak 3, 24% according to integration of areas under the peak) were generated (figure 4 B). In addition, also unmodified ubiquitin (peak 1, 21% according to integration of areas under the peak) was still present in the purified reaction product. ESI-MS analysis confirmed that peak 1 contained non-modified ubiquitin (8564.19 Da), peak 2 contained single-modified ubiquitin (8976.58 Da) and peak 3 contained mainly double-modified ubiquitin (9388.68 Da) (figure 4 C). Notably, the TAMRA-NHS ester can theoretically react with each primary amine of ubiquitin (either at the N terminal amino acid or at the ε-amino group of each of the seven lysine residues). However, tryptic digest followed by LC-MS/MS analysis proved that under the optimized reaction conditions used for coupling, mainly lysine 6 was labeled. However, also peptides

with the TAMRA modification at lysine residues 11, 33, 48, and 63 were identified (figure 4 D and E). As mainly a single TAMRA fluorophore was linked to ubiquitin, the labeled ubiquitin will be called hereafter Ub-T.

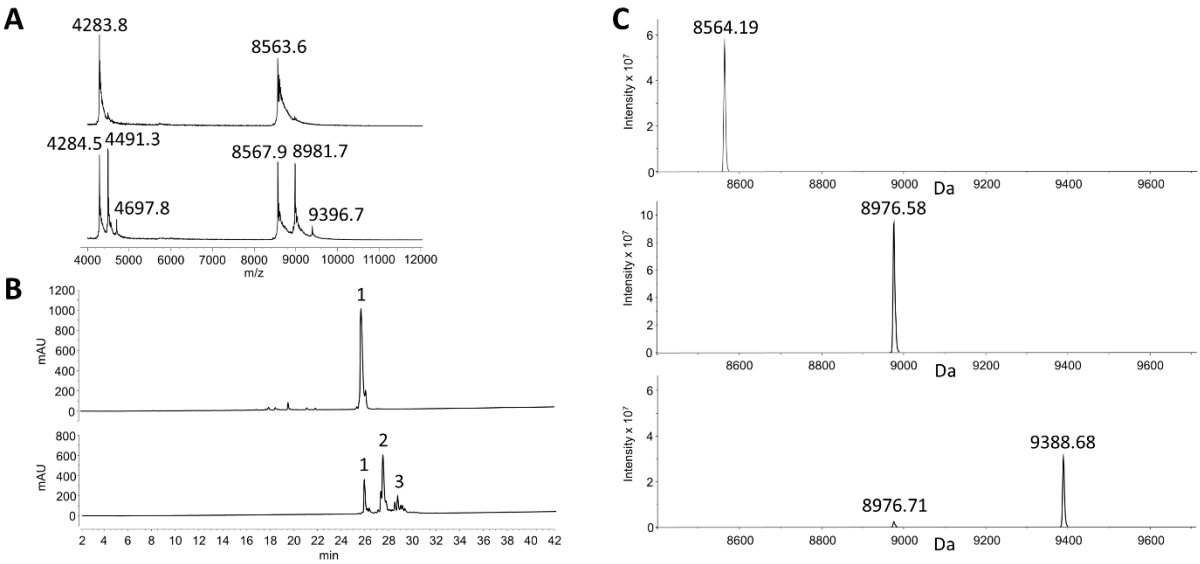

D

Sequence	# PSMs	Modifications	IonScore	Charge	MH+ [Da]	ΔM [ppm]	RT [min]
TITLEVEPSDTIENVK	37		84	2	1787,93096	2,00	28,53
ESTLHLVLR	26		66	2	1067,62175	0,88	23,35
LIFAGKQLEDGR	1		65	3	1346,74216	-0,44	20,45
TLTGkTITLEVEPSDTIENVK	5	K11(TAMRA)	52	3	2700,37296	2,74	38,17
IQDKEGIPPDQQR	7		41	3	1523,78519	2,54	9,60
TLSDYNIQK	13		36	2	1081,55351	0,99	18,40
IQDkEGIPPDQQR	17	K33(TAMRA)	34	3	1935,92978	3,18	32,08
TLSDYNIQkESTLHLVLR	1	K63(TAMRA)	33	3	2542,30039	1,05	38,79
EGIPPDQQR	22		33	2	1039,51689	0,14	14,09
LIFAGkQLEDGR	9	K48(TAMRA)	30	2	1758,88689	1,04	36,04
TLSDYNIQKESTLHLVLR	1		25	4	2130,16274	3,44	26,99
AKIQDKEGIPPDQQR	4		23	4	1722,91494	0,89	8,97
MQIFVkTLTGK	10	K6(TAMRA)	21	3	1677,87247	0,89	42,82
mQIFVkTLTGK	6	M1(Ox); K6(TAMRA)	17	3	1693,86747	0,93	35,84
ESTLHLVLRLR	1		17	3	1336,80512	-0,66	22,33

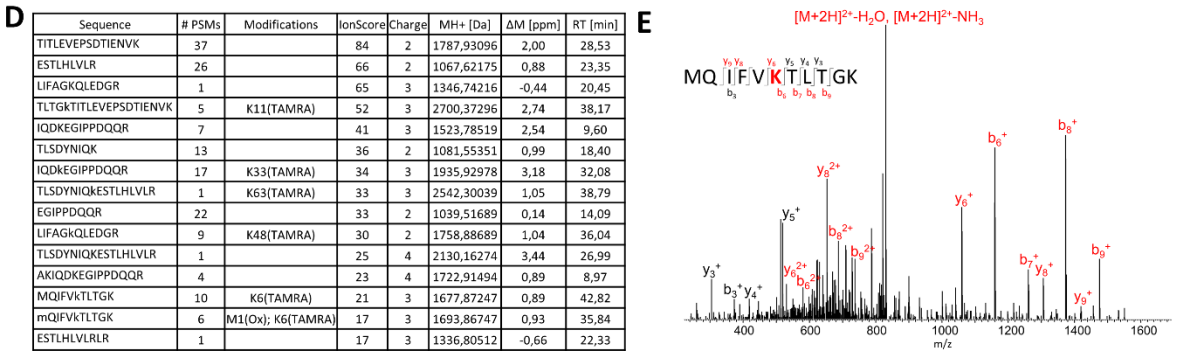

Figure 4: Analytics of TAMRA-labeled ubiquitin (Ub-T)

(A) *MALDI-TOF analysis of the reaction product from the ubiquitin-TAMRA coupling. In the upper panel as reference a spectrum of unmodified ubiquitin is shown, and in the lower panel a spectrum of the reaction product is shown. Calculated masses of the different ubiquitin species are:* M_{calc} *(Ub*$^{++}$*) = 4283 Da,* M_{calc} *(Ub-T*$^{++}$*) = 4491 Da,* M_{calc} *(Ub-T*$_2^{++}$*) = 4669 Da,* M_{calc} *(Ub*$^{+}$*) = 8565 Da,* M_{calc} *(Ub-T*$^{+}$*) = 8981 Da,* M_{calc} *(Ub-T*$_2^{+}$*) = 9397 Da. (B) HPLC chromatograms of unmodified ubiquitin as reference (upper panel) and purified Ub-T (lower panel). (C) ESI-MS analysis of the three HPLC peaks with peak 1 in the upper panel, peak 2 in the middle panel and peak 3 in the lower panel. (D) Peptides identified in LC-MS/MS analysis of tryptic digested Ub-T to identify modification sites with TAMRA. (E) Corresponding* MS^2 *spectrum of the peptide MQIFV****K****TLTGK containing the TAMRA modification at lysine 6 (marked in bold). Red color indicates peptide fragments harboring the TAMRA modification.*

4.1.2 Development of an FP-based E6AP auto-ubiquitination assay

In order to establish the FP-based ubiquitination assay, auto-ubiquitination of E6AP was investigated. E6AP was chosen as model E3 ligase due to its high pathological relevance and since it efficiently ubiquitinates itself in *in vitro* assays using a purely recombinant system.

To set up the assay, increasing concentrations of E6AP were incubated with a mixture of ATP, Ub-T, unlabeled ubiquitin (ten-fold excess to Ub-T), E1 and E2 enzymes in absence or presence of HPV-16 E6. Reactions took place in a 384 well plate format and FP values were measured every 10 min over 120 min. Free Ub-T had at 30°C FP values of 170 to 180 mP (millipolarization units), whereas values of 250 to 260 mP were reached when Ub-T was covalently attached to E6AP (figure 5 A). Furthermore, FP values increased faster for reasctions with higher E6AP concentrations. As expected (Mortensen et al., 2015), in presence of HPV-16 E6 reactions were strongly activated, as recognizable at the earlier onset and much faster increase of FP values in respective samples. Several controls were included, each with one essential component of the ubiquitination reaction missing. In absence of ATP, E1, E2, or E6AP the FP values stayed approximately at 180 mP indicating that no reaction took place. Furthermore, in presence of ATP, E1, E2 and a ligase-dead mutant of E6AP (substitution of cysteine 820 to alanine according to isoform 1) FP values stayed constant at 180 mP as well, also in presence of HPV-16 E6. Moreover, SDS-PAGE and fluorescence scan analysis of aliquots of the reaction samples showed that the increase of FP values is in line with the emergence of poly-ubiquitinated species typical for E6AP auto-ubiquitination reactions (figure 5 B). In presence of HPV-16 E6, all Ub-T is consumed and shifted to a high molecular mass smear after 60 min corresponding to constant FP values of 250 mP from 60 min onwards (figure 5 B). Due to the complex outcome of ubiquitination (multiple different lysine residues of E6AP can be ubiquitinated and different chain lengths and topologies can be formed), the actual mode of ubiquitination is difficult to determine in general. Nonetheless, the assay is clearly dependent on ubiquitination conditions and offers a great dynamic range to monitor ubiquitination in real-time.

A commonly accepted measure for robustness of a high-throughput screening assay is the Z' value that is calculated by equation: Z' = 1 - ((3*(stdev (PC) + stdev (NC)) / (mean (PC) - mean (NC))) as described by (Zhang et al., 1999). The closer the Z' value is to 1, the more robust is the assay. Assays with Z' values between 0.3 and 0.5 are considered as reliable and those with Z' values between 0.5 and 1 are considered as excellent (Zhang et al., 1999). In our case, Z' values larger than 0.8 between HPV-16 E6-activated reactions and control reactions are reached demonstrating the robustness of the FP-based ubiquitination assay.

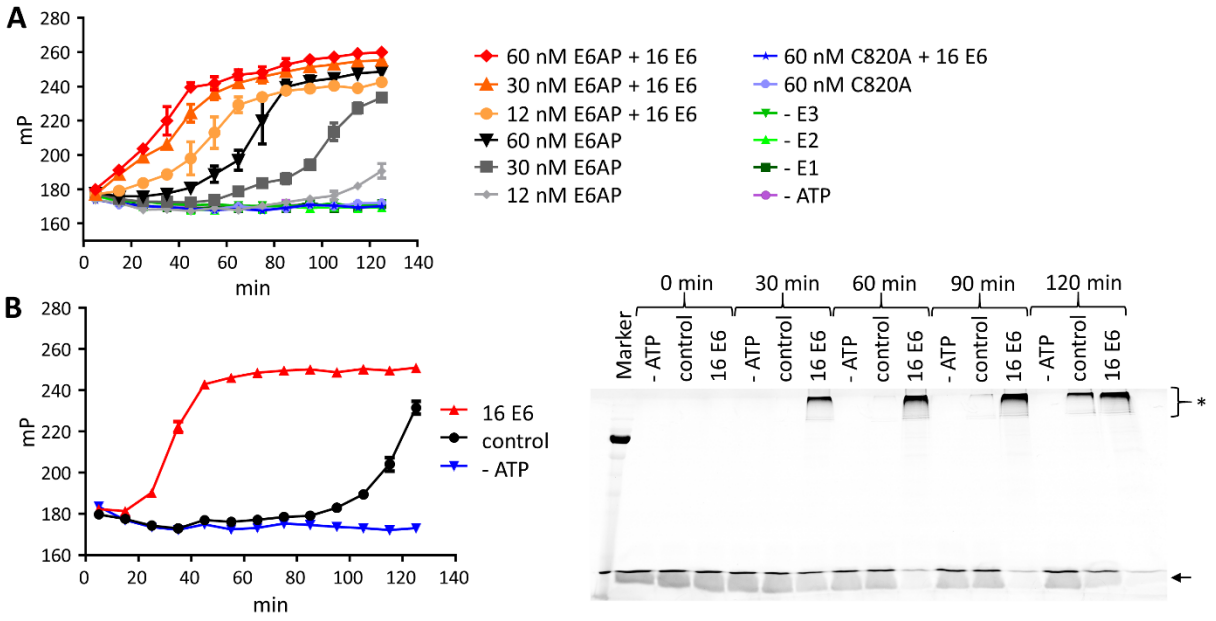

Figure 5: Development of the FP-based E6AP auto-ubiquitination assay
(A) Exemplary FP-based ubiquitination assay with different concentrations of E6AP in absence or presence of HPV-16 E6. Several controls show that increase of FP values over time is indeed dependent on the ubiquitination reaction. (B) Exemplary FP-based E6AP auto-ubiquitination assays in presence or absence of HPV-16 E6 including a control reaction without ATP. A fluorescence scan (532 nm excitation and 575 nm emission filter) of an SDS-PA gel of samples taken at the indicated reaction times is shown on the right-hand side. The marker band represents 70 kDa. Free Ub-T is marked by an arrow, while poly-ubiquitin species of Ub-T are marked with an asterisk.

4.1.3 Transfer of the FP-based ubiquitination assay to other E3 ligases

The next step was to test whether the FP-based ubiquitination assay can be transferred to other ubiquitin ligases. This would not only broaden application possibilities but could also serve later on as specificity controls for the identification of compounds that act on E6AP.

Different RING and HECT type ligases were recombinantly expressed and FP-based auto-ubiquitination assays were performed (figure 6). Aside from E6AP, an N-terminally truncated and GST-tagged version of HUWE1 (spanning the 900 C-terminal residues 3474-4374 and abbreviated as HUWE1_trunc) (Adhikary et al., 2005), full-length HDM2 as well as GST fusion constructs of its isolated RING domain (HDM2_RING) and of the RING domain of RLIM (RLIM_RING) (Ostendorff et al., 2002, Johnsen et al., 2009) were investigated. Moreover, samples with E6AP in presence of its allosteric activator HPV-16 E6 and samples with the isolated HECT domain of E6AP (E6AP_HECT) were included. A Coomassie blue stained SDS-PA gel of the proteins used for this experiment is shown (figure 6 C). Reactions with the different E3 ligases were performed over a time course of 120 min and FP values determined at different times (figure 6 A). In addition to the FP readout, aliquots of the reaction were taken after 120 min and subjected to SDS-PAGE and fluorescence scan analysis (figure 6 B). In line with the results obtained for E6AP, free Ub-T and samples without ubiquitin ligase had FP values of about 180 mP,

whereas FP values of reactions with the various ubiquitin ligases used up all Ub-T over time resulting in FP values of 260 to 280 mP. However, it should be mentioned that E6AP_HECT produces only mono- and to a smaller amount di- and tri-ubiquitinated species so that also only a slight increase of FP values to approximately 200 mP was obtained.

Taken together, the results obtained prove that the FP-based ubiquitination assay can be readily transferred to other ubiquitin ligases. In addition, the assays with different ubiquitin ligases confirmed the great dynamic range of the assay. This feature combined with the possibility to measure a sample multiple times in a 384 well plate format makes the assay well-suited for high-throughput screening for modulators of ubiquitin ligases.

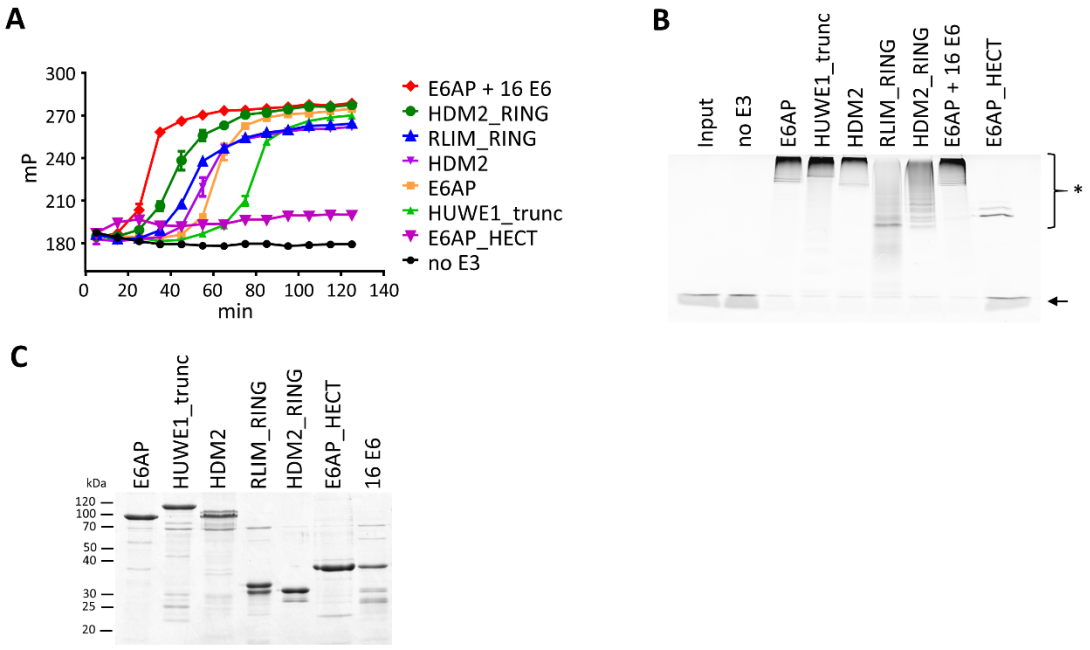

Figure 6: Transfer of the FP-based ubiquitination assay to other ubiquitin ligases
(A) FP-based auto-ubiquitination assays with different RING or HECT type ubiquitin ligases as indicated were performed with UbcH5b as E2 enzyme. Final assay concentrations of enzymes were: 60 nM E6AP, 120 nM HUWE1_trunc, 120 nM HDM2, 300 nM HDM2_RING, 120 nM RLIM_RING, 60 nM E6AP + 15 nM HPV-16 E6, 300 nM E6AP_HECT. (B) Samples of the FP-based assays were taken after reactions were finished (after 120 min) and separated via SDS-PAGE. Ub-T species were detected by fluorescence scan. The marker band represents 70 kDa. Free Ub-T is marked by an arrow while poly-ubiquitin species of Ub-T are marked by an asterisk. (C) Coomassie blue stained SDS-PA gel with recombinantly expressed proteins used for the FP-based ubiquitination assays.

4.2 Identification of small molecule inhibitors of E6-E6AP

Drugs that target HPV-induced cancers in a specific manner (i.e. not targeting uninfected tissue) are currently not available, and only a few lead structures that disrupt the E6-E6AP complex have been published in the meantime (see chapter 1.2.4.1.3). For this reason, the developed FP-based ubiquitination assay was used in a high-throughput screen (HTS) to identify small molecules that inhibit

activation of E6AP by HPV-16 E6 and, thus, may potentially disrupt the interaction of HPV-16 E6 and E6AP. Moreover, it was speculated that inhibitors of E6AP could be identified concurrently.

4.2.1 High-throughput screen for E6-E6AP inhibitors

To identify small molecule inhibitors of E6-E6AP by HTS, it was decided to measure only a single time point to be able to interleave assay plates with the aim to reduce the number of runs with different enzyme master mix solutions during the screen and to increase the throughput substantially. Protein concentrations of HPV-16 E6 (15 nM) and E6AP (12 nM) were adjusted so that E6-activated reactions reached after 35 min nearly the plateau with about 90% of their final FP value, whereas FP values of non-activated reactions did not start to increase yet. These adjustments should ensure a large window of FP values between unaffected and inhibited reactions. Negative controls (representing 0% inhibition) and positive controls without HPV-16 E6 (representing 100% inhibition of the activation of E6AP by HPV-16 E6) were included in 8 wells each on every plate.

4.2.1.1 Stability assessment of the E6-E6AP inhibitor screening assay

Before the screen was started, a pretest was performed to ensure that the enzyme master mix solutions remained stable while being stored in a Tecan Freedom Evo HTS workstation during the screen. Enzyme premixes were prepared, and automated handling was carried out exactly as planned for the HTS. Seven plates were started with 90 min in between each run so that enzyme premixes for the last plate had been stored for 9 hours (figure 7 A). Negative controls (i.e. auto-ubiquitination occurs) showed at 35 min FP values of around 240 mP whereas positive controls (no auto-ubiquitination) had FP values of around 180 mP (figure 7 B). This large separation between controls and small standard deviations of those resulted in high Z' values proving robustness of the assay and ascertaining identification of possible hits in the screen (figure 7 C). Additionally, a dilution series of Luteolin (a published E6-E6AP inhibitor) and Tyrphostin 47 (a previously identified E1 inhibitor (unpublished data)) were included. Both compounds showed a dose-dependent inhibition of the reaction with highly comparable effects in all seven runs with half maximal inhibitory concentrations (IC50s) of 3 µM (Luteolin) and 9 µM (Tyrphostin 47), respectively (figure 7 D). Accordingly, the pretest proved that the assay, the chosen concentrations of components as well as the quality of prepared enzymes as well as of Ub-T were suited for the planned HTS.

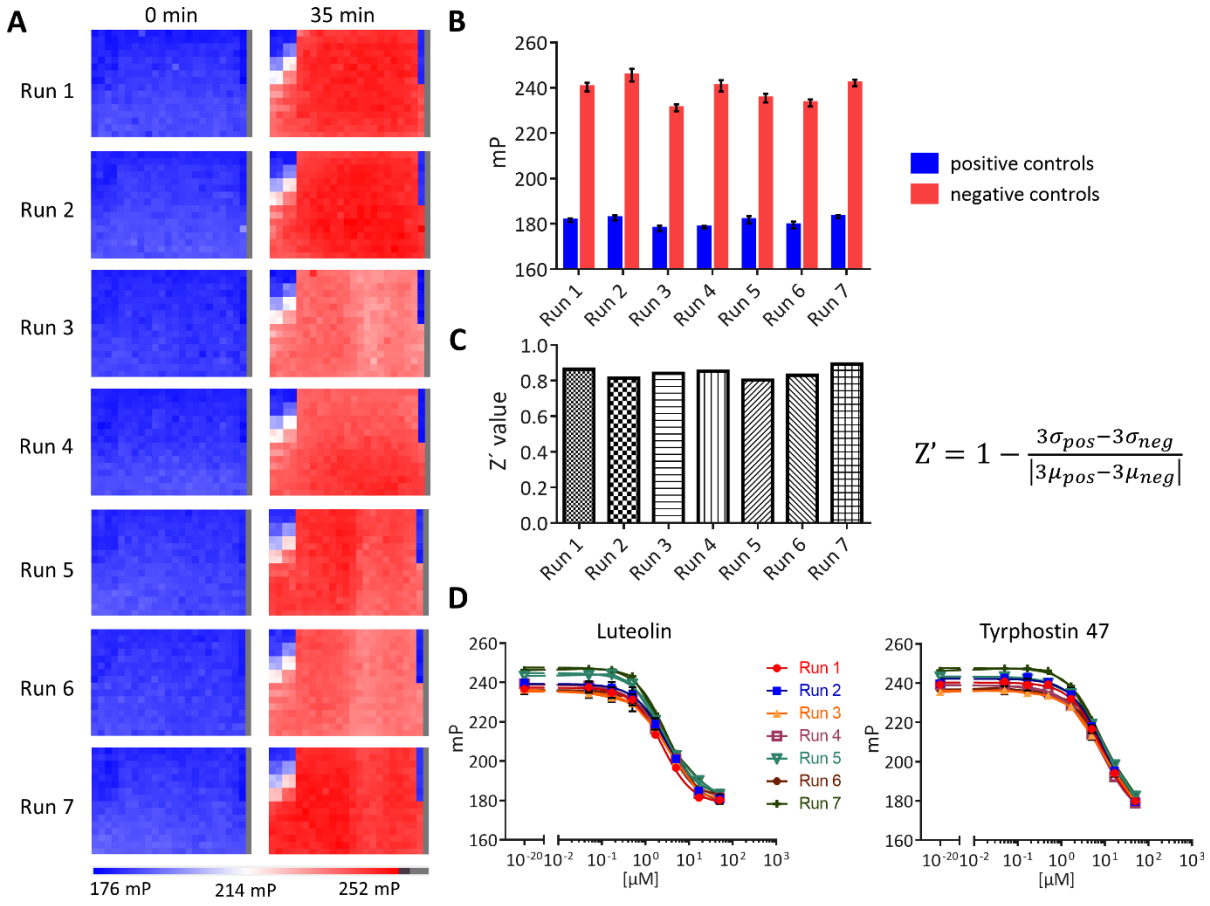

Figure 7: Stability test for the E6-E6AP inhibitor screen

To assess robustness of the assay and stability of components, a pretest for the E6-E6AP screen was performed. Assay plates with a dilution series of Luteolin (a published E6-E6AP inhibitor) and Tyrphostin 47 (a previously identified E1 inhibitor) were started with a time interval of 90 min in between with enzymes mixtures stored in open vessels at 4°C in the HTS workstation. In the first two columns quadruplicates of a serial dilution of Luteolin and in the second two columns quadruplicates of a serial dilution of Tyrphostin 47 were placed. (A) Heatmaps of the plates are shown from 0 min and 35 min reactions. The color code is indicated below. (B) Column bar graphs of the mean of FP values of the 8 positive and 8 negative control wells. Error bars indicate standard deviations. (C) Z' values and equation to calculate Z' values with standard deviations (σ) and means (µ) of positive (pos) and negative (neg) controls according to (Zhang et al., 1999). (D) IC50 determination of dilution series of Luteolin and Tyrphostin 47 by non-linear regression (fitting with a variable slope with four parameters) using GraphPad Prism.

4.2.1.2 Primary screen for E6-E6AP inhibitors

As the potential for the identification of inhibitors as well as same reaction conditions for plates started at different time points was ensured, an HTS of 156 plates with in total 50,961 compounds was performed with 50 µM compound concentration. The average Z' value of the screened plates was 0.82 ranging from 0.60 to 0.93. 48 compounds that interfered with the fluorescence readout at the 0 min time point were excluded. 9 of them showed theoretically impossible low FP values (FP (t_0) ≤ 150 mP), probably due to autofluorescence, and 39 of them showed unexpected high FP values (FP (t_0) ≥ 200 mP), probably due to precipitation of Ub-T.

To give examples of the data obtained by the HTS, heatmaps of FP values of the ten plates with the most hits as well as their Z' values are shown (figure 8). To compare the strength of inhibition, FP values of the samples were normalized relative to the controls for each plate separately (with negative controls corresponding to 0% inhibition and positive controls corresponding to 100% inhibition). According to the given definition, 351 compounds (~0.64%) showed over 50% inhibition, 200 compounds (~0.36%) showed over 75% inhibition, and 129 compounds (~0.24%) showed over 90% inhibition. Note that besides of the 8 negative control wells on each plate, additionally 3903 wells contained no compound because some library plates were not completely full. None of these 5151 reactions showed decreased FP values that would correspond to an inhibition ≥ 50%, indicating that the false positive rate was neglectable.

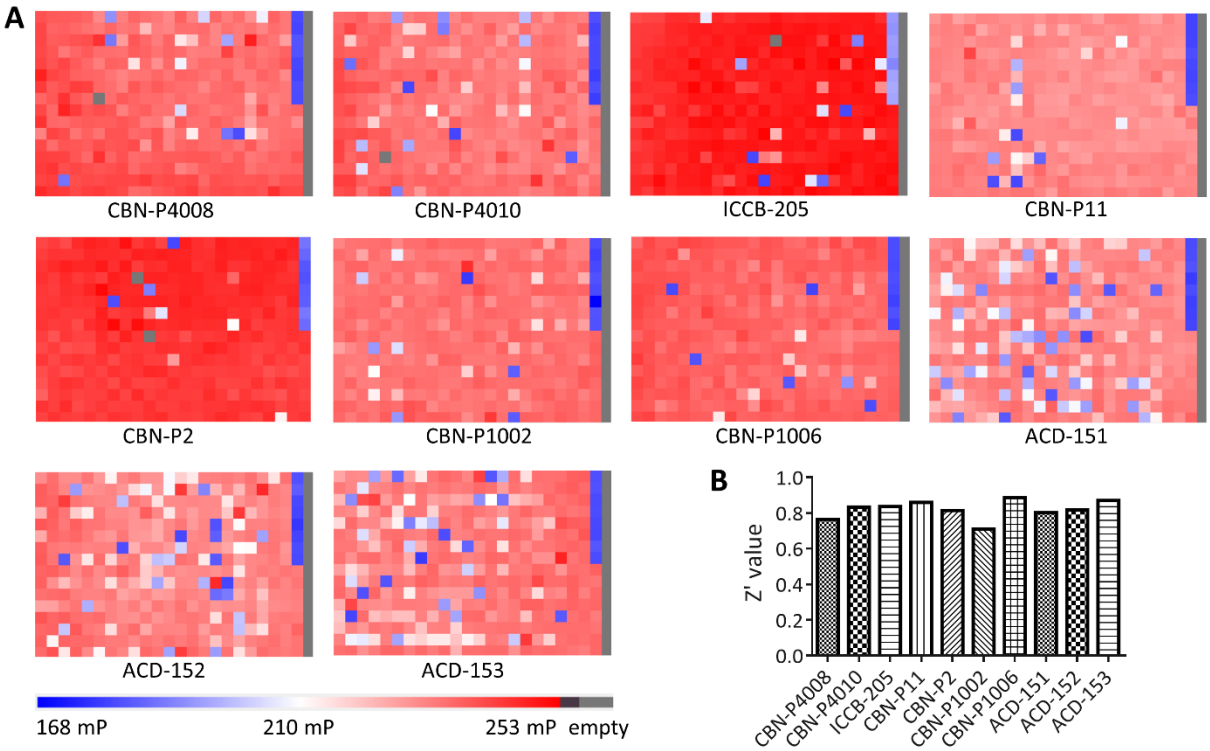

Figure 8: Exemplary data of the primary screen for E6-E6AP inhibitors
(A) *Heatmaps of FP values from the ten plates with most hits in the HTS for E6-E6AP inhibitors. The color code is given below. Grey color indicates samples with FP values ≤ 150 mP or ≥ 200 mP at 0 min that were excluded from evaluation. Data were evaluated with KNIME software. (B) Column bar graphs of corresponding Z' values of the ten shown plates.*

4.2.2 Counter screen with RLIM_RING to exclude unspecific inhibitors

A caveat of the established FP-based ubiquitination assay is that the whole ubiquitination cascade is involved so that compounds acting on E1 or E2 enzymes will inhibit the monitored reaction also. To exclude such compounds as well as compounds that interfere with the assay due to other yez unknown reasons, a counter screen was performed with RLIM_RING. RLIM_RING was previously investigated in our laboratory and is hence known to be readily prepared in large amounts and to perform efficient auto-ubiquitination (Johnsen et al., 2009) (see also figure 6). Besides, RLIM as a member of the RING E3 ligase family acts with a completely different mechanism than E6AP, so that in principle not only inhibitors of E6-E6AP but also inhibitors of E6AP (HECT ligases in general) should not act on RLIM.

4.2.2.1 Stability assessment of the inhibitor counter screen assay

First, the stability of the FP-based assay with RLIM_RING and UbcH5b (a cognate E2 enzyme of RLIM and many other human E3 ligases including E6AP) was assessed. To do so, a concentration of RLIM_RING was chosen so that comparable reaction kinetics were achieved as seen in the E6-E6AP inhibitor screen by using 100 nM RLIM_RING per sample. Samples without RLIM_RING were used as positive control and surrogate for complete inhibition. A stability test (4 runs started with 2 h time lag) with the same compound plate as used for the E6-E6AP inhibitor pretest showed clear separation between positive and negative controls as well as stability of enzyme solutions stored in the HTS workstation for the investigated period (maximum of 6 h storage) (figure 9 A and B). Z' values ≥ 0.8 confirmed robustness of the counter screen assay (figure 9 C). Interestingly, Luteolin exhibited much weaker inhibition for RLIM_RING compared to the E6-E6AP stability tests (figure 9 D), whereas Tyrphostin 47 showed a comparably strong inhibition with an IC50 of approximately 10 µM (figure 9 D).

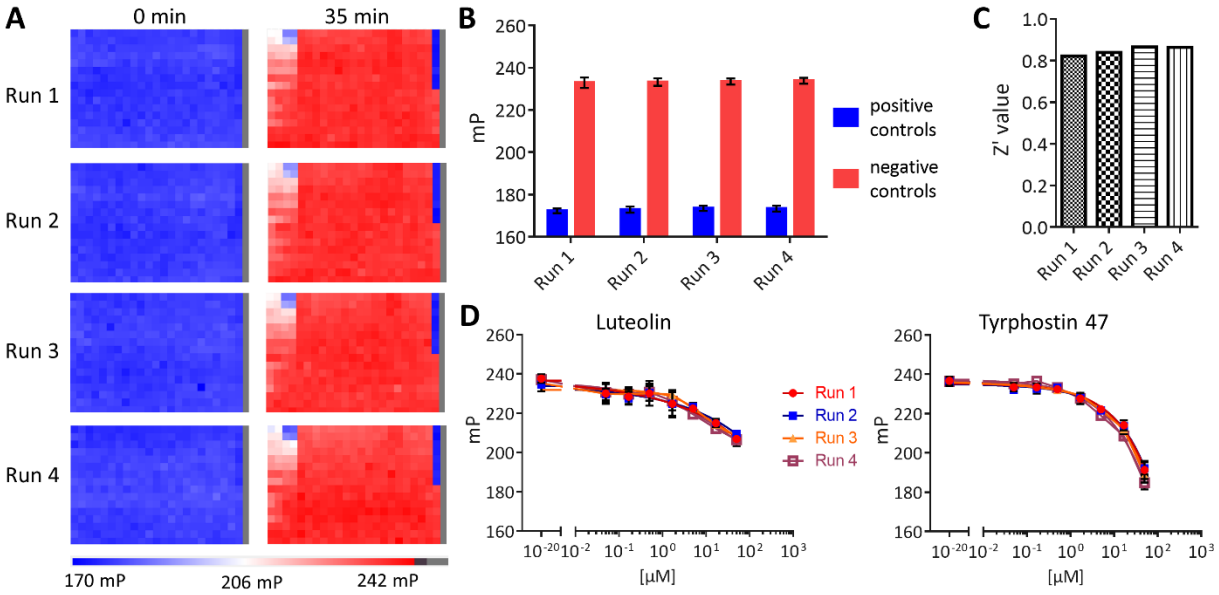

Figure 9: Stability test of the inhibitor counter screen assay
To assess robustness of the assay and stability of components, a pretest for the RLIM_RING counter screen was performed. It was designed like the pretest for the E6-E6AP inhibitor screen. Enzymes mixtures were stored in the HTS workstation at 4°C. Every 2 h an assay plate was started with a compound transfer from the compound plate containing the dilution series of Luteolin and Tyrphostin 47. In the first two columns quadruplicates of a serial dilution of Luteolin and in the second two columns quadruplicates of a serial dilution of Tyrphostin 47 were placed. Reactions were performed at 30°C temperature. (A) Heatmaps of FP values after 0 min and 35 min reaction times. The color code of the heat maps is given below. (B) Column bar graphs of the mean of the 8 positive and negative controls of the four runs are shown. Error bars indicate standard deviations. (C) Z' values of the four runs. (D) IC50 determination of the dilution series of Luteolin and Tyrphostin 47 by non-linear regression (fitting with a variable slope with four parameters) with GraphPad Prism.

4.2.2.2 Counter screen with RLIM_RING

To get an impression how trustful the hits from the primary screen are and to already evaluate as many hits as possible, the 10 plates that contained the most hits in the primary screen were chosen to be counter screened with RLIM_RING so that overall 149 hits from those with ≥ 50% were tested. Many compounds inhibited also RLIM_RING auto-ubiquitination as visible in the heatmaps of the counter screened plates (figure 10 A). Z' values ≥ 0.8 confirmed robustness of the counter screen (figure 10 B). In total, 23 of the hits showed ≤ 10% inhibition, whereas the majority (~85%) also inhibited RLIM_RING auto-ubiquitination and were thus classified as unspecific inhibitors of the ubiquitination cascade (see appendix table 1).

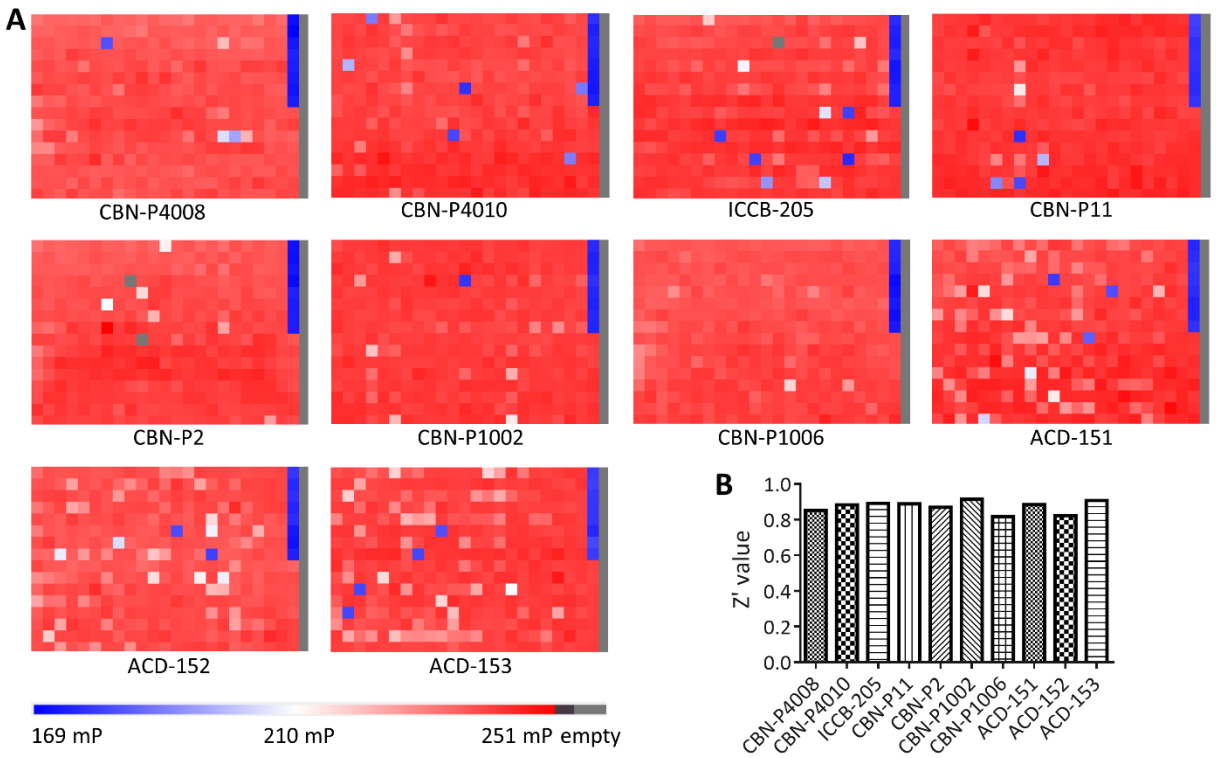

Figure 10: Inhibitor counter screen

The ten plates with most hits in the E6-E6AP inhibitor primary screen were counter screened with RLIM_RING with the same procedure as applied in the primary screen, besides that UbcH5b instead of UbcH7 was used as E2 enzyme. (A) Heatmaps of FP values with the color code indicated below. Dark grey color indicates samples that showed at 0 min FP values lower 150 mP or larger 200 mP and that were therefore excluded from further evaluation. (B) Column bar graphs of Z' values of the respective plates.

4.2.3 Secondary assays with cherry-picked screening hits

The counter screen revealed that about 85% of the 149 tested compounds had also an inhibiting effect on RLIM_RING auto-ubiquitination. Hence, specificity of the 202 other compounds needed to be confirmed as well before they were further followed. Despite the disadvantage that compounds could only be tested with a maximal final concentration of 10 µM instead of the 50 µM which was used in the primary screen, due to economic reasons it was decided not to counter screen all original plates but to retest cherry-picked compounds. Therefore, hits from the Maybridge library were cherry-picked at the Screening Centre of the University of Konstanz and hits from ChemDiv and ChemBioNet libraries were kindly supplied from Screening facilities from the FMP Berlin and the Max Planck Institute of Molecular Cell Biology and Genetics in Dresden (for small molecule libraries used in the screen, see Material and Methods, chapter 3.1).

4.2.3.1 Cherry-picked compounds from Maybridge library

22 compounds from the Maybridge library were cherry-picked and tested in the FP assay with a dilution series from 6 µM to 30 nM. Note that many of the compounds were colorful. However, since all different kinds of colors were covered, interference with the FP readout was not immediately apparent. These compounds were tested in FP-based auto-ubiquitination assays with E6-E6AP and E6AP (figure 11). One compound (MB021D08) showed preferred inhibition of E6-E6AP auto-ubiquitination, two compounds (MB021A08, MB022P17) unexpectedly inhibited preferably E6AP and 14 compounds clearly inhibited both reactions. Six compounds (MB002D11, MB006F17, MB008B03, MB009J16, MB015B08, MB027L20) showed no effect at all, with the lower concentrations used in comparison to the primary screen as possible explanation. Since no controls were included in this experiment, no percentages of inhibition can be stated. Future studies should assess specificity of the active compounds in respect to other ubiquitin ligases and especially the three compounds with preference for E6AP or E6-E6AP should be further characterized.

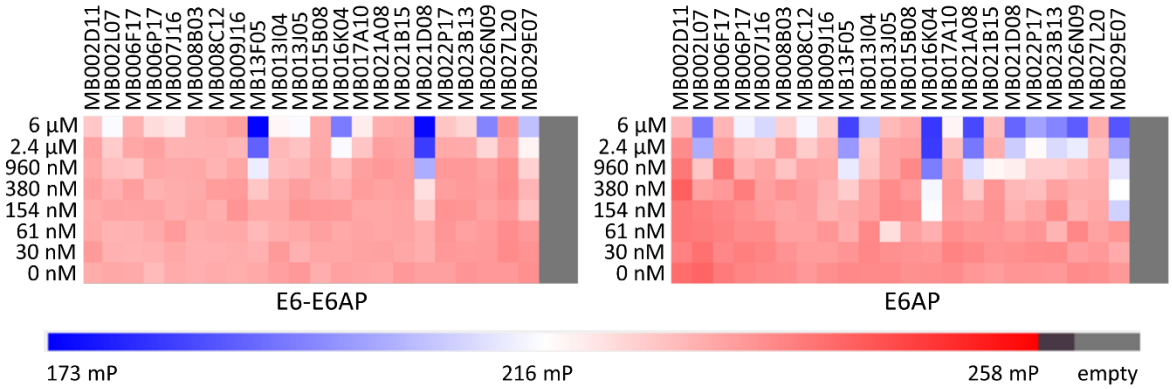

Figure 11: FP-based E6AP auto-ubiquitination assays with cherry-picked screening hits from the Maybridge library

A dilution series of the compounds in a library plate was prepared and the assays were handled like in the screen for E6-E6AP inhibitors in the HTS workstation. The 50 min time point from FP auto-ubiquitination assays with E6-E6AP and E6AP is shown. Compounds and final assay concentrations are indicated. The color code of the heatmaps is given below.

4.2.3.2 Cherry-picked compounds from ChemBioNet and ChemDiv libraries

121 hits from the ChemBioNet (CBN) and 48 hits from ChemDiv (CD) libraries were ordered to be cherry-picked (see above in chapter 4.2.3). Additionally, 14 of the 23 compounds, that were inactive in the counter screen with RLIM_RING, were purchased as they were commercially available (note that these 14 compounds were different from the cherry-picked ones). Stock solutions of all compounds were plated on a 384 well library plate and tested under the conditions used in the E6-E6AP inhibitor primary screen and the RLIM_RING counter screen, respectively. It should be emphasized, that concentrations of the cherry-picked compounds were five-times lower than in the primary screen due

to the small amounts provided so that a final assay concentration of 10 µM was obtained. For this reason, the 14 purchased compounds were also applied with 10 µM. Consequently, the threshold for E6-E6AP inhibitors was set to 30% due to the lower concentrations. Compounds that inhibited RLIM_RING auto-ubiquitination with more than 10% (this threshold corresponds also to a three-fold standard deviation of respective positive controls) were regarded as unspecific. According to these criteria, 41 of the 183 tested compounds turned out to be unspecific, 124 compounds showed no effect, and 18 compounds were specific for E6-E6AP (a comprehensive overview over results of these experiments is given in appendix table I).

4.2.4 Evaluation of purchased and synthesized screening hits

4.2.4.1 Evaluation of compounds OF101-114

14 of the 23 hits that showed promising results in the counter screen with RLIM_RING were, as mentioned above (chapter 4.2.3.2), commercially available (for structures see figure 12). In addition to the described HTS assays these compounds were also tested in further assays more extensively.

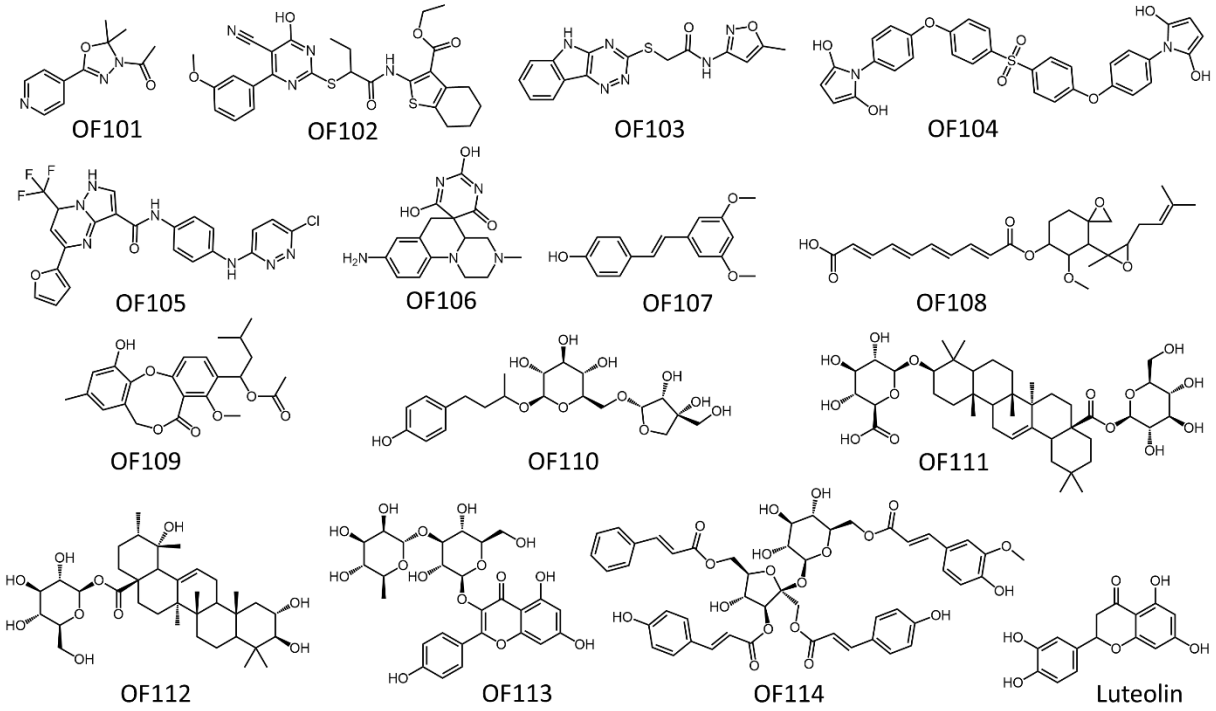

Figure 12: Chemical structures of purchased hits from the E6-E6AP inhibitor screen
All ordered compounds were numbered according to an internal name assignment with OF1XX compounds as potential E6-E6AP inhibitors. A list with these IDs, unique IDs (uiid) from the Screening Centre of the University of Konstanz, suppliers and order numbers, HTS assay results and final conclusions about the specificity is given in appendix table I.

FP auto-ubiquitination assays were performed with RLIM_RING, E6AP and E6-E6AP with 50 µM of the 14 compounds or Luteolin (figure 13 A). Four compounds (OF101, 107, 109, 110) showed no effect, four compounds (OF105, 106, 112, 113) showed complete inhibition of the three E3 ligases, and seven compounds (OF102, 103, 104, 108, 111, 114, Luteolin) showed partial inhibition of a part of or all E3 ligases. OF114 showed solubility problems and was thus excluded from further experiments. Unfortunately, none of the compounds exhibited specific inhibition of E6-E6AP or E6AP. Next, effects of the compounds on the E1 level were tested according to (Hacker et al., 2013). OF106 showed complete inhibition and OF111 showed partial inhibition of E1. In contrast, most other compounds did not affect E1 in this assay format (figure 13 B). Additionally, the 14 compounds were also tested in conventional SDS-PAGE auto-ubiquitination assays with different E3 ligases. Comparable results as in the FP auto-ubiquitination assays shown with either no significant inhibition of E6-E6AP and E6AP or unspecific inhibition also of the other E3 ligases were obtained.

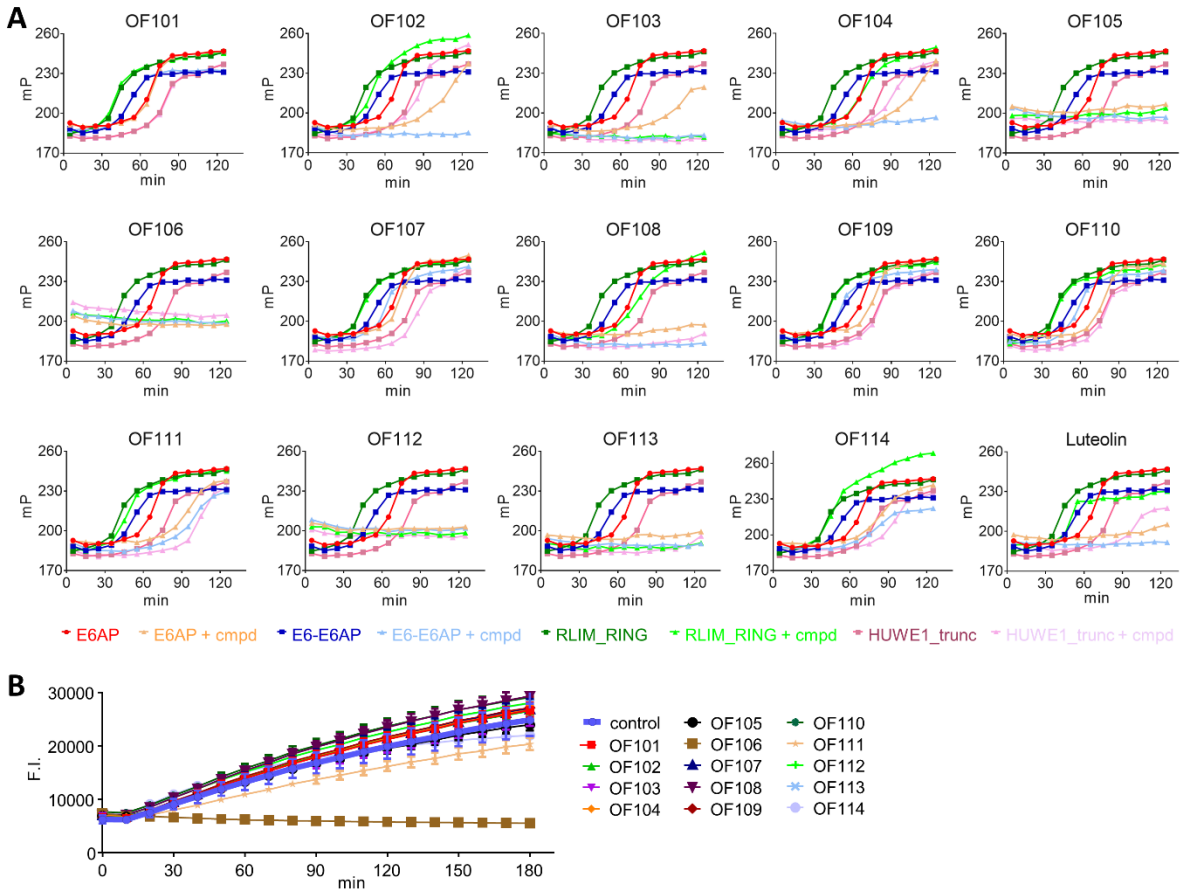

Figure 13: Reaction monitoring of 14 purchased compounds in FP-based auto-ubiquitination assays and in E1 activity assays

(A) FP assays with E6-E6AP, E6AP, RLIM_RING, and HUWE1_trunc were performed in absence and presence of 50 µM of the indicated compounds. FP values were measured every 10 min over 2 h while the assay plate was incubated in the multiwell reader at 30°C. (B) E1 activity assay with 50 µM compound concentration according to (Hacker et al., 2013). Fluorescence intensities (F.I.) were measured every 10 min over 3 h.

4.2.4.2 Synthesis and investigation of flavonoid-like compounds

In the HTS assays with cherry-picked compounds a group of three structurally related compounds OF122, OF123, and OF124 showed strong inhibition of E6-E6AP and only mild effects on RLIM_RING. Moreover, these compounds own a similar scaffold as Luteolin (figure 14 A). They showed great potency in preliminary assays to inhibit E6-E6AP-mediated ubiquitination of p53 (figure 14 B). As none of these compounds was commercially available, one of them (OF122) was synthesized in collaboration with Kathrin Götz and Lena Schneider (AG Marx, University of Konstanz) and named OF122b. FP-based ubiquitination assays with E6-E6AP, E6AP and RLIM_RING (figure 14 C) showed that not only E6-E6AP but also E6AP and RLIM_RING auto-ubiquitination was strongly inhibited. Interestingly, OF122b showed similar cytotoxic effects on HeLa cells (HPV-18-positive cancer cells) as Luteolin (figure 14 D), while OF122b showed significantly stronger E1 inhibition in *in vitro* E1 activity assays than Luteolin (figure 14 E). Therefore, it can be concluded that OF122b and Luteolin act unspecifically, however, possibly with different mechanisms.

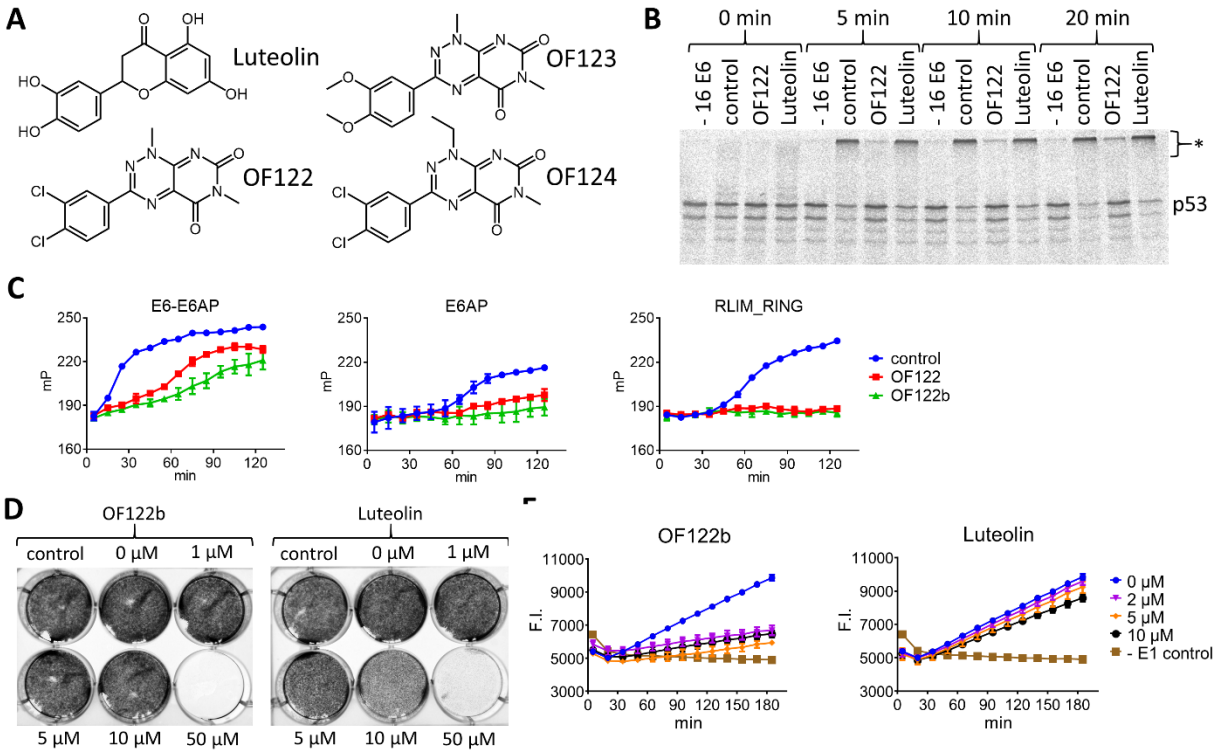

Figure 14: OF122 and structurally related flavonoid derivatives act unspecifically
(A) Structures of Luteolin and the three flavonoid derivatives identified in the primary screen and confirmed in HTS assays with cherry-picked hits are shown. (B) E6-E6AP-mediated p53 substrate ubiquitination assays in presence of 10 µM Luteolin or OF122. Polyubiquitinated species of p53 are marked with an asterisk. (C) Comparison of effects of cherry-picked (OF122) and synthesized (OF122b) compound in FP-based auto-ubiquitination assays with E6-E6AP, E6AP, or RLIM_RING with 10 µM assay concentration. (D) Colony formation cytotoxicity assays with HeLa cells treated for 24 h with the indicated concentrations of OF122b or Luteolin, respectively. (E) E1 activity assays in presence of indicated concentrations of OF122b or Luteolin according to (Hacker et al., 2013). Fluorescence intensities (F.I.) were measured every 10 min over 3 h.

4.2.5 Final experiments with purchased and synthesized compounds

Later, more potential E6-E6AP inhibitors (OF115-121) with promising results in the experiments with the cherry-picked compounds were purchased (for structures see figure 15 A). These compounds and selected compounds that were purchased previously were retested in FP-based auto-ubiquitination assays with E6-E6AP, E6AP and RLIM_RING. As additional read-out, reactions were analyzed by SDS-PAGE followed by fluorescence scan, which are exemplary shown (figure 15 B).

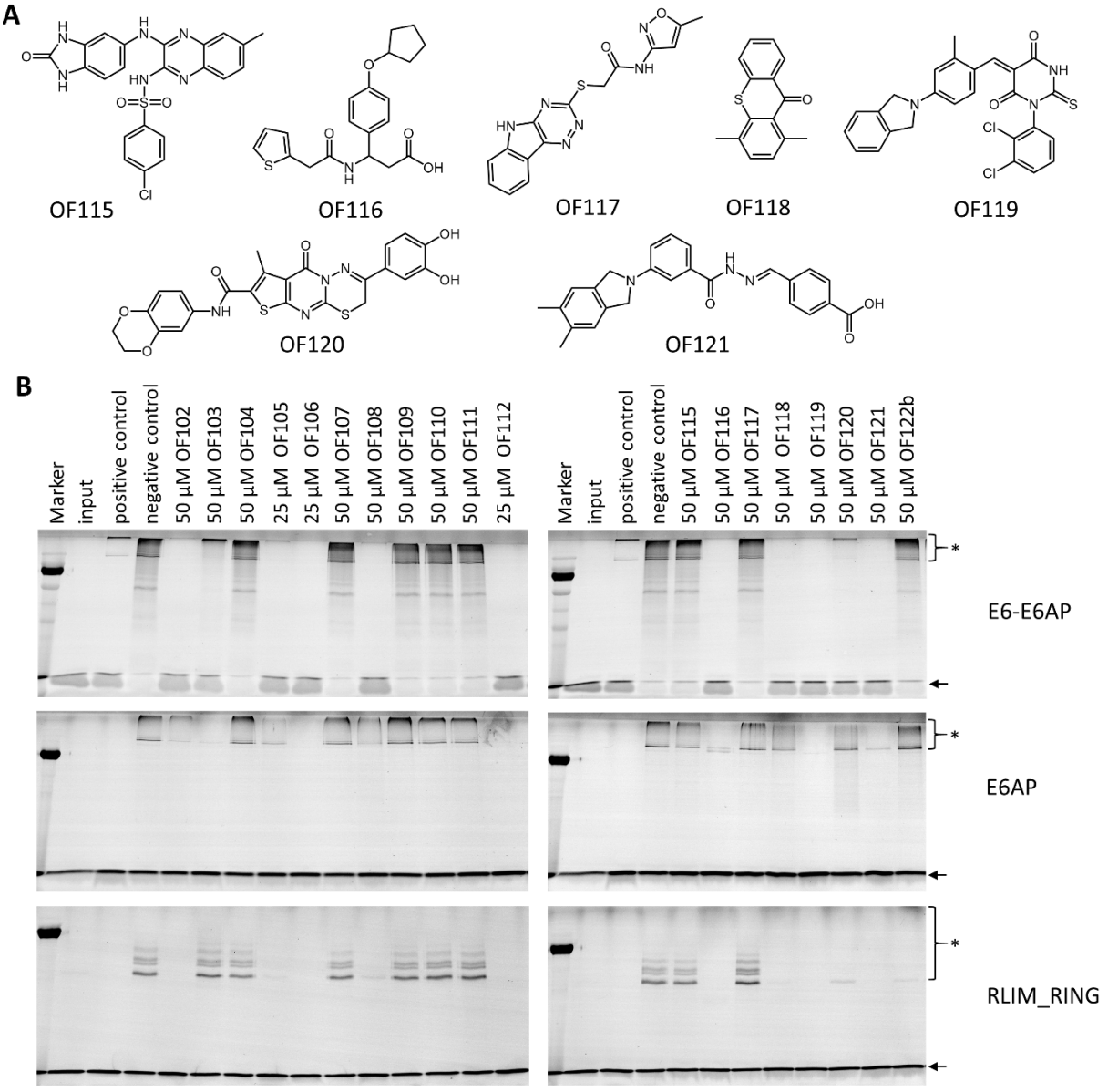

Figure 15: Final experiments with purchased and synthesized compounds
(A) Chemical structures of the newly purchased potential E6-E6AP inhibitors. (B) FP-based auto-ubiquitination assays performed with 12 nM E6AP + 15 nM HPV-16 E6; 100 nM E6AP; or 100 nM RLIM_RING. Samples of these assays were taken after 40 min and analyzed by SDS-PAGE and fluorescence scan. Free Ub-T is marked with an arrow while poly-ubiquitin species of Ub-T are marked with an asterisk. The marker band represents 70 kDa.

Unfortunately, despite the promising results in the HTS assays all tested compounds showed in these and subsequent experiments either no consistent inhibition of E6-E6AP or E6AP, or they inhibited RLIM_RING or other tested E3 ligases as well. How the discrepancies between these and the first promising preliminary results can be explained, has not been finally clarified for the reasons of time. Taken together, it can be concluded that none of the tested compounds inhibits the E6-E6AP complex or E6AP in a specific and exclusive manner. A schematic overview of the results of the HTS and secondary assays for E6-E6AP inhibitors is given in figure 16. The aim to identify specific inhibitors *in vitro* was not reached, as none of the closer characterized (i.e. purchased) hits showed a clear-cut specificity profile towards the E6-E6AP complex or E6AP that would justify more detailed *in cellula* evaluation. 51 hits were not completely evaluated, but preliminary results indicate that they too act either unspecifically or are inactive (appendix table I). Consequently, due to time reasons and since the focus was put on other aims of this study, characterization of the inhibitors was not further pursued.

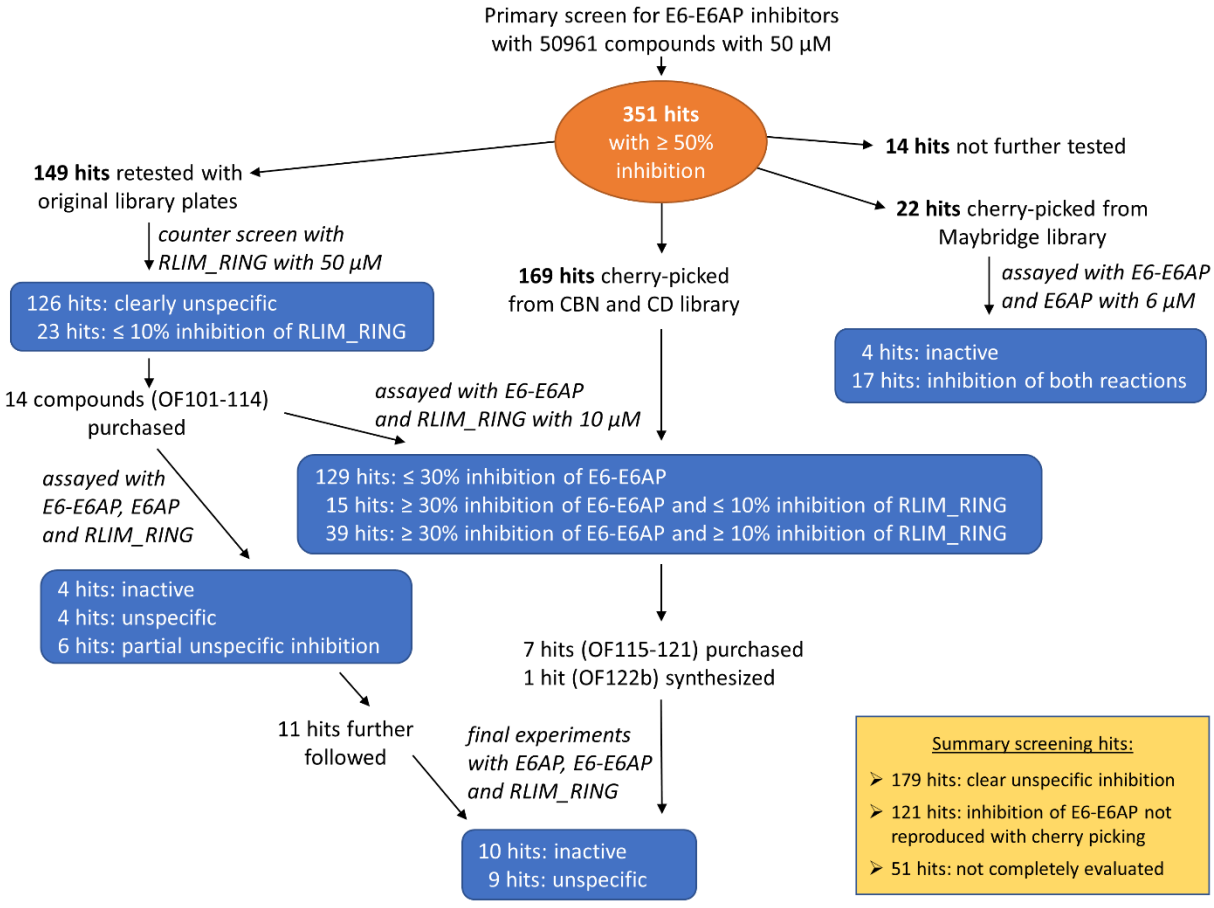

Figure 16: Schematic overview over results from the E6-E6AP inhibitor screen and secondary assays *Results from the primary screen, secondary HTS assays, and further secondary assays are displayed. The experiments are ordered in a time-related manner with early experiments in the upper part and later experiments in the lower part of the scheme. An overall summary of the screening hits is given in the lower right corner. For more details see appendix table I.*

4.3 Identification of small molecule activators of E6AP

E6 proteins from high-risk human papillomaviruses strongly activate E6AP (Mortensen et al., 2015) and E6AP can be additionally stimulated by HERC2 (Kühnle et al., 2011). Therefore, we proposed that E6AP is on its own not fully active and can be converted into more active states by interacting partners. As activation of E6AP by interacting proteins is possible, activation by small molecules is feasible as well. Real-time monitoring of E6AP ubiquitination reactions with the FP-based assay proved to be reliable; thus, we decided to perform a second HTS to identify small molecule activators of E6AP.

4.3.1 Adjustment of the FP-based ubiquitination assay for the identification of small molecule E6AP activators

For the planned screening E6AP concentrations needed to be adjusted so that a slight auto-ubiquitination reaction was obtained that could be strongly accelerated by addition of activators. However, choosing the optimal reaction time to identify activators turned out to be challenging due to the sigmoidal reaction curve. Variations in E6AP concentration did not only result in a premature or delayed start of the increase of the FP value and an altered slope of the curve but also in different final FP values as shown for a reaction with E6AP alone, a reaction containing E6AP and HPV-16 E6 and a reaction containing E6AP and Tamoxifen (a small molecule activator of E6AP described later) (figure 17 A). While stimulation by HPV-16 E6 was for all different E6AP concentrations clearly visible at all times, in the absence of HPV-16 E6 low E6AP concentrations at early reaction times bore the risk to miss some or all activators as demonstrated for Tamoxifen. Too high E6AP concentrations or too late time points were also not suitable, since FP values of non-activated reactions were rather high resulting in a smaller detection window and decreased signal to noise ratio between different reaction samples. In addition, under these conditions temperature differences were visible on the 384 well plate as the reader needs over 5 min to read out the whole plate and variations between different plates were obvious (data not shown). Furthermore, preincubation as well as temperature control was different in the HTS workstation compared to pipetting the reactions by hand (which was initially used to set-up the reaction conditions) resulting in different reaction kinetics (data not shown). Due to these reasons, we performed pretests in the HTS workstation (figure 17 B) and subsequently decided to perform reactions with low concentrations of E6AP (15 nM) and to measure FP of the assay plate at two different time points (after 45 and 55 min).

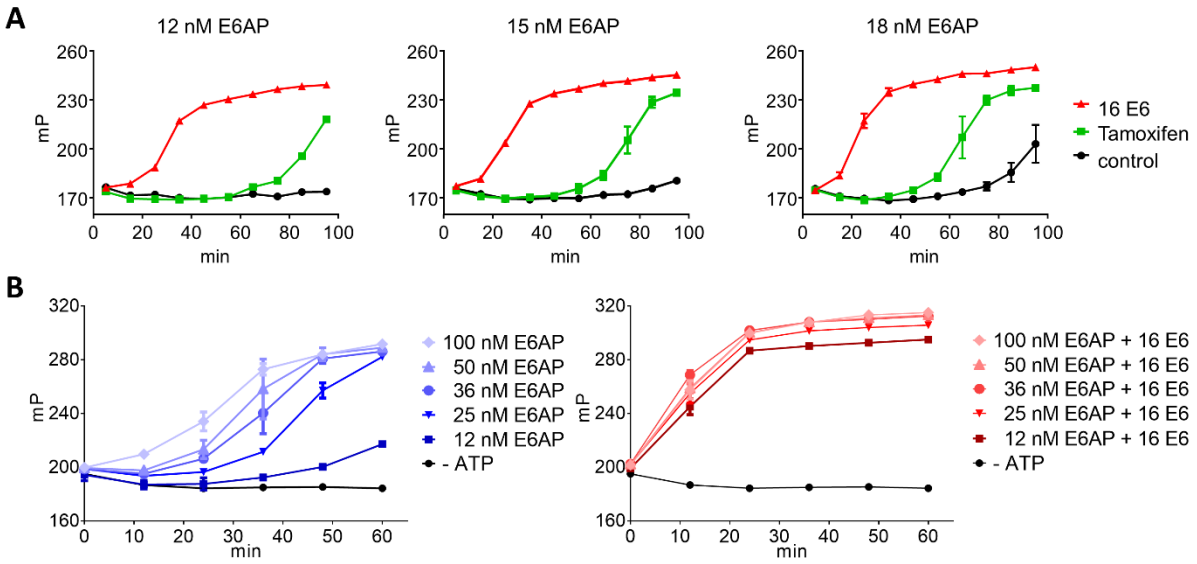

Figure 17: E6AP titration in FP-based ubiquitination assays to adjust conditions for activator screen
(A) FP-based E6AP auto-ubiquitination assays were performed with different concentrations of E6AP as indicated either for its own, with 50 µM Tamoxifen, or in presence of HPV-16 E6. The assays were pipetted manually. (B) FP-based E6AP auto-ubiquitination assays performed in absence or presence of HPV-16 E6 with the indicated amounts of E6AP in the HTS workstation. Additional controls without ATP were included. Liquid handling and temperature control were implemented as planned for the HTS.

4.3.2 Primary screen for E6AP activators

142 library plates with in total 48,077 compounds were screened with 50 µM to identify activators of E6AP. 53 hits were identified by setting a threshold of either 32% activation after 45 min or 70% activation at the 55 min time point. This corresponds to a hit rate of 0.11%. FP values of positive and negative controls were constant in an acceptable manner for most plates (figure 18 A). Due to unknown reasons, positive controls of the last 13 screened plates reached FP values of only 210 mP instead of 250. Therefore, two of the last 13 plates had Z' values between 0.2 and 0.5 resulting in an increased probability of false negative results for these plates. Z' values of all other plates were between 0.54 and 0.93 with a mean of 0.84 (figure 18 B). None of the 3263 wells containing DMSO nor any of the 1136 negative controls scored as false positive hit.

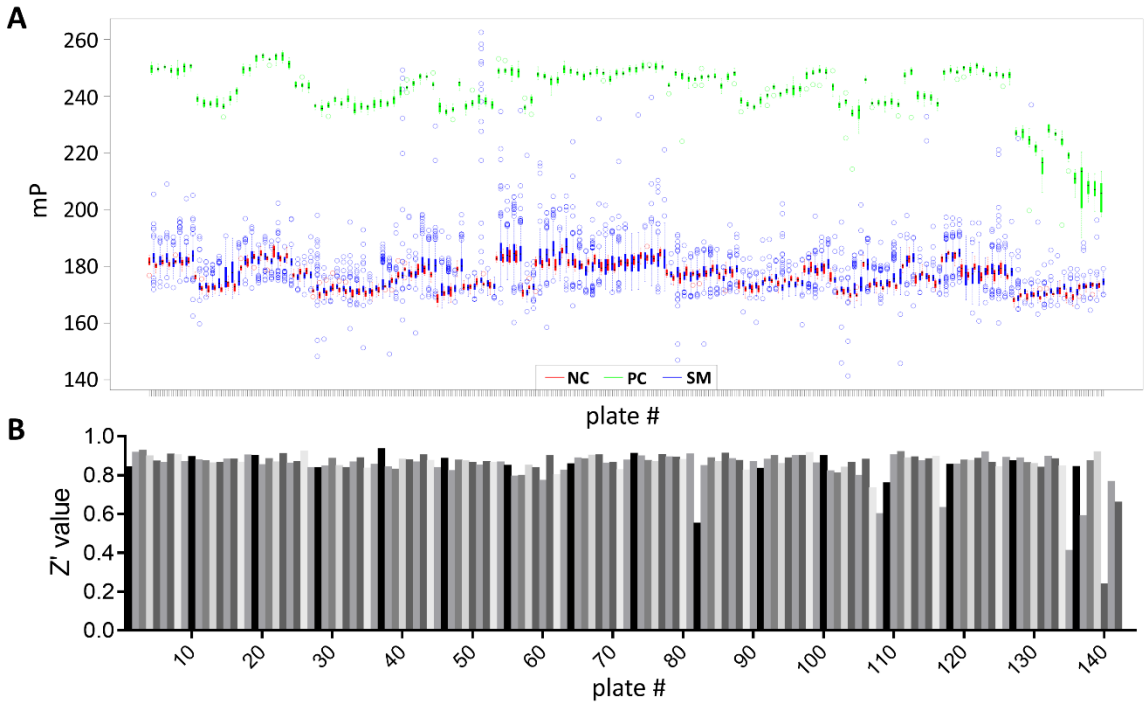

Figure 18: Results of the HTS for small molecule activators of E6AP
(A) Boxplot graphs with FP values of samples and controls from all 142 screened plates are shown. Negative controls (NC) are colored red, positive controls (PC) are colored green and samples (SM) are shown in blue. (B) Corresponding Z' values of the 142 screened plates.

4.3.3 Secondary assays with small molecule activators of E6AP

4.3.3.1 Counter screen with RLIM_RING

As with the hits from the E6-E6AP inhibitor screen, a counter screen with RLIM_RING was performed to probe whether hits from the E6AP activator screen lead to an unspecific increase of FP values and thus should be excluded from subsequent experiments. To do so, the 14 library plates with the most hits (29 hits) were counter tested. Low RLIM_RING concentrations (50 nM) were employed to monitor a possible stimulation resulting in an increase of FP values. Twice the concentration (100 nM) was used as positive control. None of the tested compounds resulted in a significant increase of FP values at the 45- or 55- min (figure 19 A and appendix table II). Importantly, the increase of the positive controls to 230 mP respective 240 mP at the two time points resulted in Z' values of about 0.8 indicated proper functioning of the counter screen (figure 19 B). Although RLIM_RING auto-ubiquitination is mechanistically not directly comparable to E6AP auto-ubiquitination, E1, E2 and Ub-T concentrations, the compounds and their concentrations, reaction temperatures, incubation times and other parameters were identical to the primary screen with E6AP so that compounds acting at a stage other than E6AP should be identified in this set-up. Consequently, as none of the compounds induced an increase of FP values, it was concluded that these compounds act specifically at the E6AP level.

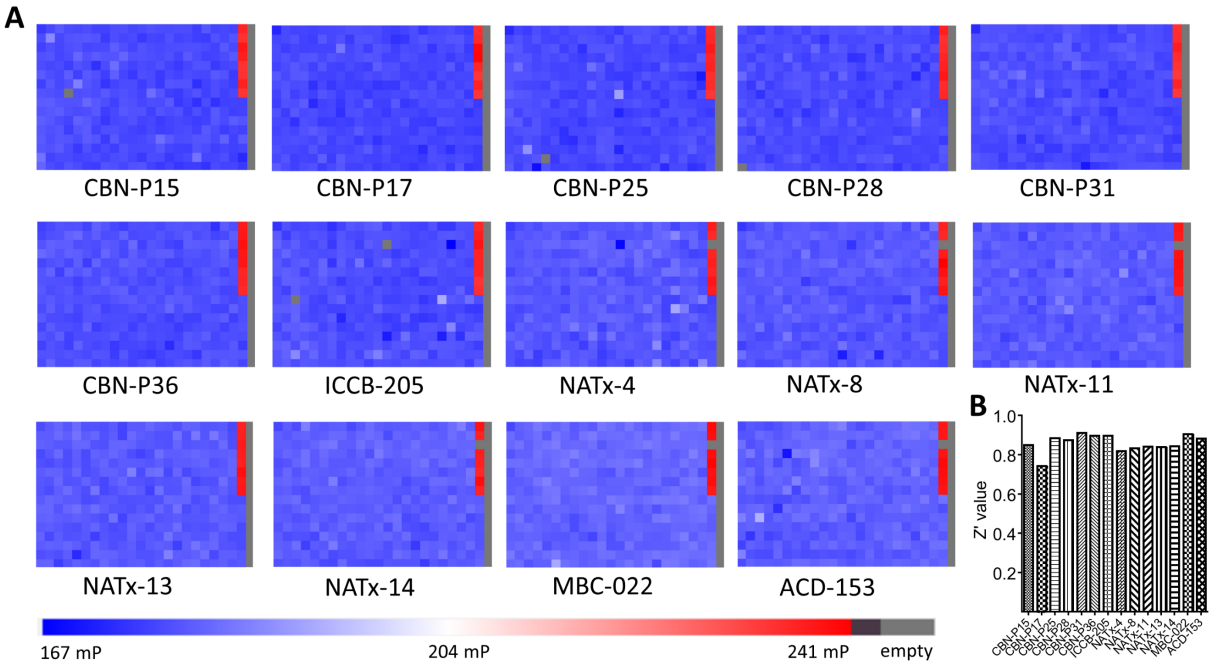

Figure 19: E6AP activators counter screen with RLIM_RING

(A) Heatmaps of FP values of the 14 counter screened plates (that were chosen as they contained the most screening hits) at 55 min reaction time are shown. The compounds were tested with assay concentrations of 50 µM like in the E6AP activator primary screen. All other concentrations and ingredients were identical to those of the E6AP activator screen. However, UbcH5b instead of UbcH7 was used as E2 enzyme. The third positive control (namely well 23 C) was due to a technical error not pipetted correctly for all plates and was thus excluded from evaluation. The color code of the heatmaps is given below them. (B) Column bar graphs with respective Z' values.

4.3.3.2 Evaluation of cherry-picked screening hits

For further evaluation, 43 compounds that scored positive in the E6AP activator screen were cherry-picked from ChemBioNet (12 hits), Maybridge (11 hits) or NATx (12 hits) libraries or purchased (8 hits). 23 of them were tested to not score in the counter screen with RLIM_RING as described above (chapter 4.3.3.1). The 43 compounds were retested with the screening assay in the HTS workstation with a concentration of 10 µM for activation of E6AP. 21 of them were reproduced with ≥ 10% activation at 55 min reaction time (corresponding to ≥ 3-fold standard deviation of the negative controls), while 22 showed less than 10% activation and were thus considered as weak activators or to be inactive (appendix table II). From the 8 purchased compounds, 4 scored active while the 4 others scored inactive according to the set threshold.

4.3.3.3 Evaluation of purchased hits

Three compounds (OF211, OF216 and OF227) from the NATx library that showed strong activation of E6AP in the experiment with the cherry-picked compounds were purchased for further evaluation. Hence 7 of the 21 hits confirmed in the cherry-picking experiments and 4 compounds that showed mild effects in this experiment were available for further experiments (all 11 structures are shown in figure 20 A). Moreover, in the meantime, five compounds (OF232-236), had been identified by Franziska Müller in our group in a screen for activators of the Angelman syndrome-derived mutant E6AP_F583S. These isoalloxazine derivatives showed strong activation of E6AP (appendix table II) so that they were included in further evaluation (structures are shown in figure 20 B).

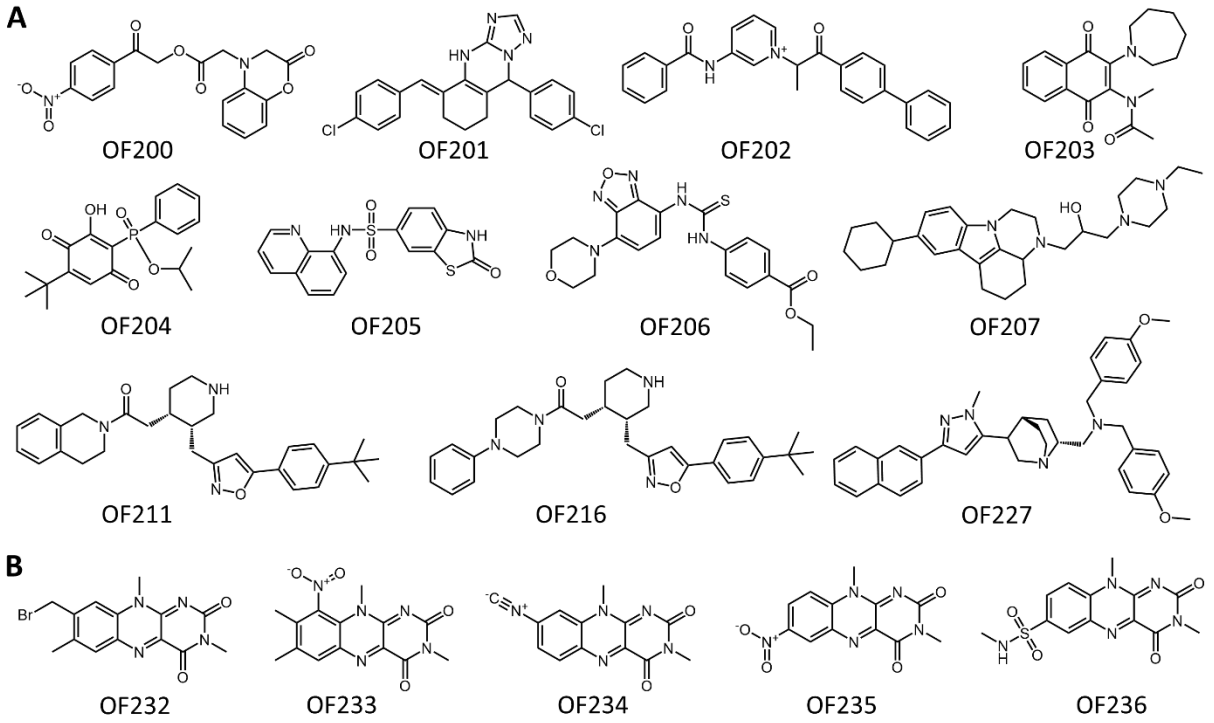

Figure 20: Chemical structures of closer investigated E6AP activators
(A) Chemical structures of purchased screening hits are displayed. (B) Chemical structures of the identified isoalloxazine derivatives are shown. These compounds were found by Franziska Müller in a screen for E6AP_F583S activators from an in-house chemical library (MDB library, note that this library was not included in the primary screen for E6AP activators). All compounds were numbered according to an internal name assignment with OF2XX as potential E6AP activators. A list with respective unique IDs (uiid) from the Screening Centre of the University of Konstanz, suppliers and order numbers as well as secondary assay results is given in appendix table II.

In secondary assays with a first group of ordered compounds (OF201 to OF207) and conditions as in the primary screen, the activating effect of the compounds on E6AP was confirmed (figure 21 A). Aside from the bacterially expressed E6AP also E6AP expressed by the baculovirus system in insect cells was tested. Reactions with baculovirus expressed E6AP were in general slower, however comparable results regarding small molecule activation were obtained. The strongest activation was by compound OF204 while the other compounds showed mild to medium effects (figure 21 A).

Next, purchased OF211, 216 and 227 were tested in the FP-based E6AP auto-ubiquitination assays together with OF204 and the isoalloxazine derivatives (OF232 to 236). As E2 enzyme either UbcH5b or UbcH7 were used, with similar results obtained for both (figure 21 B). These results further confirmed that the compounds target E6AP and not the E2 enzyme. Furthermore, the compounds were tested with the catalytically inactive E6AP_C820A mutant. No increase of FP values could be observed with any of the compounds, supporting the notion that the compounds indeed stimulate the catalytic activity of E6AP (figure 21 B). The natural product derived compounds (OF211, OF216, OF227) as well as the five isoalloxazine derivatives (OF232-236) stimulated E6AP. The strongest activation was achieved by OF227.

The two isoalloxazine derivatives OF232 and OF234 showed with concentrations lower than 10 µM clear activation of E6AP; however, both, especially OF234, showed with higher concentrations also unspecific inhibition of E6AP and of other E3 ligases (as shown below in chapter 4.3.3.8). Therefore, the effect of the most potent compounds (OF204, OF211, OF227, OF232 and OF234) on E1 activity was assessed. To do so, a refined version of the ATP sensor cleavage assay was employed (Hammler et al., 2020) showing that OF232 and OF234 act as E1 inhibitors (figure 21 C). However, follow-up experiments showed that by increasing E1 amounts, an overall activating effect towards E6AP could be achieved also with higher OF234 concentrations.

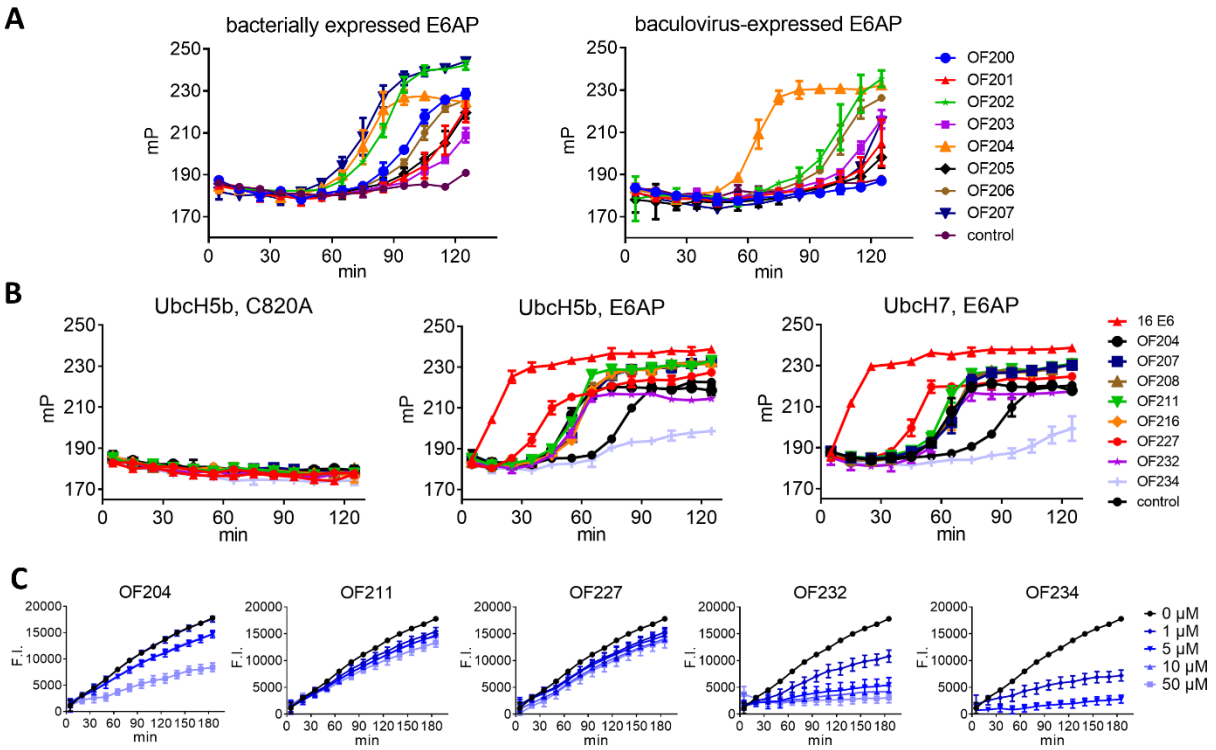

Figure 21: Purchased hits from the E6AP activator screen were evaluated in FP-based E6AP auto-ubiquitination assays and E1 activity assays

(A) FP-based auto-ubiquitination assays with bacterially expressed or baculovirus-expressed E6AP as indicated were performed to verify the purchased screening hits. (B) Further FP-based E6AP auto-ubiquitination assays with purchased compounds. The left panel shows assays with the catalytically inactive E6AP_C820A mutant. The middle and right panel show FP-based E6AP auto-ubiquitination assays with wild-type E6AP and UbcH5b or UbcH7 as E2 enzyme, respectively. Assays were performed with 10 µM compounds at 30°C. (C) E1 enzyme activity assays with a novel ATP probe according to (Hammler et al., 2020) with used compound concentrations indicated. Error bars indicate SEM of technical triplicates.

4.3.3.4 Comparison of commercially available OF211 analogues

Two of the confirmed hits (OF211 and OF216) have a highly similar scaffold. 17 analogues with a related scaffold were commercially available (OF209 to OF226). These compounds were purchased and tested in a dilution series in FP-based E6AP auto-ubiquitination assays. EC50s were determined from FP values at the 55 min reaction time from samples of a dilution series of the compounds from 50 µM to 50 nM. Structures and EC50s are shown in figure 22. Three of them showed activation with EC50s lower than 10 µM, nine showed activation between 10 µM and 75 µM, while five did not show any activating effect. These results confirmed the potency of the activators identified by HTS, while none of the additionally tested compounds showed more potent effects on E6AP activation.

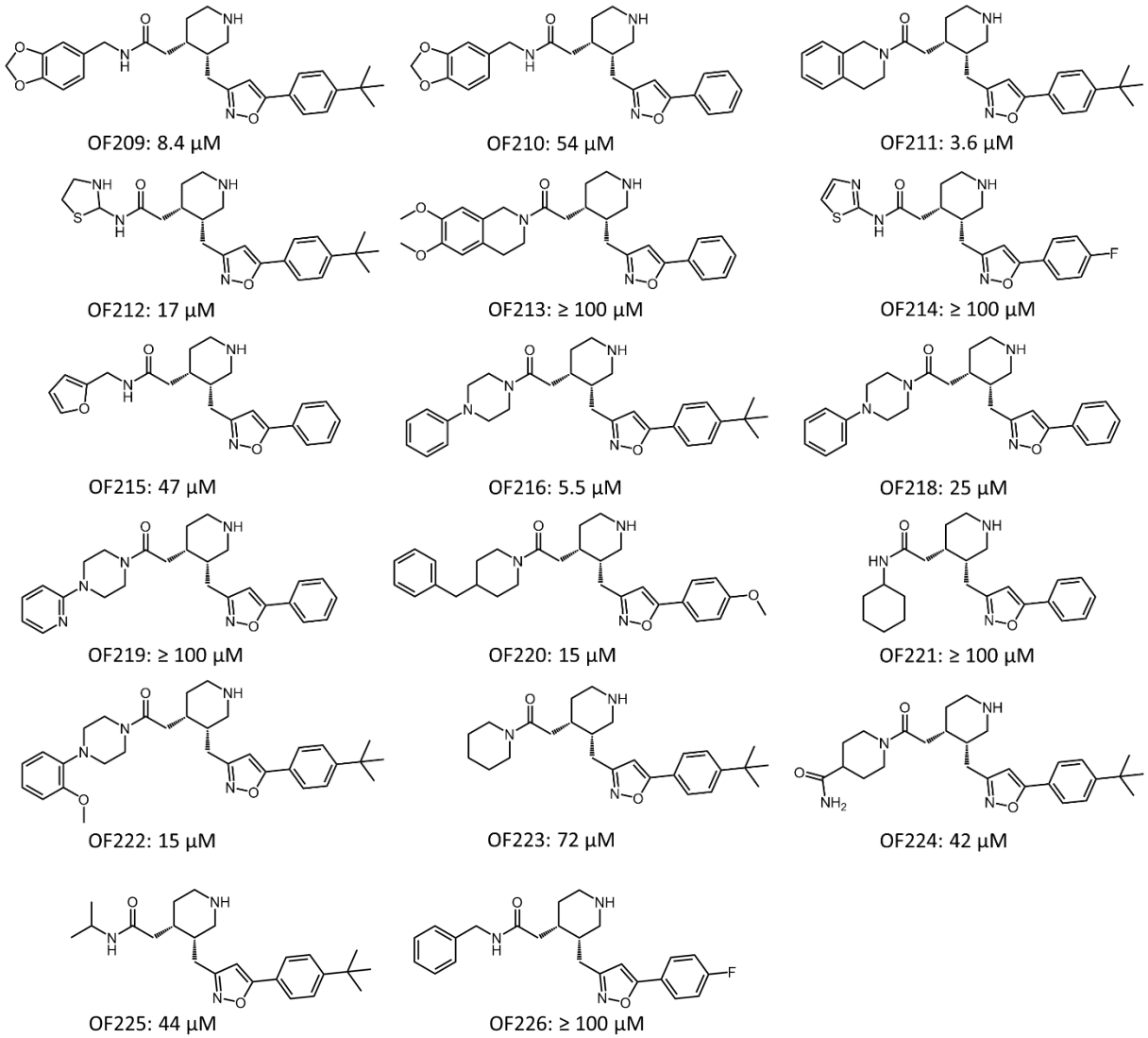

Figure 22: Comparison of purchased OF211 analogues in their potency to activate E6AP
FP-based E6AP auto-ubiquitination assays were performed with concentrations from 50 nM to 50 µM of in total 17 structurally related purchased compounds. FP values of the 55 min reaction time were used to determine the given EC50 values by non-linear regression (fitting with a variable slope with four parameters) with GraphPad Prism.

4.3.3.5 Tamoxifen and derivatives activate E6AP

Besides the screening hits another discovery was made in the present study. In the course of an early pilot screen for E6AP activators two candidate small molecules were identified (Offensperger, 2015). Their activating effects were not consistent, however, a bioinformatic tool (Reid et al., 2008) revealed that one of them owns a pharmacologic profile closely related to drugs acting on nuclear hormone receptors. Therefore, several different estradiol-related hormones and pro-hormones (β-Estradiol, Testosterone, Progesterone, Dehydroandrosterone (DHEA), Dehydroisoandrosterone, 17α-Hydroxypregnenolone) as well as drugs acting on nuclear hormone receptors (Tamoxifen, Fulvestrant, G-1, G36, MPP, DL-Aminoglutethimide, Dexamethasone) and further small molecules that may be related to E6AP or associated cellular pathways (Retinoic acid, Vitamin D3, Anastrozol, Letrozol, MDL-28170, Y27632, UO126, LY294002, Rapamycin, CHIR99021, Latrunculin A) were tested in the FP assay. Most of them showed neither activating nor inhibiting effects (data not shown). However, Tamoxifen strongly stimulated E6AP. Therefore, 4-Hydroxytamoxifen and Endoxifen (the active metabolites of Tamoxifen in estrogen receptor modulation) as well as Raloxifen, a SERM (selective estrogen receptor modulator), that is chemically closely related to Tamoxifen were purchased (figure 23 A) and tested in FP-based E6AP auto-ubiquitination assays. All four compounds showed comparably potent activation of E6AP with UbcH5b or UbcH7 as E2 enzyme (figure 23 B). In absence of E2 enzymes, no increase of FP values was observed confirming that E6AP-mediated ubiquitination was indeed needed. Noteably, although it is apparently present in the ICCB library, Tamoxifen was not identified in the HTS for unknown reasons (data not shown).

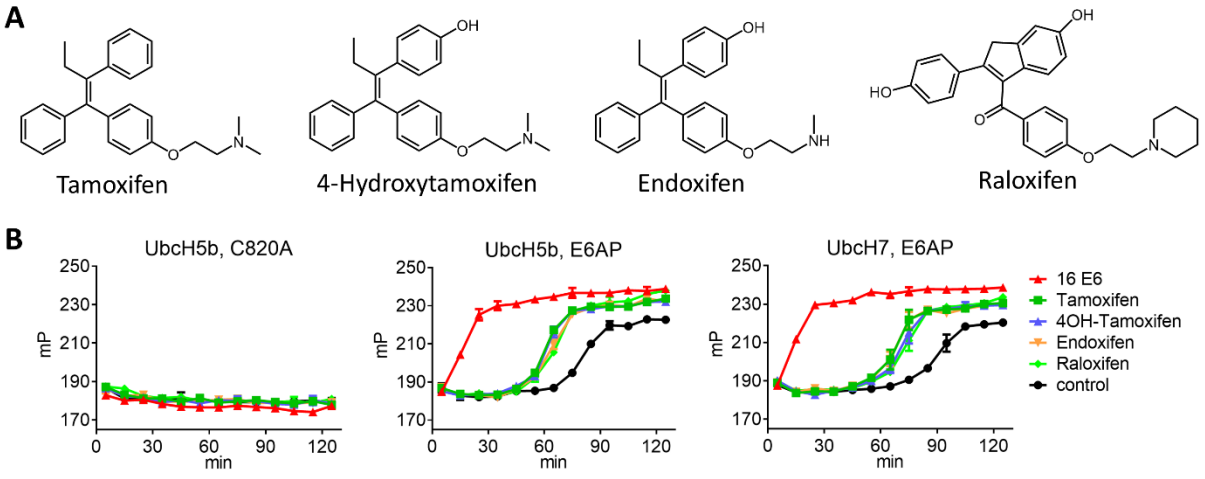

Figure 23: Tamoxifen and derivatives of it activate E6AP
(A) Chemical structures of Tamoxifen and investigated derivatives are shown. (B) FP-based E6AP auto-ubiquitination assays with 10 µM of the compounds indicated. Either UbcH5b or UbcH7 was used as E2 enzyme as indicated with wild-type E6AP or the catalytically inactive E6AP_C820A mutant.

Tamoxifen is administered as selective estrogen receptor modulator (SERM) in breast cancer therapy in pre-menopausal women (Shagufta & Ahmad, 2018). In this context, Tamoxifen is a prodrug that is metabolized by Cytochrome P450 (CYP) enzymes. CYP3A4 demethylates Tamoxifen at the terminal nitrogen and CYP2D6 hydroxylates Tamoxifen at its 4-position. The 4-hydroxy group increases affinity to estrogen receptor α (ERα) nearly 100-fold (Malet et al., 1988). The major effects of the 4-hydroxy group were underlined by solving a complex of ERα with 4-Hydroxytamoxifen (Shiau et al., 1998). As shown above in this chapter, Tamoxifen and its metabolites showed similar effects on E6AP. To increase specificity of Tamoxifen for E6AP, we hypothesized that blockage of the 4-position by a methyl group should reduce *in vivo* effects on ERα dramatically. Thus, 4-Methyltamoxifen (4Met-Tamoxifen) was synthesized (Meike Liebmann, AG Marx, University of Konstanz) and purity was confirmed by mass spectrometry and NMR (not shown). Next, FP-based E6AP auto-ubiquitination assays were performed to test whether 4Met-Tamoxifen showed the desired effects on E6AP. Indeed, different concentrations of 4Met-Tamoxifen showed comparable effects to the same concentrations of Tamoxifen or 4-Hydroxytamoxifen with the E2 enzyme used not making a difference (figure 24). Taken together, Tamoxifen and its derivatives showed consistently strong activation of E6AP.

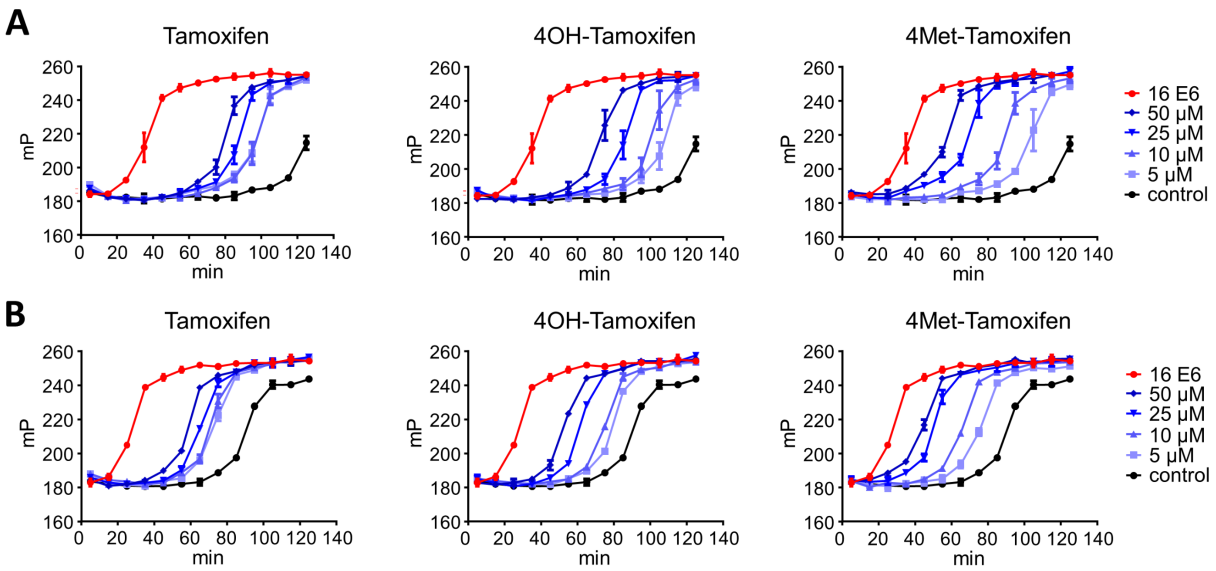

Figure 24: Comparison of Tamoxifen, 4-Hydroxytamoxifen and 4-Methyltamoxifen in FP-based E6AP auto-ubiquitination assays

FP-based E6AP auto-ubiquitination assays were performed with the indicated concentrations of Tamoxifen, 4OH-Tamoxifen or 4Met-Tamoxifen with (A) UbcH5b or (B) UbcH7 as E2 enzyme. Negative and positive (HPV-16 E6 containing) controls were included.

4.3.3.6 Evaluation of isoalloxazine-related compounds

Since compounds OF232-236 have an isoalloxazine scaffold, also known as flavin-like scaffold, different physiologically relevant flavins (Riboflavin, FMN, FAD) and polycyclic aromatic hydrocarbons (Fluorene, Fluorenone, Fluoranthrene, Phenanthrene, Anthracene) were tested for E6AP modulation. They showed neither activating nor inhibiting effects (data not shown). However, the structurally more distant Acriflavin showed a mild activation of E6AP (data not shown). Moreover, flavins are known to act as DNA intercalators and metal ion chelators (Herfeld et al., 1994). Therefore, other DNA intercalators (propidium iodide that scored also as hit in the primary screen and has a chemical structure related to Raloxifen, Cisplatin and Doxorubicin) and an ion metal chelator (EDTA) were tested (with 1, 10, 50 µM) in E6AP auto-ubiquitination assays with no obvious effects (data not shown).

4.3.3.7 Fluorescence scan of SDS-PA gels confirms stimulation of ubiquitination by small molecules

To determine whether activation of E6AP by the small molecules resulted in the same typical pattern of poly-ubiquitin smear as seen in conventional ubiquitination assays (see figure 5 for example), aliquots of the FP assays were also separated by SDS-PAGE and Ub-T was visualized by fluorescence scan. Indeed, the pattern looks identical to non-activated ubiquitination reactions and indicates typical poly-ubiquitination of E6AP. The band of free Ub-T disappears whereas a poly-ubiquitin smear appears at the junction of separating and stacking gel. Mild activation of E6AP by OF202, 204, 207 and strong activation of E6AP by Tamoxifen and OF211 can be seen in the FP assays (figure 25 A). These observations are in line with the fluorescence scans (figure 25 B).

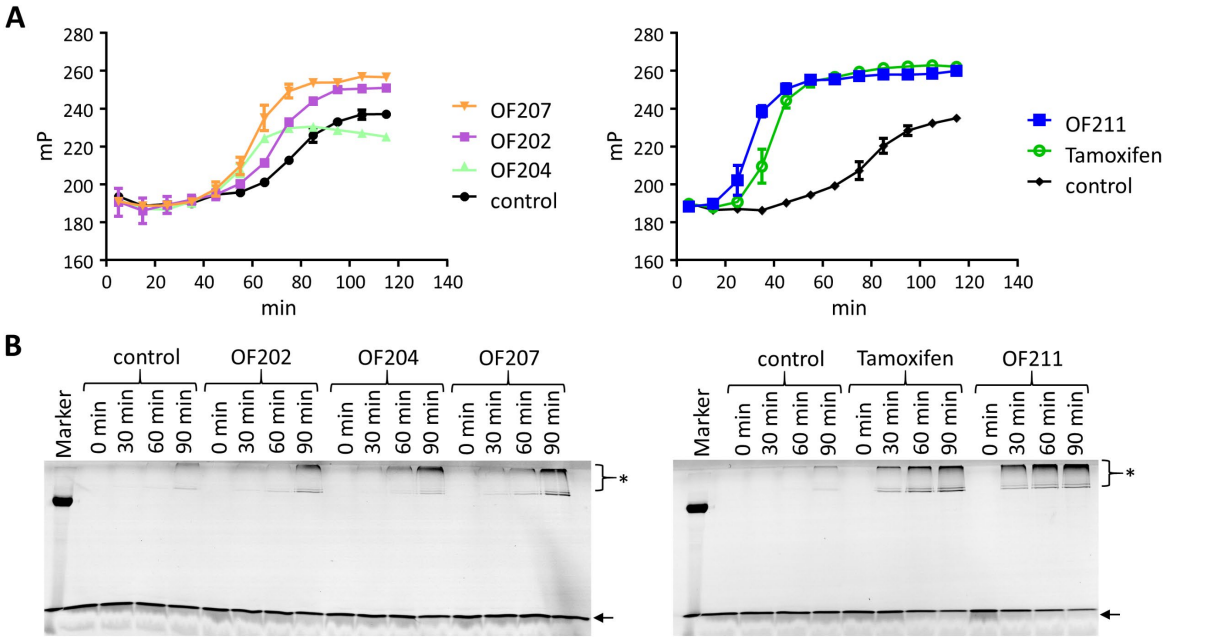

Figure 25: Fluorescence scan analysis of SDS-PA gels of FP-based E6AP auto-ubiquitination assays in presence of small molecule E6AP activators

(A) FP-based E6AP auto-ubiquitination assays were performed without or with 10 µM compound as indicated at 30°C. (B) Additional samples were incubated in the same plate in the FP reader. Samples were taken at the indicated reaction times and separated by SDS-PAGE. Ub-T was visualized by fluorescence scan. The marker band indicates 70 kDa, the arrow marks free ubiquitin and the asterisk marks poly-ubiquitin species of Ub-T.

4.3.3.8 Specificity of activators for E6AP

The results presented so far showed that the faster increase of FP values in presence of the small molecule activators was dependent on ubiquitination conditions (i.e. presence of ATP, $MgCl_2$ and all enzymes of the ubiquitination cascade) and catalytically active E6AP. The next step was to confirm that the small molecule activators were specific for E6AP. To do so, FP-based ubiquitination assays were performed with HUWE1_trunc and RLIM_RING. Their concentrations were adjusted so that a slow ubiquitination reaction was achieved. All other enzyme concentrations and parameters were maintained as in the FP-based E6AP auto-ubiquitination assays. Exemplary data from assays with Tamoxifen are shown in figure 26. A strong stimulation of E6AP but no effect on HUWE1_trunc or RLIM_RING auto-ubiquitination was observed in FP-based (figure 26 A) as well as in fluorescence scans of aliquots of reactions of the FP-based assays (figure 26 B).

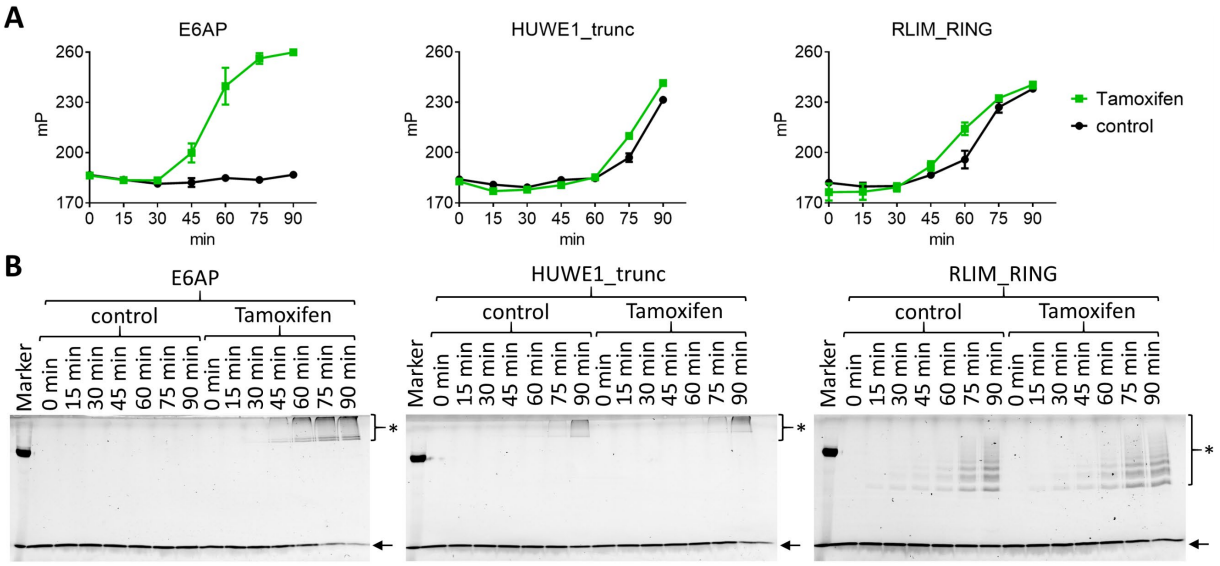

Figure 26: Tamoxifen activates E6AP auto-ubiquitination of but not of HUWE1_trunc or RLIM_RING
(A) FP-based auto-ubiquitination assays were performed with 20 nM E6AP, 100 nM HUWE1_trunc or 100 nM RLIM_RING with or without 50 µM Tamoxifen. (B) Samples incubated on the same plate were stopped after the indicated reaction times and afterwards analyzed by SDS-PAGE and fluorescence scan (532 nm excitation and 575 nm emission filter). The marker band indicates 70 kDa, the arrow marks free Ub-T, and poly-ubiquitin species of Ub-T are labeled by an asterisk.

Next, FP-based auto-ubiquitination assays were performed with different concentrations of the seven most potent small molecules with E6AP, HUWE1_trunc, RLIM_RING, or HDM2_RING (figure 27). As additional positive control, samples with the doubled E3 concentration were included for each E3 ligase. OF204, OF208, OF211, and OF216 showed with concentrations of 5, 10 and 20 µM activation of E6AP that is comparable to activity of the 2xE6AP control, but no effects on the other E3 ligases. OF227 showed a strong dose-dependent stimulation of E6AP and with higher concentrations also mild stimulating effects on HUWE1_trunc but no effects on the RING E3 ligases. For the isoalloxazine derivatives OF232 and OF234 stimulation of E6AP with concentrations up to 10 µM were observed, which turned into inhibition with higher concentrations. OF232 and OF234 also showed inhibiting effects on HUWE1_trunc and mild inhibiting effects on RLIM_RING with the low concentrations tested (figure 27).

The inhibitory effect of the compounds, especially of OF234, most likely originates from their inhibiting effects on the E1 level, as shown in figure 21. In follow-up experiments with higher E1 concentrations, overall stimulating effects on E6AP could be obtained even with higher concentrations of E1. For comparability reasons, the E1 concentration was maintained as used in the screen for the following experiments.

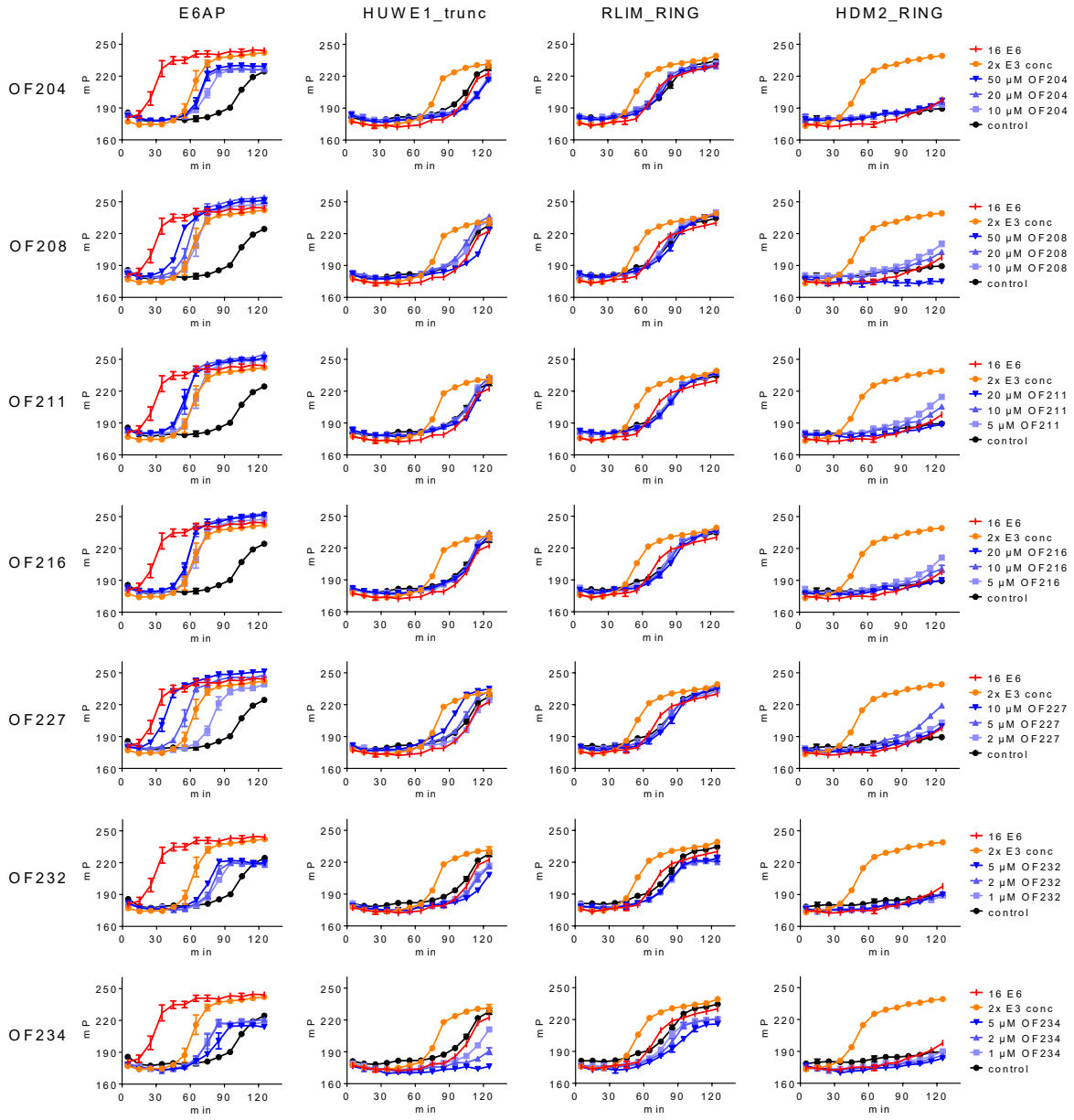

Figure 27: Specificity assessment of small molecule activators in FP-based ubiquitination assays with different E3 ligases

FP-based auto-ubiquitination assays were performed with E6AP, HUWE1_trunc, RLIM_RING or HDM2_RING. Approximately 25 nM of each E3 was used with 50 nM ot them used in the 2x E3 conc controls. Note that GST fusion proteins of HUWE1_trunc, RLIM_RING and HDM2_RING were used. Compound concentrations were used as indicated on the right hand side.

4.3.3.9 Evaluation of activators in conventional E6AP ubiquitination assays

To test whether the stimulating effects were an artifact due to the TAMRA labeling of ubiquitin, conventional *in vitro* ubiquitination assays followed by SDS-PAGE and Coomassie blue staining were performed. It should be noted that the enzyme concentrations in this type of assay are significantly higher (10x E1, 10x E2, 5x E6AP, 10x total ubiquitin) than in the FP-based assays. Furthermore, assays need to be stopped at rather early time points so that the reaction has not come to completion.

Ubiquitination assays with the eight compounds ordered first showed activation of E6AP by Tamoxifen, 4-Hydroxytamoxifen, OF204 and OF207 (figure 28 A). In a later experiment, strong stimulating effects could be confirmed for OF204, OF211, OF216, OF232, and OF234, while OF207 and OF227 showed only mild effects (figure 28 B). It was previously published that the hydrophobic patch mutant UbLIA (replacement of L8 and I44 by alanine) is impaired in E6AP auto-ubiquitination but that this defect can be rescued by HPV-16 E6 (Mortensen et al., 2015). The UbLIA defect could also be rescued by compounds OF211 and OF234 and in particular by OF204 and OF232 (figure 28 C). None of the compounds showed an effect on ligase-dead E6AP_C820A so that off-target effects could be excluded in this assay format (figure 28 D).

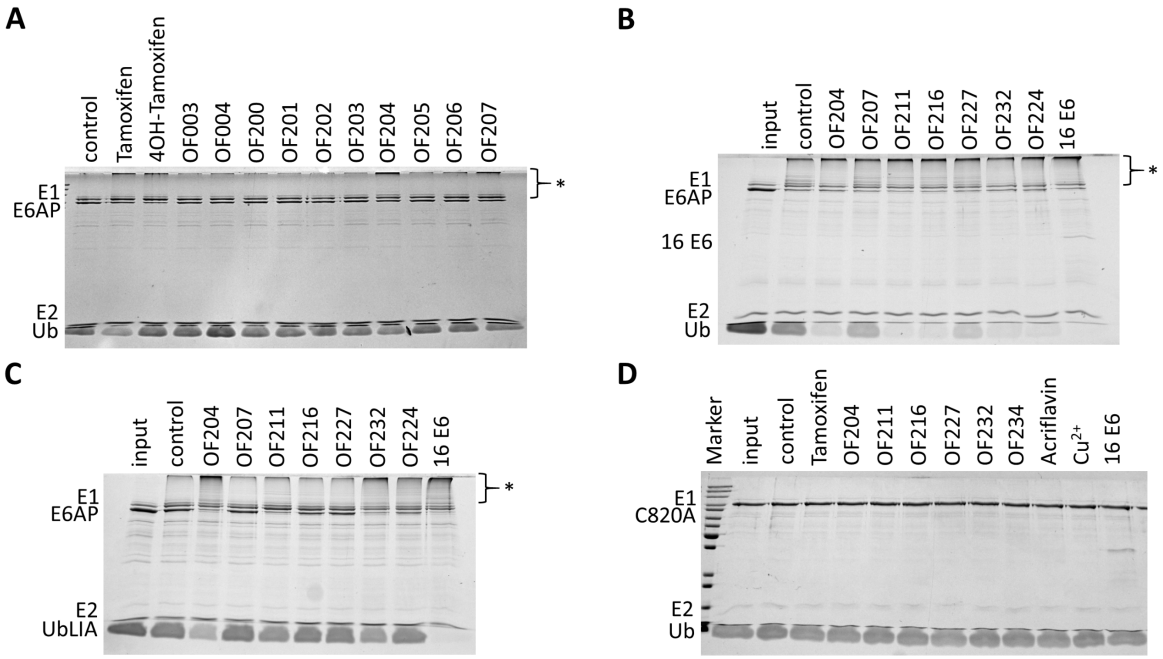

Figure 28: Evaluation of activators in conventional in vitro E6AP auto-ubiquitination assays
(A*) Conventional E6AP auto-ubiquitination assays with 50 µM compounds and stopped after 20 min at 30°C. (B) Conventional E6AP auto-ubiquitination assays with 20 µM of further compounds and stopped after 10 min at 30°C. (C) Conventional E6AP auto-ubiquitination assays with the hydrophobic patch mutant UbLIA incubated with 20 µM compounds at 37°C for 90 min. (D) Conventional E6AP auto-ubiquitination assays with the catalytic inactive E6AP_C820A mutant in presence of 20 µM compounds and incubation at 30°C for 90 min.*

Taken together, several compounds including five Tamoxifen derivatives and five isoalloxazine derivatives were identified that showed consistent, potent and specific activation in FP-based E6AP auto-ubiquitination assays. They can be classified in three groups. The first class contains compounds that show effects in FP assays. The second class contains compounds that show also effects in conventional *in vitro* E6AP ubiquitination assays analyzed by SDS-PAGE and Coomassie blue staining. The third class of compounds can additionally rescue the inability of E6AP to use UbLIA in *in vitro* E6AP auto-ubiquitination assays. A summary of our efforts to identify small molecule activators of E6AP is shown in figure 29.

Figure 29: Overview over the identification of small molecule E6AP activators
A schematic overview over results from the primary screen and secondary assays is given. Detailed primary and HTS secondary assay results as well as unique IDs (uiid) from the Screening Centre of the University of Konstanz, suppliers and order numbers of the small molecule E6AP activators are given in appendix table II.

4.4 Investigation of the effects of small molecule activators on AS-derived mutants

We identified several compounds that can reproducibly and strongly stimulate E6AP activity. Since point mutations in the *UBE3A* gene reduce the catalytic activity of respective E6AP mutants in certain cases of Angelman syndrome (AS), we investigated next whether the identified compounds are able to rescue such AS-derived E6AP mutants.

4.4.1 Characterization of AS mutants

Six different E6AP point mutations were selected ((Sadikovic et al., 2014), and F583S kindly provided by SJ Chamberlain, affiliation) with one located in the N-terminal AZUL domain (C21Y), one located in the central region of E6AP (S349P) and a cluster of four located in the middle of the N lobe of the HECT domain (ΔS582, F583S, E584Q, Q588P; called 58X AS mutants in the following) (figure 30 A). The 58X AS mutants are located at one side of the N lobe in some distance to the E2 binding site and not in direct vicinity to the C lobe (figure 30 B). Therefore, their defect is not easily explainable with the current knowledge about the catalytic activity of E6AP.

All six mutants were recombinantly expressed and characterized in auto-ubiquitination assays (figure 30 C). The C21Y mutant was as active as wild-type E6AP and therefore not further followed. With the S349P mutant, only low yields were obtained so that the protein remained impure after standard purification. Nonetheless, some, albeit impaired, ubiquitination activity was observed which could be stimulated by HPV-16 E6 to some extent. In contrast, the 58X AS mutants showed nearly complete absence of ligase activity which could however be rescued by HPV-16 E6 (figure 30 C). FP-based E6AP auto-ubiquitination assays confirmed our findings that C21Y is at least as active as wild-type E6AP, S349P is seriously impaired in catalysis and cannot be efficiently rescued by HPV-16 E6, while the 58X AS mutants are almost completely inactive on their own but can be clearly rescued by HPV-16 E6 (figure 30 D).

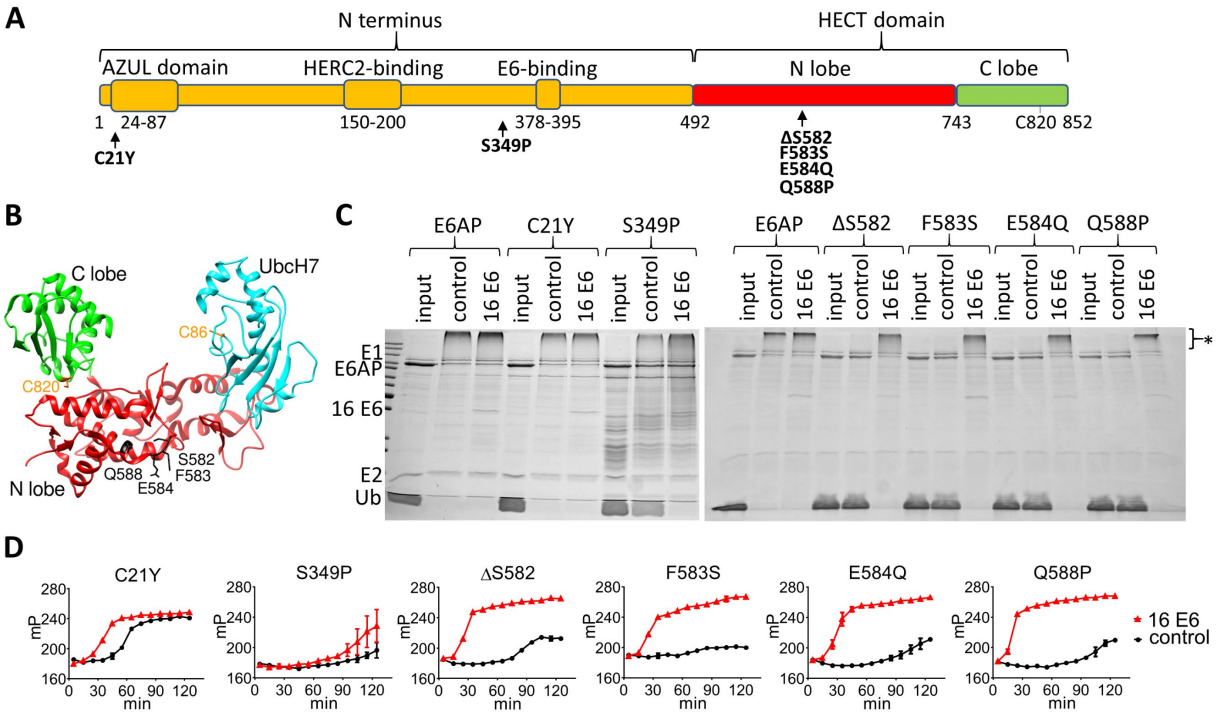

Figure 30: Characterization of AS-derived E6AP point mutants

(A) Scheme of domains and known interaction sites of E6AP with AS point mutants investigated in this study labeled in bold. (B) Illustration of the 58X AS mutations in the crystal structure of the HECT domain of E6AP (pdb:1C4Z). (C) Conventional in vitro E6AP auto-ubiquitination assays with wild-type E6AP (called E6AP) and investigated E6AP AS mutants in absence and presence of HPV-16 E6. Assays were analyzed by SDS-PAGE and Coomassie blue staining. (D) FP-based E6AP auto-ubiquitination assays with investigated AS mutants in absence and presence of HPV-16 E6. FP-based ubiquitination assays with C21Y and S349P were performed with the standard 15 nM E3 concentration at 30°C. Note that, for FP-based ubiquitination assays with catalytically impaired AS 58X mutants always 60 nM of them were used and assays were performed at 37°C.

4.4.2 Small molecule activators rescue catalytically impaired AS-derived E6AP mutants

4.4.2.1 Rescue of AS mutants by small molecules in FP auto-ubiquitination assays

Since the 58X AS mutants could be activated by HPV-16 E6, we tested all ordered activators for rescue of the 58X AS mutants in FP-based auto-ubiquitination assays (data not shown). Four compounds (OF204, OF227, OF232, OF234) showed substantial and consistent activation of all four mutants as shown for F583S (figure 31 A) and E584Q (figure 31 B). To note, higher concentrations of OF234 inhibited the reactions, due to its inhibitory effect on E1 as shown in figure 21 C.

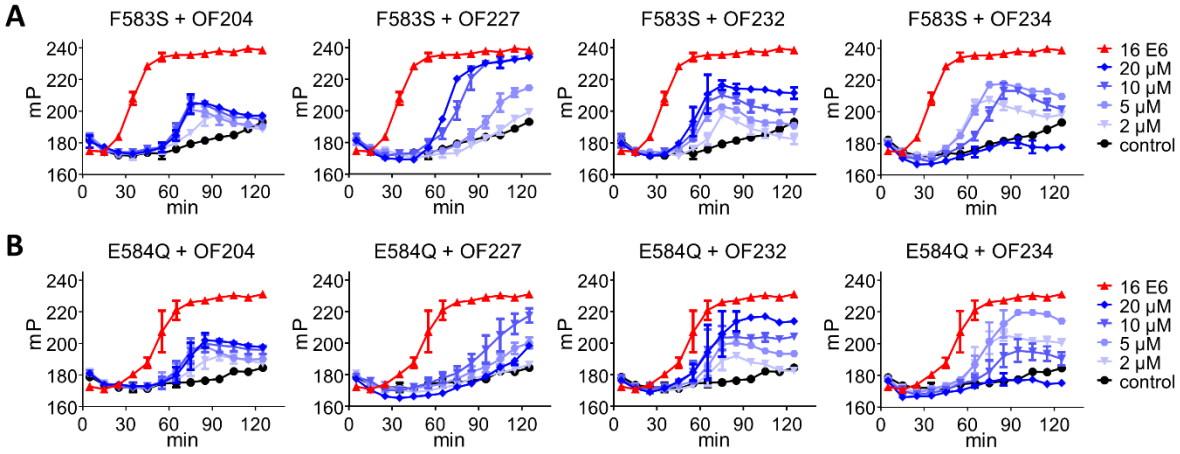

Figure 31: Rescue of 58X AS mutants by small molecules in FP-based E6AP auto-ubiquitination assays *Indicated concentrations of compounds OF204, OF227, OF232 and OF234 were tested for rescue of the strongly impaired ubiquitin ligase activity of (A) E6AP_F583S or (B) E6AP_E584Q in FP-based auto-ubiquitination assays. 60 nM of the 58X AS mutants were used and assays were performed at 37°C.*

To confirm that the increase in FP values was indeed due to ubiquitination, further FP assays were performed with different compounds and analyzed by both determing FP values and SDS-PAGE followed by fluorescence scan. Tamoxifen stimulated E6AP but did not rescue the F583S mutant. In contrast, addition of OF227 clearly resulted in an increase of poly-ubiquitinated species confirming that indeed ubiquitin chains were formed and that thus the increase of the FP signal was not due to interference with the fluorescent readout (figure 32 A). The stimulating effect of OF234 on F583S was also visible in a time course experiment with fluorescence scan of SDS-PA gels and quantitation of band intensities confirmed these results (figure 32 B).

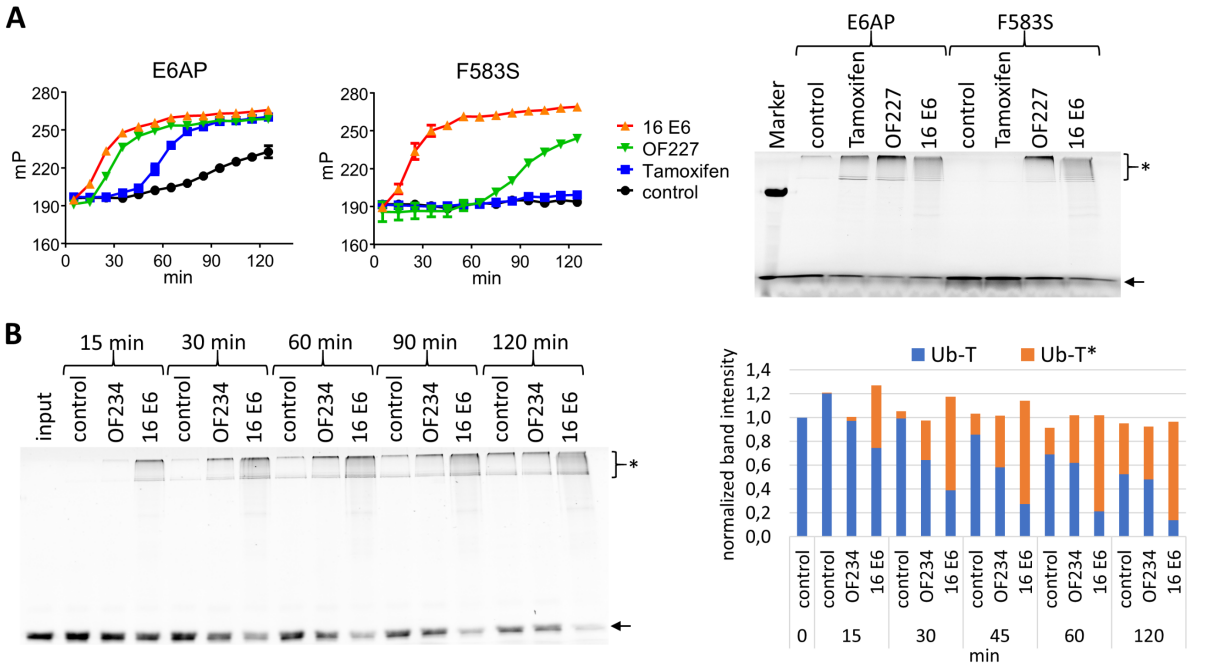

Figure 32: Fluorescence scan of SDS-PA gels of FP-based auto-ubiquitination assays supports rescue of 58X AS mutants by small molecule activators

(A) FP-based auto-ubiquitination assays with wild-type E6AP (E6AP, 15 nM) or E6AP_F583S (F583S, 60 nM) were performed at 37°C to test effects of 10 µM OF227 or Tamoxifen. After 2 h reactions were finished, and samples were analyzed by SDS-PAGE and fluorescence scan (with 532 nm excitation and 575 nm emission filter). (B) E6AP auto-ubiquitination reactions in absence or presence of 10 µM OF234 were performed under FP assay conditions, stopped at the indicated times and analyzed by SDS-PAGE and fluorescence scan. The marker band indicates 70 kDa, the arrow marks free Ub-T, and poly-ubiquitin species of Ub-T are labeled by an asterisk. Quantified band intensities are shown on the right hand side with free Ub-T shown in blue and conjugated Ub-T species shown in red.

4.4.2.2 Rescue of AS mutants by small molecules in conventional SDS-PAGE assays

Next, rescue of 58X AS mutants was investigated in conventional *in vitro* E6AP auto-ubiquitination assays analyzed by SDS-PAGE and Coomassie blue staining. Clear stimulating effects of compounds OF232 and OF234 could be seen for all four mutants, whereas OF227 showed only mild effects in this assay format (figure 33). In addition, also a mild rescue of the 58X AS mutants could be observed with OF232 and OF234 when UbLIA was used as source of ubiquitin (not shown).

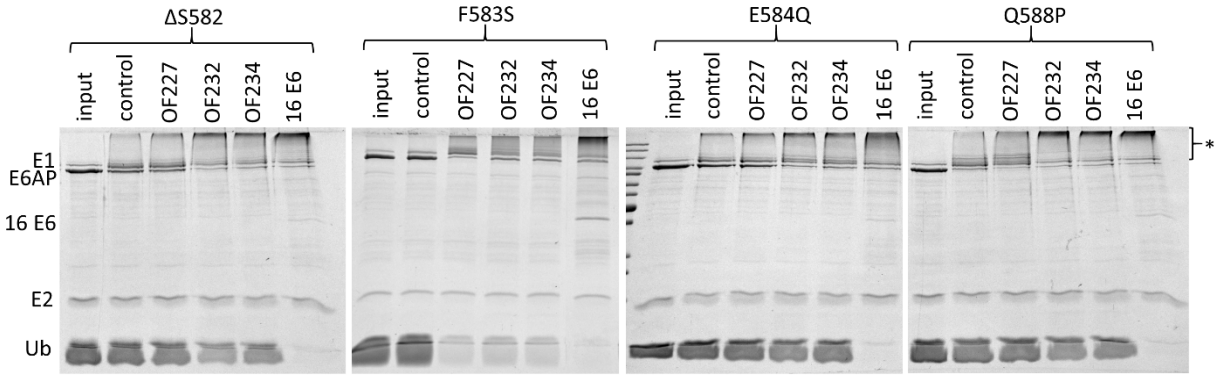

Figure 33: Conventional in vitro auto-ubiquitination assays with 58X AS mutants and small molecule activators

58X AS mutants were tested with 10 µM of compound OF227, OF232, or OF234 in conventional in vitro E6AP auto-ubiquitination assays. Reaction mixtures were incubated at 37°C for 2 h before samples were subjected to SDS-PAGE and Coomassie blue staining. Poly-ubiquitin species are labeled with an asterisk.

4.4.2.3 Investigation of the release of a potential auto-inhibitory function of the AZUL domain by compound OF232

Characterization of C21Y and ΔAZUL mutants showed that both were at least as active as wild-type E6AP if not even more active. Besides this, OF232 (and related compounds; data not shown) exhibited no activating effect on E6AP_ΔAZUL (figure 34 A). As the recombinant E6AP preparations applied in these experiments were already highly active, experiments with UbLIA instead of wild-type ubiquitin proved to be better suited to detect stimulating effects on E6AP and active mutants of it in conventional *in vitro* auto-ubiquitination assays. Yet also in experiments with UbLIA, no activating effect of OF232 on ΔAZUL was observed (figure 34 B). For these reasons, we hypothesized that the AZUL domain may act auto-inhibitory and that OF232 and similar compounds might be able to counteract this auto-inhibition. Since strong activating effects of OF232 could be observed for the 58X AS mutants, we asked whether these stimulating effects were also observed for a double mutant harboring a 58X AS mutation and lacking the AZUL domain.

Conventional *in vitro* auto-ubiquitination assays revealed that E6AP_F583S_ΔAZUL was as inactive as the F583S mutant (figure 34 C). While no activation of the double mutant was observed in conventional auto-ubiquitination assays (figure 34 C), a rescue similar as seen for the F583S mutant was observed in FP auto-ubiquitination assays (figure 34 D). Thus, regulation of E6AP's activity seems to be controlled at several layers and a more complex mechanism than just the possible auto-inhibition through the AZUL domain. In other words, the mechanism of action of OF232 (and possibly also of the other small molecules) as well as the nature of the 58X AS defect needs to be addressed by means other than the here applied mutational analysis approach.

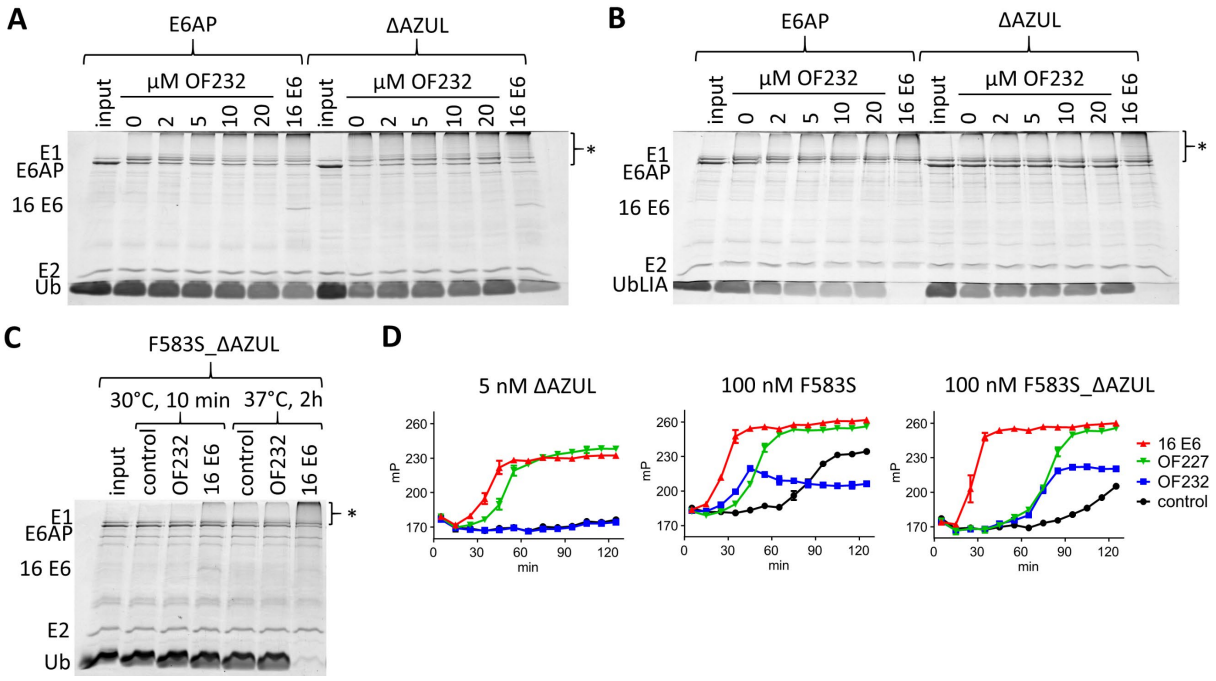

Figure 34: Investigation of a potential release of a potential auto-inhibitory function of the AZUL domain through OF232

Conventional auto-ubiquitination assays were performed with wild-type E6AP or the E6AP_ΔAZUL mutant in presence of indicated concentrations of OF232 with (A) ubiquitin (10 min reaction at 30°C). or (B) with UbLIA (2 h reaction at 37°C). (C) Same experiment with the E6AP_F583S_ΔAZUL double mutant. Reaction times and temperatures were used as indicated. (D) FP-based auto-ubiquitination assays with the indicated concentration of E6AP variants and with 10 µM of the indicated compounds. Reactions took place at 37°C.

4.5 Investigation of E6AP-mediated substrate ubiquitination

In order to regulate proteostasis, the main function of ubiquitin ligases is the modification of substrate proteins. Auto-ubiquitination is mainly thought to be an auto-regulatory mechanism and may proceed via a mechanism that is different from substrate ubiquitination. For this reason, the next step was to find out whether the identified activators are also able to stimulate substrate ubiquitination, additionally to auto-ubiquitination as investigated in all experiments so far.

4.5.1 *In vitro* Ring1B_I53S substrate ubiquitination assays with small molecules

One of the best studied and mostly used substrate of E6AP is Ring1B. As it is an E3 ligase itself (i.e. it also performs auto-ubiquitination), the catalytically inactive mutant Ring1B_I53S is usually used as substrate in ubiquitination assays. To be able to distinguish between poly-ubiquitinated E6AP and poly-ubiquitinated substrate, Ring1B_I53S is radioactively labeled (i.e. *in vitro* translated with S^{35}-methionine as sole methionine source) so that it can be detected by fluorography. Substrate ubiquitination assays were performed with all ordered activators (OF200-236), most of them showing mild effects (data not shown). However, four compounds showed consistent and potent stimulation of E6AP (figure 35 A) and, remarkably, F583S and E584Q (figure 35 B and C). For OF227, higher concentrations (50 and 100 µM) were needed to see clear-cut effects but those were highly convincing for wild-type E6AP as well as the AS-derived mutants. It is worth mentioning that these high OF227 concentrations did not result in a switch from auto- to substrate ubiquitination, as could be the case, but stimulated both reactions (data not shown). Furthermore, the overall inhibiting effect of higher concentrations (≥ 20 µM) of compounds OF232 and 234 were observed again. As shown above in figure 21 C, this issue originates presumably from inhibitory effects on the E1 enzyme.

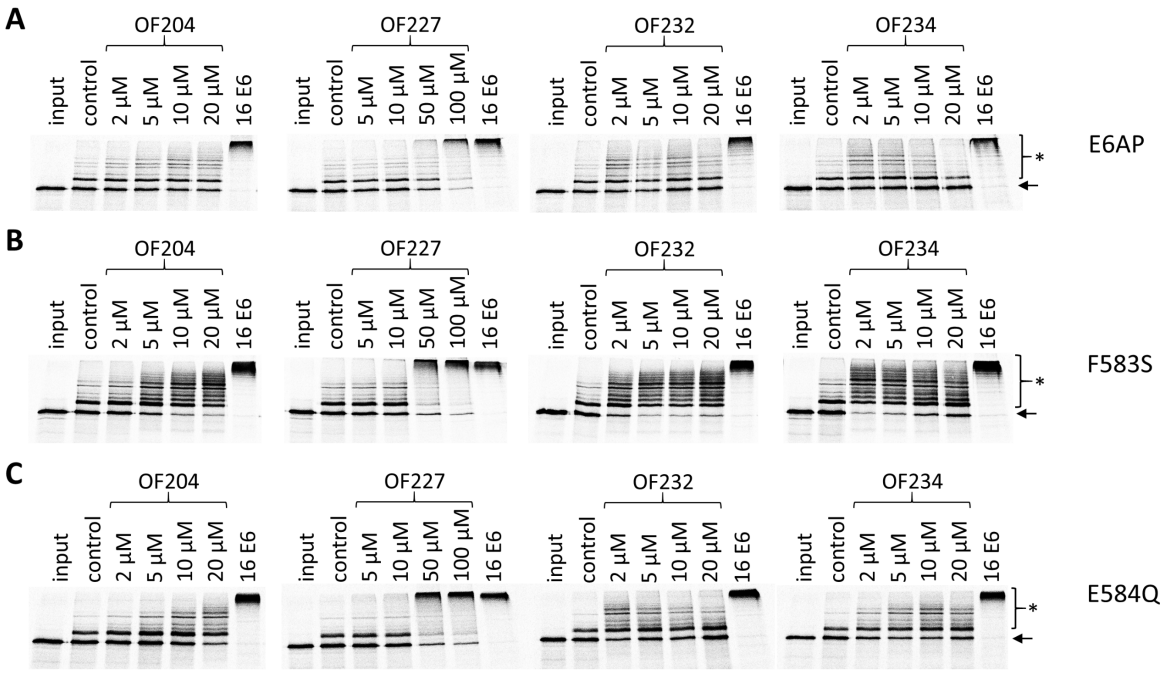

Figure 35: Stimulation of wild-type E6AP and the E6AP_F583S and E6AP_E584Q mutants by OF204, OF227, OF232 and OF234 in in vitro Ring1B_I53S substrate ubiquitination assays
In vitro substrate ubiquitination assays with radioactively labeled Ring1B_I53S were performed with the indicated concentrations of compounds. For wild-type E6AP UbLIA was used, while wild-type ubiquitin was used for the AS 58X mutants. A control reaction without any compound and a positive control reaction containing HPV-16 E6 were included. Input represents control samples stopped after 0 min while all other reactions were incubated at 37°C for 90 min. Unmodified Ring1B_I53S is marked by an arrow while ubiquitinated species are labeled with an asterisk.

4.5.2 Evaluation of small molecule activators in *in cellula* assays

In vitro assays have the great advantage that a specific enzyme can be investigated by its own. However, main drawbacks of *in vitro* assays are an altered environment of the investigated enzyme that is different from that in cells and that it cannot be excluded that the compounds of interest may also affect proteins other than the enzyme investigated. Thus, mammalian cell culture is presumably a more realistic system to investigate the effects of the identified small molecule activators. Therefore, in the next phase of this study, activation of E6AP and AS mutants was tested in *in cellula* Ring1B_I53S degradation assays, as increased ubiquitination of Ring1B_I53S by activation of E6AP should in principle lead to enhanced degradation by the proteasome and thus reduced Ring1B_I53S levels. However, first, cytotoxicity assays had to be performed to assure that depletion of Ring1B_I53S was due to increased targeted ubiquitination by E6AP and not due to cytotoxic effects of the compounds.

4.5.2.1 Cytotoxicity assays

Cytotoxicity assays were performed with H1299 parental cells, H1299 K3 cells (clonal cell line with stable knockdown of E6AP by siRNA (Kuballa et al., 2007)), and H1299 1C3 cells (clonal cell line with CRISPR-Cas knockout of E6AP (Schroff, 2017)). Western blot analysis of the cell lines with an α-E6AP antibody confirmed strong reduction or absence of E6AP in the respective cell lines (figure 36 A). OF227 showed some cytotoxicity with concentrations higher than 10 µM (figure 36 B). OF232 showed strong cytotoxicity in all three cell lines with concentrations higher than 10 µM (figure 36 C). OF234 showed even stronger cytotoxicity with no surviving cells with 5 µM in colony formation assays (figure 36 D). No difference for any of the tested compounds was visible between the different cell lines, indicating E6AP-independent cytotoxic effects.

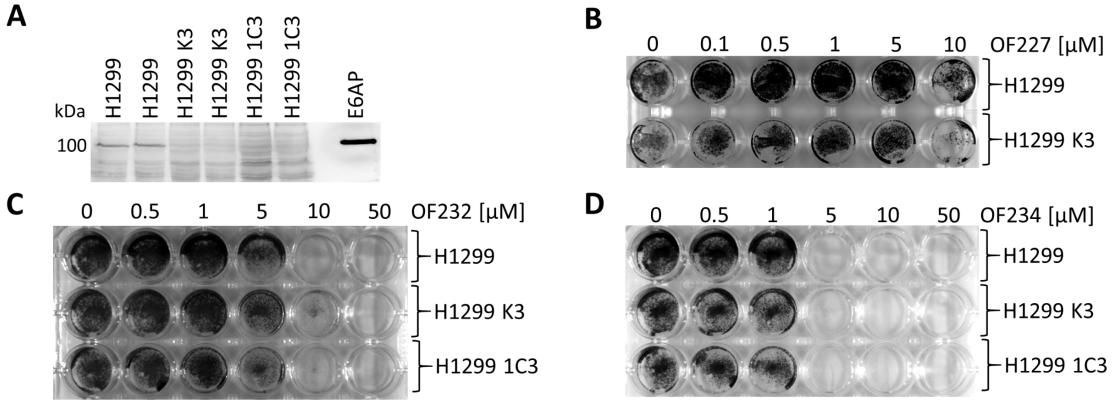

Figure 36: Cytotoxicity assays with small molecule activators OF227, OF232 and OF234
(A) Western blot analysis of two different biological samples of H1299, H1299 K3 and H1299 1C3 cells using an α-E6AP antibody. 100 ng recombinant E6AP was included as reference. (B - D) Colony formation cytotoxicity assays with the indicated cell lines and concentrations of compound OF227, OF232 and OF234, respectively.

4.5.2.2 *In cellula* Ring1B_I53S degradation assays with small molecules

As OF232 and OF234 showed inhibition of E1 (figure 21 C) and strong cytotoxic effects *in cellula* (figure 36 C and D), they were not suited for *in cellula* experiments. OF204 also showed inhibiting effects on E1 (figure 21 C) and was thus also considered as not suited for cellular experiments. Therefore, the only compound left that showed clear effects in *in vitro* Ring1B_I53S substrate ubiquitination assays was OF227. Hence, its effect on *in cellula* Ring1B_I53S degradation was examined in H1299 1C3 cells. The use of H1299 1C3 cells allowed to investigate E6AP AS point mutants in absence of any wild-type E6AP and to include controls to reveal potential E6AP-independent effects. OF227 showed a clear decrease of Ring1B_I53S levels with higher concentrations (5 to 10 µM) (figure 37). However, with 10 µM OF227, Ring1B_I53S levels were reduced also in samples with no E6AP co-transfected. Even if these effects are weaker compared to those in the presence of E6AP or 58X AS mutants, clear E6AP-

independent reduction of Ring1B_I53S was obtained with higher OF227 concentrations, presumably reflecting slight cytotoxic effects. In contrast, lower OF227 concentrations tested (2 to 5 µM) resulted in Ring1B_I53S reduction only in the presence of wild-type E6AP. With lower OF227 concentrations, no decrease of Ring1B_I53S levels in the absence of E6AP was observed but also, only a slight reduction of Ring1B_I53S levels in the presence of the 58X AS mutants. This indicates that the concentration range of OF227, in which E6AP-dependent and thus desired effects can be observed, is rather small. In addition, the reproducibility of the results obtained in transient transfection experiments proved to be limited, as significant deviations in the results obtained in several independent experiments were observed, as exemplified by the experiments shown. Therefore, a stable cell line expressing a substrate reporter construct may be superior to study the potential effects of small molecule activators on E6AP and AS mutants.

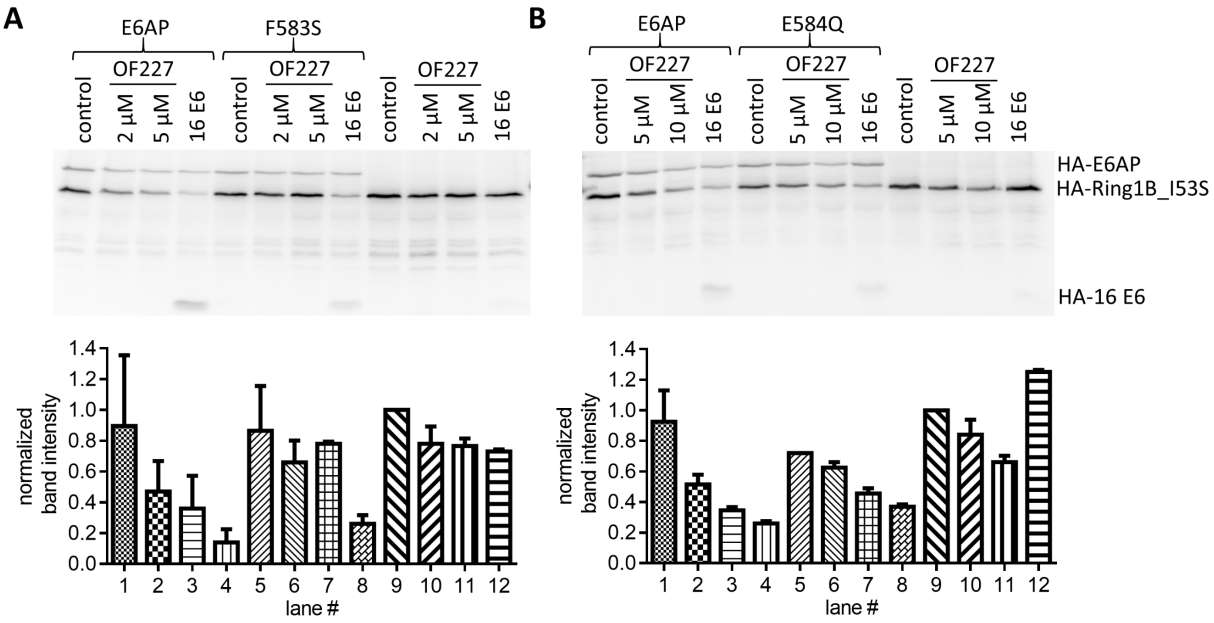

Figure 37: Evaluation of compound OF227 in in cellula substrate degradation assays
H1299 1C3 (E6AP knockout) cells were transiently transfected with 1200 ng HA-Ring1B_I53S and 300 ng beta-galactosidase expression construct. Samples were co-transfected with 900 ng HA-tagged E6AP or 58X AS mutant as indicated. Additionally, for positive control samples, 1500 ng HA-16 E6 vector was co-transfected. After 5 h, medium was exchanged with fresh medium containing compound in the indicated concentrations. After 20 h cells were harvested, and sample amounts were adjusted according to transfection efficiencies determined by beta-galactosidase activity. (A) E6AP_F583S treated with 2 or 5 µM OF227. (B) E6AP_E584Q treated with 5 or 10 µM OF227. Ring1B_I53S band intensities of two western blot replicates for each experiment were quantified with AIDA software and visualized with Prism6 software and are shown below. The column bars show the mean of the replicates and the error bars indicate standard deviations of the replicates.

4.6 Analysis of the mechanism of E6AP activation

The small molecule activators were identified in our unbiased activity-based HTS so that neither their binding site nor their mechanism of action remained unclear. However, for newly identified small molecules it is important to show that they indeed bind to their target. Ideally, X-ray crystallography is used to solve the structure of the ligand-bound protein. As for E6AP, only the structure of the HECT domain is solved, while there is no information about the structure of the full-length protein (Huang et al., 1999). Yet, the evidence obtained so far clearly indicates that the stimulating compounds require the N-terminal region of E6AP to exert their stimulating effect an that the N terminus plays a key role for the enzymatic function of E6AP (i.e. the isolated HECT domain is not fully active in auto-ubiquitination but forms mainly mono-, di- and tri-ubiquitinated species and it cannot be stimulated by the compounds). Hence, X-ray crystallography was not the method of choice in this study.

Another method to study binding is biolayer interferometry which was employed in this study by using an Octet K2 instrument from ForteBio. To do so, full-length His-tagged E6AP was immobilized on Ni-NTA biosensor tips and binding of several small molecule activators was tested. However, no significant signal changes upon potential binding could be detected (data not shown). This is likely explained by the huge size difference of the analyte (small molecules with 300 to 500 g/mol) to the immobilized molecule (E6AP with 100,000 g/mol) (i.e. the small increase in mass is below the detection limit).

4.6.1 *In vitro* thermal shift assays to investigate compound binding

Other approaches use the fact that binding of ligands often alters the thermal stability of a protein (Molina et al., 2013, Huynh & Partch, 2015). A simple variant to test this thermal shift are *in vitro* thermal shift assays (figure 38 A). While with 10 µM Tamoxifen no effects were recognizable (figure 38 B), 20 µM Tamoxifen showed mild destabilizing effects at a temperature of 60°C on E6AP and E6AP_HECT, but also on HUWE1_trunc and RLIM_RING (figure 38 C). Other tested compounds (OF227 and OF234) as well as HPV-16 E6 did also not show any remarkable effect (data not shown). Therfore, *in vitro* thermal shift assays were also not suited for E6AP.

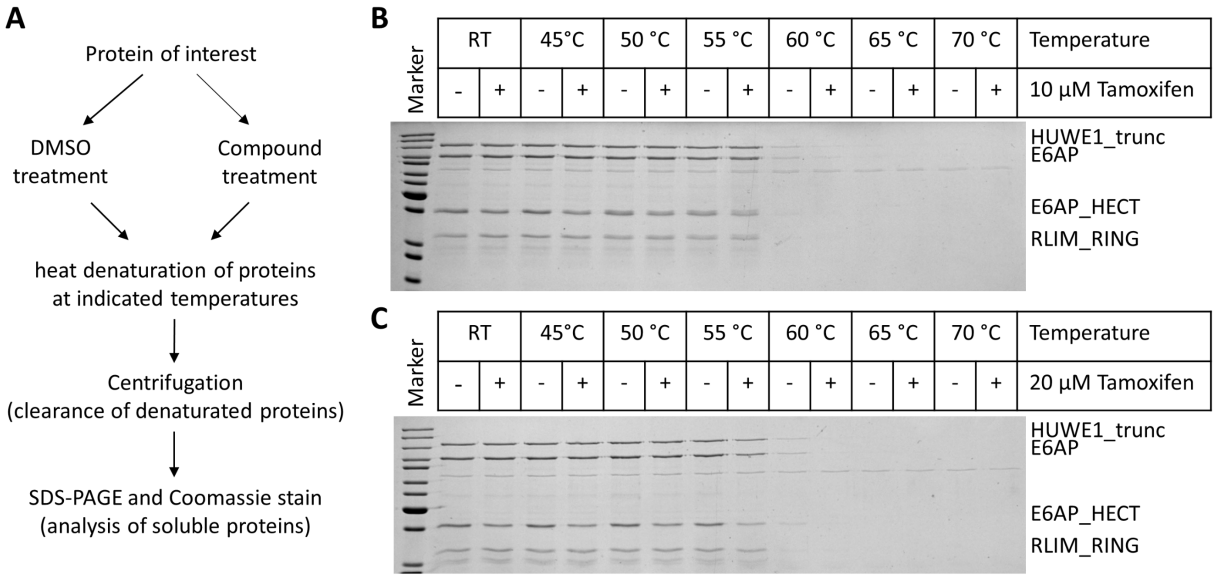

Figure 38: In vitro thermal shift assays with Tamoxifen
(A) Outline of in vitro thermal shift assays as performed. The heat denaturation step took place for two minutes in thin-walled PCR tubes in a standard PCR cycler and samples were incubated for two further minutes on ice prior to centrifugation. Similar E6AP, E6AP_HECT, HUWE1_trunc, and RLIM_RING concentrations were tested simultaneously with Tamoxifen. Shown are obtained results with (B) 10 µM and (C) 20 µM Tamoxifen.

4.6.2 Crosslinking mass spectrometry to study activation of E6AP

Chemical crosslinking coupled to mass spectrometry (XL-MS) is an emerging technique that can be used to obtain information about interactions of proteins or protein regions in protein complexes. Quantitative XL-MS (qXL-MS) can additionally allow investigation of conformational changes of protein complexes and even single proteins (Leitner et al., 2016, Chen & Rappsilber, 2018, Yu & Huang, 2018). The basic principle of XL-MS is the formation of a covalent bond between amino acid side chains of proximal proteins or protein domains by a small molecule containing two reactive groups, a so-called crosslinker. In this study, isotopically labeled disuccinimidyl suberate (DSS) was used. This homobifunctional crosslinker contains two NHS-activated carboxyl groups, which react predominantly with primary amines at pH 7 to 9, and is therefore able to link the ε-amino group of lysine residues which are in close proximity; this chemistry is used in most crosslinking studies (Iacobucci et al., 2019). For evaluation of crosslinked regions, proteins are enzymatically digested with trypsin after reduction and alkylation of cysteine residues. Afterwards, crosslinked peptides are desalted via C18 columns, enriched via size-exclusion chromatography and identified via LC-MS/MS and respective data processing and evaluation.

Identified crosslinks can either originate from different proteins (so-called interlinks) or they originate from the same protein (so-called intralinks). Crosslinks can contain a wealth of information about spatial proximity (and reactivity) of the crosslinked amino acid residues. Interlinks, on the one hand, can be used to determine neighboring proteins in protein complexes. Intralinks, on the other hand, can contain information about different conformational states of a protein. Furthermore, the entirety of crosslinks can be used as distant constraints for integrative modeling. In collaboration with Florian Stengel and his group, several XL-MS methods were applied to investigate how the E6-E6AP complex is assembled, how a substrate (i.e. p53) is positioned in the context of the full-length E6-E6AP complex and towards the catalytic center of E6AP. Moreover, effects of HPV-16 E6 and one of the small molecule activators on E6AP's structural dynamics were investigated. Finally, the crosslinking pattern of the AS mutants F583S and E584Q was compared to that of wild-type E6AP and the effect of HPV-16 E6 and the small molecules on the conformational dynamics of the 58X AS mutants was explored.

4.6.2.1 XL-MS confirms binding of HPV-16 E6 to its known binding site on E6AP and reveals proximity of HPV-16 E6 to N- and C-terminal regions of E6AP

First, the complex of full-length E6AP with HPV-16 E6 was analyzed by XL-MS. To do so, three preparations of E6AP, HPV-16 E6 and HPV-16 E6_L50E, an E6AP binding-deficient mutant (Zanier et al., 2013), were generated (figure 39 A). *In vitro* ubiquitination assays with ubiquitin (figure 39 B) and UbLIA (figure 39 C) confirmed stimulation of E6AP by HPV-16 E6 but not by HPV-16 E6_L50E. Since all proteins were functional as expected, XL-MS experiments were performed. Three different conditions, namely E6AP only, E6AP + E6 and E6AP + E6_L50E were investigated (figure 39 D). Each of those conditions was prepared with three biological replicates of E6AP. Concise technical details concerning chemical crosslinking, sample processing and mass spectrometric analysis as well as results are described in (Sailer et al., 2018). For E6AP only samples, a total of 145 unique crosslinks was identified in all three replicates (396 unique crosslinks were identified in one or two replicates only). For the E6AP + E6 sample, XL-MS analysis yielded 146 unique crosslinks with 8 interlinks between E6AP and E6 identified over all three replicates (408 identified crosslinks were identified in one or two replicates). In contrast, in the E6AP + E6_L50E samples, just one interlink was identified, although a similar number of 131 crosslinks was identified for E6AP over all three replicates (and 325 crosslinks were identified in one or two replicates), confirming the marginal binding of HPV-16 E6_L50E to E6AP and the validity of our approach. One of the identified interlinks connects lysine 350 of E6AP with lysine 94 of HPV-16 E6 and confirms so the known E6 binding site of E6AP. Besides this one, several interlinks were identified between the AZUL domain of E6AP (originating from lysine 7) and the two zinc fingers of HPV-16 E6. Moreover, several crosslinks connect the HECT domain of E6AP (lysines 708, 779, 799, 841) also with the two zinc fingers of HPV-16 E6.

Since high-resolution structures of the HECT domain of E6AP (Huang et al., 1999) and of HPV-16 E6 (Martinez-Zapien et al., 2016) are known, integrative structural modeling using crosslinks in a Bayesian scoring scheme was used to create a model of the complex (figure 39 E).

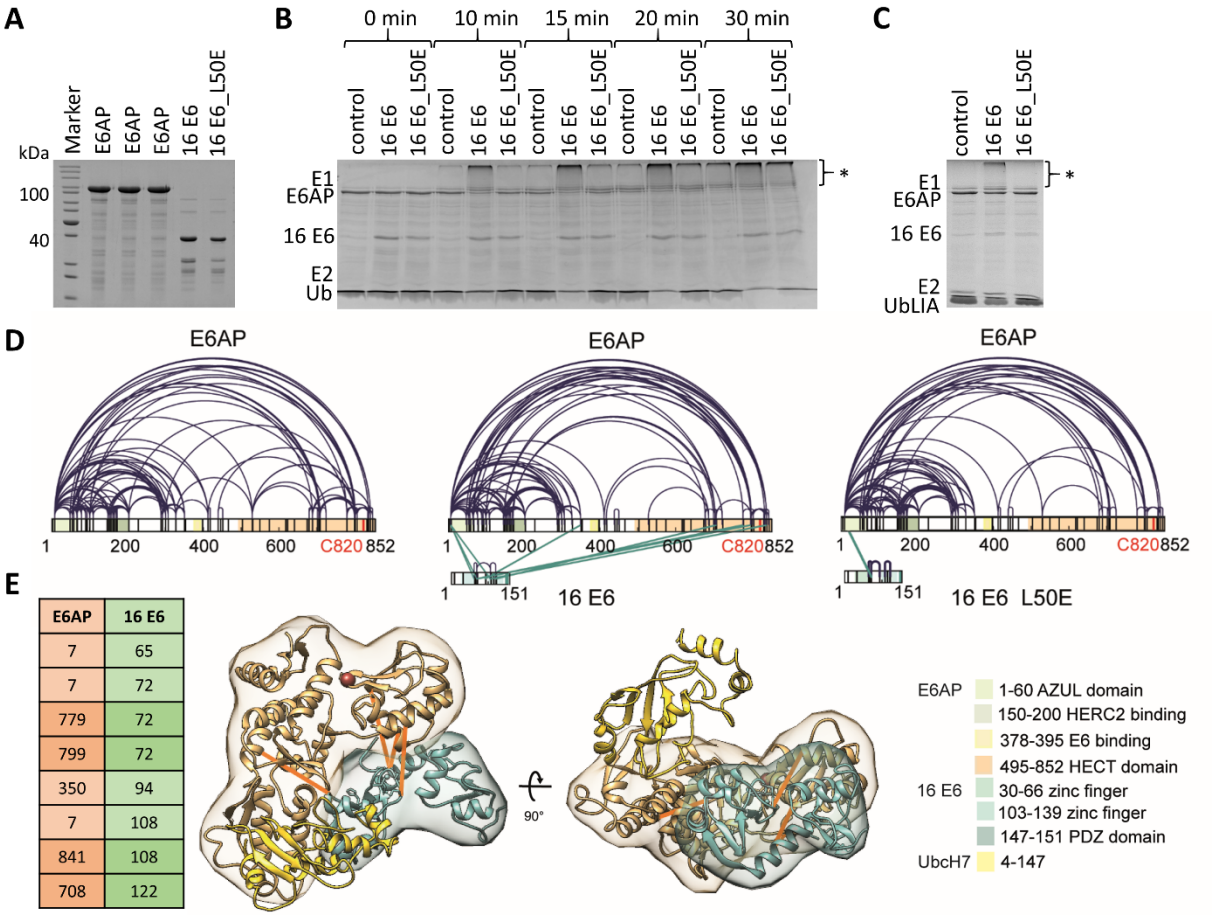

Figure 39: XL-MS confirms binding of HPV-16 E6 to its known binding site on E6AP and reveals proximity of HPV-16 E6 to N- and C-terminal regions of E6AP

(A) Coomassie stained SDS-PA gel of the protein preparations used. Note that a GST fusion construct of HPV-16 E6 was utilized. (B) Conventional in vitro E6AP auto-ubiquitination assays with HPV-16 E6 or HPV-16 E6_L50E stopped at the indicated time points. (C) Conventional in vitro E6AP auto-ubiquitination assay with HPV-16 E6 or HPV-16 E6_L50E with UbLIA. Reactions were stopped after 90 min and analyzed by SDS-PAGE and Coomassie staining. Poly-ubiquitinated species are marked by an asterisk. (D) Graphs indicating identified crosslinks with an Id-score ≥ 25 identified within all three replicates for E6AP, E6AP + E6 and E6AP + E6_L50E (sample processing, MS measurements and data evaluation were done by Carolin Sailer). (E) Table showing identified interlinks between E6AP and HPV-16 E6 with interlinks that can be mapped to existing PDB structures highlighted. Model of the complex of the HECT domain of E6AP (1C4Z) and HPV-16 E6 (4XR8) obtained from integrated modeling using the identified interlinks as restraints. Modeling experiments were done by Kai-Michael Kammer. The figure is adapted from (Sailer et al., 2018).

4.6.2.2 XL-MS data allows structural modeling of the ternary E6AP-E6-p53 complex

Furthermore, we asked the question how the transfer of ubiquitin from the catalytic center of E6AP to the substrate can be achieved. Therefore, we performed XL-MS experiments with E6AP and HPV-16 E6 and recombinantly expressed p53 (figure 40 A).

We found that the identified interlinks between E6AP and HPV-16 E6 alone were highly comparable to the previously identified interlinks between E6AP and HPV-16 E6 (figure 40 B). Furthermore, interlinks connecting the DNA binding domain of p53 (residues 92-292) with the HECT domain of E6AP, but also with its N-terminally located AZUL domain were identified in all three replicates. Integrated computational modeling including the crystal structure of the DNA binding domain of one p53 molecule in complex with HPV-16 E6 (Martinez-Zapien et al., 2016) as a single rigid body, resulted in a model with a highly comparable orientation of HPV-16 E6 towards the HECT domain of E6AP. In this model, p53 is located adjacent to the C lobe and the catalytic cysteine of E6AP so that potential ubiquitination sites of the DNA binding domain of p53 are placed closely to the catalytic center of E6AP (figure 40 C). Moreover, p53 is positioned between HPV-16 E6 and the C lobe of the HECT domain of E6AP and thus does not interfere with E2 binding to the HECT domain. Strikingly, the N-terminal AZUL domain of E6AP is also crosslinked with different lysine residues of p53 (lysine 120, 164, 357, 373). Additionally, the same lysine residues were also identified to be crosslinked with lysine residues of E6AP that are close to its catalytic center. It needs to be considered that p53 forms a homotetramer so that interactions of the apparently same residue of p53 to both the AZUL and the HECT domain of E6AP may originate from different p53 molecules within the tetramer.

In any case, the data indicates that both HPV-16 E6 and p53 are in direct vicinity to the catalytic center of E6AP and to the AZUL domain. This compact conformation opens the possibility that HPV-16 E6 may function as a cofactor in E6AP catalysis. Moreover, this model of the ternary enzyme-substrate complex may be used to identify amino acid residues on the proteins that are critical for the formation of the complex.

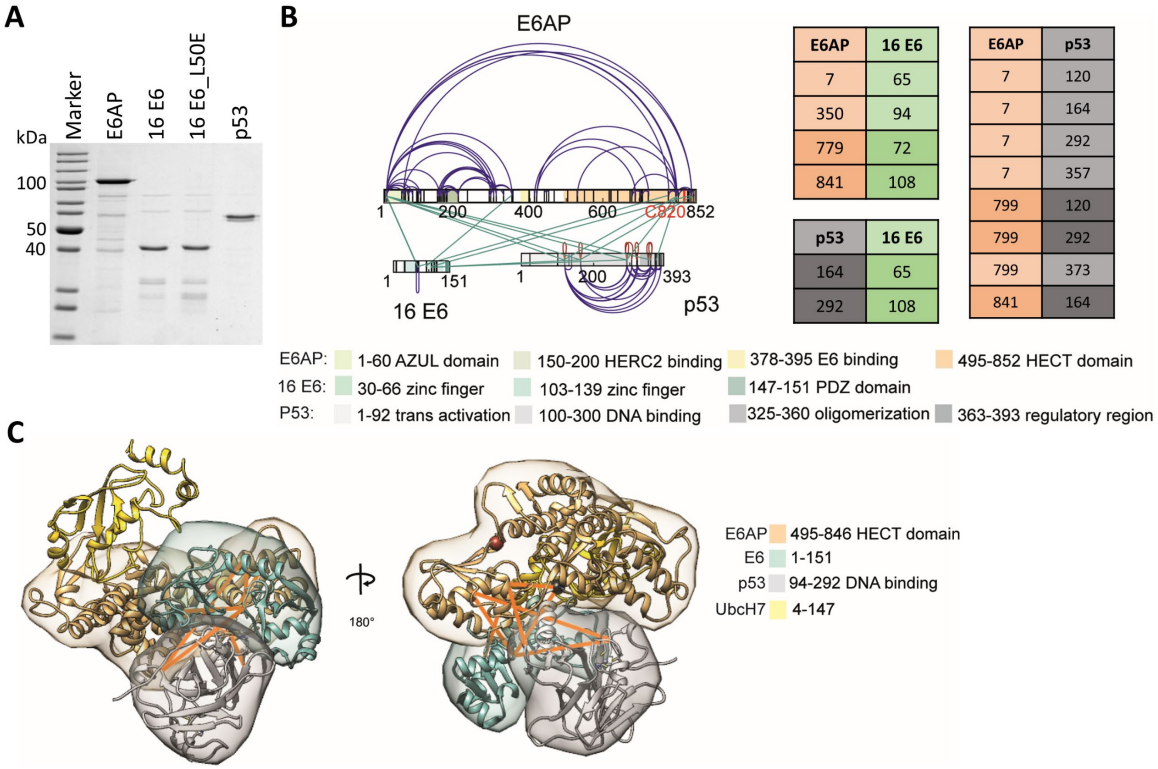

Figure 40: XL-MS-based structural model of the ternary E6AP-E6-p53 enzyme-substrate complex
(A) SDS-PAGE of protein preparations used. Recombinant p53 was provided by Alexandra Julier. (B) Graphs indicating identified crosslinks with an Id-score ≥ 25 identified within all three replicates. Tables showing identified interlinks of the ternary complex with interlinks that can be mapped to existing PDB structures highlighted. (C) Integrated modeling of the HECT domain of E6AP (1C4Z) and the complex of the DNA binding domain of p53 bound to HPV-16 E6 (4XR8) using interlinks as restraints. XL-MS sample processing, MS measurements and data evaluation were done by Carolin Sailer and computational modeling experiments were done by Kai-Michael Kammer. The figure is adapted from (Sailer et al., 2018).

4.6.2.3 SILAC-XL-MS indicates a monomeric state of E6AP in absence as well as in presence of HPV-16 E6

Conventional XL-MS is not able to discriminate interlinks between two different protomers and intralinks inside a single protomer within a homooligomer. Besides this, it needs to be considered that very high protein concentrations of E6AP of 1 µg/µL are needed for XL-MS that could trigger oligomerization. Moreover, transient interactions between different E6AP molecules may be stabilized through the crosslinker so that two E6AP molecules are coupled and subsequently erroneously heavily crosslinked. These limitations of XL-MS and the contradictory results concerning E6AP oligomerization (Ronchi et al., 2014) prompted us to ask whether the identified crosslinks between E6AP's C and N terminus are intralinks within a single E6AP molecule or interlinks between different E6AP molecules. To scrutinize this, XL-MS was combined with SILAC (stable isotope labelling in cell culture) (Chen et al., 2015).

To do so, E6AP was expressed in a strain auxotrophic for lysine and arginine (Matic et al., 2011) in M9 minimal medium with heavy (^{13}C6/^{15}N4-labeled) lysine and heavy (4,4,5,5-deuterated) arginine (called 'heavy E6AP' in this context). *In vitro* auto-ubiquitination assays ensured that heavy E6AP behaved like 'normal' E6AP (figure 41 A). Next, SILAC-XL-MS experiments were performed with a stoichiometric mixture of heavy and light E6AP. Note that in total similar numbers of E6AP intralinks were identified as before in conventional XL-MS with 379 intralinks for E6AP only (204 light-light, 168 heavy-heavy and 7 light-heavy crosslinks) and 383 for E6AP in presence of HPV-16 E6 (204 light-light, 172 heavy-heavy and 7 light-heavy links) proving that no errors emerged in the evaluation. Interestingly, while an overall similar number of crosslinks was identified compared to conventional XL-MS only two homodimeric interlinks (between E6AP and heavy E6AP) were identified. These interlinks connect two N-terminal regions (lysine 148 with 170 and 439 with 66, according to isoform 1 of E6AP) (figure 41 B). In presence of HPV-16 E6, a third homodimeric interlink was identified (between lysine 7 and 7) in addition to the two homodimeric interlinks identified in absence of HPV-16 E6. The low number of identified homodimeric interlinks suggests that E6AP is mainly in a monomeric or transient polymeric state and that the presence of HPV-16 E6 does not have an influence on the polymerization behavior of E6AP.

To corroborate these findings, we performed size-exclusion experiments. Comparison to calibration standards revealed that E6AP migrates like a 170 kDa protein (figure 41 C). This could in principle be explained by short-lived interactions between E6AP molecules leading in average to an increase in size. However, more likely, E6AP has not a globular shape but an extended conformation in solution so that its running behavior corresponds to an apparently larger protein. Several further size-exclusion chromatography experiments proved that full-length, as well as isolated HECT domains of E6AP, E6AP F727 mutants and certain disease-associated variants migrate as a monomer. Especially, no evidence for interactions of HECT domains was obtained (Engelke, 2019).

To sum up, the SILAC-XL-MS data suggest that E6AP has weak homo-oligomeric interactions that are however, not mediated through the HECT domain as previously assumed (Ronchi et al., 2014) but through N-terminal regions and that HPV-16 E6 does not alter the oligomerization behavior of E6AP.

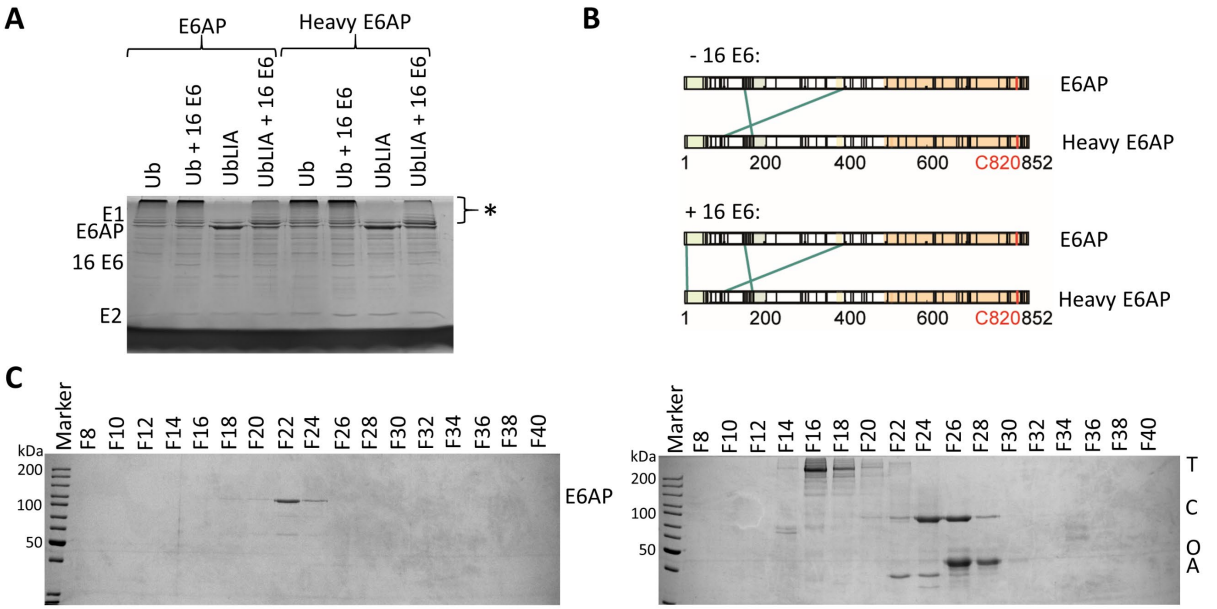

Figure 41: SILAC-XL-MS indicates a monomeric state of E6AP in absence and presence of HPV-16 E6
(A) In vitro auto-ubiquitination assays with conventional and heavy (stable isotope labeled) E6AP. (B) SILAC-XL-MS in absence and presence of HPV-16 E6. SILAC-XL-MS sample processing, MS measurements and data evaluation were done by Carolin Sailer. (C) Size-exclusion chromatography experiments with E6AP and calibration standard proteins. Fractions were analyzed by SDS-PAGE and Coomassie blue staining. High-molecular weight standards are marked with T: Thyroglobulin (669 kDa, dimer), C: Conalbumin (75 kDa), Ovalbumin (42 kDa), A: Aldolase (158 kDa, tetramer). The figure is adapted from (Sailer et al., 2018).

4.6.2.4 qXL-MS reveals structural dynamics of E6AP upon binding of HPV-16 E6

Quantitation of crosslinks via their MS1 or MS2 intensities has turned out to be a valuable method to analyze different conformations of a protein so that quantitation of intralinks can in principle be used to observe structural dynamics of a protein (Walzthoeni et al., 2015, Walker-Gray et al., 2017, Yu & Huang, 2018). Quantitation of the 106 unique high-confidence crosslinks found in all three replicates of the E6AP + E6 samples in comparison to the E6AP only samples resulted in the identification of enriched or depleted intralinks indicating indeed a conformational rearrangement of E6AP in presence of HPV-16 E6 (figure 42). In detail, the abundance of the majority of crosslinks did not change, while multiple crosslinks inside the HECT domain or connecting the HECT domain with the central regions of E6AP were decreased (log2 change ≤ -1.5) and several crosslinks connecting N and C termini of E6AP (spanning from lysines inside or close to the AZUL domain to lysines close to the catalytic center of E6AP) were increased (log2 change ≥ +1.5).

Quantitation of experiments with HPV-16 E6_L50E in comparison to E6AP only revealed marginal changes of crosslink abundances, indicating minor conformational rearrangements. This control experiment confirms that changes in crosslink abundance are due to binding and interaction and not just due to the mere presence of the HPV-16 E6 protein. Taken together, our qXL-MS data substantiate our model of stabilization or inducation of a high-activity conformation of E6AP through HPV-16 E6.

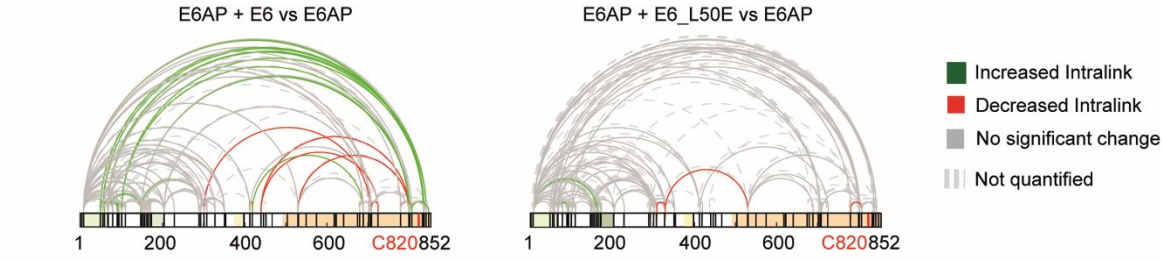

Figure 42: qXL-MS reveals structural dynamics of E6AP upon HPV-16 E6 binding
Quantitation of data shown in figure 39 revealed a distinct pattern of enriched and depleted intralinks of E6AP + E6 compared to E6AP (Id-score ≥ 25, p-value ≤ 0.01, log2 change ≥ +1.5). Quantitation of E6AP + E6_L50E with E6AP resulted in neglectable changes of intralink abundances. The figure is adapted from (Sailer et al., 2018).

4.6.2.5 qXL-MS reveals conformational rearrangements of E6AP and AS-derived E6AP mutants induced by small molecule activators comparable to those induced by HPV-16 E6

As the HPV-16 E6-mediated transition of E6AP into its high-activity conformation could be detected by qXL-MS, we wanted to investigate the 58X AS mutants with this method next. A different conformation may give hints why the mutants are deficient their catalytic activity. Possibly, an overall more open conformation would underline our model that E6AP is in its active conformation more compact. Furthermore, investigation of the impact of HPV-16 E6 and the small molecule activators on wild-type E6AP and the 58X AS mutants by qXL-MS could provide further insights into how activation is achieved. Therefore, proteins were generated in sufficient amounts and tested in biochemical activity assays. SDS-PAGE analysis of purified proteins and the structures of OF232 and Alloxazine (a structurally highly related compound to OF232 that served as control) are shown (figure 43 A and B). FP-based auto-ubiquitination assays with the protein preparations confirmed that OF232 activates E6AP and rescues the activity of F583S and E584Q, whereas Alloxazine showed no effects (figure 43 C). Conventional E6AP auto-ubiquitination assays with ubiquitin (figure 43 D) and UbLIA (figure 43 E) confirmed that OF232 and HPV-16 E6 activate wild-type E6AP and rescue the 58X AS mutants (that were in control reactions virtually inactive), whereas Alloxazine did not show activating nor inhibiting effects.

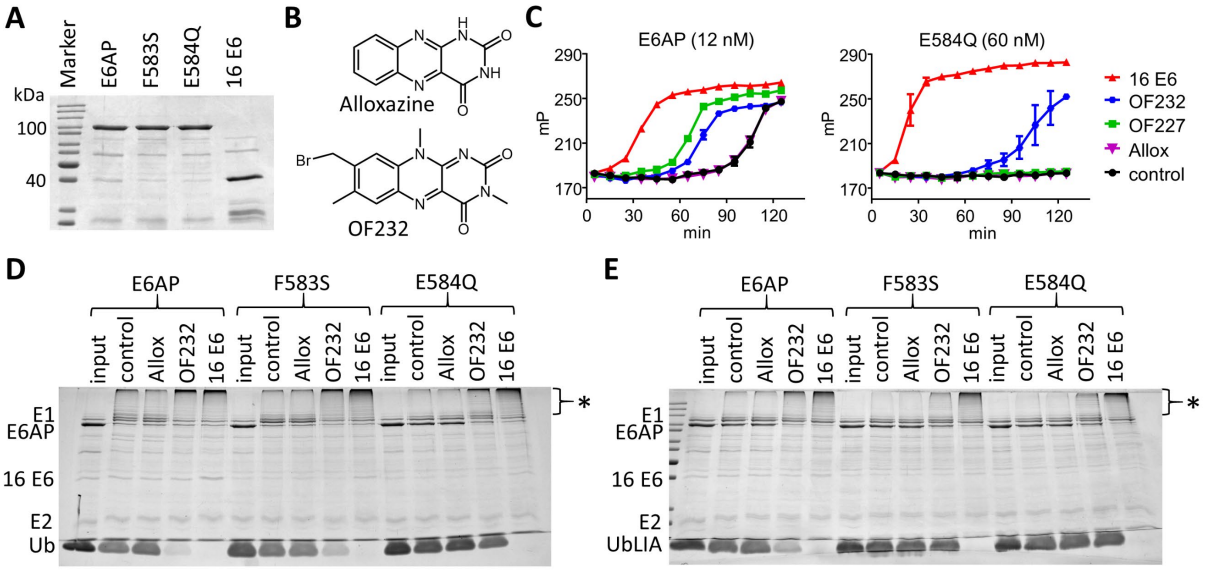

Figure 43: Quality control of reagents for XL-MS experiments with 58X AS mutants and OF232
(A) Coomassie blue stained SDS-PA gel of proteins used for the XL-MS experiments. (B) Chemical structures of OF232 and Alloxazine. (C) FP-based auto-ubiquitination assays with E6AP or E584Q with 10 µM of compounds OF227, OF232 or Alloxazine (abbreviated as Allox). A control reaction without compound as well as a positive control containing HPV-16 E6 were included. (D) In vitro E6AP auto-ubiquitination assays with protein preparations and compounds used for XL-MS with ubiquitin (reactions with E6AP were incubated for 10 min at 30°C, whereas reactions with F583S or E584Q were incubated for 90 min at 37°C). (E) Same experiment as in (D) with UbLIA (all reactions were incubated at 37°C for 90 min).

As the purified proteins performed as expected in the auto-ubiquitination assays, we performed XL-MS experiments. The three E6AP variants were investigated either on their own or in presence of OF232, Alloxazine or HPV-16 E6. First, intralinks of the 58X AS mutants were quantified against E6AP. Here, only minor changes with little increase or decrease of intralinks were obtained (figure 44). Altogether, a possible slightly more compact conformation (i.e. slightly increased interaction of N and C termini) can be construed and not a more extended conformation that would fit to an inactive conformation as our working-model implies the high-activity conformation (induced by HPV-16 E6) to be the more compact one.

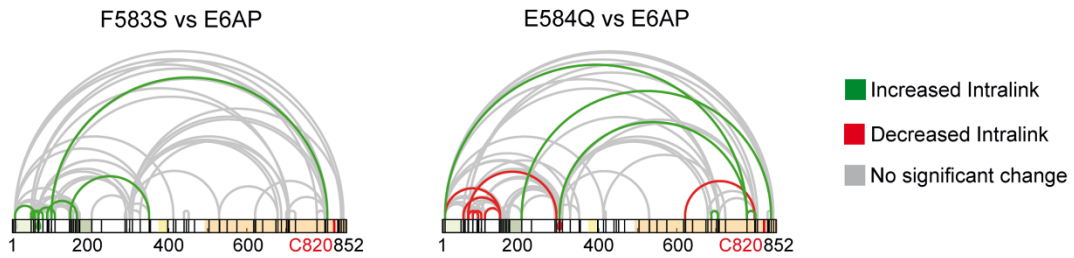

Figure 44: qXL-MS reveals only minor differences in intralink abundances identified for 58X AS mutants compared to those identified for wild-type E6AP
Quantitation of identified high-confidence crosslinks (ld-score ≥ 25, p-value ≤ 0.01) of F583S and E584Q samples in comparison to E6AP is shown. Note that samples contained 1 % DMSO (v/v) in contrast to earlier shown data. Grey lines indicate intralinks with no significant change, while green lines indicate increased intralinks (log2ratio ≤ -1) and red lines indicate decreased intralinks (log2ratio ≥1). Sample processing, MS measurements and data evaluation were done by Jasmin Jansen.

As only marginal differences in the conformation of the 58X AS mutants in comparison to wild-type E6AP were revealed, we turned our interest towards the question what impact HPV-16 E6 and OF232 may have on the conformation of 58X AS mutants. Quantitation of identified intralinks in E6AP + E6 samples versus E6AP showed an overall similar picture as the previously performed experiments (figure 45 A). In fact, binding of HPV-16 E6 led again to enhanced proximity of N and C termini of E6AP as illustrated by the green arcs connecting them. However, a large number of previously not observed decreased intralinks between the central part of E6AP and its termini appeared in presence of HPV-16 E6 (note that in these experiments a 1.5-fold molar excess of HPV-16 E6 was used in contrast to equimolar ratios used in previous experiments). Remarkably, quantitation of E6AP + OF232 with E6AP only showed a nearly identical pattern as seen for samples containing HPV-16 E6. Measurements with the highly similar compound OF234 showed a similar change in the crosslinking pattern (data not shown). In contrast, Alloxazine showed almost no effect on the intralink pattern of E6AP, with only a small number of decreased intralinks in the AZUL domain and from that to central regions of E6AP. In addition, conformational changes of F583S and E584Q induced by HPV-16 E6 and OF232 (figure 45 B and C) compare well to those seen for wild-type E6AP (figure 45 A).
To sum up, the tested small molecule activator OF232 affects the structural dynamics of E6AP and the investigated 58X AS mutants in a manner similar to HPV-16 E6. Alloxazine, which features a highly related scaffold to OF232 but does not show effects in ubiquitination assays induces minor changes of crosslink abundances for wild-type E6AP as well as for both 58X AS mutants. Therefore, it can be concluded that OF232 and HPV-16 E6 induce both a similar transition of E6AP and 58X AS mutants towards a more compact and more active conformation.

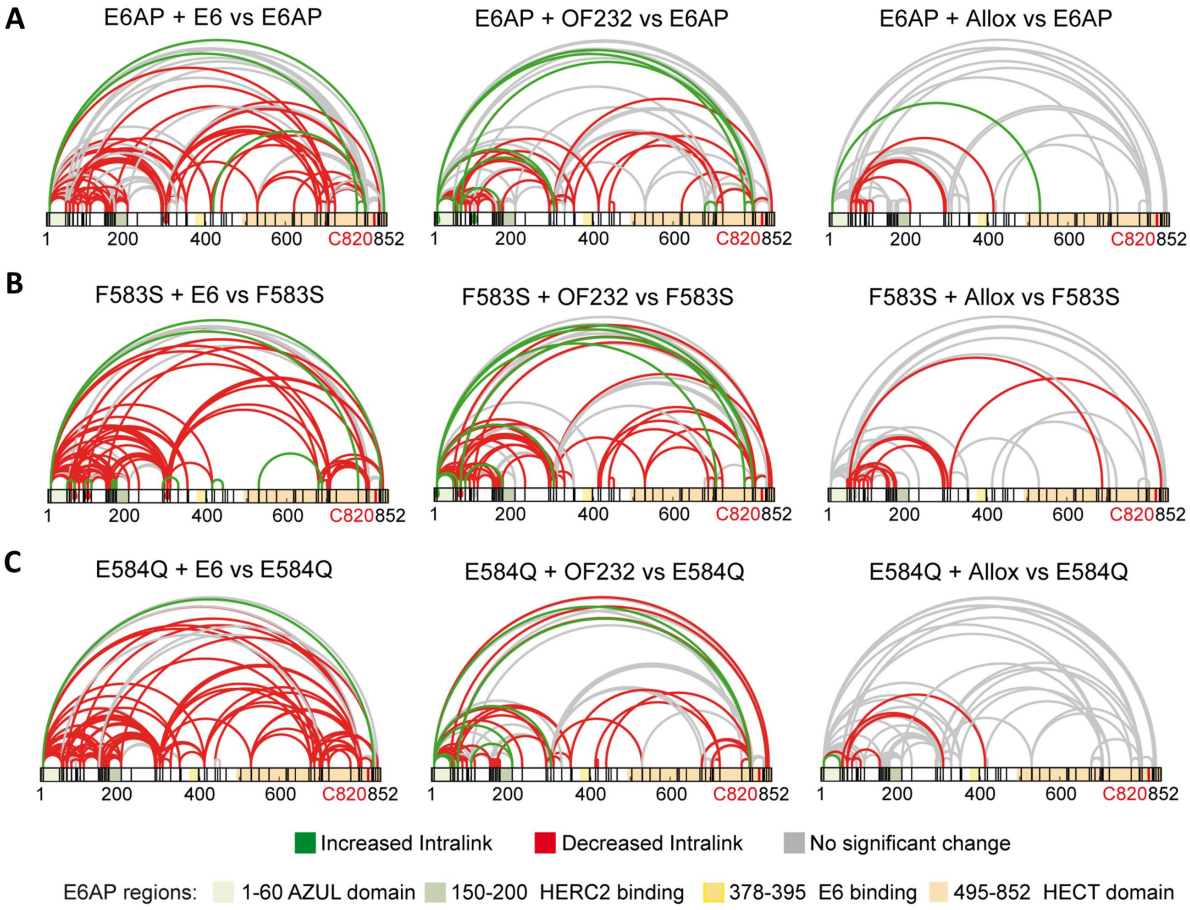

Figure 45: OF232 and HPV-16 E6 induce similar structural dynamics of both E6AP and 58X AS mutants
Quantitation of identified high-confidence crosslinks (ld-score ≥ 25, p-value ≤ 0.01) of samples of E6AP, F583S and E584Q in presence of Alloxazine (Allox), OF232 or HPV-16 E6 compared to samples of the respective E6AP variant only. Note that respective samples contained 100 µM of the compound and that all samples contained 1 % DMSO (v/v). Additionally, note that HPV-16 E6 samples contained a 1.5-fold molar excess of HPV-16 E6 to E6AP in contrast to an equimolar ratio used in earlier shown experiments. Grey lines indicate intralinks with no significant change, green lines indicate increased intralinks (log2ratio ≥ 1) and red lines indicate decreased intralinks (log2ratio ≤ -1). Sample processing, MS measurements and data evaluation were done by Jasmin Jansen.

5 Discussion

During the course of this dissertation an FP-based ubiquitination assay was developed that was used in two high-throughput screens to identify small molecule inhibitors of the E6-E6AP complex and small molecule activators of E6AP. The effect of identified activators on E6AP were studied in various ubiquitination assays, and -quantitative chemical crosslinking coupled to mass spectrometry experiments revealed that they affect the structural dynamics of E6AP in such a way that a high-activity conformation of E6AP is induced and/or stabilized. The results obtained will be discussed in the following sections.

5.1 Assessment of the developed FP-based ubiquitination assay

A novel fluorescence polarization (FP)-based assay to monitor the activity of E3 ubiquitin ligases was developed in this study. E6AP was used as model E3 ligase to establish the assay but the assay can be readily transferred to other HECT ligases and RING ligases, as shown for HUWE1 and HDM2 and RLIM, respectively. The only requirements are that the E3 ligase can be purified in sufficient amounts and performs efficient auto-ubiquitination *in vitro*. Nonetheless, it should be kept in mind that different ligases act mechanistically different (i.e. HECT vs. RING vs. RBR ligase or catalytic domain vs. full-length protein) and thus, outcome of ubiquitination may differ (i.e. linkage type, chain length, free chains vs. cis- vs. trans-auto-ubiquitination vs. substrate ubiquitination) as well as that the FP readout monitors solely ubiquitin consumption. These differences between different E3 ligases may result in different sigmoidal curves in FP-based ubiquitination assays with different onsets of increase of FP values, different slopes and different finally reached plateaus, making an accurate quantitation of the reactions challenging and impeding calculation of reaction kinetics. In addition, we have recognized that E3 ligases vary in their actual catalytic efficiency so that with similar concentrations very slow or very fast reactions are obtained, making activity changes difficult to detect. Conversely, adjustment of E3 ligase concentration to achieve a similar reaction curve of FP values, may result in unequal ratios between the analyzed E3 ligases and assayed compounds making a quantitative comparison of the effects of a compound on different E3 ligases rather difficult or even impossible. However, although, quantitative comparisons of the influence of compounds on different E3 ligases may be intricate, qualitative comparison can certainly be made. Furthermore, comparing the effects of different compounds on the same E3 ligase in a quantitative manner is readily feasible.

For technical reasons, it should be noted that the Tecan Infinite F500 reader needs (also due to the chosen 10 flashes per measurement) approximately 5 min to measure FP for a whole 384 well plate. This makes accurate measurements at the critical time when the reaction in the absence and the presence of an activating compound differs most prominently somewhat challenging. Thus, for the

identification of small molecule activators, ideally, reaction conditions should be established at which the E3 ligase is more or less inactive in the absence of compounds. This could in principle be achieved by using UbLIA, the hydrophobic patch mutant of ubiquitin used in this study for conventional ubiquitination assays. However, labeling of UbLIA with TAMRA resulted in precipitation of the protein-dye conjugate under several different conditions (not shown). An alternative approach would be the use of ubiquitin K11/48R or K48/63R mutants. They are also not efficiently used by E6AP and this impairment can also be rescued by HPV-16 E6 and possibly also by small molecule activators of E6AP. Overall, the developed FP-based ubiquitination assays proved to be easy-to-handle and robust in several applications. Recently, another group published a similar FP-based ubiquitination assay where cysteine containing ubiquitin variants were labeled with Alexa Fluor 488 C5 maleimide to investigate ubiquitin chain formation by the CUE domain of Cue1 (von Delbruck et al., 2016). Moreover, when the experimental part of this study was already finished, another FP-based ubiquitination assay was published (Franklin & Pruneda, 2019). To note, while differently labeled ubiquitins (either N-terminally TAMRA labeled ubiquitin or ubiquitin labeled at all primary amines with fluorescein) were used in that study, a 10-fold excess of unlabeled ubiquitin was necessary for an efficient reaction, similar to the reaction conditions used here. While Franklin and Pruneda addressed additional applications like tracking ubiquitin transfer in the ubiquitination cascade or cleavage of ubiquitin chains by DUBs, they also indicated the suitability of the FP-based ubiquitination assays to monitor activity of E3 ligases.

5.2 Identification of E6-E6AP inhibitors

5.2.1 High-throughput screen for E6-E6AP inhibitors

Links between HPVs and cervical cancer were suspected almost 50 years (zur Hausen, 2002). Since then DNA of specific HPV types has been found in almost every cervical cancer biopsy and epidemiological studies underlined that HPVs are the main etiological factor for cervical cancer (zur Hausen, 2002). In 2018, approximately 570,000 new cases of cervical cancer were diagnosed worldwide, and about 311,000 women died from this cancer (Gultekin et al., 2020). The key viral oncoproteins E6 and E7 were identified almost 30 years ago and have been extensively characterized in the meantime (Hoppe-Seyler et al., 2018). But how has the knowledge of the molecular mechanisms leading to cervical cancer been implicated in the development of therapeutics? Until today, no drug targeting E6 and/or E7 has been released for the treatment of cervical cancer, although several studies were able to identify lead structures for the development of small molecule inhibitors (see chapter 1.2.4.1.3 and (D'Abramo & Archambault, 2011)). However, the identified structures presumably lack potency and/or selectivity as suggested by the notion that they were not further evaluated in clinical trials. To identify new lead structures, 50,961 compounds were screened using the newly developed

FP assay with conditions optimized to identify inhibitors of E6-activated E6AP auto-ubiquitination. 351 hits (with ≥ 50% inhibition) were identified in the primary screen. As first evaluation step, about half of the hits (149 compounds) were counter screened with RLIM_RING to exclude compounds acting on ubiquitin, E1 or E2 enzyme. The counter screen revealed that approximately 85% of the tested hits were unspecific. Overall, 21 putatively specific hits were purchased and evaluated in further secondary assays with E6-E6AP, E6AP, RLIM_RING and HUWE1_trunc to distinguish inhibitors of E6-E6AP or E6AP, respectively, and to sort out false positives from the primary screen. The counter screen with RLIM_RING did apparently not work robustly, since 8 of the compounds which showed no inhibition of RLIM_RING in the counter screen showed clear inhibition of RLIM_RING in later experiments. A possible explanation could be that certain compounds precipitated on the library plates so that the primary screen was performed actually with lower concentrations. Altogether, of the 351 screening hits, 179 showed definitely unspecific inhibition, probably on the E1 or E2 level; 121 hits could not be confirmed to inhibit E6-E6AP with lower concentrations of cherry-picked compounds; and 51 hits were not finally evaluated. From these 51 not finally evaluated compounds, 14 were not followed up at all and 37 were partly tested with several of them showing mild inhibition of E6-E6AP, so that it was decided not to investigate them further. However, some specificity towards E6-E6AP, E6AP and HECT ligases in general may exist (data not shown) and needs to be addressed in future studies. Independent of the obtained results, possible applications of the different classes of inhibitors will be discussed in the following sections.

5.2.2 Assessment of E1 and E2 inhibitors

Interestingly, most of the hits tested in the counter screen (126 of 149) showed additional inhibition of RLIM_RING suggesting a mode of action on the E1 or E2 enzyme level.

In general, E1 inhibitors are also of interest since alterations in ubiquitination are observed in a wide range of pathologic conditions so that the ubiquitin-proteasome system is a therapeutic target, e.g. in cancers like leukemia and multiple myeloma (Yang et al., 2007). Previously, several studies aimed to identify E1 inhibitors (Yang et al., 2007, Xu et al., 2010, Ungermannova et al., 2012, Huang & Dixit, 2016). An assay to monitor E1 activity, e.g. the assays used in this study (Hacker et al., 2013, Hammler et al., 2020), could be used to differentiate further at which stage the different compounds identified in the present study act. It is worth mentioning that Hacker et al. screened 1,279 compounds (AD151, AD153, ICCB204, ICCB205) for E1 inhibition that were also screened for inhibition of the E6-E6AP complex. In that study, four of five hits were confirmed, including β-Lapachon. All four compounds were identified to act inhibitory in this study, too (not shown).

Inhibitors of E2 enzymes may also be of interest since recent work suggested that E2 enzymes do not only serve as 'ubiquitin carriers', but can dictate chain linkage and length and determine substrate specificity in several cases (Streich & Lima, 2014, Huang & Dixit, 2016). Furthermore, given that there are 38 E2 enzymes in humans, but only 2 E1 enzymes, E2 inhibition is at least in theory more specific than E1 inhibition (Ye & Rape, 2009, Harper & King, 2011). However, although the inhibitors identified here could be further characterized, this was not done as the focus of this study was to identify inhibitors of the E6-E6AP complex and/or E6AP.

5.2.3 Assessment of E6AP inhibitors

A common and highly penetrant genetic form of ASD results from maternally inherited 15q11-13 amplification causing an increase of E6AP levels. For this reason, small molecule E6AP inhibitors are conceivable as therapeutics. Only two inhibitors of HECT ubiquitin ligases have been reported so far. Heclin was published to inhibit several members of the HECT ligase family (Mund et al., 2014) and Clomipramine was published to inhibit ITCH but also showed some effects on E6AP (Rossi et al., 2014). In the present study, it was speculated that E6AP inhibitors might be identified simultaneously in the screen for E6-E6AP inhibitors. Moreover, the existence of inhibitors acting on several or even all members of the HECT ligase family is well possible due to high conservation of the catalytic HECT domain (Lorenz, 2018). To distinguish between the different classes of inhibitors (i.e. specific for E6AP or acting on HECT E3s in general), potential hits were tested with HUWE1. However, no compound with clear-cut properties (i.e. either acting only on E6AP or on HECT ligases without showing any unspecific effect on RLIM_RING) was identified in this study. A possible explanation may be that the reaction conditions were optimized to identify inhibitors of the E6-E6AP complex. Since HPV-16 E6 stabilizes the active conformation of E6AP, it might be that inhibitors of E6AP that recognize the ''low activity'' conformation were not detectable. Even if inhibitors of E6AP may bind to the high-activity conformation, their inhibiting effects may be compensated by the impressively strong activation of E6AP by HPV-16 E6. Therefore, a separate screen with higher enzyme concentrations of E6AP in absence of HPV-16 E6 would be the strategy of choice to identify E6AP inhibitors.

5.2.4 Assessment of E6-E6AP inhibitors

Fourteen already preliminary confirmed hits were purchased and tested in secondary assays. However, none of them inhibited the E6-E6AP complex specifically. Moreover, Luteolin, a flavonoid that was published as inhibitor of the E6-E6AP complex (Cherry et al., 2013, Kumar et al., 2015, Yuan et al., 2016), showed unspecific inhibition of auto-ubiquitination of other tested E3 ligases. Application of the TRASE assay (Hacker et al., 2013) showed that Luteolin and likely also other published flavonoids,

inhibit also the E1 enzyme. These results fit to other studies revealing that flavonoids are promiscuous inhibitors targeting numerous different enzymes (Dangles & Dufour, 2008, Tritsch et al., 2015, Liu et al., 2017a) and multiple cellular pathways (Lin et al., 2008, Tang, 2016). However, cytotoxic side effects would be less problematic if the drug could be specifically delivered to cervical cancer. Therefore, the identified compounds, even if they have unspecific properties in addition to the disruption of the E6-E6AP complex, may still be regarded as lead structures for cervical cancer therapy.

Another issue may be that in all experiments E6 and E6AP were first mixed and afterwards compounds were added. It seems possible that the 15 min preincubation time before the assays were started were to short or to put it in other words, that the E6-E6AP complex is too stable so that the compounds had no chance to disrupt the complex. A possible improvement would therefore be to incubate HPV-16 E6 with the compounds first so that these can bind to the binding groove of HPV-16 E6, thereby occupying the binding site of the α-helical LXXLL binding motif of E6AP. Furthermore, a recent study showed that interaction of HPV-16 E6 and E6AP is more complex than just an interaction of the α-helical LXXLL motif with the E6 binding groove, that is, other regions of E6AP interact with HPV-16 E6 and these interactions seem to be important for ubiquitin ligase stimulation (Drews et al., 2020). Thus, these additional regions may also represent potential target sites for small molecules.

Taken together, our results go unfortunately hand in hand with the fact that until today no drug for cervical cancer targeting the E6 protein was released. This underlines the immense challenge of identifying inhibitors specific for the E6-E6AP complex. The knowledge that formation of the E6-E6AP complex plays a key role in the development of cervical and other HPV-related cancers and presents thus a great target for drugs, hence still awaits a small molecule that can disrupt this complex efficiently and without severe side effects. Be it is it may, this study added a novel tool to identify and evaluate such small molecules that might hopefully be helpful in the future.

5.3 Identification of small molecule activators of E6AP

E6AP plays a key role in the two neurodevelopmental disorders Angelman syndrome and Dup15q syndrome as described above (chapters 1.2.4.2 and 1.2.4.3, respectively). Despite increasing research efforts, mechanisms of E6AP regulation and how malfunction of E6AP results in these disorders are still only partially understood. Furthermore, incomplete knowledge of the mechanism and the structural basis of E6AP-mediated catalysis has precluded rational approaches to target E6AP therapeutically (Chen et al., 2018). Therefore, a further aim of this study was to identify small molecule activators of E6AP that could serve as tools for its characterization. Compounds with such properties could beyond that serve as lead compounds in drug discovery for Angelman syndrome therapeutics.

5.3.1 High-throughput screen for E6AP activators

Until now, no small molecules that stimulate enzymatic activity of E6AP or any other ubiquitin ligase (meaning directly enhancing enzymatic activity and not increasing ubiquitination of a specific target as e.g. PROTACs do) are known. Therefore, we decided to screen libraries of drug-like small molecules to identify activators specific for E6AP. According to our selection criteria 53 small molecules out of 48,077 tested compounds were identified. From those, 43 were retested with the FP screening assays with 10 µM instead of 50 µM as used in the primary screen, as due to limited amounts of cherry-picked compounds higher concentrations were not possible. 50 µM is a rather high concentration for high-throughput screenings, but it was used as it was unknown whether E6AP activators exist at all and we did not to miss any due to too low compound concentrations. 21 of the 43 retested hits could be confirmed to stimulate E6AP also with the lower concentration used. The other 22 hits may be characterized and optimized later, but 21 potent compounds sufficed to be followed-up in this study.
As next step, twelve compounds that were cherry-picked and confirmed were commercially available and were further tested in conventional SDS-PAGE-based auto-ubiquitination assays with seven of them showing clear stimulation of E6AP. At this stage, it needs to be mentioned that it is expected that not all compounds identified in the screen score positive in other assays as enzyme concentrations differ between FP-based and conventional E6AP auto-ubiquitination assays with about 10-fold higher E1, 10-fold higher E2, 20-fold higher E6AP, and 30-fold higher ubiquitin concentrations in conventional E6AP auto-ubiquitination assays. The reason for this is that when the FP assay was developed, Ub-T concentrations were set to 20 nM (as this concentration can be readily detected by the reader and due to limited amounts of Ub-T) and the other enzyme concentrations were reduced accordingly. In detail, E1 and E2 concentrations were adjusted to 10-fold higher concentrations than necessary for optimal auto-ubiquitination and E6AP concentration was adjusted so that a slow, which means activatable, reaction was obtained. In SDS-PAGE assays, higher concentrations are commonly used to be able to visualize proteins by Coomassie blue staining. Another point that needs to be considered for conventional E6AP auto-ubiquitination assays is the speed of the reaction that needs to be stopped early on before reactions have reached completion. At these early time points, weak activation can be difficult to observe due to only slight differences in band intensities. However, activation of E6AP by HPV-16 E6 is clearly visible such assays, and four compounds (OF204, OF227, OF232, OF234) show also clear-cut activation of E6AP (figure 28).

For this reason, E6AP auto-ubiquitination assays with a hydrophobic patch mutant of ubiquitin (UbLIA, substitution of L8 and I44 to alanine) that is poorly used by E6AP are preferred as unambiguous differences between control and activated reactions are obtained. The rationale to do so is that E6AP experiences a defect in isopeptide bond formation with UbLIA, while the first step of HECT ligase catalysis, the transthiolation reaction, is unaffected (Mortensen et al., 2015). Interestingly, three (OF204, OF232, OF234) of the four compounds that show activation with wild-type ubiquitin also rescue the UbLIA defect of E6AP. This suggests that these compounds act, like HPV-16 E6 (Mortensen et al., 2015), on the isopeptide bond formation step, providing first evidence evidence about their mechanism of action.

Two of the four most extensively characterized activators (OF204 and OF227) show stronger activation of wild-type E6AP while the isoalloxazine derivatives (OF232 and OF234) are more proficient in rescuing the activity of 58X AS mutants. From OF204 (CBP31F04), a derivative (CBP31H04) with just an additional hydroxyl group was identified in the primary screen. This compound was not commercially available and was thus not further characterized, but it strengthens the notion that OF204 is an E6AP activator. OF227 is a derivatized natural product that activates E6AP potently in FP-based auto-ubiquitination assays. Also, mild effects in conventional E6AP auto-ubiquitination assays (figure 28) and with concentrations larger than 20 µM strong effects in Ring1B_I53S substrate ubiquitination assays were obtained (figure 35). OF232 and OF234 are structurally closely related alloxazine derivatives that show the strongest effects of all identified compounds in rescuing the 58X AS mutants (figures 31, 33, and 43). While several different synthesized alloxazine derivatives scored positive, other tested derivatives from the same library and the naturally occurring isoalloxazine containing molecules FMN, FAD and Riboflavin showed no activation of E6AP. The decisive difference could so far not be unraveled, but it can be speculated that alloxazine and OF232 bind both to the N terminus of E6AP as suggested by the qXL-MS data (indicated by altered crosslink abundancies in N terminal regions with bot compounds but globally changed crosslink abundancies with OF232 (figure 45). The activating compounds interact presumably additionally with other regions of E6AP inducing thus structural rearrangements and enzyme activation.

Notably, larger concentrations of some of the identified compounds (especially OF232 and OF234) lead to inhibition of E6AP auto-ubiquitination. It might sound contradictory that those compounds were identified in the screen with high concentrations (50 µM for the primary screen; and 12.5 µM for the MDB plates containing OF232 and OF234). However, this may be explained by the notion that as stock solutions of many compounds on the library plates tend to precipitate so that actually lower assay concentrations were obtained.

Nonetheless, a serious disadvantage of the identified molecules remains, namely their off-target, inhibiting effect on E1 and their cytotoxicity. The cytotoxicity is probably associated with E1 inhibition or due to DNA intercalation that can be anticipated due to their chemical structure (Herfeld et al., 1994). For this reason, the identified compounds must be regarded as scaffolds that need to be derivatized and pharmacologically optimized before they can be tested in AS patient-derived iPSC systems or AS mouse models (Fink et al., 2017, Sonzogni et al., 2018). Several screening hits were not fully characterized in respect to specificity and further properties like cytotoxicity. These compounds may potentially be better suited candidates. Notwithstanding, this study could identify ''first-in-class'' E6AP activators and could prove that the developed FP-based ubiquitination assay is suited not only to screen for inhibitors but also activators of ubiquitin ligases.

5.3.2 Evaluation of Tamoxifen and derivatives

In this study, Tamoxifen was identified as potent activator of E6AP. Since 1990, Tamoxifen is an FDA-approved drug for breast cancer therapy. Tamoxifen blocks binding of estrogen to estrogen receptor alpha (ERα). ERα is a ligand-activated transcription factor with divergent functions in different tissues with some of these playing a critical role in the etiology of breast cancer (Couse & Korach, 1999). Tamoxifen belongs to a group of drugs named selective estrogen receptor modulators (SERMs), which act as either ERα agonists or antagonists depending on the tissue and environmental context and is thus applied for treating breast cancer in pre- and postmenopausal women (Wu et al., 2005, Deroo & Korach, 2006, Shagufta & Ahmad, 2018).

Tamoxifen was not directly identified in our high-throughput screen but by bioinformatic analysis of the obtained hits as some of them were found to have a pharmacologic profile closely related to drugs acting on ERα. Endoxifen and 4-Hydroxytamoxifen, the active metabolites of Tamoxifen in ERα modulation (Sanchez-Spitman et al., 2019) and Raloxifen, a structurally related SERM, were also tested and shown to activate E6AP while estrogen, its prohormones and related hormones and other tested SERMs (like Fulvestrant) showed no effect. This means that Tamoxifen-induced effects on ERα and E6AP are presumably a coincidence. However, due to its ability to modulate ERα, Tamoxifen might have side effects when used as medication for Angelman syndrome. Though, possible side effects may not be too severe as Tamoxifen is approved as a drug and hence tested thoroughly.

Furthermore, it needs to be recalled that Tamoxifen is a prodrug that is metabolized to hydroxylated forms at its position 4. These hydroxylated forms are 50-100 times more potent than Tamoxifen ((Jordan et al., 1977, Fabian et al., 1981)). A crystal structure of 4-Hydroxytamoxifen and ERα explains the strongly enhanced binding as the 4-hydroxy group forms distinct hydrogen bonds to ERα (Shiau et al., 1998). We hypothesized that blockage of position 4 by a methyl group should have minor effects on E6AP (as Tamoxifen and 4-Hydroxytamoxifen have similar activation potencies).

Conversely, a methyl group should dramatically decrease effects on ERα. 4-Methyltamoxifen was, thus, kindly synthesized by Meike Liebmann (AG Marx, University of Konstanz) and showed indeed a potent activation of E6AP similar to Tamoxifen. Effects of 4-Methyltamoxifen on ERα has still to be evaluated in future studies, but it is likely that mild, if any, effects will be obtained. If so, 4-Methyltamoxifen would exemplify how rational drug design can help to minimize adverse or unwanted effects of a drug that acts on more than one known cellular target.

Another issue to consider in this context is that besides its function as E3 ligase, a possible role of E6AP as transcriptional cofactor was suggested (Nawaz et al., 1999, Kühnle et al., 2013). Hence, it seems possible that Tamoxifen plays a yet unknown role in the crosstalk between E6AP and ERα in transcriptional regulation that might be unveiled in the future. Besides this, an independent proteomics study identified E6AP as molecular target of Tamoxifen in MCF-7 cells (Lochab et al., 2012). It was shown that Tamoxifen treatment reduces E6AP levels. As mechanism of E6AP depletion, it was indicated that Tamoxifen affects nuclear export of E6AP. With the knowledge from the present study, an alternative explanation might be that Tamoxifen activates E6AP auto-ubiquitination resulting in its proteasomal degradation and thus in its depletion.

5.3.3 Small molecule activators of E6AP as potential treatment for AS

This study identified several small molecule activators of E6AP, giving proof of principle that small molecules can be used to stimulate E6AP's ubiquitin ligase activity. In general, small molecule activators of E6AP can be envisioned for application as therapeutic regimen in AS. To do so, two different scenarios of their usage can be imagined.

First, in the majority of AS individuals the paternal allele is intact but is imprinted. Yet, long-noncoding RNA (lncRNA)-mediated imprinting may not completely silence expression of the paternal allele, so that low levels E6AP are still present (Daily et al., 2012). If these remaining small amounts could be activated, overall substrate ubiquitination by E6AP may be shifted to more physiological conditions. Another feasible option could be the combination of small molecule activators of E6AP with approaches to unsilence paternal *UBE3A* which are currently under investigation. Such approaches bear great potential, but it is not clear yet, whether reconstitution of paternal *UBE3A* expression results in physiological E6AP levels (Meng et al., 2012, Meng et al., 2013, Meng et al., 2015). Thus, simultaneous activation of wild-type E6AP by small molecules should prove beneficial.

The second scenario is the rescue of catalytically inactive point mutants of E6AP. Approximately 10% of AS individuals carry a point mutation in the maternal allele leading to expression of full-length but functionally impaired E6AP (Bird, 2014). These point mutations can be subdivided into mutants that are not stable (i.e. have a short half-life) and are removed by the cellular quality control system or into stable mutants (i.e. half life is comparable to wild-type E6AP) with disturbed protein-protein interaction properties and/or reduced ubiquitin ligase function (Cooper et al., 2004, Yi et al., 2015). In the present study, six AS-derived mutants were characterized. One (C21Y) showed ligase activity similar to the one of wild-type E6AP and another (S349P) showed decreased activity and only low yields were obtained from bacterial expression, probably due to folding defects. On the contrary, a cluster of four point mutants (ΔS582, F583S, E584Q, Q588P; called here 58X AS mutants) were obtained in high yields upon bacterial expression. Their ability to form thioester complexes with ubiquitin was not affected (Franziska Müller, unpublished observation) but they were strongly deficient in isopeptide bond formation. Excitingly, this defect could be rescued by HPV-16 E6 as well as by four of the identified small molecule activators (figures 31, 33, and 43). S582 was described to be 'located at the middle of the N lobe of the HECT domain and thus to play a key role in bridging two roughly globular substructures of the N lobe' (Sadikovic et al., 2014). These atomic interactions remain relatively stable after ubiquitin binding, highlighting the importance of the S582 residue in maintaining the overall structure stability (Sadikovic et al., 2014). In contrast, the other three mutants that are located also between the two parts of the N lobe are facing outwards in the crystal structure of the HECT domain (Huang et al., 1999), so that different mechanisms leading to the defect in E3 activity than the one proposed for S582 may apply.

AS-derived E6AP point mutants differ in their defect (Cooper et al., 2004, Sadikovic et al., 2014) and it is possible that not all can be rescued by small molecules. Moreover, certain AS mutants are enzymatically as active as wild-type E6AP. An example for this subgroup of mutants is E6AP C21Y. Disturbed interactions of E6AP C21Y with other proteins were suggested as cause for its dysfunction (Kühnle et al., 2018). Nonetheless, further screenings for activators should be performed with E6AP mutants other than the 58X ones but with affected ubiquitin ligase activity, as it is likely that different causes underlie the catalytic dysfunction of different AS mutants (e.g. some mutations interfere with the ability of E6AP to form thioester complexes with ubiquitin, others affect the ability to catalyze isopeptide bond formation). From a clinical point of view, it would be interesting to know whether AS point mutants can be grouped into distinct subclasses based on which step of E6AP-mediated catalysis is affected. If such subgroups could exist, new cases that fit into one subgroup could be tackled in a shorter time frame (as their activity may be rescued by already knwon small molecules.

A possible drawback of small molecule-induced E6AP activation is that increased auto-ubiquitination may lead to a decrease in E6AP levels due to increased proteasomal degradation and thus overall effects on substrate protein levels may be difficult to predict. Therefore, it needs to be tested *in vivo* whether small molecule activators of E6AP are indeed effective in enhancing substrate ubiquitination. For AS, several different mouse models have been created, and test batteries for their phenotype have been established that are well-suited to evaluate possible therapies for AS (Sonzogni et al., 2018, Rotaru et al., 2020). Alternatively, patient-derived inducible pluripotent stem cell (iPSC) systems are close to reality models to evaluate E6AP activators (Chamberlain et al., 2010, Fink et al., 2017). Determing efficiency of therapies with AS individuals according to FDA-approved regimes appears to be rather difficult due to the rare number of AS individuals. Similarly, chances to find identical twins for a placebo-controlled trial are very low (and ethically questionable), even though such a study was performed recently (Han et al., 2019). Furthermore, a major concern is that most likely AS needs to be treated in the first months of life, while it is currently diagnosed as late as at an age of nine months to six years (Zylka, 2019).

In conclusion, while it is still a long way with several obstacles to overcome towards an AS therapy with small molecule E6AP activators, this study hopefully makes a first into this direction step by showing that E6AP as well as certain AS-derived E6AP mutants can be activated by small molecules. While the most potent compounds (OF204, OF227, OF232, OF234) need to be derivatized to reduce cytotoxicity, Tamoxifen and 4-Methyltamoxifen should be tested in AS mouse and iPSC models in the near future.

5.4 Mechanism of E6AP activation

The identified small molecules proved to be able to activate E6AP in several different experiments. The mechanism by which the activity of E3 ligases can be regulated in general and a possible mechanism how the small molecules activate E6AP will be discussed in the following sections.

5.4.1 Activability of ubiquitin ligases in general and of E6AP in particular

Our laboratory previously showed that E6AP can be activated by HPV-16 E6 (Mortensen et al., 2015) and by HERC2, another ubiquitin ligase (Kühnle et al., 2011). In general, it is not surprising that E6AP can be activated, since it is a common feature of many enzymes to be not fully active in their naturally occurring state and to be transferred into more active states for example by post-translational modifications, binding of cofactors or by interaction or complex formation with other proteins (Oliveira & Sauer, 2012). Furthermore, it is known that also ubiquitin ligases can be activated as described in this chapter.

For instance, several HECT ligases are kept in a catalytically inactive state by intramolecular interactions between N-terminal regions (either the C2 linker or the linker region between the WW domains) and the HECT domain (Weber et al., 2019). Auto-inhibition of these ligases was uncovered when removal of specific domains increased their activity (Wiesner et al., 2007, Weber et al., 2019). However, since E6AP does not contain comparable N-terminal regions, it is unlikely that E6AP is regulated by a similar auto-inhibitory mechanism. Nonetheless, N-terminal regions of E6AP and probably interactions of these with the HECT domain seem to be decisive for its ligase activity, as supported by the facts that (I) the HECT domain of E6AP by its own is catalytically rather inactive, (II) an AZUL domain deletion mutant is more active than full-length E6AP and (III) qXL-MS indicated conformational rearrangements of all domains of E6AP when it is transferred into a high-activity conformation.

For other members of the HECT family, non-covalent interactions of the HECT domain with ubiquitin seem to be important to control catalysis but E6AP seems to behave differently also in this respect (Jackl et al., 2018). Furthermore, inhibition by homodimerization as proposed for HUWE1 (Sander et al., 2017) or activation by trimerization as suggested for E6AP itself (Ronchi et al., 2014) are unlikely as size-exclusion chromatography and SILAC-XL-MS experiments performed in this study indicate a monomeric state of E6AP (figure 41). However, additional mechanisms of regulation exist for ubiquitin ligases, as most, if not all, RBR E3s are for example known to be auto-inhibited, yet by different mechanisms (reviewed in (Dove & Klevit, 2017)). Furthermore, a study using high-throughput mutagenesis of Ube4b (an RBR ligase) could identify activity-enhancing point mutations (Starita et al., 2013). This shows that small changes like substitution of a single amino acid can have major effects on the activity of ubiquitin ligases which may also be achieved by post-translational modifications or

bound small molecules. Indeed, also for E6AP a hyperactive point mutant (T485A, numbering according to isoform 1) was identified in an ASD individual (Yi et al., 2015). In line with these results, it could be shown that E6AP K847R is more active than wild-type E6AP (Krist & Statsyuk, 2015). These findings were confirmed during the present study (not shown) and emphasize the notion that also small differences can result in large activity changes of E6AP.

Interestingly, E6AP shows certain similarity to several RBR ligases as both have to make large domain movements to allow ubiquitin transfer from the E2~Ub thioester to the active site cysteine (Huang et al., 1999, Dove & Klevit, 2017). In support of this hypothesis, regions of E6AP close to the E6 binding site are disordered, indicating conformational flexibility that allows domains to adopt distant locations (as in the proposed low-activity conformation) as well as proximal ones (as in the proposed high-activity conformation).

5.4.2 Interaction between N and C termini of E6AP as regulatory mechanism

Quantitative XL-MS experiments could show that N and C termini of E6AP get in closer proximity when E6AP is prevalently in its high-activity conformation (figures 42 and 45). Interestingly, this conformational rearrangement was obtained for wild-type E6AP as well as for the F583S and E584Q mutants by addition of HPV-16 E6 or of small molecule activators (as shown with OF232 in this study). In each case, an enrichment of crosslinks between N and C termini and a decrease of crosslinks between the HECT domain and central regions was observed (figures 45). Comparison of the crosslinking patterns of wild-type E6AP and the investigated 58X AS mutants did not reveal major differences (figure 44). These results fit to the fact that these mutants are capable of forming ubiquitin-thioesters and are not completely impaired in their ligase activity. The underlying mechanism of the defect of the 58X AS mutants in isopeptide bond formation could not be solved yet. The defect seems to be independent of the interaction with the AZUL domain as a double mutant (E6AP_F583S_ΔAZUL) is as strongly impaired as the AS mutant itself. Regardless, an interaction of N and C termini seems to be characteristic for a high-activity conformation of both E6AP and the AS-derived point mutants as summarized in the current model of E6AP activation (figure 46).

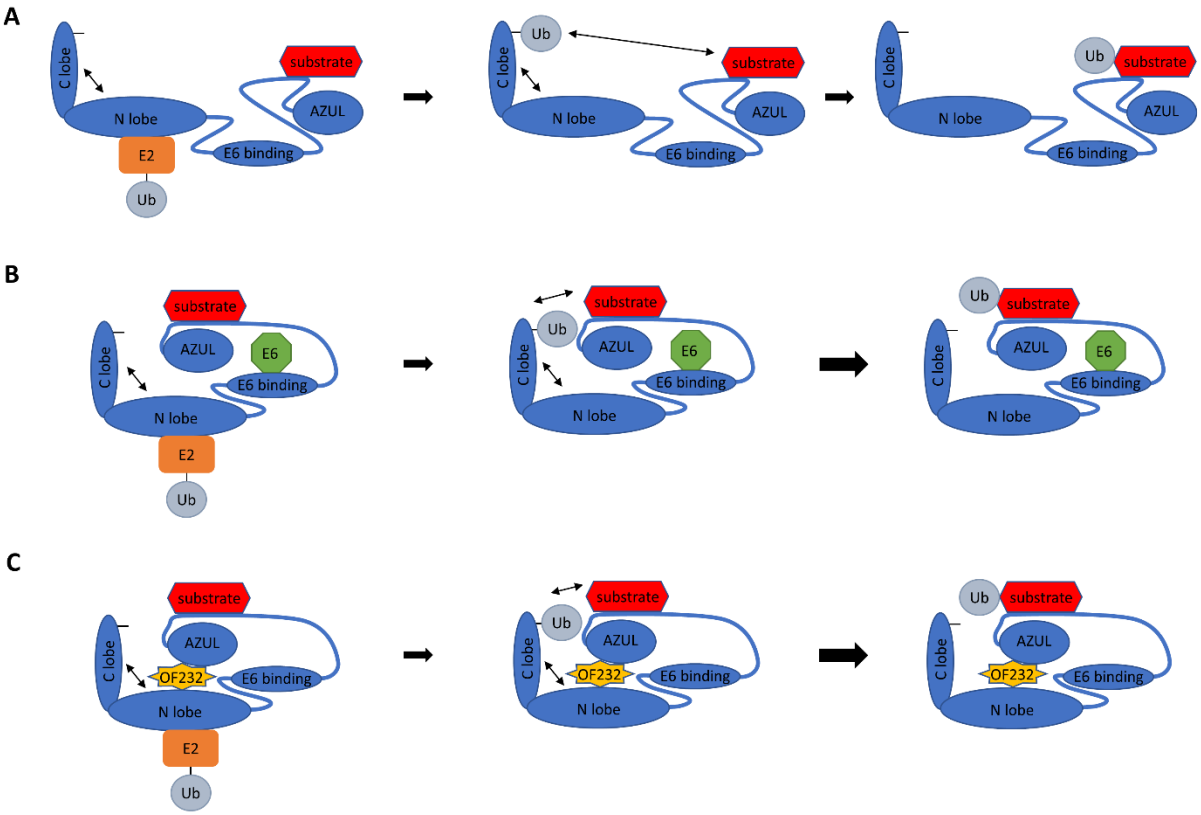

Figure 46: Model of the mechanism of E6AP activation by HPV-16 E6 and OF232
A hypothetical model of the mechanism of activation of E6AP-mediated ubiquitination is shown for (A) E6AP alone, (B) E6AP in presence of HPV-16 E6, and (C) E6AP in presence of the small molecule activator OF232. The first reaction step, namely the transthiolation reaction (the transfer of ubiquitin from the E2 enzyme to the catalytic center of E6AP) is unaffected by both allosteric activators. In contrast, the second reaction step, namely the isopeptide bond formation (transfer of ubiquitin from the catalytic center of E6AP to a lysine residues of the substrate) is stimulated by both HPV-16 E6 and the small molecule activator (as indicated by larger reaction arrows). Note that the model is valid not only for wild-type E6AP but also for the E6AP 58X AS mutants. Binding of HPV-16 E6 or OF232 results in similar structural rearrangements of E6AP in such a way that N-terminal regions (e.g. the AZUL domain) get into closer proximity to the HECT domain (N lobe and C lobe harboring the catalytic center of E6AP). E6AP is colored blue, E2 is colored orange, the substrate is colored red, ubiquitin is colored grey, HPV-16 E6 is colored green, and OF232 is colored yellow. Arrows indicate the two reaction steps of the catalysis. Double-headed arrows indicate structural flexibility and/or movements of E6AP.

Interaction of very N and C termini of E6AP could also be seen in alternative experiments (data not shown). E6AP auto-ubiquitination shows always mono- and to a smaller extent diubiquitinated species at very early time points that rapidly shift to high-molecular mass smear indicating poly-ubiquitination. Mass spectrometric analysis revealed that main mono-ubiquitination sites are lysine 54, 78 and 847 (numbering according to isoform 1 (Yamamoto et al., 1997), data not shown). These lysine residues need to be proximal to the catalytic center to be ubiquitinated, that is, that the AZUL domain needs to be in short distance to the HECT domain when ubiquitin is passed onto them. While lysine 847 was already known to play an important role in catalysis (Krist & Statsyuk, 2015), mono-ubiquitination of

lysine 54 and 78 needs to be elaborated in more detail, especially in presence of activators or for AS-derived E6AP mutants.

First results by mutational analysis of the respective lysines to alanine or arginine suggests that mono-ubiquitination of E6AP in the very N terminus indeed regulates E6AP activity as the mutants are less active than wild-type E6AP (Benedikt Steinle, under supervision). This fits to the notion that release of auto-inhibited states by auto-ubiquitination is a more common feature of E3 ligases, as previously demonstrated for HDM2 (Ranaweera & Yang, 2013). However, the precise impact of E6AP mono-ubiquitination and possible structural rearrangements, especially regarding positioning of the AZUL domain, needs to await solution of structures of respective species. So far, it remains unanswered whether mono-ubiquitination of E6AP's N terminus happens accidentally in *in vitro* assays or whether it truly plays a regulating role in E6AP auto- or substrate ubiquitination.

Mono-ubiquitination may be one mechanism of E6AP regulation, but several further layers exist for sure, as it was already shown for phosphorylation (i.e. T485 (Yi et al., 2015)) and interacting proteins like HERC2, HPV-16 E6 (Kühnle et al., 2011, Mortensen et al., 2015). Therefore, it remains interesting to not only obtain structures of full-length E6AP in different stages of the catalytic cycle but also in differently active conformations induced by post-translational modifications or allosteric activators. With such structures in hand, it could be rationalized which domains or residues of E6AP are critical for regulation of its activity. This information could be used to fine-tune E6AP activity. Furthermore, such structures could ultimately explain the deleterious effects of AS-derived point mutations. The activators identified in this study can perhaps contribute in this case by stabilizing certain conformations so that E6AP can be crystallized, which is on-going work in collaboration. In addition, the recent progress in cryo-electron microscopy (Nogales & Scheres, 2015, Ognjenovic et al., 2019) offers a promising alternative approach to solve the structure of normal and high-activity conformations of E6AP.

Taken together, we obtained evidence that allosteric activators of E6AP act by inducing conformational rearrangements bringing N and C termini into closer proximity. Consequently, a model could be that in the absence of interacting proteins or molecules, E6AP is mainly in a conformation in which the HECT domain interacts with central regions (e.g. E6-binding or neighboring regions). Binding of HPV-16 E6 could disperse these interactions leading to far-reaching conformational rearrangements that favor interaction of the N-terminal domain with the HECT domain resulting in a high-activity conformation. Whether or not this model is correct and how HPV-16 E6 and the small molecule activator OF232 achieve this conformational rearrangement, will have to await high-resolution structures of full-length E6AP with bound HPV-16 E6 or OF232, respectively.

6 Conclusions and Outlook

6.1 Conclusions

In the present study, a novel FP-based ubiquitination assay was developed. The assay can be used to monitor enzymatic activity of ubiquitin ligases in real-time thus allowing several consecutive measurements in multiwell plates, increasing throughput and simplifying reaction monitoring. The assay proved to be functional in two independent high-throughput screens to identify small molecule inhibitors as well as activators. Furthermore, the FP assay was transferred to different E3 ubiquitin ligases including full-length E6AP and its isolated HECT domain, a truncated variant of HUWE1, full-length HDM2 and its isolated RING domain and the isolated RING domain of RLIM. Thus, in principle, the FP assay should be transferable to many other HECT ligases, RING ligases and RBR ligases as well as to enzymes conjugating ubiquitin-like proteins like SUMO and NEDD8. The only criterion is that the ligase performs efficient in auto- or substrate ubiquitination. Moreover, the assay could be used to identify modulators of E1 and E2 enzymes or of deubiquitinating enzymes, enabling the identification of modulators of all members of the previously as undruggable designated ubiquitination system (Huang & Dixit, 2016). However, the main application of the FP assay is likely to remain the identification of small molecule modulators of ubiquitin ligases or disease-related point mutants of those. Identified modulators are promising lead structures for drug development for associated diseases and will contribute to a deeper understanding of the physiological roles of the respective ligases.

Our efforts to identify small molecule inhibitors of the E6-E6AP complex resulted, unfortunately, in the lesson learned that the great majority of identified hits inhibits also auto-ubiquitination of mechanistically unrelated RING ligases. Although protein-protein interactions are known to be difficult to target, multiple examples emerged recently showing that protein-protein interactions can be interrupted by small molecules (Ivanov et al., 2013, Arkin et al., 2014). Moreover, since the binding pocket of HPV-16 E6 was characterized as druggable (Zanier et al., 2014), it is not immediately clear why no inhibitor that acts unequivocally on the HPV-16 E6-induced activation of E6AP was identified in our study. Thus, the screen should be continued with further compounds and possibly with altered screening conditions in order to find a desired candidate.

In contrast to the inhibitor screen, the screen for activators of E6AP yielded the identification of diverse compounds that stimulate E6AP not only for auto- but also for substrate ubiquitination. Furthermore, certain AS-associated mutants of E6AP could be rescued by a subset of the identified activators. The investigated 58X AS mutants were characterized to be defective in isopeptide bond formation.

Interestingly, the same compounds that rescue the 58X AS mutants also rescue the UbLIA defect of wild-type E6AP, supporting the notion that the compounds act on the isopeptide bond formation step. Finally, qXL-MS was introduced as a method to study conformational rearrangements of E6AP. The structure of E6AP has not been investigated so far by other methods as E6AP appears to resist crystal formation for X-ray analysis and is too large for NMR. In any case, qXL-MS could show that distinct structural rearrangements of E6AP are induced by HPV-16 E6 and small molecule activators. Both types of allosteric activators induce or stabilize a conformation with the main characteristic that N and C termini are in closer proximity compared to E6AP or the 58X AS mutants in the absence of the activators. Furthermore, qXL-MS came in handy, as standard methods to verify binding of small molecules did not work for E6AP. In other words, structural rearrangements, as observed in this study by qXL-MS, induced by a compound provide strong evidence for the interaction of the compound with the protein of interest.

In conclusion, the present study introduces the FP-based ubiquitination assay as a novel tool to study enzymes involved in ubiquitination reactions and to identify promising compounds that may either be used as chemical probes or as lead structures for drug development in scientific and pharmaceutical research.

6.2 Outlook

In the future, the FP-based ubiquitination assay will hopefully be adapted by others for small molecule screenings or to characterize mutants of ubiquitin ligases in a high-throughput manner. Furthermore, either published E6-E6AP inhibitors will be verified or further small molecule libraries will be screened to identify such desired compounds. Besides this, a screen for E6AP inhibitors should be performed to eventually identify compounds for basic research with E6AP or lead structures for therapeutics in the context of Dup15q syndrome. Moreover, if not already in progress, screens for inhibitors of HUWE1_trunc, RLIM_RING and HDM2 should be performed since these ubiquitin ligases are of significant scientific and medicinal interest. Last but not least, AS-derived ligase-deficient mutants of E6AP should be screened for activators to obtain additional lead compounds and to characterize possible catalytic differences between the mutants.

In line with this, it would be exciting to investigate further AS mutants or hyperactive E6AP variants (i.e. Y533A, C21Y, and T485A) by qXL-MS to characterize them on a structural level. Moreover, structural dynamics of E6AP in presence of HERC2 or its RLD2 domain (that was shown to be sufficient for E6AP activation (Kühnle et al., 2011)) were not performed yet and should be done to complete the picture of E6AP activation. It is well imaginable that similar structural dynamics as for HPV-16 E6 are obtained. However, also other mechanisms of activation are conceivable, which could also be valid for a subset of the identified small molecule activators.

Another issue that needs to be addressed in future studies is the optimization of the identified small molecule activators of E6AP. They should be examined by medicinal chemistry experts to improve them for tests in AS iPSC systems or AS mouse model test batteries. Additionally, it would be exciting to explore the influence of the small molecule activators on ubiquitination of different substrates of E6AP. In the same direction, activators could be used to identify new bona-fide substrates of E6AP in quantitative proteomics. If future work identifies a substrate that plays a key role in Angelman syndrome, activators of E6AP might possibly be used to develop PROTACs (proteolysis targeting chimeras) (Burslem & Crews, 2020) for targeted and efficient ubiquitination of that single protein while other substrates would be less affected. However, since only a narrow range of activity alteration of E6AP appears to be allowed for normal neural development, it may be extremely challenging to fine-tune E6AP activity properly, in particular in imprinting-affected neurons of AS individuals. Nonetheless, the identified small molecule activators of E6AP present a further step towards understanding regulation and physiological functions of E6AP and possibly towards novel therapeutics for AS.

7 References

Adhikary S, Marinoni F, Hock A, Hulleman E, Popov N, Beier R, Bernard S, Quarto M, Capra M, Goettig S, Kogel U, Scheffner M, Helin K, Eilers M (2005) The ubiquitin ligase HectH9 regulates transcriptional activation by Myc and is essential for tumor cell proliferation. Cell; 123: 409-21

Albrecht U, Sutcliffe JS, Cattanach BM, Beechey CV, Armstrong D, Eichele G, Beaudet AL (1997) Imprinted expression of the murine Angelman syndrome gene, Ube3a, in hippocampal and Purkinje neurons. Nat Genet; 17: 75-78

Angelman H (1965) Puppet Children - a Report on 3 Cases. Dev Med Child Neurol; 7: 681-&

Arkin MR, Tang Y, Wells JA (2014) Small-molecule inhibitors of protein-protein interactions: progressing toward the reality. Chem Biol; 21: 1102-14

Aronchik I, Kundu A, Quirit JG, Firestone GL (2014) The Antiproliferative Response of Indole-3-Carbinol in Human Melanoma Cells Is Triggered by an Interaction with NEDD4-1 and Disruption of Wild-Type PTEN Degradation. Mol Cancer Res; 12: 1621-1634

Attali I, Tobelaim WS, Persaud A, Motamedchaboki K, Simpson-Lavy KJ, Mashahreh B, Levin-Kravets O, Keren-Kaplan T, Pilzer I, Kupiec M, Wiener R, Wolf DA, Rotin D, Prag G (2017) Ubiquitylation-dependent oligomerization regulates activity of Nedd4 ligases. Embo Journal; 36: 425-440

Avagliano Trezza R, Sonzogni M, Bossuyt SNV, Zampeta FI, Punt AM, van den Berg M, Rotaru DC, Koene LMC, Munshi ST, Stedehouder J, Kros JM, Williams M, Heussler H, de Vrij FMS, Mientjes EJ, van Woerden GM, Kushner SA, Distel B, Elgersma Y (2019) Loss of nuclear UBE3A causes electrophysiological and behavioral deficits in mice and is associated with Angelman syndrome. Nat Neurosci; 22: 1235-1247

Bacino CA, Goddard-Finegold J, Turcich M, Glaze D, O'Brien W, Beaudet AL (2001) A double blind therapeutic trial in Angelman syndrome using betaine and folic acid. Am J Hum Genet; 69: 679-679

Baleja JD, Cherry JJ, Liu ZG, Gao H, Nicklaus MC, Voigt JH, Chen JJ, Androphy EJ (2006) Identification of inhibitors to papillomavirus type 16 E6 protein based on three-dimensional structures of interacting proteins. Antivir Res; 72: 49-59

Bandilovska I, Keam SP, Gamell C, Machicado C, Haupt S, Haupt Y (2019) E6AP goes viral: the role of E6AP in viral- and non-viral-related cancers. Carcinogenesis; 40: 707-714

Bard JAM, Goodall EA, Greene ER, Jonsson E, Dong KC, Martin A (2018) Structure and Function of the 26S Proteasome. Annu Rev Biochem; 87: 697-724

Baxter AJ, Brugha TS, Erskine HE, Scheurer RW, Vos T, Scott JG (2015) The epidemiology and global burden of autism spectrum disorders. Psychol Med; 45: 601-13

Be XB, Hong YH, Wei J, Androphy EJ, Chen JJ, Baleja JD (2001) Solution structure determination and mutational analysis of the papillomavirus E6 interacting peptide of E6AP. Biochemistry; 40: 1293-1299

Beal R, Deveraux Q, Xia G, Rechsteiner M, Pickart C (1996) Surface hydrophobic residues of multiubiquitin chains essential for proteolytic targeting. Proc Natl Acad Sci U S A; 93: 861-6

Beasley SA, Bardhi R, Spratt DE (2019) H-1, C-13, and N-15 resonance assignments of the C-terminal lobe of the human HECT E3 ubiquitin ligase ITCH. Biomol Nmr Assign; 13: 15-20

Beaudenon S, Huibregtse JM (2008) HPV E6, E6AP and cervical cancer. Bmc Biochemistry; 9

Beerheide W, Bernard HU, Tan YJ, Ganesan A, Rice WG, Ting AE (1999) Potential drugs against cervical cancer: zinc-ejecting inhibitors of the human papillomavirus type 16 E6 oncoprotein. J Natl Cancer Inst; 91: 1211-20

BeerRomero P, Glass S, Rolfe M (1997) Antisense targeting of E6AP elevates p53 in HPV-infected cells but not in normal cells. Oncogene; 14: 595-602

Ben-Saadon R, Zaaroor D, Ziv T, Ciechanover A (2006) The polycomb protein Ring1B generates self atypical mixed ubiquitin chains required for its in vitro histone H2A ligase activity. Mol Cell; 24: 701-711

Berthold MR, Cebron N, Dill F, Gabriel TR, Kotter T, Meinl T, Ohl P, Sieb C, Thiel K, Wiswedel B (2008) KNIME: The Konstanz Information Miner. Stud Class Data Anal: 319-326

Bielskiene K, Bagdoniene L, Mozuraitiene J, Kazbariene B, Janulionis E (2015) E3 ubiquitin ligases as drug targets and prognostic biomarkers in melanoma. Medicina-Lithuania; 51: 1-9

Bindels-de Heus K, Mous SE, Ten Hooven-Radstaake M, van Iperen-Kolk BM, Navis C, Rietman AB, Ten Hoopen LW, Brooks AS, AS EECf, Elgersma Y, Moll HA, de Wit MY (2019) An overview of health issues and development in a large clinical cohort of children with Angelman syndrome. Am J Med Genet A;

Birch SE, Kench JG, Takano E, Chan P, Chan AL, Chiam K, Veillard AS, Stricker P, Haupt S, Haupt Y, Horvath L, Fox SB (2014) Expression of E6AP and PML predicts for prostate cancer progression and cancer-specific death. Ann Oncol; 25: 2392-7

Bird LM (2014) Angelman syndrome: review of clinical and molecular aspects. Appl Clin Genet; 7: 93-104

Boisclair MD, McClure C, Josiah S, Glass S, Bottomley S, Kamerkar S, Hemmila I (2000) Development of a ubiquitin transfer assay for high throughput screening by fluorescence resonance energy transfer. J Biomol Screen; 5: 319-28

Bonati MT, Russo S, Finelli P, Valsecchi MR, Cogliati F, Cavalleri F, Roberts W, Elia M, Larizza L (2007) Evaluation of autism traits in Angelman syndrome: a resource to unfold autism genes. Neurogenetics; 8: 169-78

Borgatti R, Piccinelli P, Passoni D, Dalpra L, Miozzo M, Micheli R, Gagliardi C, Balottin U (2001) Relationship between clinical and genetic features in "inverted duplicated chromosome 15" patients. Pediatr Neurol; 24: 111-116

Bosch FX, Broker TR, Forman D, Moscicki AB, Gillison ML, Doorbar J, Stern PL, Stanley M, Arbyn M, Poljak M, Cuzick J, Castle PE, Schiller JT, Markowitz LE, Fisher WA, Canfell K, Denny LA, Franco EL, Steben M, Kane MA, Schiffman M, Meijer CJLM, Sankaranarayanan R, Castellsague X, Kim JJ, Brotons M, Alemany L, Albero G, Diaz M, de Sanjose S, Conto IMC (2013) Comprehensive Control of Human Papillomavirus Infections and Related Diseases. Vaccine; 31: H1-H31

Braun JA, Herrmann AL, Blase JI, Frensemeier K, Bulkescher J, Scheffner M, Galy B, Hoppe-Seyler K, Hoppe-Seyler F (2019) Effects of the antifungal agent ciclopirox in HPV-positive cancer cells: Repression of viral E6/E7 oncogene expression and induction of senescence and apoptosis. Int J Cancer;

Browne CE, Dennis NR, Maher E, Long FL, Nicholson JC, Sillibourne J, Barber JCK (1997) Inherited interstitial duplications of proximal 15q: Genotype-phenotype correlations. Am J Hum Genet; 61: 1342-1352

Buckley DL, Crews CM (2014) Small-Molecule Control of Intracellular Protein Levels through Modulation of the Ubiquitin Proteasome System. Angew Chem Int Edit; 53: 2312-2330

Buckley RH, Dinno N, Weber P (1998) Angelman syndrome: are the estimates too low? Am J Med Genet; 80: 385-90

Buel GR, Chen X, Chari R, O'Neill MJ, Ebelle DL, Jenkins C, Sridharan V, Tarasov SG, Tarasova NI, Andresson T, Walters KJ (2020) Structure of E3 ligase E6AP with a proteasome-binding site provided by substrate receptor hRpn10. Nat Commun; 11: 1291

Burette AC, Judson MC, Burette S, Phend KD, Philpot BD, Weinberg RJ (2017) Subcellular organization of UBE3A in neurons. J Comp Neurol; 525: 233-251

Burette AC, Judson MC, Li AN, Chang EF, Seeley WW, Philpot BD, Weinberg RJ (2018) Subcellular organization of UBE3A in human cerebral cortex. Mol Autism; 9: 54

Burslem GM, Crews CM (2020) Proteolysis-Targeting Chimeras as Therapeutics and Tools for Biological Discovery. Cell; 181: 102-114

Butz K, Denk C, Ullmann A, Scheffner M, Hoppe-Seyler F (2000) Induction of apoptosis in human papillomaviruspositive cancer cells by peptide aptamers targeting the viral E6 oncoprotein. Proc Natl Acad Sci U S A; 97: 6693-7

Butz K, Ristriani T, Hengstermann A, Denk C, Scheffner M, Hoppe-Seyler F (2003) siRNA targeting of the viral E6 oncogene efficiently kills human papillomavirus-positive cancer cells. Oncogene; 22: 5938-5945

Cao Y, Wang C, Zhang XL, Xing GC, Lu KF, Gu YQ, He FC, Zhang LQ (2014) Selective Small Molecule Compounds Increase BMP-2 Responsiveness by Inhibiting Smurf1-mediated Smad1/5 Degradation. Sci Rep-Uk; 4

Celegato M, Messa L, Goracci L, Mercorelli B, Bertagnin C, Spyrakis F, Suarez I, Cousido-Siah A, Trave G, Banks L, Cruciani G, Palu G, Loregian A (2019) A novel small-molecule inhibitor of the human papillomavirus E6-p53 interaction that reactivates p53 function and blocks cancer cells growth. Cancer Lett;

Chamberlain SJ, Brannan CI (2001) The Prader-Willi syndrome imprinting center activates the paternally expressed murine Ube3a antisense transcript but represses paternal Ube3a. Genomics; 73: 316-22

Chamberlain SJ, Chen PF, Ng KY, Bourgois-Rocha F, Lemtiri-Chlieh F, Levine ES, Lalande M (2010) Induced pluripotent stem cell models of the genomic imprinting disorders Angelman and Prader-Willi syndromes. P Natl Acad Sci USA; 107: 17668-17673

Chan AL, Grossman T, Zuckerman V, Campigli Di Giammartino D, Moshel O, Scheffner M, Monahan B, Pilling P, Jiang YH, Haupt S, Schueler-Furman O, Haupt Y (2013) c-Abl phosphorylates E6AP and regulates its E3 ubiquitin ligase activity. Biochemistry; 52: 3119-29

Chen D, Gehringer M, Lorenz S (2018) Developing Small-Molecule Inhibitors of HECT-Type Ubiquitin Ligases for Therapeutic Applications: Challenges and Opportunities. Chembiochem; 19: 2123-2135

Chen X, Wei S, Ji Y, Guo X, Yang F (2015) Quantitative proteomics using SILAC: Principles, applications, and developments. Proteomics; 15: 3175-92

Chen Z, Jiang HJ, Xu W, Li XG, Dempsey DR, Zhang XB, Devreotes P, Wolberger C, Amzel LM, Gabelli SB, Cole PA (2017) A Tunable Brake for HECT Ubiquitin Ligases. Molecular Cell; 66: 345-+

Chen ZA, Rappsilber J (2018) Protein Dynamics in Solution by Quantitative Crosslinking/Mass Spectrometry. Trends Biochem Sci; 43: 908-920

Cherry JJ, Rietz A, Malinkevich A, Liu Y, Xie M, Bartolowits M, Davisson VJ, Baleja JD, Androphy EJ (2013) Structure based identification and characterization of flavonoids that disrupt human papillomavirus-16 E6 function. PLoS One; 8: e84506

Clayton-Smith J (1993) Clinical Research on Angelman Syndrome in the United-Kingdom - Observations on 82 Affected Individuals. Am J Med Genet; 46: 12-15

Clayton-Smith J, Laan L (2003) Angelman syndrome: a review of the clinical and genetic aspects. Journal of Medical Genetics; 40: 87-95

Clayton-Smith J, Pembrey ME (1992) Angelman syndrome. J Med Genet; 29: 412-5

Clerici M, Luna-Vargas MP, Faesen AC, Sixma TK (2014) The DUSP-Ubl domain of USP4 enhances its catalytic efficiency by promoting ubiquitin exchange. Nat Commun; 5: 5399

Cook EH, Lindgren V, Leventhal BL, Courchesne R, Lincoln A, Shulman C, Lord C, Courchesne E (1997) Autism or atypical autism in maternally but not paternally derived proximal 15q duplication. Am J Hum Genet; 60: 928-934

Cooper EM, Hudson AW, Amos J, Wagstaff J, Howley PM (2004) Biochemical analysis of Angelman syndrome-associated mutations in the E3 ubiquitin ligase E6-associated protein. J Biol Chem; 279: 41208-17

Copping NA, Christian SGB, Ritter DJ, Islam MS, Buscher N, Zolkowska D, Pride MC, Berg EL, LaSalle JM, Ellegood J, Lerch JP, Reiter LT, Silverman JL, Dindot SV (2017) Neuronal overexpression of Ube3a isoform 2 causes behavioral impairments and neuroanatomical pathology relevant to 15q11.2-q13.3 duplication syndrome. Hum Mol Genet; 26: 3995-4010

Couse JF, Korach KS (1999) Estrogen receptor null mice: what have we learned and where will they lead us? (vol 20, pg 358, 1999). Endocr Rev; 20: 459-459

Cubillos-Rojas M, Schneider T, Hadjebi O, Pedrazza L, de Oliveira JR, Langa F, Guenet JL, Duran J, de Anta JM, Alcantara S, Ruiz R, Perez-Villegas EM, Aguilar-Montilla FJ, Carrion AM, Armengol JA, Baple E, Crosby AH, Bartrons R, Ventura F, Rosa JL (2016) The HERC2 ubiquitin ligase is essential for embryonic development and regulates motor coordination. Oncotarget; 7: 56083-56106

D'Abramo CM, Archambault J (2011) Small molecule inhibitors of human papillomavirus protein - protein interactions. Open Virol J; 5: 80-95

Daily J, Smith AG, Weeber EJ (2012) Spatial and temporal silencing of the human maternal UBE3A gene. Eur J Paediatr Neurol; 16: 587-91

Dangles O, Dufour C (2008) Flavonoid-Protein Binding Processes and their Potential Impact on Human Health. Rec Adv Polyphen Res; 1: 67-87

Davydov IV, Woods D, Safiran YJ, Oberoi P, Fearnhead HO, Fang S, Jensen JP, Weissman AM, Kenten JH, Vousden KH (2004) Assay for ubiquitin ligase activity: High-throughput screen for inhibitors of HDM2. Journal of Biomolecular Screening; 9: 695-703

de Bie P, Ciechanover A (2011) Ubiquitination of E3 ligases: self-regulation of the ubiquitin system via proteolytic and non-proteolytic mechanisms. Cell Death Differ; 18: 1393-402

De Cesare V, Johnson C, Barlow V, Hastie J, Knebel A, Trost M (2018) The MALDI-TOF E2/E3 Ligase Assay as Universal Tool for Drug Discovery in the Ubiquitin Pathway. Cell Chemical Biology; 25: 1117-+

de Martel C, Plummer M, Vignat J, Franceschi S (2017) Worldwide burden of cancer attributable to HPV by site, country and HPV type. International Journal of Cancer; 141: 664-670

Deol KK, Lorenz S, Strieter ER (2019) Enzymatic Logic of Ubiquitin Chain Assembly. Frontiers in Physiology; 10

Deroo BJ, Korach KS (2006) Estrogen receptors and human disease. J Clin Invest; 116: 561-70

Deshaies RJ, Joazeiro CA (2009) RING domain E3 ubiquitin ligases. Annual review of biochemistry; 78: 399-434

Dhamodharan, Ponnusamy, Odumpatta, Lulu, Arumugam (2018) Computational investigation of marine bioactive compounds against E6 oncoprotein of Human Papilloma Virus-HPV16. J App Pharm Sci,; 8(04): 023-032

Dhananjayan SC, Ramamoorthy S, Khan OY, Ismail A, Sun J, Slingerland J, O'Malley BW, Nawaz Z (2006) WW domain binding protein-2, an E6-associated protein interacting protein, acts as a coactivator of estrogen and progesterone receptors. Mol Endocrinol; 20: 2343-2354

Dikic I (2017) Proteasomal and Autophagic Degradation Systems. Annual Review of Biochemistry, Vol 86; 86: 193-224

Dikic I, Wakatsuki S, Walters KJ (2009) Ubiquitin-binding domains - from structures to functions. Nature reviews Molecular cell biology; 10: 659-71

Dindot SV, Antalffy BA, Bhattacharjee MB, Beaudet AL (2008) The Angelman syndrome ubiquitin ligase localizes to the synapse and nucleus, and maternal deficiency results in abnormal dendritic spine morphology. Hum Mol Genet; 17: 111-8

Doorbar J, Egawa N, Griffin H, Kranjec C, Murakami I (2015) Human papillomavirus molecular biology and disease association. Rev Med Virol; 25 Suppl 1: 2-23

Dove KK, Klevit RE (2017) RING-Between-RING E3 Ligases: Emerging Themes amid the Variations. J Mol Biol; 429: 3363-3375

Drews CM, Brimer N, Vande Pol SB (2020) Multiple regions of E6AP (UBE3A) contribute to interaction with papillomavirus E6 proteins and the activation of ubiquitin ligase activity. PLoS Pathog; 16: e1008295

Driscoll DJ, Miller JL, Schwartz S, Cassidy SB (2017) Prader-Willi Syndrome. In Book, Prader-Willi Syndrome, Adam MP, Ardinger HH, Pagon RA, Wallace SE, Bean LJH, Stephens K, Amemiya A (eds) Seattle (WA):

Du JL, Strieter ER (2018) A fluorescence polarization-based competition assay for measuring interactions between unlabeled ubiquitin chains and UCH37 center dot RPN13. Anal Biochem; 550: 84-89

Du YH (2015) Fluorescence Polarization Assay to Quantify Protein-Protein Interactions in an HTS Format. Protein-Protein Interactions: Methods and Applications, 2nd Edition; 1278: 529-544

Dymalla S, Scheffner M, Weber E, Sehr P, Lohrey C, Hoppe-Seyler F, Hoppe-Seyler K (2009) A novel peptide motif binding to and blocking the intracellular activity of the human papillomavirus E6 oncoprotein. J Mol Med (Berl); 87: 321-31

Ebner F (2019) Deregulation of protein ubiquitination by HPV E6 proteins. Doctoral thesis, AG Scheffner, University of Konstanz;

Eisenhaber B, Chumak N, Eisenhaber F, Hauser MT (2007) The ring between ring fingers (RBR) protein family. Genome Biol; 8: 209

El Hokayem J, Weeber E, Nawaz Z (2018) Loss of Angelman Syndrome Protein E6AP Disrupts a Novel Antagonistic Estrogen-Retinoic Acid Transcriptional Crosstalk in Neurons. Mol Neurobiol; 55: 7187-7200

Eletr ZM, Kuhlman B (2007) Sequence determinants of E2-E6AP binding affinity and specificity. J Mol Biol; 369: 419-28

Engelke J (2019) Structural characterization of E6AP and disease-related E6AP variants. Masterthesis, AG Scheffner, University of Konstanz;

Escobedo A, Gomes T, Aragon E, Martin-Malpartida P, Ruiz L, Macias MJ (2014) Structural Basis of the Activation and Degradation Mechanisms of the E3 Ubiquitin Ligase Nedd4L. Structure; 22: 1446-1457

Fabian C, Tilzer L, Sternson L (1981) Comparative binding affinities of tamoxifen, 4-hydroxytamoxifen, and desmethyltamoxifen for estrogen receptors isolated from human breast carcinoma: correlation with blood levels in patients with metastatic breast cancer. Biopharm Drug Dispos; 2: 381-90

Fang P, Lev-Lehman E, Tsai TF, Matsuura T, Benton CS, Sutcliffe JS, Christian SL, Kubota T, Halley DJ, Meijers-Heijboer H, Langlois S, Graham JM, Beuten J, Willems PJ, Ledbetter DH, Beaudet AL (1999) The spectrum of mutations in UBE3A causing Angelman syndrome. Hum Mol Genet; 8: 129-135

Feng YM, Sessions EH, Zhang F, Ban FQ, Placencio-Hickok V, Ma CT, Zeng FY, Pass I, Terry DB, Cadwell G, Bankston LA, Liddington RC, Chung TDY, Pinkerton AB, Sergienko E, Gleave M, Bhowmick NA, Jackson MR, Cherkasov A, Ronai ZA (2019) Identification and characterization of small molecule

inhibitors of the ubiquitin ligases Siah1/2 in melanoma and prostate cancer cells. Cancer Letters; 449: 145-162

Fink JJ, Robinson TM, Germain ND, Sirois CL, Bolduc KA, Ward AJ, Rigo F, Chamberlain SJ, Levine ES (2017) Disrupted neuronal maturation in Angelman syndrome-derived induced pluripotent stem cells. Nat Commun; 8: 15038

Finucane BM, Lusk L, Arkilo D, Chamberlain S, Devinsky O, Dindot S, Jeste SS, LaSalle JM, Reiter LT, Schanen NC, Spence SJ, Thibert RL, Calvert G, Luchsinger K, Cook EH (2016) 15q Duplication Syndrome and Related Disorders. In Book, 15q Duplication Syndrome and Related Disorders, Adam MP, Ardinger HH, Pagon RA, Wallace SE, Bean LJH, Stephens K, Amemiya A (eds) Seattle (WA):

Foster SA, Phelps WC (1999) Zn(2+) fingers and cervical cancer. J Natl Cancer Inst; 91: 1180-1

Franklin TG, Pruneda JN (2019) A High-Throughput Assay for Monitoring Ubiquitination in Real Time. Front Chem; 7: 816

Frints SGM, Ozanturk A, Criado GR, Grasshoff U, de Hoon B, Field M, Manouvrier-Hanu S, Hickey SE, Kammoun M, Gripp KW, Bauer C, Schroeder C, Toutain A, Mosher TM, Kelly BJ, White P, Dufke A, Rentmeester E, Moon S, Koboldt DC, van Roozendaal KEP, Hu H, Haas SA, Ropers HH, Murray L, Haan E, Shaw M, Carroll R, Friend K, Liebelt J, Hobson L, De Rademaeker M, Geraedts J, Fryns JP, Vermeesch J, Raynaud M, Riess O, Gribnau J, Katsanis N, Devriendt K, Bauer P, Gecz J, Golzio C, Gontan C, Kalscheuer VM (2019) Pathogenic variants in E3 ubiquitin ligase RLIM/RNF12 lead to a syndromic X-linked intellectual disability and behavior disorder. Mol Psychiatr; 24: 1748-1768

Gallagher E, Gao M, Liu YC, Karin M (2006) Activation of the E3 ubiquitin ligase Itch through a phosphorylation-induced conformational change. P Natl Acad Sci USA; 103: 1717-1722

Gamell C, Bandilovska I, Gulati T, Kogan A, Lim SC, Kovacevic Z, Takano EA, Timpone C, Agupitan AD, Litchfield C, Blandino G, Horvath LG, Fox SB, Williams SG, Russo A, Gallo E, Paul PJ, Mitchell C, Sandhu S, Keam SP, Haupt S, Richardson DR, Haupt Y (2019) E6AP Promotes a Metastatic Phenotype in Prostate Cancer. iScience; 22: 1-15

Gamell C, Gulati T, Levav-Cohen Y, Young RJ, Do H, Pilling P, Takano E, Watkins N, Fox SB, Russell P, Ginsberg D, Monahan BJ, Wright G, Dobrovic A, Haupt S, Solomon B, Haupt Y (2017) Reduced abundance of the E3 ubiquitin ligase E6AP contributes to decreased expression of the INK4/ARF locus in non-small cell lung cancer. Sci Signal; 10

George AJ, Hoffiz YC, Charles AJ, Zhu Y, Mabb AM (2018) A Comprehensive Atlas of E3 Ubiquitin Ligase Mutations in Neurological Disorders. Front Genet; 9: 29

Geurink PP, El Oualid F, Jonker A, Hameed DS, Ovaa H (2012) A General Chemical Ligation Approach Towards Isopeptide-Linked Ubiquitin and Ubiquitin-Like Assay Reagents. Chembiochem; 13: 293-297

Giuliano AR, Tortolero-Luna G, Ferrer E, Burchell AN, de Sanjose S, Kjaer SK, Munoz N, Schiffman M, Bosch FX (2008) Epidemiology of Human Papillomavirus Infection in Men, Cancers other than Cervical and Benign Conditions. Vaccine; 26: K17-K28

Glessner JT, Wang K, Cai G, Korvatska O, Kim CE, Wood S, Zhang H, Estes A, Brune CW, Bradfield JP, Imielinski M, Frackelton EC, Reichert J, Crawford EL, Munson J, Sleiman PM, Chiavacci R, Annaiah K, Thomas K, Hou C, Glaberson W, Flory J, Otieno F, Garris M, Soorya L, Klei L, Piven J, Meyer KJ, Anagnostou E, Sakurai T, Game RM, Rudd DS, Zurawiecki D, McDougle CJ, Davis LK, Miller J, Posey DJ,

Michaels S, Kolevzon A, Silverman JM, Bernier R, Levy SE, Schultz RT, Dawson G, Owley T, McMahon WM, Wassink TH, Sweeney JA, Nurnberger JI, Coon H, Sutcliffe JS, Minshew NJ, Grant SF, Bucan M, Cook EH, Buxbaum JD, Devlin B, Schellenberg GD, Hakonarson H (2009) Autism genome-wide copy number variation reveals ubiquitin and neuronal genes. Nature; 459: 569-73

Goodwin EC, DiMaio D (2000) Repression of human papillomavirus oncogenes in HeLa cervical carcinoma cells causes the orderly reactivation of dormant tumor suppressor pathways. P Natl Acad Sci USA; 97: 12513-12518

Goodwin EC, Yang E, Lee CJ, Lee HW, DiMaio D, Hwang ES (2000) Rapid induction of senescence in human cervical carcinoma cells. P Natl Acad Sci USA; 97: 10978-10983

Gossan NC, Zhang F, Guo BQ, Jin D, Yoshitane H, Yao AY, Glossop N, Zhang YQ, Fukada Y, Meng QJ (2014) The E3 ubiquitin ligase UBE3A is an integral component of the molecular circadian clock through regulating the BMAL1 transcription factor. Nucleic Acids Research; 42: 5765-5775

Greer PL, Hanayama R, Bloodgood BL, Mardinly AR, Lipton DM, Flavell SW, Kim TK, Griffith EC, Waldon Z, Maehr R, Ploegh HL, Chowdhury S, Worley PF, Steen J, Greenberg ME (2010) The Angelman Syndrome Protein Ube3A Regulates Synapse Development by Ubiquitinating Arc. Cell; 140: 704-716

Grier MD, Carson RP, Lagrange AH (2015) Toward a Broader View of Ube3a in a Mouse Model of Angelman Syndrome: Expression in Brain, Spinal Cord, Sciatic Nerve and Glial Cells. PLoS One; 10: e0124649

Griffin H, Elston R, Jackson D, Ansell K, Coleman M, Winter G, Doorbar J (2006) Inhibition of papillomavirus protein function in cervical cancer cells by intrabody targeting. J Mol Biol; 355: 360-378

Gu B, Carstens KE, Judson MC, Dalton KA, Rougie M, Clark EP, Dudek SM, Philpot BD (2019) Ube3a reinstatement mitigates epileptogenesis in Angelman syndrome model mice. J Clin Invest; 129: 163-168

Gulati T, Huang C, Caramia F, Raghu D, Paul PJ, Goode RJA, Keam SP, Williams SG, Haupt S, Kleifeld O, Schittenhelm RB, Gamell C, Haupt Y (2018) Proteotranscriptomic Measurements of E6-Associated Protein (E6AP) Targets in DU145 Prostate Cancer Cells. Molecular & Cellular Proteomics; 17: 1170-1183

Gultekin M, Ramirez PT, Broutet N, Hutubessy R (2020) World Health Organization call for action to eliminate cervical cancer globally. Int J Gynecol Cancer;

Gururaja TL, Pray TR, Lowe R, Dong GQ, Huang JN, Daniel-Issakani S, Payan DG (2005) A homogeneous FRET assay system for multiubiquitin chain assembly and disassembly. Method Enzymol; 399: 663-682

Gustin RM, Bichell TJ, Bubser M, Daily J, Filonova I, Mrelashvili D, Deutch AY, Colbran RJ, Weeber EJ, Haas KF (2010) Tissue-specific variation of Ube3a protein expression in rodents and in a mouse model of Angelman syndrome. Neurobiol Dis; 39: 283-291

Hacker SM, Pagliarini D, Tischer T, Hardt N, Schneider D, Mex M, Mayer TU, Scheffner M, Marx A (2013) Fluorogenic ATP analogues for online monitoring of ATP consumption: observing ubiquitin activation in real time. Angew Chem Int Ed Engl; 52: 11916-9

Hall MD, Yasgar A, Peryea T, Braisted JC, Jadhav A, Simeonov A, Coussens NP (2016) Fluorescence polarization assays in high-throughput screening and drug discovery: a review. Methods Appl Fluores; 4

Hammler D, Stuber K, Offensperger F, Scheffner M, Zumbusch A, Marx A (2020) Novel fluorescently labelled ATP analogues for direct monitoring of ubiquitin activation. Chemistry;

Han J, Bichell TJ, Golden S, Anselm I, Waisbren S, Bacino CA, Peters SU, Bird LM, Kimonis V (2019) A placebo-controlled trial of folic acid and betaine in identical twins with Angelman syndrome. Orphanet J Rare Dis; 14: 232

Harbord M (2001) Levodopa responsive Parkinsonism in adults with Angelman Syndrome. J Clin Neurosci; 8: 421-422

Harlalka GV, Baple EL, Cross H, Kühnle S, Cubillos-Rojas M, Matentzoglu K, Patton MA, Wagner K, Coblentz R, Ford DL, Mackay DJ, Chioza BA, Scheffner M, Rosa JL, Crosby AH (2013) Mutation of HERC2 causes developmental delay with Angelman-like features. J Med Genet; 50: 65-73

Harper JW, King RW (2011) Stuck in the middle: drugging the ubiquitin system at the e2 step. Cell; 145: 1007-9

Hatakeyama S, Jensen JP, Weissman AM (1997) Subcellular localization and ubiquitin-conjugating enzyme (E2) interactions of mammalian HECT family ubiquitin protein ligases. Journal of Biological Chemistry; 272: 15085-15092

Haupt Y, Maya R, Kazaz A, Oren M (1997) Mdm2 promotes the rapid degradation of p53. Nature; 387: 296-9

Heery DM, Kalkhoven E, Hoare S, Parker MG (1997) A signature motif in transcriptional co-activators mediates binding to nuclear receptors. Nature; 387: 733-6

Hegde AN, Upadhya SC (2011) Role of ubiquitin-proteasome-mediated proteolysis in nervous system disease. Biochimica et biophysica acta; 1809: 128-40

Herfeld P, Helissey P, Giorgi-Renault S, Goulaouic H, Pager J, Auclair C (1994) Poly(pyrrolecarboxamides) linked to photoactivable chromophore isoalloxazine. Synthesis, selective binding, and DNA cleaving properties. Bioconjug Chem; 5: 67-76

Herman AG, Hayano M, Poyurovsky MV, Shimada K, Skouta R, Prives C, Stockwell BR (2011) Discovery of Mdm2-MdmX E3 Ligase Inhibitors Using a Cell-Based Ubiquitination Assay. Cancer Discov; 1: 312-325

Hershko A, Ciechanover A, Varshavsky A (2000) The ubiquitin system. Nat Med; 6: 1073-1081

Hillman PR, Christian SGB, Doan R, Cohen ND, Konganti K, Douglas K, Wang X, Samollow PB, Dindot SV (2017) Genomic imprinting does not reduce the dosage of UBE3A in neurons. Epigenetics Chromatin; 10: 27

Hoeller D, Hecker CM, Dikic I (2006) Ubiquitin and ubiquitin-like proteins in cancer pathogenesis. Nature reviews Cancer; 6: 776-88

Hogart A, Wu D, LaSalle JM, Schanen NC (2010) The comorbidity of autism with the genomic disorders of chromosome 15q11.2-q13. Neurobiol Dis; 38: 181-91

Honda R, Tanaka H, Yasuda H (1997) Oncoprotein MDM2 is a ubiquitin ligase E3 for tumor suppressor p53. FEBS Lett; 420: 25-7

Hong CA, Swearingen E, Mallari R, Gao X, Cao ZD, North A, Young SW, Huang SG (2003) Development of a high throughput time-resolved fluorescence resonance energy transfer assay for TRAF6 ubiquitin polymerization. Assay Drug Dev Techn; 1: 175-180

Hoppe-Seyler K, Bossler F, Braun JA, Herrmann AL, Hoppe-Seyler F (2018) The HPV E6/E7 Oncogenes: Key Factors for Viral Carcinogenesis and Therapeutic Targets. Trends Microbiol; 26: 158-168

Hoppe-Seyler K, Bossler F, Lohrey C, Bulkescher J, Rosl F, Jansen L, Mayer A, Vaupel P, Durst M, Hoppe-Seyler F (2017) Induction of dormancy in hypoxic human papillomavirus-positive cancer cells. P Natl Acad Sci USA; 114: E990-E998

Hornbeck PV, Zhang B, Murray B, Kornhauser JM, Latham V, Skrzypek E (2015) PhosphoSitePlus, 2014: mutations, PTMs and recalibrations. Nucleic Acids Res; 43: D512-20

Howie HL, Katzenellenbogen RA, Galloway DA (2009) Papillomavirus E6 proteins. Virology; 384: 324-34

Huang HS, Allen JA, Mabb AM, King IF, Miriyala J, Taylor-Blake B, Sciaky N, Dutton JW, Lee HM, Chen X, Jin J, Bridges AS, Zylka MJ, Roth BL, Philpot BD (2012) Topoisomerase Inhibitors Unsilence the Dormant Allele of UBE3A in Neurons. Biol Psychiat; 71: 45s-45s

Huang L, Kinnucan E, Wang G, Beaudenon S, Howley PM, Huibregtse JM, Pavletich NP (1999) Structure of an E6AP-UbcH7 complex: insights into ubiquitination by the E2-E3 enzyme cascade. Science; 286: 1321-6

Huang X, Dixit VM (2016) Drugging the undruggables: exploring the ubiquitin system for drug development. Cell Res; 26: 484-98

Huibregtse JM, Scheffner M, Beaudenon S, Howley PM (1995) A family of proteins structurally and functionally related to the E6-AP ubiquitin-protein ligase. Proc Natl Acad Sci U S A; 92: 5249

Huibregtse JM, Scheffner M, Howley PM (1991) A cellular protein mediates association of p53 with the E6 oncoprotein of human papillomavirus types 16 or 18. EMBO J; 10: 4129-35

Huibregtse JM, Scheffner M, Howley PM (1993a) Cloning and expression of the cDNA for E6-AP, a protein that mediates the interaction of the human papillomavirus E6 oncoprotein with p53. Mol Cell Biol; 13: 775-84

Huibregtse JM, Scheffner M, Howley PM (1993b) Localization of the E6-AP regions that direct human papillomavirus E6 binding, association with p53, and ubiquitination of associated proteins. Mol Cell Biol; 13: 4918-27

Huynh K, Partch CL (2015) Analysis of protein stability and ligand interactions by thermal shift assay. Curr Protoc Protein Sci; 79: 28 9 1-28 9 14

Iacobucci C, Piotrowski C, Aebersold R, Amaral BC, Andrews P, Bernfur K, Borchers C, Brodie NI, Bruce JE, Cao Y, Chaignepain S, Chavez JD, Claverol S, Cox J, Davis T, Degliesposti G, Dong MQ, Edinger N, Emanuelsson C, Gay M, Gotze M, Gomes-Neto F, Gozzo FC, Gutierrez C, Haupt C, Heck AJR, Herzog F, Huang L, Hoopmann MR, Kalisman N, Klykov O, Kukacka Z, Liu F, MacCoss MJ, Mechtler K, Mesika R,

Moritz RL, Nagaraj N, Nesati V, Neves-Ferreira AGC, Ninnis R, Novak P, O'Reilly FJ, Pelzing M, Petrotchenko E, Piersimoni L, Plasencia M, Pukala T, Rand KD, Rappsilber J, Reichmann D, Sailer C, Sarnowski CP, Scheltema RA, Schmidt C, Schriemer DC, Shi Y, Skehel JM, Slavin M, Sobott F, Solis-Mezarino V, Stephanowitz H, Stengel F, Stieger CE, Trabjerg E, Trnka M, Vilaseca M, Viner R, Xiang Y, Yilmaz S, Zelter A, Ziemianowicz D, Leitner A, Sinz A (2019) First Community-Wide, Comparative Cross-Linking Mass Spectrometry Study. Anal Chem; 91: 6953-6961

Iossifov I, O'Roak BJ, Sanders SJ, Ronemus M, Krumm N, Levy D, Stessman HA, Witherspoon KT, Vives L, Patterson KE, Smith JD, Paeper B, Nickerson DA, Dea J, Dong S, Gonzalez LE, Mandell JD, Mane SM, Murtha MT, Sullivan CA, Walker MF, Waqar Z, Wei LP, Willsey AJ, Yamrom B, Lee YH, Grabowska E, Dalkic E, Wang ZH, Marks S, Andrews P, Leotta A, Kendall J, Hakker I, Rosenbaum J, Ma BC, Rodgers L, Troge J, Narzisi G, Yoon S, Schatz MC, Ye K, McCombie WR, Shendure J, Eichler EE, State MW, Wigler M (2014) The contribution of de novo coding mutations to autism spectrum disorder. Nature; 515: 216-U136

Ivanov AA, Khuri FR, Fu H (2013) Targeting protein-protein interactions as an anticancer strategy. Trends Pharmacol Sci; 34: 393-400

Jabbar S, Strati K, Shin MK, Pitot HC, Lambert PF (2010) Human papillomavirus type 16 E6 and E7 oncoproteins act synergistically to cause head and neck cancer in mice. Virology; 407: 60-7

Jackl M, Stollmaier C, Strohaker T, Hyz K, Maspero E, Polo S, Wiesner S (2018) beta-Sheet Augmentation Is a Conserved Mechanism of Priming HECT E3 Ligases for Ubiquitin Ligation. J Mol Biol; 430: 3218-3233

Jacobson AD, MacFadden A, Wu ZP, Peng JM, Liu CW (2014) Autoregulation of the 26S proteasome by in situ ubiquitination. Mol Biol Cell; 25: 1824-1835

Jiang YH, Armstrong D, Albrecht U, Atkins CM, Noebels JL, Eichele G, Sweatt JD, Beaudet AL (1998) Mutation of the Angelman ubiquitin ligase in mice causes increased cytoplasmic p53 and deficits of contextual learning and long-term potentiation. Neuron; 21: 799-811

Johnsen SA, Gungor C, Prenzel T, Riethdorf S, Riethdorf L, Taniguchi-Ishigaki N, Rau T, Tursun B, Furlow JD, Sauter G, Scheffner M, Pantel K, Gannon F, Bach I (2009) Regulation of estrogen-dependent transcription by the LIM cofactors CLIM and RLIM in breast cancer. Cancer Res; 69: 128-36

Jones KA, Han JE, DeBruyne JP, Philpot BD (2016) Persistent neuronal Ube3a expression in the suprachiasmatic nucleus of Angelman syndrome model mice. Sci Rep; 6: 28238

Jordan VC, Collins MM, Rowsby L, Prestwich G (1977) A monohydroxylated metabolite of tamoxifen with potent antioestrogenic activity. J Endocrinol; 75: 305-16

Judson MC, Sosa-Pagan JO, Del Cid WA, Han JE, Philpot BD (2014) Allelic specificity of Ube3a expression in the mouse brain during postnatal development. J Comp Neurol; 522: 1874-96

Kamadurai HB, Souphron J, Scott DC, Duda DM, Miller DJ, Stringer D, Piper RC, Schulman BA (2009) Insights into ubiquitin transfer cascades from a structure of a UbcH5B approximately ubiquitin-HECT(NEDD4L) complex. Mol Cell; 36: 1095-102

Kao SH, Wu HT, Wu KJ (2018) Ubiquitination by HUWE1 in tumorigenesis and beyond. J Biomed Sci; 25: 67

Kao WH, Beaudenon SL, Talis AL, Huibregtse JM, Howley PM (2000) Human papillomavirus type 16 E6 induces self-ubiquitination of the E6AP ubiquitin-protein ligase. Journal of Virology; 74: 6408-6417

Kapoor I, Kanaujiya J, Kumar Y, Thota JR, Bhatt MLB, Chattopadhyay N, Sanyal S, Trivedi AK (2016) Proteomic discovery of MNT as a novel interacting partner of E3 ubiquitin ligase E6AP and a key mediator of myeloid differentiation. Oncotarget; 7: 7640-7656

Kathman SG, Span I, Smith AT, Xu ZY, Zhan J, Rosenzweig AC, Statsyuk AV (2015) A Small Molecule That Switches a Ubiquitin Ligase From a Processive to a Distributive Enzymatic Mechanism. Journal of the American Chemical Society; 137: 12442-12445

Kerscher O, Felberbaum R, Hochstrasser M (2006) Modification of proteins by ubiquitin and ubiquitin-like proteins. Annu Rev Cell Dev Biol; 22: 159-80

Khatri N, Gilbert JP, Huo Y, Sharaflari R, Nee M, Qiao H, Man HY (2018) The Autism Protein Ube3A/E6AP Remodels Neuronal Dendritic Arborization via Caspase-Dependent Microtubule Destabilization. J Neurosci; 38: 363-378

Khatri N, Man HY (2019) The Autism and Angelman Syndrome Protein Ube3A/E6AP: The Gene, E3 Ligase Ubiquitination Targets and Neurobiological Functions. Front Mol Neurosci; 12: 109

Kim HC, Huibregtse JM (2009) Polyubiquitination by HECT E3s and the determinants of chain type specificity. Mol Cell Biol; 29: 3307-18

Kim TG, Lee JH, Lee MY, Kim KU, Lee JH, Park CH, Lee BH, Oh KS (2017) Development of a High-Throughput Assay for Inhibitors of the Polo-Box Domain of Polo-Like Kinase 1 Based on Time-Resolved Fluorescence Energy Transfer. Biol Pharm Bull; 40: 1454-1462

Kishino T, Lalande M, Wagstaff J (1997) UBE3A/E6-AP mutations cause Angelman syndrome. Nat Genet; 15: 70-3

Kleijnen MF, Alarcon RM, Howley PM (2003) The ubiquitin-associated domain of hPLIC-2 interacts with the proteasome. Mol Biol Cell; 14: 3868-3875

Kleijnen MF, Shih AH, Zhou PB, Kumar S, Soccio RE, Kedersha NL, Gill G, Howley PM (2000) The hPLIC proteins may provide a link between the ubiquitination machinery and the proteasome. Molecular Cell; 6: 409-419

Klingelhutz AJ, Roman A (2012) Cellular transformation by human papillomaviruses: Lessons learned by comparing high- and low-risk viruses. Virology; 424: 77-98

Kobayashi F, Nishiuchi T, Takaki K, Konno H (2018) Ubiquitin chain specificities of E6AP E3 ligase and its HECT domain. Biochem Biophys Res Commun; 496: 686-692

Komander D, Rape M (2012) The Ubiquitin Code. Annu Rev Biochem; 81: 203-229

Koszela J, Pham NT, Evans D, Mann S, Perez-Pi I, Shave S, Ceccarelli DFJ, Sicheri F, Tyers M, Auer M (2018) Real-time tracking of complex ubiquitination cascades using a fluorescent confocal on-bead assay. Bmc Biol; 16

Krishnan V, Stoppel DC, Nong Y, Johnson MA, Nadler MJ, Ozkaynak E, Teng BL, Nagakura I, Mohammad F, Silva MA, Peterson S, Cruz TJ, Kasper EM, Arnaout R, Anderson MP (2017) Autism gene Ube3a and seizures impair sociability by repressing VTA Cbln1. Nature; 543: 507-512

Krist DT, Park S, Boneh GH, Rice SE, Statsyuk AV (2016) UbFluor: a mechanism-based probe for HECT E3 ligases. Chemical Science; 7: 5587-5595

Krist DT, Statsyuk AV (2015) Catalytically Important Residues of E6AP Ubiquitin Ligase Identified Using Acid-Cleavable Photo-Cross-Linkers. Biochemistry; 54: 4411-4

Kuballa P, Matentzoglu K, Scheffner M (2007) The role of the ubiquitin ligase E6-AP in human papillomavirus E6-mediated degradation of PDZ domain-containing proteins. J Biol Chem; 282: 65-71

Kubbutat MH, Jones SN, Vousden KH (1997) Regulation of p53 stability by Mdm2. Nature; 387: 299-303

Kuhne C, Banks L (1998) ES ubiquitin ligase E6-AP links multicopy maintenance protein 7 to the ubiquitination pathway by a novel motif, the L2G box. Journal of Biological Chemistry; 273: 34302-34309

Kühnle S, Kogel U, Glockzin S, Marquardt A, Ciechanover A, Matentzoglu K, Scheffner M (2011) Physical and functional interaction of the HECT ubiquitin-protein ligases E6AP and HERC2. J Biol Chem; 286: 19410-6

Kühnle S, Martinez-Noel G, Leclere F, Hayes SD, Harper JW, Howley PM (2018) Angelman syndrome-associated point mutations in the Zn(2+)-binding N-terminal (AZUL) domain of UBE3A ubiquitin ligase inhibit binding to the proteasome. J Biol Chem; 293: 18387-18399

Kühnle S, Mothes B, Matentzoglu K, Scheffner M (2013) Role of the ubiquitin ligase E6AP/UBE3A in controlling levels of the synaptic protein Arc. Proc Natl Acad Sci U S A; 110: 8888-93

Kumar A, Kuhn LT, Balbach J (2018) A Cu2+ complex induces the aggregation of human papillomavirus oncoprotein E6 and stabilizes p53. Febs Journal; 285: 3013-3025

Kumar S, Jena L, Mohod K, Daf S, Varma AK (2015) Virtual Screening for Potential Inhibitors of High-Risk Human Papillomavirus 16 E6 Protein. Interdiscip Sci; 7: 136-42

Kumar S, Talis AL, Howley PM (1999) Identification of HHR23A as a substrate for E6-associated protein-mediated ubiquitination. Journal of Biological Chemistry; 274: 18785-18792

Kuslansky Y, Sominsky S, Jackman A, Gamell C, Monahan BJ, Haupt Y, Rosin-Arbesfeld R, Sherman L (2016) Ubiquitin ligase E6AP mediates nonproteolytic polyubiquitylation of beta-catenin independent of the E6 oncoprotein. Journal of General Virology; 97: 3313-3330

Kwon YT, Ciechanover A (2017) The Ubiquitin Code in the Ubiquitin-Proteasome System and Autophagy. Trends Biochem Sci; 42: 873-886

Lagrange M, Boulade-Ladame C, Mailly L, Weiss E, Orfanoudakis G, Deryckere F (2007) Intracellular scFvs against the viral E6 oncoprotein provoke apoptosis in human papillomavirus-positive cancer cells. Biochem Bioph Res Co; 361: 487-492

Lai MC, Lombardo MV, Baron-Cohen S (2014) Autism. Lancet; 383: 896-910

Lakowicz JR (2006) Principles of fluorescence spectroscopy. Springer, New York

Lalande M, Calciano MA (2007) Molecular epigenetics of Angelman syndrome. Cell Mol Life Sci; 64: 947-60

Landre V, Rotblat B, Melino S, Bernassola F, Melino G (2014) Screening for E3-Ubiquitin ligase inhibitors: challenges and opportunities. Oncotarget; 5: 7988-8013

Lea WA, Simeonov A (2011) Fluorescence polarization assays in small molecule screening. Expert Opin Drug Dis; 6: 17-32

Lee HM, Clark EP, Kuijer MB, Cushman M, Pommier Y, Philpot BD (2018) Characterization and structure-activity relationships of indenoisoquinoline-derived topoisomerase I inhibitors in unsilencing the dormant Ube3a gene associated with Angelman syndrome. Molecular Autism; 9

Lee SY, Ramirez J, Franco M, Lectez B, Gonzalez M, Barrio R, Mayor U (2014) Ube3a, the E3 ubiquitin ligase causing Angelman syndrome and linked to autism, regulates protein homeostasis through the proteasomal shuttle Rpn10. Cellular and Molecular Life Sciences; 71: 2747-2758

Lehoux M, D'Abramo CM, Archambault J (2009) Molecular Mechanisms of Human Papillomavirus-Induced Carcinogenesis. Public Health Genom; 12: 268-280

Leitner A, Faini M, Stengel F, Aebersold R (2016) Crosslinking and Mass Spectrometry: An Integrated Technology to Understand the Structure and Function of Molecular Machines. Trends Biochem Sci; 41: 20-32

Lemak A, Yee A, Bezsonova I, Dhe-Paganon S, Arrowsmith CH (2011) Zn-binding AZUL domain of human ubiquitin protein ligase Ube3A. J Biomol NMR; 51: 185-90

Levav-Cohen Y, Wolyniec K, Alsheich-Bartok O, Chan AL, Woods SJ, Jiang YH, Haupt S, Haupt Y (2012) E6AP is required for replicative and oncogene-induced senescence in mouse embryo fibroblasts. Oncogene; 31: 2199-209

Levy SE, Mandell DS, Schultz RT (2009) Autism. Lancet; 374: 1627-1638

Li L, Li ZG, Howley PM, Sacks DB (2006) E6AP and calmodulin reciprocally regulate estrogen receptor stability. Journal of Biological Chemistry; 281: 1978-1985

Li S, Hong X, Wei Z, Xie M, Li W, Liu G, Guo H, Yang J, Wei W, Zhang S (2019) Ubiquitination of the HPV Oncoprotein E6 Is Critical for E6/E6AP-Mediated p53 Degradation. Front Microbiol; 10: 2483

Li W, Bengtson MH, Ulbrich A, Matsuda A, Reddy VA, Orth A, Chanda SK, Batalov S, Joazeiro CA (2008) Genome-wide and functional annotation of human E3 ubiquitin ligases identifies MULAN, a mitochondrial E3 that regulates the organelle's dynamics and signaling. PloS one; 3: e1487

Lin Y, Shi RX, Wang X, Shen HM (2008) Luteolin, a Flavonoid with Potential for Cancer Prevention and Therapy. Curr Cancer Drug Tar; 8: 634-646

Liu F, Xu K, Xu Z, de Las Rivas M, Wang C, Li X, Lu J, Zhou Y, Delso I, Merino P, Hurtado-Guerrero R, Zhang Y, Wu F (2017a) The small molecule luteolin inhibits N-acetyl-alpha-galactosaminyltransferases and reduces mucin-type O-glycosylation of amyloid precursor protein. J Biol Chem; 292: 21304-21319

Liu YM, HuangFu WC, Huang HL, Wu WC, Chen YL, Yen Y, Huang HL, Nien CY, Lai MJ, Pan SL, Liou JP (2017b) 1,4-Naphthoquinones as inhibitors of Itch, a HECT domain-E3 ligase, and tumor growth suppressors in multiple myeloma. Eur J Med Chem; 140: 84-91

Liu YQ, Liu ZG, Androphy E, Chen J, Baleja JD (2004) Design and characterization of helical peptides that inhibit the E6 protein of papillornavirus. Biochemistry; 43: 7421-7431

Lochab S, Pal P, Kanaujiya JK, Tripathi SB, Kapoor I, Bhatt ML, Sanyal S, Behre G, Trivedi AK (2012) Proteomic identification of E6AP as a molecular target of tamoxifen in MCF7 cells. Proteomics; 12: 1363-77

Lopez SJ, Segal DJ, LaSalle JM (2019) UBE3A: An E3 Ubiquitin Ligase With Genome-Wide Impact in Neurodevelopmental Disease. Frontiers in Molecular Neuroscience; 11

Lorenz S (2018) Structural mechanisms of HECT-type ubiquitin ligases. Biol Chem; 399: 127-145

Lossie AC, Whitney MM, Amidon D, Dong HJ, Chen P, Theriaque D, Hutson A, Nicholls RD, Zori RT, Williams CA, Driscoll DJ (2001) Distinct phenotypes distinguish the molecular classes of Angelman syndrome. Journal of Medical Genetics; 38: 834-845

Louria-Hayon I, Alsheich-Bartok O, Levav-Cohen Y, Silberman I, Berger M, Grossman T, Matentzoglu K, Jiang YH, Muller S, Scheffner M, Haupt S, Haupt Y (2009) E6AP promotes the degradation of the PML tumor suppressor. Cell Death Differ; 16: 1156-66

Luk HM (2016) Angelman-Like Syndrome: A Genetic Approach to Diagnosis with Illustrative Cases. Case Rep Genet; 2016: 9790169

Lyall K, Croen L, Daniels J, Fallin MD, Ladd-Acosta C, Lee BK, Park BY, Snyder NW, Schendel D, Volk H, Windham GC, Newschaffer C (2017) The Changing Epidemiology of Autism Spectrum Disorders. Annu Rev Publ Health; 38: 81-102

Mabb AM, Judson MC, Zylka MJ, Philpot BD (2011) Angelman syndrome: insights into genomic imprinting and neurodevelopmental phenotypes. Trends Neurosci; 34: 293-303

Magenis RE, Brown MG, Lacy DA, Budden S, Lafranchi S (1987) Is Angelman Syndrome an Alternate Result of Del(15)(Q11q13). Am J Med Genet; 28: 829-838

Malecka KA, Fera D, Schultz DC, Hodawadekar S, Reichman M, Donover PS, Murphy ME, Marmorstein R (2014) Identification and Characterization of Small Molecule Human Papillomavirus E6 Inhibitors. Acs Chem Biol; 9: 1603-1612

Malet C, Gompel A, Spritzer P, Bricout N, Yaneva H, Mowszowicz I, Kuttenn F, Mauvais-Jarvis P (1988) Tamoxifen and hydroxytamoxifen isomers versus estradiol effects on normal human breast cells in culture. Cancer Res; 48: 7193-9

Mansour M, Haupt S, Chan AL, Godde N, Rizzitelli A, Loi S, Caramia F, Deb S, Takano EA, Bishton M, Johnstone C, Monahan B, Levav-Cohen Y, Jiang YH, Yap AS, Fox S, Bernard O, Anderson R, Haupt Y (2016) The E3-ligase E6AP Represses Breast Cancer Metastasis via Regulation of ECT2-Rho Signaling. Cancer Res; 76: 4236-48

Mansour M, Haupt S, Chan AL, Godde N, Rizzitelli A, Loi S, Caramia F, Deb S, Takano EA, Bishton M, Johnstone C, Monahan B, Levav-Cohen Y, Jiang YH, Yap AS, Fox S, Bernard O, Anderson R, Haupt Y (2019) Retraction: The E3-ligase E6AP Represses Breast Cancer Metastasis via Regulation of ECT2-Rho Signaling. Cancer Res; 79: 3008

Manzo-Merino J, Thomas M, Fuentes-Gonzalez AM, Lizano M, Banks L (2013) HPV E6 oncoprotein as a potential therapeutic target in HPV related cancers. Expert Opin Ther Tar; 17: 1357-1368

Mao R, Jalal SM, Snow K, Michels VV, Szabo SM, Babovic-Vuksanovic D (2000) Characteristics of two cases with dup(15)(q11.2-q12): one of maternal and one of paternal origin. Genet Med; 2: 131-135

Margolis SS, Salogiannis J, Lipton DM, Mandel-Brehm C, Wills ZP, Mardinly AR, Hu LD, Greer PL, Bikoff JB, Ho HYH, Soskis MJ, Sahin M, Greenberg ME (2010) EphB-Mediated Degradation of the RhoA GEF Ephexin5 Relieves a Developmental Brake on Excitatory Synapse Formation. Cell; 143: 442-455

Mari S, Ruetalo N, Maspero E, Stoffregen MC, Pasqualato S, Polo S, Wiesner S (2014) Structural and Functional Framework for the Autoinhibition of Nedd4-Family Ubiquitin Ligases. Structure; 22: 1639-1649

Martinez-Noel G, Galligan JT, Sowa ME, Arndt V, Overton TM, Harper JW, Howley PM (2012) Identification and proteomic analysis of distinct UBE3A/E6AP protein complexes. Mol Cell Biol; 32: 3095-106

Martinez-Noel G, Luck K, Kühnle S, Desbuleux A, Szajner P, Galligan JT, Rodriguez D, Zheng L, Boyland K, Leclere F, Zhong Q, Hill DE, Vidal M, Howley PM (2018) Network Analysis of UBE3A/E6AP-Associated Proteins Provides Connections to Several Distinct Cellular Processes. J Mol Biol; 430: 1024-1050

Martinez-Zapien D, Ruiz FX, Poirson J, Mitschler A, Ramirez J, Forster A, Cousido-Siah A, Masson M, Vande Pol S, Podjarny A, Trave G, Zanier K (2016) Structure of the E6/E6AP/p53 complex required for HPV-mediated degradation of p53. Nature; 529: 541-+

Maspero E, Mari S, Valentini E, Musacchio A, Fish A, Pasqualato S, Polo S (2011) Structure of the HECT:ubiquitin complex and its role in ubiquitin chain elongation. Embo Rep; 12: 342-349

Maspero E, Valentini E, Mari S, Cecatiello V, Soffientini P, Pasqualato S, Polo S (2013) Structure of a ubiquitin-loaded HECT ligase reveals the molecular basis for catalytic priming. Nat Struct Mol Biol; 20: 696-701

Masuda Y, Saeki Y, Arai N, Kawai H, Kukimoto I, Tanaka K, Masutani C (2019) Stepwise multipolyubiquitination of p53 by the E6AP-E6 ubiquitin ligase complex. J Biol Chem; 294: 14860-14875

Mata-Cantero L, Cid C, Gomez-Lorenzo MG, Xolalpa W, Aillet F, Martin JJ, Rodriguez MS (2015) Development of two novel high-throughput assays to quantify ubiquitylated proteins in cell lysates: application to screening of new anti-malarials. Malar J; 14: 200

Matentzoglu K, Scheffner M (2008) Ubiquitin ligase E6-AP and its role in human disease. Biochem Soc Trans; 36: 797-801

Matic I, Jaffray EG, Oxenham SK, Groves MJ, Barratt CL, Tauro S, Stanley-Wall NR, Hay RT (2011) Absolute SILAC-compatible expression strain allows Sumo-2 copy number determination in clinical samples. J Proteome Res; 10: 4869-75

Matsuoka S, Ballif BA, Smogorzewska A, McDonald ER, Hurov KE, Luo J, Bakalarski CE, Zhao ZM, Solimini N, Lerenthal Y, Shiloh Y, Gygi SP, Elledge SJ (2007) ATM and ATR substrate analysis reveals extensive protein networks responsive to DNA damage. Science; 316: 1160-1166

Matsuura T, Sutcliffe JS, Fang P, Galjaard RJ, Jiang YH, Benton CS, Rommens JM, Beaudet AL (1997) De novo truncating mutations in E6-AP ubiquitin-protein ligase gene (UBE3A) in Angelman syndrome. Nat Genet; 15: 74-7

Mayya V, Lundgren DH, Hwang SI, Rezaul K, Wu LF, Eng JK, Rodionov V, Han DK (2009) Quantitative Phosphoproteomic Analysis of T Cell Receptor Signaling Reveals System-Wide Modulation of Protein-Protein Interactions. Sci Signal; 2

Melvin AT, Woss GS, Park JH, Waters ML, Allbritton NL (2013) Measuring activity in the ubiquitin-proteasome system: from large scale discoveries to single cells analysis. Cell Biochem Biophys; 67: 75-89

Meng L, Person RE, Huang W, Zhu PJ, Costa-Mattioli M, Beaudet AL (2013) Truncation of Ube3a-ATS unsilences paternal Ube3a and ameliorates behavioral defects in the Angelman syndrome mouse model. PLoS Genet; 9: e1004039

Meng LY, Person RE, Beaudet AL (2012) Ube3a-ATS is an atypical RNA polymerase II transcript that represses the paternal expression of Ube3a. Hum Mol Genet; 21: 3001-3012

Meng LY, Ward AJ, Chun S, Bennett CF, Beaudet AL, Rigo F (2015) Towards a therapy for Angelman syndrome by targeting a long non-coding RNA. Nature; 518: 409-412

Mertz LGB, Christensen R, Vogel I, Hertz JM, Nielsen KB, Gronskov K, Ostergaard JR (2013) Angelman Syndrome in Denmark. Birth Incidence, Genetic Findings, and Age at Diagnosis. Am J Med Genet A; 161: 2197-2203

Messa L, Celegato M, Bertagnin C, Mercorelli B, Nannetti G, Palu G, Loregian A (2018) A quantitative LumiFluo assay to test inhibitory compounds blocking p53 degradation induced by human papillomavirus oncoprotein E6 in living cells. Sci Rep-Uk; 8

Metzger MB, Pruneda JN, Klevit RE, Weissman AM (2014) RING-type E3 ligases: master manipulators of E2 ubiquitin-conjugating enzymes and ubiquitination. Biochim Biophys Acta; 1843: 47-60

Mishra M, Sharma A, Thacker G, Trivedi AK (2019) Nano-LC based proteomic approach identifies that E6AP interacts with ENO1 and targets it for degradation in breast cancer cells. IUBMB Life;

Mitchell KJ (2015) The Genetics of Neurodevelopmental Disorders Foreword. Genetics of Neurodevelopmental Disorders: Ix-Xii

Mittal S, Banks L (2017) Molecular mechanisms underlying human papillomavirus E6 and E7 oncoprotein-induced cell transformation. Mutat Res Rev Mutat Res; 772: 23-35

Miura K, Kishino T, Li E, Webber H, Dikkes P, Holmes GL, Wagstaff J (2002) Neurobehavioral and electroencephalographic abnormalities in Ube3a maternal-deficient mice. Neurobiol Dis; 9: 149-59

Molina DM, Jafari R, Ignatushchenko M, Seki T, Larsson EA, Dan C, Sreekumar L, Cao YH, Nordlund P (2013) Monitoring Drug Target Engagement in Cells and Tissues Using the Cellular Thermal Shift Assay. Science; 341: 84-87

Morrow EM, Yoo SY, Flavell SW, Kim TK, Lin Y, Hill RS, Mukaddes NM, Balkhy S, Gascon G, Hashmi A, Al-Saad S, Ware J, Joseph RM, Greenblatt R, Gleason D, Ertelt JA, Apse KA, Bodell A, Partlow JN, Barry B, Yao H, Markianos K, Ferland RJ, Greenberg ME, Walsh CA (2008) Identifying autism loci and genes by tracing recent shared ancestry. Science; 321: 218-23

Mortensen F, Schneider D, Barbic T, Sladewska-Marquardt A, Kühnle S, Marx A, Scheffner M (2015) Role of ubiquitin and the HPV E6 oncoprotein in E6AP-mediated ubiquitination. Proc Natl Acad Sci U S A; 112: 9872-7

Mot AC, Prell E, Klecker M, Naumann C, Faden F, Westermann B, Dissmeyer N (2018) Real-time detection of N-end rule-mediated ubiquitination via fluorescently labeled substrate probes. New Phytol; 217: 613-624

Mulherkar SA, Sharma J, Jana NR (2009) The ubiquitin ligase E6-AP promotes degradation of alpha-synuclein. J Neurochem; 110: 1955-64

Mund T, Lewis MJ, Maslen S, Pelham HR (2014) Peptide and small molecule inhibitors of HECT-type ubiquitin ligases. P Natl Acad Sci USA; 111: 16736-16741

Murray MF, Jurewicz AJ, Martin JD, Ho TF, Zhang H, Johanson KO, Kirkpatrick RB, Ma JH, Lor LA, Thrall SH, Schwartz B (2007) A high-throughput screen measuring ubiquitination of p53 by human mdm2. Journal of Biomolecular Screening; 12: 1050-1058

Nakao M, Sutcliffe JS, Durtschi B, Mutirangura A, Ledbetter DH, Beaudet AL (1994) Imprinting analysis of three genes in the Prader-Willi/Angelman region: SNRPN, E6-associated protein, and PAR-2 (D15S225E). Hum Mol Genet; 3: 309-15

Nalepa G, Rolfe M, Harper JW (2006) Drug discovery in the ubiquitin-proteasome system. Nat Rev Drug Discov; 5: 596-613

Nasu J, Murakami K, Miyagawa S, Yamashita R, Ichimura T, Wakita T, Hotta H, Miyamura T, Suzuki T, Satoh T, Shoji I (2010) E6AP Ubiquitin Ligase Mediates Ubiquitin-Dependent Degradation of Peroxiredoxin 1. J Cell Biochem; 111: 676-685

Nath D, Shadan S (2009) The ubiquitin system. Nature; 458: 421

Nawaz Z, Lonard DH, Smith CL, Lev-Lehman E, Tsai SY, Tsai MJ, O'Malley BW (1999) The Angelman syndrome-associated protein, E6-AP, is a coactivator for the nuclear hormone receptor superfamily. Molecular and Cellular Biology; 19: 1182-1189

Nogales E, Scheres SH (2015) Cryo-EM: A Unique Tool for the Visualization of Macromolecular Complexity. Mol Cell; 58: 677-89

Noor A, Dupuis L, Mittal K, Lionel AC, Marshall CR, Scherer SW, Stockley T, Vincent JB, Mendoza-Londono R, Stavropoulos DJ (2015) 15q11.2 Duplication Encompassing Only the UBE3A Gene Is Associated with Developmental Delay and Neuropsychiatric Phenotypes. Human Mutation; 36: 689-693

Nuber U, Schwarz SE, Scheffner M (1998) The ubiquitin-protein ligase E6-associated protein (E6-AP) serves as its own substrate. European Journal of Biochemistry; 254: 643-649

Obeid JP, Zeidan YH, Zafar N, El Hokayem J (2018) E6-Associated Protein Dependent Estrogen Receptor Regulation of Protein Kinase A Regulatory Subunit R2A Expression in Neuroblastoma. Mol Neurobiol; 55: 1714-1724

Oda H, Kumar S, Howley PM (1999) Regulation of the Src family tyrosine kinase Blk through E6AP-mediated ubiquitination. P Natl Acad Sci USA; 96: 9557-9562

Offensperger F (2015) Establishment of an HTS assay for the identification of small molecule modulators of E6AP. Masterthesis, AG Scheffner, University of Konstanz;

Ognjenovic J, Grisshammer R, Subramaniam S (2019) Frontiers in Cryo Electron Microscopy of Complex Macromolecular Assemblies. Annu Rev Biomed Eng; 21: 395-415

Ogunjimi AA, Briant DJ, Pece-Barbara N, Le Roy C, Di Guglielmo GM, Kavsak P, Rasmussen RK, Seet BT, Sicheri F, Wrana JL (2005) Regulation of Smurf2 ubiquitin ligase activity by anchoring the E2 to the HECT domain. Molecular Cell; 19: 297-308

Oh E, Akopian D, Rape M (2018) Principles of Ubiquitin-Dependent Signaling. Annu Rev Cell Dev Biol; 34: 137-162

Oliveira AP, Sauer U (2012) The importance of post-translational modifications in regulating Saccharomyces cerevisiae metabolism. FEMS Yeast Res; 12: 104-17

Ong J, Torres J (2019) E3 Ubiquitin Ligases in Cancer and Their Pharmacological Targeting. IntechOpen: Ubiquitin Proteasome System - Current Insights into Mechanism Cellular Regulation and Disease;

Ostendorff HP, Bossenz M, Mincheva A, Copeland NG, Gilbert DJ, Jenkins NA, Lichter P, Bach I (2000) Functional characterization of the gene encoding RLIM, the corepressor of LIM homeodomain factors. Genomics; 69: 120-30

Ostendorff HP, Peirano RI, Peters MA, Schluter A, Bossenz M, Scheffner M, Bach I (2002) Ubiquitination-dependent cofactor exchange on LIM homeodomain transcription factors. Nature; 416: 99-103

Oughtred R, Stark C, Breitkreutz BJ, Rust J, Boucher L, Chang C, Kolas N, O'Donnell L, Leung G, McAdam R, Zhang F, Dolma S, Willems A, Coulombe-Huntington J, Chatr-aryamontri A, Dolinski K, Tyers M (2019) The BioGRID interaction database: 2019 update. Nucleic Acids Research; 47: D529-D541

Park SJ, Foote PK, Krist DT, Rice SE, Statsyuk AV (2017) UbMES and UbFluor: Novel probes for ring-between-ring (RBR) E3 ubiquitin ligase PARKIN. Journal of Biological Chemistry; 292: 16539-16553

Pembrey M, Fennell SJ, Vandenberghe J, Fitchett M, Summers D, Butler L, Clarke C, Griffiths M, Thompson E, Super M, Baraitser M (1989) The Association of Angelmans Syndrome with Deletions within 15q11-13. Journal of Medical Genetics; 26: 73-77

Peter S, Bultinck J, Myant K, Jaenicke LA, Walz S, Muller J, Gmachl M, Treu M, Boehmelt G, Ade CP, Schmitz W, Wiegering A, Otto C, Popov N, Sansom O, Kraut N, Eilers M (2014) Tumor cell-specific inhibition of MYC function using small molecule inhibitors of the HUWE1 ubiquitin ligase. EMBO Mol Med; 6: 1525-41

Peters SU, Bird LM, Kimonis V, Glaze DG, Shinawi UM, Bichell TJ, Barbieri-Welge R, Nespeca M, Anselm I, Waisbren S, Sanborn E, Sun Q, O'Brien WE, Beaudet AL, Bacino CA (2010) Double-Blind Therapeutic Trial in Angelman Syndrome Using Betaine and Folic Acid. Am J Med Genet A; 152a: 1994-2001

Petersen MB, Brondum-Nielsen K, Hansen LK, Wulff K (1995) Clinical, cytogenetic, and molecular diagnosis of Angelman syndrome: estimated prevalence rate in a Danish county. Am J Med Genet; 60: 261-2

Pettersen EF, Goddard TD, Huang CC, Couch GS, Greenblatt DM, Meng EC, Ferrin TE (2004) UCSF Chimera--a visualization system for exploratory research and analysis. J Comput Chem; 25: 1605-12

Pierce NW, Kleiger G, Shan SO, Deshaies RJ (2009) Detection of sequential polyubiquitylation on a millisecond timescale. Nature; 462: 615-9

Pinto D, Pagnamenta AT, Klei L, Anney R, Merico D, Regan R, Conroy J, Magalhaes TR, Correia C, Abrahams BS, Almeida J, Bacchelli E, Bader GD, Bailey AJ, Baird G, Battaglia A, Berney T, Bolshakova N, Bolte S, Bolton PF, Bourgeron T, Brennan S, Brian J, Bryson SE, Carson AR, Casallo G, Casey J, Chung BH, Cochrane L, Corsello C, Crawford EL, Crossett A, Cytrynbaum C, Dawson G, de Jonge M, Delorme R, Drmic I, Duketis E, Duque F, Estes A, Farrar P, Fernandez BA, Folstein SE, Fombonne E, Freitag CM, Gilbert J, Gillberg C, Glessner JT, Goldberg J, Green A, Green J, Guter SJ, Hakonarson H, Heron EA, Hill M, Holt R, Howe JL, Hughes G, Hus V, Igliozzi R, Kim C, Klauck SM, Kolevzon A, Korvatska O, Kustanovich V, Lajonchere CM, Lamb JA, Laskawiec M, Leboyer M, Le Couteur A, Leventhal BL, Lionel AC, Liu XQ, Lord C, Lotspeich L, Lund SC, Maestrini E, Mahoney W, Mantoulan C, Marshall CR, McConachie H, McDougle CJ, McGrath J, McMahon WM, Merikangas A, Migita O, Minshew NJ, Mirza GK, Munson J, Nelson SF, Noakes C, Noor A, Nygren G, Oliveira G, Papanikolaou K, Parr JR, Parrini B, Paton T, Pickles A, Pilorge M, Piven J, Ponting CP, Posey DJ, Poustka A, Poustka F, Prasad A, Ragoussis J, Renshaw K, Rickaby J, Roberts W, Roeder K, Roge B, Rutter ML, Bierut LJ, Rice JP, Salt J, Sansom K, Sato D, Segurado R, Sequeira AF, Senman L, Shah N, Sheffield VC, Soorya L, Sousa I, Stein O, Sykes N, Stoppioni V, Strawbridge C, Tancredi R, Tansey K, Thiruvahindrapduram B, Thompson AP, Thomson S, Tryfon A, Tsiantis J, Van Engeland H, Vincent JB, Volkmar F, Wallace S, Wang K, Wang Z, Wassink TH, Webber C, Weksberg R, Wing K, Wittemeyer K, Wood S, Wu J, Yaspan BL, Zurawiecki D, Zwaigenbaum L, Buxbaum JD, Cantor RM, Cook EH, Coon H, Cuccaro ML, Devlin B, Ennis S, Gallagher L, Geschwind DH, Gill M, Haines JL, Hallmayer J, Miller J, Monaco AP, Nurnberger JI, Jr., Paterson AD, Pericak-Vance MA, Schellenberg GD, Szatmari P, Vicente AM, Vieland VJ, Wijsman EM, Scherer SW, Sutcliffe JS, Betancur C (2010) Functional impact of global rare copy number variation in autism spectrum disorders. Nature; 466: 368-72

Puffenberger EG, Jinks RN, Wang H, Xin BZ, Fiorentini C, Sherman EA, Degrazio D, Shaw C, Sougnez C, Cibulskis K, Gabriel S, Kelley RI, Morton DH, Strauss KA (2012) A homozygous missense mutation in HERC2 associated with global developmental delay and autism spectrum disorder. Human Mutation; 33: 1639-1646

Pyeon D, Rojas VK, Price L, Kim S, Meharvan S, Park IW (2019) HIV-1 Impairment via UBE3A and HIV-1 Nef Interactions Utilizing the Ubiquitin Proteasome System. Viruses; 11

Quirit JG, Lavrenov SN, Poindexter K, Xu J, Kyauk C, Durkin KA, Aronchik I, Tomasiak T, Solomatin YA, Preobrazhenskaya MN, Firestone GL (2017) Indole-3-carbinol (I3C) analogues are potent small molecule inhibitors of NEDD4-1 ubiquitin ligase activity that disrupt proliferation of human melanoma cells. Biochem Pharmacol; 127: 13-27

Raimondo D, Giorgetti A, Bernassola F, Melino G, Tramontano A (2008) Modelling and molecular dynamics of the interaction between the E3 ubiquitin ligase itch and the E2 UbcH7. Biochem Pharmacol; 76: 1620-1627

Ramamoorthy S, Tufail R, Hokayem JE, Jorda M, Zhao W, Reis Z, Nawaz Z (2012) Overexpression of ligase defective E6-associated protein, E6-AP, results in mammary tumorigenesis. Breast Cancer Res Treat; 132: 97-108

Ranaweera RS, Yang X (2013) Auto-ubiquitination of Mdm2 enhances its substrate ubiquitin ligase activity. J Biol Chem; 288: 18939-46

Reid D, Sadjad BS, Zsoldos Z, Simon A (2008) LASSO-ligand activity by surface similarity order: a new tool for ligand based virtual screening. J Comput Aided Mol Des; 22: 479-87

Reis A, Greger V, Lalande M, Sperling K (1993) Imprinting Mutations Suggested by Abnormal DNA Methylation Patterns in Angelman Syndrome. Am J Hum Genet; 53: 723-723

Reiter KH, Klevit RE (2018) Characterization of RING-Between-RING E3 Ubiquitin Transfer Mechanisms. Ubiquitin Proteasome System: Methods and Protocols; 1844: 3-17

Ricci-Lopez J, Vidal-Limon A, Zunniga M, Jimenez VA, Alderete JB, Brizuela CA, Aguila S (2019) Molecular modeling simulation studies reveal new potential inhibitors against HPV E6 protein. PLoS One; 14: e0213028

Ries LK, Sander B, Deol KK, Letzelter MA, Strieter ER, Lorenz S (2019) Analysis of ubiquitin recognition by the HECT ligase E6AP provides insight into its linkage specificity. J Biol Chem; 294: 6113-6129

Rietz A, Petrov DP, Bartolowits M, DeSmet M, Davisson VJ, Androphy EJ (2016) Molecular Probing of the HPV-16 E6 Protein Alpha Helix Binding Groove with Small Molecule Inhibitors. Plos One; 11

Riley BE, Lougheed JC, Callaway K, Velasquez M, Brecht E, Nguyen L, Shaler T, Walker D, Yang Y, Regnstrom K, Diep L, Zhang Z, Chiou S, Bova M, Artis DR, Yao N, Baker J, Yednock T, Johnston JA (2013) Structure and function of Parkin E3 ubiquitin ligase reveals aspects of RING and HECT ligases. Nat Commun; 4: 1982

Riling C, Kamadurai H, Kumar S, O'Leary CE, Wu KP, Manion EE, Ying M, Schulman BA, Oliver PM (2015) Itch WW Domains Inhibit Its E3 Ubiquitin Ligase Activity by Blocking E2-E3 Ligase Trans-thiolation. Journal of Biological Chemistry; 290: 23875-23887

Rinken A, Lavogina D, Kopanchuk S (2018) Assays with Detection of Fluorescence Anisotropy: Challenges and Possibilities for Characterizing Ligand Binding to GPCRs. Trends Pharmacol Sci; 39: 187-199

Ronchi VP, Kim ED, Summa CM, Klein JM, Haas AL (2017) In silico modeling of the cryptic E2 approximately ubiquitin-binding site of E6-associated protein (E6AP)/UBE3A reveals the mechanism of polyubiquitin chain assembly. J Biol Chem; 292: 18006-18023

Ronchi VP, Klein JM, Edwards DJ, Haas AL (2014) The active form of E6-associated protein (E6AP)/UBE3A ubiquitin ligase is an oligomer. J Biol Chem; 289: 1033-48

Ronchi VP, Klein JM, Haas AL (2013) E6AP/UBE3A ubiquitin ligase harbors two E2~ubiquitin binding sites. J Biol Chem; 288: 10349-60

Rossi M, Rotblat B, Ansell K, Amelio I, Caraglia M, Misso G, Bernassola F, Cavasotto CN, Knight RA, Ciechanover A, Melino G (2014) High throughput screening for inhibitors of the HECT ubiquitin E3 ligase ITCH identifies antidepressant drugs as regulators of autophagy. Cell Death Dis; 5

Rotaru DC, Mientjes EJ, Elgersma Y (2020) Angelman Syndrome: From Mouse Models to Therapy. Neuroscience;

Rotaru DC, van Woerden GM, Wallaard I, Elgersma Y (2018) Adult Ube3a Gene Reinstatement Restores the Electrophysiological Deficits of Prefrontal Cortex Layer 5 Neurons in a Mouse Model of Angelman Syndrome. J Neurosci; 38: 8011-8030

Rotin D, Kumar S (2009) Physiological functions of the HECT family of ubiquitin ligases. Nature reviews Molecular cell biology; 10: 398-409

Rougeulle C, Cardoso C, Fontes M, Colleaux L, Lalande M (1998) An imprinted antisense RNA overlaps UBE3A and a second maternally expressed transcript. Nat Genet; 19: 15-16

Rougeulle C, Glatt H, Lalande M (1997) The Angelman syndrome candidate gene, UBE3A/E6-AP, is imprinted in brain. Nature genetics; 17: 14-5

Roxburgh P, Hock AK, Dickens MP, Mezna M, Fischer PM, Vousden KH (2012) Small molecules that bind the Mdm2 RING stabilize and activate p53. Carcinogenesis; 33: 791-798

Runte M, Huttenhofer A, Gross S, Kiefmann M, Horsthemke B, Buiting K (2001) The IC-SNURF-SNRPN transcript serves as a host for multiple small nucleolar RNA species and as an antisense RNA for UBE3A. Hum Mol Genet; 10: 2687-2700

Sadikovic B, Fernandes P, Zhang VW, Ward PA, Miloslavskaya I, Rhead W, Rosenbaum R, Gin R, Roa B, Fang P (2014) Mutation Update for UBE3A variants in Angelman syndrome. Hum Mutat; 35: 1407-17

Sailer C, Offensperger F, Julier A, Kammer KM, Walker-Gray R, Gold MG, Scheffner M, Stengel F (2018) Structural dynamics of the E6AP/UBE3A-E6-p53 enzyme-substrate complex. Nat Commun; 9: 4441

Saitoh S, Buiting K, Cassidy SB, Conroy JM, Driscoll DJ, Gabriel JM, Gillessen-Kaesbach G, Glenn CC, Greenswag LR, Horsthemke B, Kondo I, Kuwajima K, Niikawa N, Rogan PK, Schwartz S, Seip J, Williams CA, Nicholls RD (1997) Clinical spectrum and molecular diagnosis of Angelman and Prader-Willi syndrome patients with an imprinting mutation. Am J Med Genet; 68: 195-206

Sakamoto H, Egashira S, Saito N, Kirisako T, Miller S, Sasaki Y, Matsumoto T, Shimonishi M, Komatsu T, Terai T, Ueno T, Hanaoka K, Kojima H, Okabe T, Wakatsuki S, Iwai K, Nagano T (2015) Gliotoxin suppresses NF-kappaB activation by selectively inhibiting linear ubiquitin chain assembly complex (LUBAC). Acs Chem Biol; 10: 675-81

Samaco RC, Hogart A, LaSalle JM (2005) Epigenetic overlap in autism-spectrum neurodevelopmental disorders: MECP2 deficiency causes reduced expression of UBE3A and GABRB3. Human molecular genetics; 14: 483-92

Sanchez-Spitman AB, Swen JJ, Dezentje VO, Moes D, Gelderblom H, Guchelaar HJ (2019) Clinical pharmacokinetics and pharmacogenetics of tamoxifen and endoxifen. Expert Rev Clin Pharmacol; 12: 523-536

Sander B, Xu WS, Eilers M, Popov N, Lorenz S (2017) A conformational switch regulates the ubiquitin ligase HUWE1. Elife; 6

Sato M, Stryker MP (2010) Genomic imprinting of experience-dependent cortical plasticity by the ubiquitin ligase gene Ube3a. P Natl Acad Sci USA; 107: 5611-5616

Scheffner M, Huibregtse JM, Vierstra RD, Howley PM (1993) The HPV-16 E6 and E6-AP complex functions as a ubiquitin-protein ligase in the ubiquitination of p53. Cell; 75: 495-505

Scheffner M, Kumar S (2014) Mammalian HECT ubiquitin-protein ligases: biological and pathophysiological aspects. Biochim Biophys Acta; 1843: 61-74

Scheffner M, Werness BA, Huibregtse JM, Levine AJ, Howley PM (1990) The E6 Oncoprotein Encoded by Human Papillomavirus Type-16 and Type-18 Promotes the Degradation of P53. Cell; 63: 1129-1136

Scheffner M, Whitaker NJ (2003) Human papillomavirus-induced carcinogenesis and the ubiquitin-proteasome system. Semin Cancer Biol; 13: 59-67

Schiffman M, Doorbar J, Wentzensen N, de Sanjose S, Fakhry C, Monk BJ, Stanley MA, Franceschi S (2016) Carcinogenic human papillomavirus infection. Nat Rev Dis Primers; 2

Schroff A (2017) Small molecules to study the E3-Ubiquitin-Ligase E6AP. Masterthesis, AG Scheffner, University of Konstanz;

Sehr P, Pawlita M, Lewis J (2007) Evaluation of different glutathione S-transferase-tagged protein captures for screening E6/E6AP interaction inhibitors using AlphaScreen. J Biomol Screen; 12: 560-7

Shagufta, Ahmad I (2018) Tamoxifen a pioneering drug: An update on the therapeutic potential of tamoxifen derivatives. Eur J Med Chem; 143: 515-531

Shai A, Pitot HC, Lambert PF (2010) E6-associated protein is required for human papillomavirus type 16 E6 to cause cervical cancer in mice. Cancer Res; 70: 5064-73

Shang F, Deng G, Liu Q, Guo W, Haas AL, Crosas B, Finley D, Taylor A (2005) Lys6-modified ubiquitin inhibits ubiquitin-dependent protein degradation. J Biol Chem; 280: 20365-74

Sheaffer AK, Lee MS, Qi HL, Chaniewski S, Zheng XF, Farr GA, Esposito K, Harden D, Lei M, Schweizer L, Friborg J, Agler M, McPhee F, Gentles R, Beno BR, Chupak L, Mason S (2016) A Small Molecule Inhibitor Selectively Induces Apoptosis in Cells Transformed by High Risk Human Papilloma Viruses. Plos One; 11

Shiau AK, Barstad D, Loria PM, Cheng L, Kushner PJ, Agard DA, Greene GL (1998) The structural basis of estrogen receptor/coactivator recognition and the antagonism of this interaction by tamoxifen. Cell; 95: 927-37

Shimoji T, Murakami K, Sugiyama Y, Matsuda M, Inubushi S, Nasu J, Shirakura M, Suzuki T, Wakita T, Kishino T, Hotta H, Miyamura T, Shoji I (2009) Identification of Annexin A1 as a Novel Substrate for HAP-Mediated Ubiquitylation. J Cell Biochem; 106: 1123-1135

Shirakura M, Murakami K, Ichimura T, Suzuki R, Shimoji T, Fukuda K, Abe K, Sato S, Fukasawa M, Yamakawa Y, Nishijima M, Moriishi K, Matsuura Y, Wakita T, Suzuki T, Howley PM, Miyamura T, Shoji I

(2007) E6AP ubiquitin ligase mediates ubiquitylation and degradation of hepatitis C virus core protein. Journal of Virology; 81: 1174-1185

Shoji I, Murakami K, Fukuda K, Osaki M, Suzu T, Miyamura T, Wakita T (2007) Molecular determinants of E6AP-dependent degradation of hepatitis C virus core protein. Hepatology; 46: 451a-451a

Silva-Santos S, van Woerden GM, Bruinsma CF, Mientjes E, Jolfaei MA, Distel B, Kushner SA, Elgersma Y (2015) Ube3a reinstatement identifies distinct developmental windows in a murine Angelman syndrome model. J Clin Invest; 125: 2069-76

Singh RK, Kazansky Y, Wathieu D, Fushman D (2017) Hydrophobic Patch of Ubiquitin is Important for its Optimal Activation by Ubiquitin Activating Enzyme E1. Anal Chem; 89: 7852-7860

Sloper-Mould KE, Jemc JC, Pickart CM, Hicke L (2001) Distinct functional surface regions on ubiquitin. J Biol Chem; 276: 30483-9

Sluimer J, Distel B (2018) Regulating the human HECT E3 ligases. Cell Mol Life Sci; 75: 3121-3141

Smith SEP, Zhou YD, Zhang GP, Jin Z, Stoppel DC, Anderson MP (2011) Increased Gene Dosage of Ube3a Results in Autism Traits and Decreased Glutamate Synaptic Transmission in Mice. Sci Transl Med; 3

Sondo E, Falchi F, Caci E, Ferrera L, Giacomini E, Pesce E, Tomati V, Bertozzi SM, Goldoni L, Armirotti A, Ravazzolo R, Cavalli A, Pedemonte N (2018) Pharmacological Inhibition of the Ubiquitin Ligase RNF5 Rescues F508del-CFTR in Cystic Fibrosis Airway Epithelia. Cell Chemical Biology; 25: 891-+

Sonzogni M, Hakonen J, Kleijn MB, Silva-Santos S, Judson MC, Philpot BD, van Woerden GM, Elgersma Y (2019) Delayed loss of UBE3A reduces the expression of Angelman syndrome-associated phenotypes. Molecular Autism; 10

Sonzogni M, Wallaard I, Santos SS, Kingma J, du Mee D, van Woerden GM, Elgersma Y (2018) A behavioral test battery for mouse models of Angelman syndrome: a powerful tool for testing drugs and novel Ube3a mutants. Molecular Autism; 9

Srinivasan S, Nawaz Z (2011) E3 ubiquitin protein ligase, E6-associated protein (E6-AP) regulates PI3K-Akt signaling and prostate cell growth. Biochim Biophys Acta; 1809: 119-27

Stanurova J, Neureiter A, Hiber M, de Oliveira Kessler H, Stolp K, Goetzke R, Klein D, Bankfalvi A, Klump H, Steenpass L (2016) Angelman syndrome-derived neurons display late onset of paternal UBE3A silencing. Sci Rep; 6: 30792

Starita LM, Pruneda JN, Lo RS, Fowler DM, Kim HJ, Hiatt JB, Shendure J, Brzovic PS, Fields S, Klevit RE (2013) Activity-enhancing mutations in an E3 ubiquitin ligase identified by high-throughput mutagenesis. Proc Natl Acad Sci U S A; 110: E1263-72

Steffenburg S, Gillberg CL, Steffenburg U, Kyllerman M (1996) Autism in Angelman syndrome: a population-based study. Pediatr Neurol; 14: 131-6

Stewart MD, Ritterhoff T, Klevit RE, Brzovic PS (2016) E2 enzymes: more than just middle men. Cell Res; 26: 423-40

Street I, Lackovic K, Haupt Y, Monahan B, Wolyniec K, Haupt S, Chan A, Falk H, Allan L, Pilling P (2012) A High Throughput Screening Platform for the Identification of Small Molecule Inhibitors of the E3 Ligase E6AP. Eur J Cancer; 48: S250-S250

Streich FC, Jr., Lima CD (2014) Structural and functional insights to ubiquitin-like protein conjugation. Annu Rev Biophys; 43: 357-79

Stutz C, Reinz E, Honegger A, Bulkescher J, Schweizer J, Zanier K, Trave G, Lohrey C, Hoppe-Seyler K, Hoppe-Seyler F (2015) Intracellular Analysis of the Interaction between the Human Papillomavirus Type 16 E6 Oncoprotein and Inhibitory Peptides. Plos One; 10

Su AI, Wiltshire T, Batalov S, Lapp H, Ching KA, Block D, Zhang J, Soden R, Hayakawa M, Kreiman G, Cooke MP, Walker JR, Hogenesch JB (2004) A gene atlas of the mouse and human protein-encoding transcriptomes. P Natl Acad Sci USA; 101: 6062-6067

Suarez I, Trave G (2018) Structural Insights in Multifunctional Papillomavirus Oncoproteins. Viruses; 10

Sun AX, Yuan Q, Fukuda M, Yu W, Yan H, Lim GGY, Nai MH, D'Agostino GA, Tran HD, Itahana Y, Wang D, Lokman H, Itahana K, Lim SWL, Tang J, Chang YY, Zhang M, Cook SA, Rackham OJL, Lim CT, Tan EK, Ng HH, Lim KL, Jiang YH, Je HS (2019) Potassium channel dysfunction in human neuronal models of Angelman syndrome. Science; 366: 1486-1492

Sun J, Liu Y, Jia Y, Hao X, Lin WJ, Tran J, Lynch G, Baudry M, Bi X (2018) UBE3A-mediated p18/LAMTOR1 ubiquitination and degradation regulate mTORC1 activity and synaptic plasticity. Elife; 7

Sun JD, Zhu GQ, Liu Y, Standley S, Ji A, Tunuguntla R, Wang YB, Claus C, Luo Y, Baudry M, Bi XN (2015) UBE3A Regulates Synaptic Plasticity and Learning and Memory by Controlling SK2 Channel Endocytosis. Cell Rep; 12: 449-461

Swatek KN, Komander D (2016) Ubiquitin modifications. Cell Res; 26: 399-422

Takahashi Y, Wu J, Suzuki K, Martinez-Redondo P, Li M, Liao HK, Wu MZ, Hernandez-Benitez R, Hishida T, Shokhirev MN, Esteban CR, Sancho-Martinez I, Belmonte JCI (2017) Integration of CpG-free DNA induces de novo methylation of CpG islands in pluripotent stem cells. Science; 356: 503-+

Tan WH, Bird LM, Thibert RL, Williams CA (2014) If Not Angelman, What Is It? A Review of Angelman-like Syndromes. Am J Med Genet A; 164: 975-992

Tang GY (2016) Why Polyphenols have Promiscuous Actions? An Investigation by Chemical Bioinformatics. Nat Prod Commun; 11: 655-6

Tang H-C (2017) Insights into the Tumor Suppressor p53: Physiological Function and Proteolytic Regulation. Doctoral thesis, AG Scheffner, University of Konstanz;

Thomas JA, Johnson J, Peterson Kraai TL, Wilson R, Tartaglia N, LeRoux J, Beischel L, McGavran L, Hagerman RJ (2003) Genetic and clinical characterization of patients with an interstitial duplication 15q11-q13, emphasizing behavioral phenotype and response to treatment. Am J Med Genet A; 119A: 111-20

Tian MY, Zeng TL, Liu MD, Han S, Lin HY, Lin Q, Li L, Jiang TT, Li G, Lin H, Zhang T, Kang QF, Deng XM, Wang HR (2019) A cell-based high-throughput screening method based on a ubiquitin-reference technique for identifying modulators of E3 ligases. Journal of Biological Chemistry; 294: 2880-2891

Tirat A, Schilb A, Riou V, Leder L, Gerhartz B, Zimmermann J, Worpenberg S, Eldhoff U, Freuler F, Stettler T, Mayr L, Ottl J, Leuenberger B, Filipuzzi I (2005) Synthesis and characterization of fluorescent ubiquitin derivatives as highly sensitive substrates for the deubiquitinating enzymes UCH-L3 and USP-2. Anal Biochem; 343: 244-255

Tomaic V, Pim D, Thomas M, Massimi P, Myers MP, Banks L (2011) Regulation of the human papillomavirus type 18 E6/E6AP ubiquitin ligase complex by the HECT domain-containing protein EDD. J Virol; 85: 3120-7

Tritsch D, Zingle C, Rohmer M, Grosdemange-Billiard C (2015) Flavonoids: true or promiscuous inhibitors of enzyme? The case of deoxyxylulose phosphate reductoisomerase. Bioorg Chem; 59: 140-4

Ungermannova D, Parker SJ, Nasveschuk CG, Chapnick DA, Phillips AJ, Kuchta RD, Liu X (2012) Identification and mechanistic studies of a novel ubiquitin E1 inhibitor. J Biomol Screen; 17: 421-34

Urso L, Calabrese F, Favaretto A, Conte P, Pasello G (2016) Critical review about MDM2 in cancer: Possible role in malignant mesothelioma and implications for treatment. Crit Rev Oncol Hematol; 97: 220-30

Valluy J, Bicker S, Aksoy-Aksel A, Lackinger M, Sumer S, Fiore R, Wust T, Seffer D, Metge F, Dieterich C, Wohr M, Schwarting R, Schratt G (2015) A coding-independent function of an alternative Ube3a transcript during neuronal development. Nature Neuroscience; 18: 666-+

Vande Pol SB, Klingelhutz AJ (2013) Papillomavirus E6 oncoproteins. Virology; 445: 115-137

Varshavsky A (2012) The ubiquitin system, an immense realm. Annu Rev Biochem; 81: 167-76

Vatsa N, Jana NR (2018) UBE3A and Its Link With Autism. Front Mol Neurosci; 11: 448

Verdecia MA, Joazeiro CA, Wells NJ, Ferrer JL, Bowman ME, Hunter T, Noel JP (2003) Conformational flexibility underlies ubiquitin ligation mediated by the WWP1 HECT domain E3 ligase. Mol Cell; 11: 249-59

Vijay-Kumar S, Bugg CE, Cook WJ (1987) Structure of ubiquitin refined at 1.8 A resolution. Journal of molecular biology; 194: 531-44

Voges D, Zwickl P, Baumeister W (1999) The 26S proteasome: a molecular machine designed for controlled proteolysis. Annu Rev Biochem; 68: 1015-68

von Delbruck M, Kniss A, Rogov VV, Pluska L, Bagola K, Lohr F, Guntert P, Sommer T, Dotsch V (2016) The CUE Domain of Cue1 Aligns Growing Ubiquitin Chains with Ubc7 for Rapid Elongation. Mol Cell; 62: 918-928

Vu TH, Hoffman AR (1997) Imprinting of the Angelman syndrome gene, UBE3A, is restricted to brain. Nature genetics; 17: 12-3

Wagstaff J, Knoll JHM, Glatt KA, Shugart YY, Sommer A, Lalande M (1992) Maternal but Not Paternal Transmission of 15q11-13-Linked Nondeletion Angelman Syndrome Leads to Phenotypic-Expression. Nat Genet; 1: 291-294

Walker-Gray R, Stengel F, Gold MG (2017) Mechanisms for restraining cAMP-dependent protein kinase revealed by subunit quantitation and cross-linking approaches. Proc Natl Acad Sci U S A; 114: 10414-10419

Walzthoeni T, Joachimiak LA, Rosenberger G, Rost HL, Malmstrom L, Leitner A, Frydman J, Aebersold R (2015) xTract: software for characterizing conformational changes of protein complexes by quantitative cross-linking mass spectrometry. Nat Methods; 12: 1185-90

Wan LX, Zou WG, Gao DM, Inuzuka H, Fukushima H, Berg AH, Drapp R, Shaik S, Hu D, Lester C, Eguren M, Malumbres M, Glimcher LH, Wei WY (2011) Cdh1 Regulates Osteoblast Function through an APC/C-Independent Modulation of Smurf1. Molecular Cell; 44: 721-733

Wang D, Ma LN, Wang B, Liu J, Wei WY (2017a) E3 ubiquitin ligases in cancer and implications for therapies. Cancer Metast Rev; 36: 683-702

Wang J, Lou SS, Wang TT, Wu RJ, Li GY, Zhao M, Lu B, Li YY, Zhang J, Cheng XW, Shen Y, Wang X, Zhu ZC, Li MJ, Takumi T, Yang H, Yu X, Liao LJ, Xiong ZQ (2019) UBE3A-mediated PTPA ubiquitination and degradation regulate PP2A activity and dendritic spine morphology. P Natl Acad Sci USA; 116: 12500-12505

Wang M, Pickart CM (2005) Different HECT domain ubiquitin ligases employ distinct mechanisms of polyubiquitin chain synthesis. EMBO J; 24: 4324-33

Wang YY, Liu XP, Zhou L, Duong D, Bhuripanyo K, Zhao B, Zhou H, Liu RC, Bi YT, Kiyokawa H, Yin J (2017b) Identifying the ubiquitination targets of E6AP by orthogonal ubiquitin transfer. Nature Communications; 8

Weber J, Polo S, Maspero E (2019) HECT E3 Ligases: A Tale With Multiple Facets. Front Physiol; 10: 370

Weinstein IB, Joe A (2008) Oncogene addiction. Cancer Research; 68: 3077-3080

Wells SI, Francis DA, Karpova AY, Dowhanick JJ, End JDB, Benson JD, Howley PM (2000) Papillomavirus E2 induces senescence in HPV-positive cells via pRB- and p21(CIP)-dependent pathways. Embo Journal; 19: 5762-5771

Wenzel DM, Lissounov A, Brzovic PS, Klevit RE (2011) UBCH7 reactivity profile reveals parkin and HHARI to be RING/HECT hybrids. Nature; 474: 105-U136

Wiesner S, Ogunjimi AA, Wang HR, Rotin D, Sicheri F, Wrana JL, Forman-Kay JD (2007) Autoinhibition of the HECT-Type ubiquitin ligase smurf2 through its c2 domain. Cell; 130: 651-662

Williams CA, Angelman H, Claytonsmith J, Driscoll DJ, Hendrickson JE, Knoll JHM, Magenis RE, Schinzel A, Wagstaff J, Whidden EM, Zori RT (1995) Angelman Syndrome - Consensus for Diagnostic-Criteria. Am J Med Genet; 56: 237-238

Williams CA, Beaudet AL, Clayton-Smith J, Knoll JH, Kyllerman M, Laan LA, Magenis RE, Moncla A, Schinzel AA, Summers JA, Wagstaff J (2006) Angelman syndrome 2005: Updated consensus for diagnostic criteria. Am J Med Genet A; 140a: 413-418

Wolyniec K, Shortt J, de Stanchina E, Levav-Cohen Y, Alsheich-Bartok O, Louria-Hayon I, Corneille V, Kumar B, Woods SJ, Opat S, Johnstone RW, Scott CL, Segal D, Pandolfi PP, Fox S, Strasser A, Jiang YH,

Lowe SW, Haupt S, Haupt Y (2012) E6AP ubiquitin ligase regulates PML-induced senescence in Myc-driven lymphomagenesis. Blood; 120: 822-32

Wu YL, Yang XJ, Ren Z, McDonnell DP, Norris JD, Willson TM, Greene GL (2005) Structural basis for an unexpected mode of SERM-mediated ER antagonism. Molecular Cell; 18: 413-424

Xu GW, Ali M, Wood TE, Wong D, Maclean N, Wang X, Gronda M, Skrtic M, Li X, Hurren R, Mao X, Venkatesan M, Beheshti Zavareh R, Ketela T, Reed JC, Rose D, Moffat J, Batey RA, Dhe-Paganon S, Schimmer AD (2010) The ubiquitin-activating enzyme E1 as a therapeutic target for the treatment of leukemia and multiple myeloma. Blood; 115: 2251-9

Yamagishi Y, Shoji I, Miyagawa S, Kawakami T, Katoh T, Goto Y, Suga H (2011) Natural Product-Like Macrocyclic N-Methyl-Peptide Inhibitors against a Ubiquitin Ligase Uncovered from a Ribosome-Expressed De Novo Library. Chemistry & Biology; 18: 1562-1570

Yamamoto Y, Huibregtse JM, Howley PM (1997) The human E6-AP gene (UBE3A) encodes three potential protein isoforms generated by differential splicing. Genomics; 41: 263-6

Yamasaki K, Joh K, Ohta T, Masuzaki H, Ishimaru T, Mukai T, Niikawa N, Ogawa M, Wagstaff J, Kishino T (2003) Neurons but not glial cells show reciprocal imprinting of sense and antisense transcripts of Ube3a. Hum Mol Genet; 12: 837-47

Yamato K, Fen J, Kobuchi H, Nasu Y, Yamada T, Nishihara T, Ikeda Y, Kizaki M, Yoshinouchi M (2006) Induction of cell death in human papillomavirus 18-positive cervical cancer cells by E6 siRNA. Cancer Gene Ther; 13: 234-241

Yang Y, Kitagaki J, Dai RM, Tsai YC, Lorick KL, Ludwig RL, Pierre SA, Jensen JP, Davydov IV, Oberoi P, Li CC, Kenten JH, Beutler JA, Vousden KH, Weissman AM (2007) Inhibitors of ubiquitin-activating enzyme (E1), a new class of potential cancer therapeutics. Cancer Res; 67: 9472-81

Yang YL, Ludwig RL, Jensen JP, Pierre SA, Medaglia MV, Davydov IV, Safiran YJ, Oberoi P, Kenten JH, Phillips AC, Weissman AM, Vousden KH (2005) Small molecule inhibitors of HDM2 ubiquitin ligase activity stabilize and activate p53 in cells. Cancer Cell; 7: 547-559

Ye Y, Rape M (2009) Building ubiquitin chains: E2 enzymes at work. Nat Rev Mol Cell Biol; 10: 755-64

Yi JJ, Berrios J, Newbern JM, Snider WD, Philpot BD, Hahn KM, Zylka MJ (2015) An Autism-Linked Mutation Disables Phosphorylation Control of UBE3A. Cell; 162: 795-807

Yu C, Huang L (2018) Cross-Linking Mass Spectrometry: An Emerging Technology for Interactomics and Structural Biology. Anal Chem; 90: 144-165

Yuan CH, Filippova M, Krstenansky JL, Duerksen-Hughes PJ (2016) Flavonol and imidazole derivatives block HPV16 E6 activities and reactivate apoptotic pathways in HPV+ cells. Cell Death Dis; 7

Zaaroor-Regev D, de Bie P, Scheffner M, Noy T, Shemer R, Heled M, Stein I, Pikarsky E, Ciechanover A (2010) Regulation of the polycomb protein Ring1B by self-ubiquitination or by E6-AP may have implications to the pathogenesis of Angelman syndrome. Proc Natl Acad Sci U S A; 107: 6788-93

Zanier K, Charbonnier S, Sidi AOMO, McEwen AG, Ferrario MG, Poussin-Courmontagne P, Cura V, Brimer N, Babah KO, Ansari T, Muller I, Stote RH, Cavarelli J, Pol SV, Trave G (2013) Structural Basis for Hijacking of Cellular LxxLL Motifs by Papillomavirus E6 Oncoproteins. Science; 339: 694-698

Zanier K, Stutz C, Kintscher S, Reinz E, Sehr P, Bulkescher J, Hoppe-Seyler K, Trave G, Hoppe-Seyler F (2014) The E6AP Binding Pocket of the HPV16 E6 Oncoprotein Provides a Docking Site for a Small Inhibitory Peptide Unrelated to E6AP, Indicating Druggability of E6. Plos One; 9

Zhang JH, Chung TD, Oldenburg KR (1999) A Simple Statistical Parameter for Use in Evaluation and Validation of High Throughput Screening Assays. J Biomol Screen; 4: 67-73

Zhang W, Sidhu SS (2014) Development of inhibitors in the ubiquitination cascade. FEBS letters; 588: 356-67

Zhang Y, Wang C, Cao Y, Gu YQ, Zhang LQ (2017) Selective compounds enhance osteoblastic activity by targeting HECT domain of ubiquitin ligase Smurf1. Oncotarget; 8: 50521-50533

Zheng L, Ding HR, Lu ZM, Li Y, Pan YQ, Ning T, Ke Y (2008) E3 ubiquitin ligase E6AP-mediated TSC2 turnover in the presence and absence of HPV16 E6. Genes Cells; 13: 285-294

Zheng N, Shabek N (2017) Ubiquitin Ligases: Structure, Function, and Regulation. Annual Review of Biochemistry, Vol 86; 86: 129-157

Zhu K, Shan ZL, Chen X, Cai YQ, Cui L, Yao WY, Wang Z, Shi P, Tian CL, Lou JZ, Xie YL, Wen WY (2017) Allosteric auto-inhibition and activation of the Nedd4 family E3 ligase Itch. Embo Rep; 18: 1618-1630

zur Hausen H (2002) Papillomaviruses and cancer: From basic studies to clinical application. Nat Rev Cancer; 2: 342-350

zurHausen H (1996) Papillomavirus infections - A major cause of human cancers. Bba-Rev Cancer; 1288: F55-F78

Zylka MJ (2019) Prenatal Treatment Path for Angelman Syndrome and Other Neurodevelopmental Disorders. Autism Res;

8 Danksagung

An dieser Stelle möchte ich mich bei einer Vielzahl von Personen bedanken, ohne deren Zusammenarbeit und/oder Unterstützung diese Arbeit nicht das geworden wäre was sie nun ist und meine Zeit als Doktorand in Konstanz nicht so schön gewesen wäre wie sie es war!

An allererster Stelle möchte ich mich bei Prof. Martin Scheffner bedanken, und zwar für die Aufnahme in seine Arbeitsgruppe, das spannende Projekt, seine fachlichen Ratschläge und klare Kommunikationsweise, aber auch für die Freiräume, die er mir als Doktorand gelassen hat.

Außerdem möchte ich Prof. Florian Stengel für die erfolgreiche Zusammenarbeit und die Übernahme des Gutachtens danken. Bei Prof. Andreas Marx möchte ich mich für die Zusammenarbeit, die Betreuung als Mitglied meines Thesiskomitees in der KoRS-CB und die Übernahme des Prüfungsvorsitzes bedanken. Bei Prof. Thomas Mayer möchte ich mich sowohl für die Möglichkeit in seinem Labor und im Screening Centre arbeiten zu dürfen als auch für den Input als Mitglied meines Thesiskomitees bedanken.

Desweiteren danke ich Ania, Thomas, Nicole und Silke für die Einarbeitung in die Laborpraktiken und für die technische Unterstützung im Laboralltag. Dann möchte ich mich bei allen ehemaligen und jetzigen Kollegen aus der AG Scheffner, nämlich bei Daniel, Stefan, Elli, Franziska, Toto, Hongjian, Felix, Alex, Franzi, Simon, Katrin, Matze, Daniela, Anja und Jeannine sowohl für die sehr schöne gemeinsame Zeit im Labor und die Mittwochabend Pokerrunden, als auch für alle privaten Feiern und Aktivitäten bedanken. Mein besonderer Dank gilt Franzi, Jasmin und Caro, die gemeinsam mit mir an der Charakterisierung E6APs und der Angelman-Syndrom Mutanten gearbeitet haben und Alex, Franzi, Jasmin und Caro für das Korrekturlesen dieser Dissertation.

Bedanken möchte ich mich auch bei allen Studenten, die ich allein oder gemeinsam mit Franzi betreut habe, und zwar bei Anja, Jeannine, Jasmin, Paulina, Valeria, Louis, Ella, Aurelia, Verena, Bene, Katharina, Julia, Sharif und Thomas. Des Weiteren möchte ich mich bei Julius, Caro, Kai, Marie und Jasmin aus der AG Stengel für die Zusammenarbeit und gemeinsamen Seminare und Ausflüge bedanken. Ebenso bei Stephan Hacker, Kathrin Götz, Joachim, Xiaohui, Daniel Hammler, Lena und Matthias Frese aus der AG Marx, und bei Martin, Lars, Martina und Melanie aus der AG TUM. Schließlich möchte ich Alex Fillbrunn und Patrick für die Unterstützung mit KNIME, bei Silke vom Screening Centre und bei Ania und Andi von der Proteomics facility sowie der KoRS-CB, dem SFB969 und dem Zukunftskolleg für jegliche Unterstützung danken.

Zu guter Letzt bedanke ich mich bei meinen Eltern, Geschwistern, Verwandten und Freunden, die ich in Konstanz während des Studiums und meiner Doktorarbeit, an der Uni oder in meiner Freizeit kennen lernen durfte, und die mir alle mit Sicherheit Stärke und Motivation zum Gelingen dieser Arbeit mitgeben konnten. Außerdem danke ich Alex für alles.

9 Appendix

9.1 Abbreviations

16 E6	HPV type 16 early protein 6
4Met-Tamoxifen	4-Methyltamoxifen
4OH-Tamoxifen	4-Hydroxytamoxifen
AS	Angelman syndrome
ASD	Autism spectrum disorder
AZUL	Amino-terminal Zn-finger of Ube3a Ligase
DTT	Dithiothreitol
E1	Ubiquitin-activating enzyme
E2	Ubiquitin-conjugating enzyme
E3	Ubiquitin ligase
E6	HPV early protein 6
E6AP	E6 Associated Protein
ERα	Estrogen Receptor alpha
FP	Fluorescence polarization
HECT	Homologous to E6AP C terminus
HPV	Human papillomavirus
HTS	High-throughput screen
iPSC	inducible Pluripotent Stem Cell
qXL-MS	quantitative XL-MS
RBR	RING-in between-RING
RING	Really interesting new gene
SDS-PAGE	Sodium dodecyl sulfate-polyacrylamide gel electrophoresis
SERM	Selective estrogen receptor modulator
TAMRA	5/6-Carboxytetramethylrhodamine
$T_{25}N_{50}$	25 mM Tris and 50 mM NaCl containing buffer
TRIS	Tris(hydroxymethyl)-aminomethan
UBE3A	Ubiquitin-protein ligase E3A; E6AP
UbLIA	Ubiquitin with substitution of L8 and I44 to alanine
Ub-T	Ubiquitin-TAMRA
XL-MS	Crosslinking coupled to mass spectrometry

9.2 Appendix table I: Small molecule E6-E6AP inhibitors

Primary screen and secondary assay results of hits from E6-E6AP inhibitor screening

uiid Screening Centre Uni Konstanz	Internal ID	Chemical structure shown in figure	Supplier with order number	% Inhibition E6-E6AP in primary screen	% Inhibition of RLIM_RING in counter screen	% Inhibition of E6-E6AP with cherry-picked compounds	% Inhibition of RLIM_RING with cherry-picked compounds	Final result
CBP1006K06	OF106	12	Vitas-M STK598610	93	10	87	-5	unspecific
CBP4008A07	OF101	12	Vitas-M STK151319	108	-4	3	-4	inactive
CBP4008O03	OF105	12	Vitas-M STL414410	92	4	14	-6	unspecific
CBP4008E13	OF103/OF117	12/15	Vitas-M STK121570	61	3	42	-11	unspecific
CBP4008I13	OF104	12	Vitas-M STL181347	52	-15	-3	-2	inactive
CBP4008A15	OF102	12	Vitas-M STK125413	50	-3	-2	-2	unspecific
AD151J11	OF107	12	Analyticon NP-000876	73	10	3	-6	inactive
AD151M19	OF113	12	Analyticon NP-011196	53	12	10	0	unspecific
AD151P07	OF108	12	Analyticon NP-000129	92	2	6	0	inactive
AD152L05	OF109	12	Analyticon NP-000872	64	9	-1	-1	inactive
AD152P12	OF110	12	Analyticon NP-001438	71	0	15	-1	inactive
AD153A04	OF111	12	Analyticon NP-000502	72	6	16	-3	inactive
AD153E15	OF112	12	Analyticon NP-000841	50	8	49	31	unspecific
CBP3I01				63		9	3	inactive
CBP3F05				63		21	11	inactive
CBP3L09				95		41	11	unspecific
CBP4I12				68		39	13	unspecific
CBP4H05				88		60	24	unspecific
CBP4M07				76		28	-7	inactive
CBP4C12				97		49	36	unspecific
CBP4H22				84		10	-4	inactive
CBP5L11				95		32	3	not finally tested
CBP6E14				69		17	7	inactive
CBP6K14				76		28	24	unspecific
CBP7G02				94		54	28	unspecific
CBP7I02				68		51	17	unspecific
CBP7J06				64		14	-3	inactive
CBP7I11				93		3	-2	inactive
CBP7K14				79		5	-5	inactive
CBP7O14				60		10	7	inactive
CBP8F10				106		41	31	unspecific
CBP8F17	OF118	15	Vitas-M STK762336	101		35	-10	unspecific
CBP8P20				86		40	11	unspecific
CBP9E13				52		35	5	not finally tested
CBP9G13	OF115	15	Vitas-M STL431978	55		72	12	inactive
CBP10D03				103		38	13	unspecific
CBP10I17				71		23	11	unspecific
CBP10H22				71		11	3	inactive
CBP12D16				76		8	-5	inactive
CBP12N21				84		11	4	inactive
CBP13D18				60		2	-2	inactive
CBP15E07				76		29	-8	inactive
CBP15O08				65		0	-2	inactive
CBP15A19				61		11	-7	inactive
CBP16J20				89		9	-1	inactive
CBP17A21				78		4	0	inactive
CBP17N20				52		13	5	inactive
CBP19I04				51		23	-4	inactive
CBP20B13				70		4	3	inactive
CBP21J03				70		24	9	inactive
CBP22D15				86		13	-1	inactive
CBP25E02				51		20	-2	inactive
CBP25L06				64		7	-24	inactive
CBP25H13				60		13	-14	inactive
CBP25J13				101		45	19	unspecific
CBP25F22				54		30	4	not finally tested
CBP26I10				64		14	8	inactive
CBP26L10				86		18	-4	inactive
CBP27M14				102		71	16	unspecific
CBP27H19				61		47	14	unspecific
CBP28F18				52		28	8	inactive
CBP29L03				84		14	-3	inactive
CBP29E05				66		9	0	inactive
CBP29F05				51		7	-5	inactive
CBP29G07				63		8	-3	inactive
CBP29K13				51		18	3	inactive
CBP31H08	OF116	15	Vitas-M STK683738	96		33	7	unspecific
CBP34L05				80		27	11	unspecific
CBP35K11				79		2	-3	inactive

CBP36E06				107		-6	-25	inactive
CBP36E07	OF120	15	ChemDiv K310-0067	63		32	-6	unspecific
CBP36A20				100		-2	1	inactive
CBP38C02				99		-1	1	inactive
CBP39E19				94		30	8	not finally tested
CBP42L22				82		8	-3	inactive
CBP42P22				81		11	-8	inactive
CBP45J06				113		25	7	inactive
CBP47F21				83		39	7	not finally tested
CBP1003M05				74		16	-2	inactive
CBP1003N15				79		6	-1	inactive
CBP1004L01				99		23	5	inactive
CBP1005J12				88		15	-2	inactive
CBP1005K12				66		35	32	unspecific
CBP1007K16				102		26	9	inactive
CBP1007K18				92		17	-2	inactive
CBP1007K22				93		11	-2	inactive
CBP1007N16				107		78	45	unspecific
CBP1008N02				75		10	-12	inactive
CBP1009L07				59		-20	-23	inactive
CBP1011F05				100		21	6	inactive
CBP1011J14				78		18	7	inactive
CBP1011F19				107		26	22	inactive
CBP1011M19				106		47	21	unspecific
CBP1012F04				113		45	14	unspecific
CBP1012P09				60		8	5	inactive
CBP1013B02				59		18	6	inactive
CBP1013M06				118		41	12	unspecific
CBP1014N22				103		20	7	inactive
CBP1015M01				54		-4	6	inactive
CBP1015L05				88		-3	-4	inactive
CBP1015J21				106		36	12	unspecific
CBP1016F18				73		32	12	unspecific
CBP1016F03				73		8	1	inactive
CBP1016M13				63		9	-8	inactive
CBP1016K20				66		11	5	inactive
CBP1016H21				97		46	30	unspecific
CBP1016I22				78		6	-3	inactive
CBP1017D14				84		30	9	not finally tested
CBP1017K21				68		34	15	unspecific
CBP1018L16				89		24	9	inactive
CBP1018I22				63		11	-1	inactive
CBP1018P17				53		4	-9	inactive
CBP1018I19				90		14	12	inactive
CBP1019M03				76		20	1	inactive
CBP1019B06				101		32	13	unspecific
CBP1019D14				79		-1	-2	inactive
CBP1020K12				70		11	-2	inactive
CBP1022B08				58		16	-4	inactive
CBP4009P16				81		25	-1	inactive
CBP4009B08				99		12	3	inactive
CBP4009D11				71		-3	-7	inactive
CBP4009A18				77		3	-3	inactive
CBP4009D21				100		20	1	inactive
CBP4011B04				119		8	-5	inactive
CBP4011A06				121		2	7	inactive
CBP4012C10				106		6	-5	inactive
CBP4012J11				107		72	50	unspecific
CBP3001O01				91		101	66	unspecific
CBP3001I09				64		18	4	inactive
CBP3001G11				66		34	5	not finally tested
CBP3006D12				108		38	15	unspecific
CBP3006A17				61		5	-1	inactive
CBP3006C19				70		-1	-4	inactive
CBP3012G06				52		-3	-4	inactive
CBP3012F07				61		3	1	inactive
CD101G01				59		48	6	not finally tested
CD101G18				88		16	-6	inactive
CD101N18				63		0	-3	inactive
CD102I20				62		-1	-5	inactive
CD103H17				76		6	-4	inactive
CD104B10				52		51	29	unspecific
CD104D08				103		66	38	unspecific
CD104F08				72		44	18	unspecific
CD104F19				102		20	7	inactive
CD104H08				100		94	51	unspecific
CD104P08				102		69	58	unspecific
CD105C03	OF122	14		57		53	0	unspecific

CD105E03	OF123	14		70		43	1	unspecific
CD105G03	OF124	14		78		35	-5	unspecific
CD105I03				55		28	-5	inactive
CD107F19				61		8	-2	inactive
CD108D16				76		24	0	inactive
CD108F17				78		6	-1	inactive
CD108H17				70		5	-4	inactive
CD109J19				90		5	-1	inactive
CD110J08				104		-6	-2	inactive
CD110J16				65		15	-1	inactive
CD112K10				106		2	-6	inactive
CD113O04				88		77	48	unspecific
CD114G20				109		34	15	unspecific
CD114P19				100		9	-1	inactive
CD116C20				79		19	-1	inactive
CD116E13				71		14	2	inactive
CD117A01				129		41	53	unspecific
CD117G13				78		12	2	inactive
CD118I08				90		50	25	unspecific
CD119L16				98		3	-1	inactive
CD122A05				101		54	16	unspecific
CD123A11				77		19	0	inactive
CD123F02				82		47	22	unspecific
CD123O11				96		5	-2	inactive
CD124E08				99		23	-4	inactive
CD124I08				97		20	-4	inactive
CD124J14				88		22	-2	inactive
CD126B04				85		24	-1	inactive
CD126D04	OF119	15	ChemDiv 4243-1246	81		41	7	unspecific
CD126D08				51		16	3	inactive
CD126H02				109		25	13	inactive
CD126H08				83		12	-15	inactive
CD126J02				52		51	20	unspecific
CD126J06				61		11	-3	inactive
CD126L06	OF121	15	ChemDiv 8008-3444	106		30	-6	unspecific
CD126L08				110		10	-17	inactive
CBP2G11				65	25			unspecific
CBP2F07				111	39			unspecific
CBP2E10				101	32			unspecific
CBP2I10				122	106			unspecific
CBP2A12				108	39			unspecific
CBP2H17				53	20			unspecific
CBP11M06				72	15			unspecific
CBP11O06				98	78			unspecific
CBP11E08				62	21			unspecific
CBP11G08				75	46			unspecific
CBP11K08				101	99			unspecific
CBP11O08				107	90			unspecific
CBP11M10				93	66			unspecific
ICCB205A07				70	26			unspecific
ICCB205C20				105	19			unspecific
ICCB205E10				107	53			unspecific
ICCB205E22				73	11			unspecific
ICCB205I17				85	58			unspecific
ICCB205I19				140	101			unspecific
ICCB205M11				133	103			unspecific
ICCB205O12				133	78			unspecific
ICCB205O16				81	16			unspecific
ICCB205O17				126	69			unspecific
CBP1002D03				58	23			unspecific
CBP1002D12				107	100			unspecific
CBP1002P16				98	41			unspecific
CBP1002J04				78	32			unspecific
CBP1002J06				58	12			unspecific
CBP1002L16				97	29			unspecific
CBP1002P06				71	27			unspecific
CBP1006E16				100	13			unspecific
CBP1006E04				100	16			unspecific
CBP1006M14				98	41			unspecific
CBP1006M19				80	25			unspecific
CBP1006O21				96	15			unspecific
CBP4008C07				107	93			unspecific
CBP4008C17				76	20			unspecific
CBP4008K17				88	55			unspecific
CBP4008K18				107	69			unspecific
CBP4008K19				50	36			unspecific
CBP4010E02				88	66			unspecific
CBP4010L03				67	15			unspecific

CBP4010N03				51	8			not finally tested
CBP4010A06				73	25			unspecific
CBP4010P06				80	20			unspecific
CBP4010G07				98	19			unspecific
CBP4010L07				73	5			not finally tested
CBP4010A10				81	1			not finally tested
CBP4010B10				83	10			unspecific
CBP4010K11				101	92			unspecific
CBP4010A17				61	10			unspecific
CBP4010C17				66	18			unspecific
CBP4010M21				100	84			unspecific
AD151B09				71	26			unspecific
AD151B19				55	18			unspecific
AD151C13				61	15			unspecific
AD151D07				51	21			unspecific
AD151D11				101	97			unspecific
AD151E05				79	34			unspecific
AD151E13				79	14			unspecific
AD151E16				105	102			unspecific
AD151E20				96	30			unspecific
AD151G07				61	42			unspecific
AD151L04				65	5			not finally tested
AD151G03				67	17			unspecific
AD151G13				78	22			unspecific
AD151G14				58	7			not finally tested
AD151I08				64	27			unspecific
AD151I09				67	23			unspecific
AD151I10				77	31			unspecific
AD151I12				74	21			unspecific
AD151I14				102	92			unspecific
AD151K07				73	16			unspecific
AD151L01				55	16			unspecific
AD151L09				94	58			unspecific
AD151L11				56	17			unspecific
AD151M02				77	22			unspecific
AD151M09				61	24			unspecific
AD151M13				72	14			unspecific
AD151M18				70	17			unspecific
AD151N07				56	6			not finally tested
AD151N11				95	44			unspecific
AD151O12				54	26			unspecific
AD151O14				65	26			unspecific
AD151O18				76	14			unspecific
AD151P03				80	23			unspecific
AD151P19				64	22			unspecific
AD152B04				73	17			unspecific
AD152B15				81	26			unspecific
AD152C08				57	21			unspecific
AD152E16				104	42			unspecific
AD152F13				109	95			unspecific
AD152F16				93	50			unspecific
AD152G13				57	4			not finally tested
AD152F20				72	28			unspecific
AD152G08				100	53			unspecific
AD152H03				92	50			unspecific
AD152H11				61	29			unspecific
AD152H12				57	21			unspecific
AD152H16				108	102			unspecific
AD152J11				67	38			unspecific
AD152J15				66	39			unspecific
AD152J17				104	50			unspecific
AD152K16				89	27			unspecific
AD152K17				90	25			unspecific
AD152N03				57	16			unspecific
AD152M18				62	19			unspecific
AD152N18				62	19			unspecific
AD152P16				71	-2			not finally tested
AD153A06				90	35			unspecific
AD153A14				107	46			unspecific
AD153A15				73	24			unspecific
AD153C02				75	29			unspecific
AD153C13				82	19			unspecific
AD153C15				90	26			unspecific
AD153E07				86	26			unspecific
AD153E09				64	25			unspecific
AD153F03				50	18			unspecific
AD153F10				108	103			unspecific
AD153G07				61	18			unspecific

AD153G12	OF114	12	AD NP-003818	92	13			unspecific
AD153H08				105	93			unspecific
AD153I12				58	13			unspecific
AD153J02				51	18			unspecific
AD153J05				96	37			unspecific
AD153K03				106	99			unspecific
AD153K13				79	26			unspecific
AD153L10				73	36			unspecific
AD153M11				68	32			unspecific
AD153M02				102	96			unspecific
AD153M20				98	28			unspecific
AD153O06				71	32			unspecific
AD153O16				63	-2			not finally tested
MB029E07				96				not finally tested
CD121A06				100				not finally tested
CD121E18				59				not finally tested
CD121I12				98				not finally tested
NATx6K04				74				not finally tested
NATx11G15				54				not finally tested
MB009J16				51				not finally tested
MB002D11				104				not finally tested
MB002L07				101				not finally tested
MB006F17				77				not finally tested
MB006P17				95				not finally tested
MB007J16				100				not finally tested
MB008B03				57				not finally tested
MB008C12				74				not finally tested
MB013F05				104				not finally tested
MB013I04				98				not finally tested
MB013J05				97				not finally tested
MB015B08				73				not finally tested
MB016K04				100				not finally tested
MB017A10				68				not finally tested
MB021A08				63				not finally tested
MB021B15				59				not finally tested
MB021D08				97				not finally tested
MB022P17				92				not finally tested
MB023B13				97				not finally tested
MB026N09				52				not finally tested
MB027L20				60				not finally tested
CBP1K01				101				not finally tested
CBP1M04				101				not finally tested
CBP1M18				107				not finally tested
ICCB204B08	β-Lapachon		Sigma L2037	89				unspecific
ICCB204F14				115				not finally tested
ICCB204F18				112				not finally tested
ICCB204L18				57				not finally tested
ICCB204P19				115				not finally tested

9.3 Appendix table II: Small molecule E6AP activators

Overview primary and secondary screening assays for small molecule activators of E6AP

Uiid Screening Centre University of Konstanz	Internal ID or common name	Chemical structure shown in figure	Supplier and order number	Primary screen (% activation of E6AP)		Counter screen (% activation of RLIM_RING)		Confirmation of cherry-picked or purchased compounds (% activation of E6AP)	
				t = 45 min	t = 55 min	t = 45 min	t = 55 min	t = 45 min	t = 55 min
Screening hits									
AD152J04				25	76				
AD153M07				20	62	1	-8		
AD153O18				24	63	-3	-7		
CBP1001G05				40	53			1	-2
CBP14P15	OF200	20	Vitas-M STK208427	20	72			-1	6
CBP15G01				83	85	4	-1	-2	6
CBP16I03				30	77				
CBP17N05				32	83	1	3	14	34
CBP25C01				40	68	-6	-1	-1	-3
CBP25D12				56	71	-3	1	17	33
CBP25P04				37	64	-7	-19	8	14
CBP27E14	OF203	20	Vitas-M STK760173	17	61			6	13
CBP28J08				40	62	-8	-6	3	2
CBP28P11				81	78	2	0	2	2
CBP31F04	OF204	20	Vitas-M STK682896	51	73	-9	-1	3	16
CBP31H04				54	64	-2	-1	8	26
CBP31P13	OF205	20	Vitas-M STK777064	49	77	-12	-15	-1	-3
CBP35K22				17	53			8	1
CBP36H12				49	83	-4	0	-1	-1
CBP36P02				60	68	3	8	17	33
CBP4007J04	OF206	20	Vitas-M STK306587	18	78			1	-7
CBP7B01	OF201	20	Vitas-M STK327397	22	76			2	1
CBP7M10	OF202	20	Vitas-M STL353122	25	69			8	19
CD120M08	OF207/ OF208	20	Vitas-M STK722575	28	82			78	78
ICCB204B11	Dichloro-benzamil			18	62				
ICCB204B22	U-74389G			12	61				
ICCB205K08	TPEN			58	77	-13	-14		
ICCB205K14	Tunicamycin			28	77	-4	-9		
ICCB205M15	Mastoparan			33	76	-6	0		
ICCB205M19	Gliotoxin			60	81	-5	-15		
MB002O11				38	63			3	4
MB004I16				20	68			0	12
MB005F03				32	66			0	3
MB006O12				36	72			8	20
MB007F03				28	84			8	23
MB009J02				37	74			3	6
MB013P14				22	78			9	16
MB015L17				20	62			10	30
MB020H01				24	60			8	10

MB022E08				21	63	4	-2	2	3
MB022I06				16	62	-2	-1	2	-7
NATx03D15	OF227	20	Analyticon NAT13-262412	21	55			89	86
NATx04P08	OF222	22	Analyticon NAT14-350408	76	82	-2	-2	4	14
NATx05A13				12	62			8	15
NATx08F05				13	64	-2	4	2	0
NATx08O12				56	85	-9	-21	8	8
NATx11F07				77	79	-17	-10	-1	3
NATx13O05				40	78	1	-7	0	0
NATx13P03				90	89	0	-4	17	26
NATx14H04				36	79	-10	-9	6	8
NATx14L12	OF216	20	Analyticon NAT14-350412	41	70	1	-3	62	84
NATx14N04				38	79	-1	-6	5	8
NATx15H20	OF211	20	Analyticon NAT14-350422	29	69			81	82
Further compounds characterized in this study									
MDB1H12	OF233	22	Screening Centre #144						
MDB1H22	OF236	22	Screening Centre #332						
MDB1I08	OF232	22	Screening Centre #147						
MDB1J12	OF234	22	Screening Centre #156						
MDB1P02	OF235	22	Screening Centre #88						
NATx13L11	OF209	23	Analyticon NAT14-350417	27	60				
NATx15D20	OF210	23	Analyticon NAT14-350137	-11	-38				
NATx16M13	OF212	23	Analyticon NAT14-350393	3	6				
NATx8E22	OF213	23	Analyticon NAT14-350133	-7	-24				
NATx5K17	OF214	23	Analyticon NAT14-349953	1	2				
NATx9N18	OF215	23	Analyticon NAT14-350124	-6	-26				
NATx4G06	OF218	23	Analyticon NAT14-350132	3	15				
NATx4K12	OF219	23	Analyticon NAT14-350143	-5	1				
NATx4M12	OF220	23	Analyticon NAT14-350454	28	67				
NATx4O12	OF221	23	Analyticon NAT14-350119	-3	-4				
NATx4J20	OF223	23	Analyticon NAT14-350416	-2	-9				
NATx5M03	OF224	23	Analyticon NAT14-350424	8	27				
NATx5M13	OF225	23	Analyticon NAT14-350405	-6	-18				
NATx5I19	OF226	23	Analyticon NAT14-349955	-19	-44				
ICCB205I12	Tamoxifen							31	68
	4OH-Tamoxifen							25	52
	Endoxifen							23	51
	Raloxifen							4	15

9.4 Publications

Parts of this thesis have been published as:

Sailer C[1], **Offensperger F**[1], Julier A, Kammer KM, Walker-Gray R, Gold MG, Scheffner M, Stengel F (2018) Structural dynamics of the E6AP/UBE3A-E6-p53 enzyme-substrate complex. Nat Commun 9: 4441, [1]These authors contributed equally.

Offensperger F, Müller F, Jansen J, Hammler D, Götz KH, Marx A, Sirois CL, Chamberlain S, Stengel F, Scheffner M (2020) Identification of small molecule activators of the ubiquitin ligase E6AP/UBE3A and Angelman syndrome-derived E6AP/UBE3A variants. Manuscript.